

LEABHARLANN CHOLÁISTE NA TRÍONÓIDE, BAILE ÁTHA CLIATH | TRINITY COLLEGE LIBRARY DUBLIN
Ollscoil Átha Cliath | The University of Dublin

Terms and Conditions of Use of Digitised Theses from Trinity College Library Dublin

Copyright statement

All material supplied by Trinity College Library is protected by copyright (under the Copyright and Related Rights Act, 2000 as amended) and other relevant Intellectual Property Rights. By accessing and using a Digitised Thesis from Trinity College Library you acknowledge that all Intellectual Property Rights in any Works supplied are the sole and exclusive property of the copyright and/or other IPR holder. Specific copyright holders may not be explicitly identified. Use of materials from other sources within a thesis should not be construed as a claim over them.

A non-exclusive, non-transferable licence is hereby granted to those using or reproducing, in whole or in part, the material for valid purposes, providing the copyright owners are acknowledged using the normal conventions. Where specific permission to use material is required, this is identified and such permission must be sought from the copyright holder or agency cited.

Liability statement

By using a Digitised Thesis, I accept that Trinity College Dublin bears no legal responsibility for the accuracy, legality or comprehensiveness of materials contained within the thesis, and that Trinity College Dublin accepts no liability for indirect, consequential, or incidental, damages or losses arising from use of the thesis for whatever reason. Information located in a thesis may be subject to specific use constraints, details of which may not be explicitly described. It is the responsibility of potential and actual users to be aware of such constraints and to abide by them. By making use of material from a digitised thesis, you accept these copyright and disclaimer provisions. Where it is brought to the attention of Trinity College Library that there may be a breach of copyright or other restraint, it is the policy to withdraw or take down access to a thesis while the issue is being resolved.

Access Agreement

By using a Digitised Thesis from Trinity College Library you are bound by the following Terms & Conditions. Please read them carefully.

I have read and I understand the following statement: All material supplied via a Digitised Thesis from Trinity College Library is protected by copyright and other intellectual property rights, and duplication or sale of all or part of any of a thesis is not permitted, except that material may be duplicated by you for your research use or for educational purposes in electronic or print form providing the copyright owners are acknowledged using the normal conventions. You must obtain permission for any other use. Electronic or print copies may not be offered, whether for sale or otherwise to anyone. This copy has been supplied on the understanding that it is copyright material and that no quotation from the thesis may be published without proper acknowledgement.

Exploring an immune function for murine SARM

Thesis submitted to the University of Dublin for the degree of Doctor of Philosophy

by

Claudia Gürtler

(Dipl. hum. biol.)

School of Biochemistry and Immunology

Trinity College Dublin

Ireland



2012

TRINITY COLLEGE
2 4 MAY 2013
LIBRARY DUBLIN

Thesis 9807

Declaration

This thesis is submitted by the undersigned to the University of Dublin for the examination of Doctorate in Philosophy. The work herein is entirely my own and has not been submitted as an exercise for a degree in any other university. The library at Trinity College, Dublin, has my full permission to lend or copy this thesis on request.



Table of contents

I. List of figures **6**
II. List of tables **9**
III. List of abbreviations **10**
IV. Abstract **13**
1 Introduction **15**
1.1 The Immune system 15
1.2 Pattern recognition receptors (PRRs) 18
1.2.1 Toll-like receptors (TLRs) 19
1.2.2 C-type lectin receptors (CLRs) 28
1.2.3 RIG-I-like receptors (RLRs) 32
1.2.4 Cytosolic DNA receptors 36
1.2.5 NOD-like receptors (NLRs) 40
1.3 The IFN system 45
1.4 SARM 48
1.5 Aims 55
2 Materials & Methods **57**
2.1 Materials 57
2.1.1 Cells and cell culture reagents 57
2.1.2 Cell receptor ligands and siRNA 59
2.1.3 Antibodies 60
2.1.4 Primers 61
2.1.5 Method-specific materials 62
2.1.6 Buffers 64
2.2 Methods 67
2.2.1 Cell handling 67
2.2.2 Cell transfection using Lipofectamine 2000 68
2.2.3 Generation of M-CSF- and GM-CSF-conditioned medium 69
2.2.4 Generation of pBMDMs and pBMDCs 70
2.2.5 Generation of iBMDMs 72
2.2.6 Isolation of human PBMCs 72
2.2.7 Murine tissue RNA and protein preparation 73

2.2.8 Quantitative real-time PCR 73
2.2.9 Genomic DNA extraction 76
2.2.10 Genotyping of *Sarm*$^{-/-}$ cells 76
2.2.11 PCR for sequencing the 5'-*Ccl5* gene locus 77
2.2.12 Enzyme-linked immunosorbent assay (ELISA) 78
2.2.13 Western Blotting 79
2.2.14 Luciferase reporter gene assay 81
2.2.15 Chromatin immunoprecipitation (ChIP) assay 82
2.2.16 Fluorescence activated cell sorting (FACS) staining 84
2.2.17 Confocal microscopy 85
2.2.18 Amplification and purification of plasmid DNA 86
2.2.19 Cloning of mSARM-C-Flag into pLV-CMV 87
2.2.20 Cloning of murine *Ccl5* promoter constructs into pGL3 90
2.2.21 Statistical analysis 91

3 SARM expression in human and murine cells and implications for immune responses 93

3.1 Introduction 93
3.2 Results 95
3.2.1 SARM expression and its downregulation following immune stimulation 95
3.2.2 Divergent effects of siRNA-mediated SARM knockdown on PRR-induced cytokine responses 99
3.3 Discussion 102

4 Characterising SARM function in murine BMDCs and BMDMs 117

4.1 Introduction 117
4.2 Results 119
4.2.1 Role for SARM in TLR4-induced CCL5 and IFN-β expression in primary BMDCs 119
4.2.2 SARM has no role in TLR-induced DC maturation and endotoxin tolerance 121
4.2.3 Role for SARM in TLR- and non-TLR-induced CCL5 expression in primary and immortalised BMDMs 123
4.2.4 SARM is additionally required for IFN-β expression in immortalised, but not in primary BMDMs 124

4.2.5 TLR4-induced CCL5 is a primary response gene in BMDMs 127
4.2.6 SARM is also required for type I and type II IFN-induced CCL5, while it is dispensable for most other IFN-dependent responses 129
4.3 Discussion 131
5 Investigating the CCL5-regulatory mechanism of SARM in murine BMDMs. 159
5.1 Introduction 159
5.2 Results 161
5.2.1 SARM is not required for the activation of MAPKs and the transcription factors NF-κB and IRF3 161
5.2.2 SARM has a role in enhancing basal IRF3 expression in immortalised BMDMs 163
5.2.3 SARM is dispensable for the induced upregulation of the transcription factors IRF1 and IRF8 166
5.2.4 *Sarm*$^{-/-}$ mice harbour a polymorphism in the *Ccl5* gene promoter, which did not affect gene expression 167
5.2.5 Recruitment of RNA Polymerase II and transcription factors to the *Ccl5* promoter in the absence of SARM 170
5.3 Discussion 173
6 Final discussion 201
V. Acknowledgements 211
VI. References 213

I. List of figures

Figure 1.1: Subcellular localisation of TLRs and their selective usage of TIR adaptors 24
Figure 1.2: Overview of TLR signalling pathways 27
Figure 1.3: Dectin1 signalling 30
Figure 1.4: RLR signalling 35
Figure 1.5: Overview of cytosolic DNA receptors and their signalling pathways 39
Figure 1.6: Activation process of the NLRP3 inflammasome 42
Figure 1.7: NOD1 and NOD2 signalling 44
Figure 1.8: Type I and type II IFN signalling 47
Figure 1.9: Schematic of protein domains and motifs found in the human TIR adaptor family 49
Figure 1.10: Overview of SARM functions in *C. elegans* and mammals 52
Figure 2.1: Schematic of the mutated *Sarm* locus in *Sarm*$^{-/-}$ mice (by A. Ding) 76
Figure 2.2: pLV-CMV-GFP vector map 87
Figure 2.3: PCR product mSARM-C-Flag insert 88
Figure 2.4: Screening of minipreps for pLV-mSARM-C-Flag following *Spe*I/*Xho*I-digest 89
Figure 2.5: pGL3-luciferase vector map 90
Figure 2.6: PCR products *Ccl5* promoter constructs 91
Figure 3.1: SARM is expressed in human PBMCs and *SARM* mRNA is downregulated following TLR stimulation 109
Figure 3.2: SARM detection in murine BMDMs and the downregulation of *Sarm* mRNA following TLR4 and IFNAR stimulation 110
Figure 3.3: SARM is predominantly expressed in murine brain compared with other murine tissues and BMDMs 111
Figure 3.4: Overexpressed mSARM-C-Flag localises to punctate structures in the cytoplasm of murine NIH3T3 cells 112
Figure 3.5: Effect of SARM siRNA on TLR4-induced CCL5 expression in human HEK293-TLR4 cells 113
Figure 3.6: Effect of SARM siRNA on RLR-induced CCL5 expression in human HEK293 cells 114

Figure 3.7: Divergent effects of SARM siRNA on RLR-induced CCL5 expression in human HEK293 cells 115
Figure 4.1: Role for SARM in TLR4-induced CCL5 and IFN-β expression in primary BMDCs 139
Figure 4.2: SARM is dispensable for non-TLR-induced CCL5 and IFN-β expression in primary BMDCs 140
Figure 4.3: SARM is dispensable for TLR-induced maturation of primary BMDCs 142
Figure 4.4: SARM has no role in endotoxin tolerance in primary BMDCs and BMDMs 143
Figure 4.5: SARM is required for TLR4-induced CCL5 expression in primary BMDMs 144
Figure 4.6: SARM promotes TLR- and non-TLR-induced CCL5 expression in primary BMDMs 145
Figure 4.7: SARM is required for TLR4-induced CCL5 expression in immortalised BMDMs 146
Figure 4.8: SARM promotes non-TLR-induced CCL5 expression in immortalised BMDMs 147
Figure 4.9: SARM is required for TLR- and non-TLR-induced IFN-β expression in immortalised, but not in primary BMDMs 148
Figure 4.10: SARM is required for TLR4-mediated IFN-dependent responses in immortalised, but not in primary BMDMs 149
Figure 4.11: Overview of the effect of SARM-deficiency on TLR- and non-TLR-induced cytokines in primary and immortalised BMDMs 150
Figure 4.12: Signalling pathways potentially involved in PRR-mediated CCL5 expression 151
Figure 4.13: TLR4-induced TNF-α, CCL5 and IFN-β are primary response genes in BMDMs 154
Figure 4.14: SARM is required for IFNAR-induced CCL5 expression, but dispensable for other IFN-mediated responses in primary BMDMs 155
Figure 4.15: SARM is required for IFNAR- and IFNGR-induced CCL5 expression, but mostly dispensable for other IFN-mediated responses in immortalised BMDMs 157
Figure 4.16: Signalling pathways showing SARM-dependent CCL5 expression in BMDMs 158
Figure 5.1: SARM is dispensable for TLR4-mediated activation of NF-κB and MAPKs in primary and immortalised BMDMs 180

Figure 5.2: SARM is dispensable for TLR4-mediated IRF3 activation in primary and immortalised BMDMs 181
Figure 5.3: SARM is dispensable for TLR4- and non-TLR-mediated p65 and IRF3 nuclear translocation in primary and immortalised BMDMs 184
Figure 5.4: SARM is required for the elevated basal IRF3 expression in immortalised BMDMs, but dispensable for the IRF3 expression in primary BMDMs 185
Figure 5.5: IRF3 expression is independent of type I IFNs in immortalised BMDMs 186
Figure 5.6: IRF3 mRNA stability is not regulated by SARM in immortalised BMDMs.. 187
Figure 5.7: SARM is dispensable for TLR4- and IFNAR/IFNGR-mediated upregulation of IRF1 and IRF8 in primary and immortalised BMDMs 189
Figure 5.8: *Sarm*$^{-/-}$ mice harbour a 1-2bp G-insertion in the proximal *Ccl5* gene promoter 191
Figure 5.9: Sequence variations within the Poly(G:C) region of the *Ccl5* promoter in different mouse strains 192
Figure 5.10: The 1-2bp G-insertion in the *Ccl5* promoter does not affect its activity 194
Figure 5.11: The Poly(G)-sequence variation does not affect endogenous CCL5 expression in *Trif*- and *Tram*-knockout immortalised BMDMs 195
Figure 5.12: Optimisations for the Chromatin Immunoprecipitation (ChIP) assay 196
Figure 5.13: ChIP analysis of RNA Polymerase II and transcription factor binding to the *Ccl5* promoter in immortalised BMDMs in the presence and absence of SARM 198
Figure 5.14: Optimisation of quantitative ChIP analysis in immortalised wt BMDMs 199
Figure 6.1: Potential mechanisms of SARM-mediated CCL5 regulation in BMDMs..... 209

II. List of tables

Table 1.1: TLR receptors and their major ligands 22
Table 1.2: Selection of signal-generating CLRs relevant in innate and adaptive immunity31
Table 1.3: Inflammasome-forming receptors and a selection of non-inflammasome NLRs 45
Table 2.1: Cell types 58
Table 2.2: Cell culture reagents 59
Table 2.3: Cell receptor ligands 59
Table 2.4: siRNA 60
Table 2.5: Antibodies 61
Table 2.6: Primer pairs 62
Table 2.7: Method-specific materials 64
Table 2.8: Buffers 66
Table 2.9: cDNA synthesis protocol 74
Table 2.10: Real-time PCR protocol 75
Table 2.11: PCR protocol for *Sarm*$^{-/-}$ genotyping 77
Table 2.12: PCR protocol to amplify a 5'-*Ccl5* gene DNA-fragment for sequencing 77
Table 2.13: Composition of 10% SDS gels 79
Table 2.14: Composition of 8% native gels 80
Table 2.15: PCR protocol for semi-quantitative ChIP analysis 84
Table 2.16: Fluorescent-labeled antibodies used in DC maturation assay (FACS) 85
Table 2.17: Antibody concentrations used in confocal microscopy 86
Table 2.18: PCR protocol to generate the mSARM-C-Flag insert 88
Table 2.19: Digestion protocols of mSARM-C-Flag insert and pLV-CMV plasmid 88
Table 2.20: Ligation reaction mix 89
Table 2.21: PCR protocol to generate the *Ccl5* promoter constructs 91
Table 4.1: Overview of the effect of SARM-deficiency on TLR- and non-TLR-induced cytokines in primary BMDCs 141

III. List of abbreviations

AIM2	Absent in melanoma 2
ALR	AIM2-like receptor
AP-1	Activator protein 1
APS	Ammonium persulfate
ARE	AU-rich element
ASC	Apoptosis-associated speck-like protein containing a CARD
ASK1	Apoptosis signal-regulating kinase 1
Bcl10	B cell lymphoma 10
BCR	B cell receptor
BM	Bone marrow
BSA	Bovine serum albumin
CARD	Caspase activation and recruitment domain
CBP	CREB-binding protein
CCL5	Chemokine (C-C motif) ligand 5
cDNA	Complementary DNA
ChIP	Chromatin Immunoprecipitation
CHX	Cycloheximide
CLR	C-type lectin receptor
CNS	Central nervous system
CREB	cAMP response element-binding
DAI	DNA-dependent activator of IRFs
DAMP	Danger-associated molecular pattern
DAPI	4',6-diamidino-2-phenylindole
DC	Dendritic cell
DD	Death domain
DDX	DEAD box protein
Dectin	DC-associated C-type lectin
DHX	DExD/H-box helicase
DMEM	Dulbecco's Modified Eagle Medium
DMSO	Dimethyl sulfoxide
DNA	Deoxyribonucleic acid
DNase	Deoxyribonuclease
ds	double-stranded
DTT	Dithiothreitol
EDTA	Ethylenediaminetetraacetic acid
ELISA	Enzyme-linked immunosorbent assay
EMCV	Encephalomyocarditis virus
ER	Endoplasmic reticulum
ERK1/2	Extracellular signal-regulated kinases 1 and 2
FADD	Fas-associated death domain protein
FBS/FCS	Foetal bovine serum / Foetal calf serum
FcR	Fc receptor
GM-CSF	Granulocyte-macrophage colony-stimulating factor
HEK	Human embryonic kidney
HIV-1	Human immunodeficiency virus-1

HPV	Human papilloma virus
HSV1/2	Herpes simplex virus 1/2
iBMDMs	Immortalised bone marrow-derived macrophages
IFI16	IFNγ-inducible protein 16
IFN	Interferon
IFNAR	Interferon-α/β receptor (type I IFN receptor)
IFNGR	Interferon-gamma receptor (type II IFN receptor)
IKK	IκB kinase
IRAK	IL-1 receptor associated kinase
IRF	IFN-regulatory factor
ISG	IFN-stimulated gene
ITAM	Immunoreceptor tyrosine-based activation motif
ITIM	Immunoreceptor tyrosine-based inhibitory motif
IκB	Inhibitor of NF-κB
JEV	Japanese encephalitis virus
KAP1	KRAB-associated protein1
KLF13	Krüppel-like factor 13
LBP	LPS-binding protein
LGP2	Laboratory of genetics and physiology 2
LPS	Lipopolysaccharide
LRR	Leucine-rich repeat
LRRFIP1	Leucine-rich repeat flightless-interacting protein 1
MAL	MyD88-adaptor like protein
Malt1	Mucosa-associated lymphoid tissue lymphoma translocation protein 1
MAPK	Mitogen-activated protein kinase
MAVS	Mitochondrial antiviral signalling
MCMV	Murine cytomegalovirus
MCP-1	Monocyte chemotactic protein-1
M-CSF	Macrophage colony-stimulating factor
MDA5	Melanoma differentiation-associated gene 5
MHCI/II	Major histocompatibility complex class I and class II
miRNA	MicroRNA
MMTV	Mouse mammary tumor virus
mRNA	Messenger RNA
MyD88	Myeloid differentiation factor-88
NAP1	NF-κB-activating kinase-associated protein 1
NBD	Nucleotide binding domain
NEMO	NF-κB essential modulator
NFAT	Nuclear factor of activated T cells
NF-κB	Nuclear factor kappa B
NIK	NF-κB-inducing kinase
NLR	NOD-like receptor
NOD	Nucleotide-binding oligomerization domain
OAS2	2'-5' oligoadenylate synthase type 2
PAMP	Pathogen-associated molecular pattern
PBMCs	Peripheral blood mononuclear cells
pBMDCs	Primary bone marrow-derived dendritic cells
pBMDMs	Primary bone marrow-derived macrophages
PBS	Phosphate buffered saline
PI3K	Phosphoinositide 3-kinase

PIP2	Phosphatidyl-inositol-4,5-bisphosphate
Pol II	RNA polymerase II
Poly(I:C)	Polyinosinic-polycytidylic acid
PRG	Primary response gene
PRR	Pattern-recognition receptor
PVDF	Polyvinylidene fluoride
PYD	Pyrin domain
RANTES	Regulated on activation, normal T cell expressed and secreted
RHIM	RIP homotypic interaction motif
RIG-I	Retinoic acid-inducible gene I
RIP	Receptor-interacting protein
RLR	RIG-I-like receptor
RNA	Ribonucleic acid
ROS	Reactive oxygen species
RSV	Respiratory syncytial virus
RT	Room temperature
SARM	Sterile α and armadillo motif containing protein
Sdc2	Syndecan-2
SDS	Sodium dodecyl sulfate
SFM	Serum-free medium
SFV	Semliki Forest virus
SINTBAD	Similar to NAP1 TBK1 adaptor
siRNA	Small interfering RNA
ss	Single-stranded
SSC	Sideward scatter
STAT	Signal transducer and activator of transcription
STING	Stimulator of IFN genes
Syk	Spleen tyrosine kinase
TAB2/3	TAK binding proteins 2 and 3
TAK1	TGF-β-activated kinase 1
TANK	TRAF family member-associated NF-κB activator
TCR	T cell receptor
TEMED	Tetramethylethylenediamine
TIR	Toll/IL-1 receptor
TLR	Toll-like receptor
TNF	Tumor necrosis factor
Tpl2	Tumor progression locus
TRADD	TNF-receptor 1-associated death domain
TRAF	TNF receptor-associated factor
TRAM	TRIF-related adaptor molecule
TRIF	TIR domain-containing adaptor inducing IFN-β
UTR	Untranslated region
VSV	Vesicular stomatitis virus
WB	Western Blotting
WNV	West Nile virus
wt	Wild-type

IV. Abstract

Innate immune cells, such as tissue-residing macrophages and dendritic cells (DCs) play a key role in initiating an immune response following the detection of invading pathogens via germline-encoded pattern-recognition receptors (PRRs) present on the cell surface or in intracellular compartments and the cytosol. PRRs selectively recognise conserved molecular features of the microbe and subsequently initiate distinct signalling cascades leading to transcription factor activation and the induction of proinflammatory cytokines (e.g. TNF-α), chemokines (e.g. CCL5/RANTES) and type I interferons (i.e. IFN-α and IFN-β). One major family of PRRs are the membrane-bound Toll-like receptors (TLRs), which signal via the Toll/IL-1 receptor (TIR) domain-containing adaptor proteins MyD88, MAL, TRIF and TRAM. The immunological function of the fifth most evolutionarily conserved TIR adaptor sterile alpha and HEAT/Armadillo motif protein (SARM) is still enigmatic.

In human peripheral blood mononuclear cells (PBMCs), SARM has been shown to interact with TRIF and negatively regulate TRIF-dependent gene induction, such as TLR4-induced TNF-α. For murine SARM roles have been described in the central nervous system (CNS), where it is preferentially expressed and involved in stress-induced neuronal cell death, neuronal morphology and restriction of West Nile virus pathogenesis. The latter function was linked to a requirement for SARM for TNF-α production and activation of CNS inflammatory cells in the brainstem. However, bone marrow-derived macrophages (BMDMs) from SARM-deficient mice showed normal TNF-α and MCP-1 production following TLR stimulation, which was explained by the weak expression of SARM in this and other myeloid cell types.

Therefore this project aimed to explore the immune function of murine SARM in more detail. First, it was established that immune cells, such as human PBMCs and murine BMDMs, express SARM and *SARM* mRNA was found to be downregulated following TLR and type I IFN receptor stimulation, suggesting a role for SARM in immune responses in these immune cell types. A detailed characterisation of TLR-dependent and -independent cytokine responses in murine wild-type and SARM-deficient primary and immortalised BMDMs and primary BMDCs revealed a requirement for SARM for optimal CCL5 mRNA and protein expression in BMDMs, while it was dispensable for induction of TNF-α. Interestingly, this CCL5-regulatory function of SARM was not restricted to TRIF and TLR pathways, as cytosolic RNA and DNA sensors as well as type I and type II IFN receptors selectively required SARM for CCL5 expression, while other IFN-stimulated genes (ISGs), such as IRF7, IFIT2 and viperin, were induced independently of SARM. Further it was established that PRRs upregulated CCL5 in the primary pathway and not in a secondary response via secreted type I IFNs. Thus, SARM acted downstream of both PRR and IFN pathways to mediate CCL5 induction.

However the activation of MAP kinases and the main transcription factors implicated in CCL5 induction, including NF-κB, IRF3, IFN-stimulated STAT1 and the upregulation of IRF1 and IRF8 were normal in the absence of SARM. Thus SARM was likely to function downstream of transcription factor activation by regulating transcriptional initiation at the *Ccl5* promoter or a posttranscriptional event, such as RNA splicing. In light of the pivotal role of CCL5 in immune responses by recruiting various immune cells to sites of infected tissue, but also its implication in autoimmune diseases and cancer, it is most relevant to elucidate the exact mechanism of its regulation. This may also lead to the design of new therapies to selectively modulate CCL5 expression.

1 Introduction

1.1 The Immune system

Constantly surrounded by microbes, multicellular organisms like plants and animals developed a remarkable diversity of innate defence mechanisms to protect themselves against invading pathogens. This ancient form of host defence is evolutionarily conserved throughout the animal kingdom and referred to as the innate immune system. However, in vertebrates, a secondary, more sophisticated arm of defence has evolved; the adaptive immune system. This complementary arm is activated and directed by the innate part to cooperate and successfully eliminate any potential pathogen or toxin (1, 2).

The innate immune system is the first line of defence to protect the body against the invasion of microbes. The entry of microorganisms into the host system is generally inhibited by physical barriers, such as the skin and internal ciliated or mucosal epithelia, and secreted chemicals like destructive enzymes and acids. In addition, the normal population of epithelia with commensal bacteria inhibits the growth and invasion of pathogenic microbes. However, once a microbe has overcome these barriers, it will immediately be recognised by germline-encoded secreted or cell-associated pattern-recognition receptors (PRRs) that bind to distinct microbial structures of bacteria, viruses, parasites and fungi (3). The detected motifs are known as pathogen-associated molecular patterns (PAMPs), even though they are not unique to pathogens, but instead expressed within a given class of microbes; therefore the term microbe-associated molecular pattern (MAMP) was proposed but has not been established yet. The PRR-mediated detection of PAMPs is well suited for the initial discrimination of infectious non-self (pathogens) from non-infectious self and with it the decision to respond or not to respond to a particular ligand, because PAMPs differ from host molecules and are highly conserved and not vulnerable to mutations due to their requirement for microbial survival. One of the main innate effector mechanisms upon microbial recognition is phagocytosis, where the innate immune cell engulfs the pathogen and degrades it in internal vesicles; a process first described by Metchnikoff in 1883. Tissue-residing phagocytes, such as macrophages and dendritic cells (DCs), as well as endothelial cells and fibroblasts harbour signal-generating PRRs that lead to gene expression of various antimicrobial peptides, cytokines (e.g. TNF-α) and chemokines (e.g. CCL5/RANTES) to initiate a rapid inflammatory response characteristic of the innate immune system. This involves recruitment and activation of

other innate effector cells like monocytes, neutrophils, eosinophils, basophils and natural killer (NK) cells from the bloodstream into the infected tissue; cells, which also exhibit various PRRs and strategies to destroy the pathogen. Furthermore, an increase of vascular permeability allows plasma proteins like the complement system to enter the site of infection. These events cause the typical signs of inflammation, such as swelling, redness, heat, pain and loss of function. Finally, the inflammatory response also initiates the healing of the damaged tissue. It is noteworthy, that PRRs are also activated by endogenous, non-infectious components released from dying cells or degraded extracellular matrix caused by infection or trauma. These stress signals, known as danger-associated molecular patterns (DAMPs), induce inflammatory responses and tissue repair, but are unable to trigger an adaptive immune response, thus preventing autoimmunity (4). However, during infection the simultaneous recognition of PAMPs and DAMPs probably alerts the host immune system of the invasion of viable, harmful pathogens to subsequently trigger a more robust immune response. Five immune checkpoints were recently proposed to evaluate the microbial threat during microbial encounter and to adjust the immune response to minimise tissue damage (5). First, the innate immune cell discriminates between soluble or particulate PAMPs. A whole microorganism exhibits various PAMPs, which stimulate several PRRs that subsequently integrate the signal. Another important checkpoint is to distinguish live from dead microbes and specific vita-PAMPs have been described that are only associated with live organisms, like bacterial mRNA. The importance of vita-PAMPs to trigger an effective adaptive immune response was also shown for the more successful live vaccines compared to inactivated vaccines. Third, by detecting the activity of specific virulence factors, such as bacterial secretion systems and toxins, the host can measure the pathogenic potential of an invading microorganism. Furthermore, discrimination between microbial colonisation and invasion exists that goes beyond the physical separation of the host from microbes by epithelial barriers and might depend on microbial features that are less understood. Finally, regulation of the immune response is specific to the tissue and its associated immune cells that come into contact with the invading microbe.

In parallel to the immediate inflammatory response, the innate immune system activates a second arm of defence, named the adaptive/acquired immune response. This response is delayed by 3 to 5 days, but due to its specificity is very effective in eliminating the pathogen. It relies mainly on T and B lymphocytes, which express unique, antigen-

specific T and B cell receptors (TCRs, BCRs) that are not encoded in the germ line. Instead these receptors are generated in each cell individually by somatic gene rearrangements from a limited set of receptor genes during lymphocyte development in the primary lympoid organs thymus and bone marrow, respectively. This provides an almost infinite diversity to recognise virtually any potential antigen. Mature naïve lymphocytes then circulate between blood and secondary lymphoid tissues, such as lymph nodes, spleen and mucosa-associated lymphoid tissue (MALT), until they encounter their specific antigen. The initial activation of T cells is mediated by antigen-presenting DCs that provide the essential link between innate and adaptive immunity. Once immature DCs have recognised and engulfed a pathogen in peripheral tissue, they get activated, migrate to the draining lymph node and acquire a mature phenotype in a process called DC maturation. This is characterised by the upregulation of major histocompatibility complex (MHC) class I and class II molecules and the costimulatory proteins CD80, CD86 and CD40, which mediate the activation of antigen-specific naïve T cells. The specific TCRs on lymphocytes recognise their specific antigen only presented by a particular MHC molecule; $CD8^+$ T cells are restricted to MHC class I-presented peptides that usually originate from the cytosol, whereas $CD4^+$ helper T cells respond to MHC class II-presented antigen derived from the endocytotic compartment. T cells are further stimulated by DC-secreted cytokines that instruct the T cell on the pathogen that was originally encountered and directs the transition of the naïve T cell into an appropriate effector cell. Five main $CD4^+$ T cell subsets have been defined: T_h1, T_h2, T_h17, follicular and regulatory T cells (fT_h, T_{reg}), whose main function is to regulate other immune cells by secreting selected cytokines. The $CD8^+$ cytotoxic T cells, on the other hand, can directly induce apoptotic cell death of an infected cell. In contrast to T lymphocytes and their local effector functions against intracellular pathogens, B cells fight infection "at a distance" by secreting highly specific antibodies into blood and tissue fluids that can bind and initiate elimination of extracellular pathogens and toxins. The antigen specificity of the antibodies is identical with the individual cell surface BCR. Initially, the specific binding of the BCR to soluble antigen in the presence of auxiliary cells and cytokines leads to differentiation of naïve B cells into antibody-producing plasma cells. In both cases, antigen recognition induces proliferation of the specific T and B lymphocytes, thus increasing the number of specific effector cells to eliminate the pathogen during infection, a process known as clonal selection. Some of these cells are long-lived and establish an immune memory that allows a faster and more

vigorous response by a second encounter with the same pathogen. Also vaccination uses this memory function to protect the body against infection with a particular microbe. Although memory was long considered as being a hallmark of adaptive immunity, increasing evidence suggests adaptive-like features in innate immune cells, for example in NK cells (6, 7). Reciprocally, some lymphocyte subsets, such as B1 cells, γδ T cells and invariant NKT cells, show innate characteristics and a rapid response to antigen.

1.2 Pattern recognition receptors (PRRs)

In 1989, Janeway proposed that the innate immune system senses microbial infection via germline-encoded cellular PRRs that detect evolutionary conserved molecular signatures of the pathogen (PAMPs) to subsequently initiate an immune response (3). In 1996 Jules Hoffmann's group strongly supported this hypothesis by discovering that fruit flies, *Drosophila melanogaster*, carrying a mutation in the *Toll* gene were highly susceptible to fungal infection due to defective expression of antimicrobial peptides (8). Subsequently, its human homologue, now known as TLR4, and its function in innate immunity was described (9). Since then, a huge variety of signal-generating PRRs present in distinct cellular compartments have been identified. They recognise different but overlapping microbial molecules including proteins, lipids, lipoproteins, glycans and nucleic acids derived from bacteria, viruses, parasites and fungi. However, it became apparent in recent years that the original paradigm of selective "pathogen" recognition needs to be revisited, as PRRs also sense commensal microbes and endogenous host molecules released from damaged tissue (DAMPs). Upon ligand recognition, PRRs trigger a signalling cascade leading to induction of genes involved in immune responses, such as inflammatory cytokines, chemokines and antimicrobial peptides. The first identified and best characterised family of PRRs are the membrane-bound Toll-like receptors (TLRs), that detect PAMPs either on the cell surface or in intracellular vesicles such as endosomes and lysosomes. Also localised on the cellular membrane are C-type lectin receptors (CLRs) that mainly mediate fungal recognition. Besides these sensors of extracellular pathogens, cells exhibit a broad cytosolic detection system for sensing intracellular pathogens, which explains their ubiquitous expression in most cell types, while the transmembrane PRRs are mainly found in immune cells. Those cytosolic receptors include NOD-like receptors (NLRs), RIG-I-like receptors (RLRs) and DNA receptors, including the new family of

AIM2-like receptors (ALRs). More recently it emerged that other members of the DExD/H-box helicase superfamily, apart from RLRs, may play roles in cytosolic RNA- and DNA-sensing.

It is important to bear in mind, that pathogens generally contain multiple PAMPs and also induce the release of DAMPs that subsequently engage with various PRRs of different families that integrate the various signals and initiate together an appropriate immune response to successfully eliminate the pathogen. Although PRRs are essential for protective immunity against infection, overwhelming responses would cause acute and chronic inflammation and autoimmune diseases. Therefore multiple negative regulatory systems are in place to control immune responses.

1.2.1 Toll-like receptors (TLRs)

Toll-like receptors (TLRs) are a major family of signal-generating, transmembrane PRRs with 10 functional members identified in human and 12 in mouse. TLR1 to TLR9 are conserved in both species, while TLR10 is only expressed in human, as the murine *tlr10* gene is disrupted by a retroviral insertion (10). Instead mice express three TLR members that have been lost from the human genome, TLR11 to TLR13. All TLRs are type I integral membrane proteins with an N-terminal extracellular domain for ligand binding, a single transmembrane helix and a C-terminal cytoplasmic Toll/IL-1 receptor (TIR) domain initiating downstream signalling via homotypic interaction with TIR domain-containing adaptor proteins (11). The ectodomain (ECD) is constructed of 19-25 consecutive leucine-rich repeats (LRRs) that harbour the conserved "LxxLxLxxN" motif and that are each 22-29 residues in length, causing the typical horseshoe-shaped structure of this domain. Ligand binding leads to formation of a symmetrical "m"-shaped TLR homo- or heterodimer, which often sandwiches the ligand in between and interacts with each other at the membrane proximal region of the ECD (12). This causes dimerisation of the cytoplasmic TIR domains, creating a scaffold for the recruitment of TIR adaptors that subsequently activate downstream signalling.

TLRs can be divided into two groups due to their subcellular localisation. TLR1, 2, 4, 5 and 6 are found on the plasma membrane, where they recognise surface molecules of extracellular pathogens such as lipids, proteins and lipoproteins. TLR3, 7, 8 and 9, on the other hand, are exclusively expressed in endocytic compartments to sense nucleic acids

derived from bacteria and viruses following their endosomal degradation. Thus, the localisation of TLRs is important for accessibility of the specific ligand, but also for initiation of a particular signalling cascade and immunological response appropriate to the infecting microbe (described later). The strict location of the nucleic acid-sensing TLRs to the endosome is also a strategy to avoid recognition of self and to maintain tolerance. The innate immune system's ability to detect nucleic acids allows protective immune responses to a wide range of pathogens, especially viruses, which have not many other features suitable for detection. This bears the risk of self recognition, as nucleic acids, unlike most other PAMPs, are highly abundant in the host. Therefore, PRR compartmentalisation is one mechanism to circumvent unwanted detection of self and thus autoimmune and autoinflammatory diseases (13). The location of TLRs is regulated by several chaperones. In resting cells, nucleic acid-sensing TLRs are retained in the endoplasmic reticulum (ER) and are transported to endolysosomes upon stimulation, regulated by the ER-protein UNC93B1 (14). A similar mechanism applies to the murine endosomal receptors TLR11 and TLR13 (15, 16). Another ER-chaperone, PRAT4A, is additionally involved in regulating the traffic of TLR9, but also of the surface TLRs, TLR1, 2 and 4 (17); while gp96 appears to be a more general chaperone for TLRs (18). As another mechanism to prevent self-DNA recognition, TLR9 is kept non-functional until it is cleaved by cathepsins in the endolysosomal compartment (19).

Each TLR recognises a selective set of PAMPs (see Table 1.1). The founding member of the TLR family is TLR4, which detects lipopolysaccharide (LPS), an essential component of the outer membrane of gram-negative bacteria and a main cause of septic shock (20). LPS interacts with a complex of TLR4 and its associated coreceptor MD-2 to which it is delivered by the soluble LPS-binding protein (LBP) and the membrane-anchored CD14 protein (21). Besides bacterial LPS, TLR4 also responds to virus surface proteins such as respiratory syncytial virus (RSV) fusion protein or the envelope protein of mouse mammary tumor virus (MMTV). TLR2, another receptor on the plasma membrane, recognises a huge variety of bacterial PAMPs, as well as other components from viruses, fungi and parasites. TLR2 forms a heterodimer with TLR1 or TLR6, which selectively detect triacylated lipopetides from gram-negative bacteria (e.g. Pam_3CSK_4) or diacylated lipopeptides from gram-positive bacteria (e.g. MALP-2), respectively. TLR2/6 is also important for the immune response to RSV. Additionally, the coreceptors CD36 and CD14 have been reported to participate in ligand recognition of TLR2 heterodimer (22, 23). The

last member of cell surface TLRs is TLR5, which senses the protein flagellin of the bacterial flagella. TLR5 is proposed to have major immune functions in the small intestine, where it is highly expressed in lamina propria DCs (24). The expression of nucleic acid-sensing TLRs is restricted to membranes of the endosomal compartment, where they sample the lumen for ligands mostly derived from phagocytosed pathogens or infected apoptotic cells. Here, TLR3 specifically recognises viral double-stranded RNA (dsRNA), such as the genomic dsRNA from reoviruses or dsRNA generated during replication of single-stranded (ss) RNA viruses like RSV, encephalomyocarditis virus (EMCV), Semliki Forest virus (SFV) and West Nile virus (WNV) and some DNA viruses. The recognition of dsRNA is largely sequence independent, but requires a minimum length of 40 base pairs (bp) (25). TLR3 also detects certain small interfering RNAs (siRNAs) and the synthetic dsRNA analog polyinosinic-polycytidylic acid (Poly(I:C)). TLR7 and 8, on the other hand, sense guanosine/uridine-rich ssRNA of RNA viruses, such as vesicular stomatitis virus (VSV), influenza A virus and human immunodeficiency virus-1 (HIV-1) (26). Synthetic ligands that activate TLR7 are imidazoquinoline derivates, like imiquimod and resiquimod (R848), Poly(U) RNA and some siRNAs. In contrast to human, the function of murine TLR8 is still debatable (27). TLR9 is the only DNA-sensing TLR and specifically binds nonmethylated cytosine-guanosine (CpG)-containing DNA motifs present in bacteria and DNA viruses, but rare in the mammalian genome (28). Among the detected viruses are murine cytomegalovirus (MCMV), herpes simplex virus 1/2 (HSV1/2), human papilloma virus (HPV) and adenovirus. Additionally, TLR9 senses hemozoin, a byproduct formed during digestion of host hemoglobin by the parasite *Plasmodium falciparum*. The function of human TLR10 is still unknown, but phylogenetic analysis revealed that it is most related to TLR1 and TLR6 (29). Human TLR10 was shown to dimerise with TLR2, detected similar agonists as the TLR1/2 dimer and recruited MyD88, however the activated signalling pathway is still unknown and most likely differs from the typical TLR2-induced signalling cascade. The murine endosomal TLR11 detects the profilin-like protein of protozoan parasites like *Toxoplasma gondii* (30), while the role of murine TLR12 is still enigmatic. Murine endosomal TLR13 was recently identified as the receptor for bacterial RNA, detecting a specific, conserved sequence in bacterial 23S ribosomal RNA (31, 32). (reviewed in (33)).

TLR	Major ligand
TLR1/2	Triacylated lipopeptides from gram-negative bacteria and mycobacteria
TLR2	Lipopeptides (Pam_3CSK_4, MALP2) from bacteria, peptidoglycan and lipoteichoic acid from gram-positive bacteria, lipoarabinomannan from mycobacteria, mycoplasma, phospholipomannan from fungi, tGPI-mucin from *Trypanosoma cruzi*, hemagglutinin protein from measles virus
TLR3	Viral dsRNA of reoviruses, RSV, EMCV, SFV, WNV; synthetic Poly(I:C), siRNAs
TLR4	LPS from gram-negative bacteria, mannan from *Candida albicans*, glycoinositolphospholipids from *Trypanosoma*, viral envelope proteins from RSV and MMTV
TLR5	Bacterial flagellin
TLR6/2	Diacylated lipopeptides from gram-positive bacteria, RSV, zymosan from fungi
TLR7	Viral ssRNA from VSV, influenza A virus, HIV; synthetic imiquimod and resiquimod (R848), Poly(U) RNA, siRNAs
TLR8	Viral ssRNA; synthetic resiquimod (R848)
TLR9	Nonmethylated CpG DNA from bacteria and DNA viruses (e.g. MCMV, HSV1/2, HPV); hemozoin
hTLR10	Unknown (potentially senses triacylated lipopeptides in cooperation with TLR2)
mTLR11	Profilin of *T. gondii*, uropathogenic *E. coli*
mTLR12	Unknown
mTLR13	Bacterial 23S rRNA, VSV

Table 1.1: TLR receptors and their major ligands

Specific ligand binding leads to TLR dimerisation and formation of a signalling platform at the receptor cytosolic face, which subsequently recruits distinct TIR adaptor proteins that initiate downstream signalling (Figure 1.1). To date, five TIR domain-containing adaptor proteins have been identified (34). The first identified member was myeloid differentiation factor-88 (MyD88), which was shown to be involved in IL-1 receptor I signalling and subsequently implicated in signalling by all TLRs, except TLR3. TLR3 solely uses the adaptor TIR domain-containing adaptor inducing IFN-β (TRIF) to signal. TRIF also mediates the MyD88-independent pathway of TLR4 (35). TLR4 is specific in that it also requires two "bridging" TIR adaptors, MyD88-adaptor like protein (MAL) and TRIF-related adaptor molecule (TRAM), to recruit the cytosolic MyD88 and TRIF to the receptor, respectively. The bridging adaptors MAL and TRAM exhibit localisation motifs at their N-termini, namely a phosphatidyl-inositol-4,5-bisphosphate

(PIP2)-binding motif and a myristoylation site to target them preferentially either to the plasma membrane or the early endosomes, respectively (36, 37). This leads in the case of TLR4 also to separation of two signalling events, with activation of the MAL/MyD88-dependent pathway at the plasma membrane, followed by TLR4 internalisation and subsequent TRAM/TRIF signalling from endolysosomes (38). Furthermore, the bridging adaptors provide an additional control mechanism for TLR4 due to their tight regulation by modifications. MAL for example gets phosphorylated by Bruton's tyrosine kinase (Btk) or IRAK1/4 leading to its degradation (39-41), while TRAM is phosphorylated by protein kinase C ε (42). MAL is also involved in bridging MyD88 to TLR2, whereas the other TLRs, like TLR 5, 7, 8 and 9, recruit MyD88 directly. The selective and combinatorial adaptor usage of TLRs provides specificity of response to various pathogens. However, signalling variability is restricted as it is either controlled by the MyD88- or the TRIF-dependent pathway. While the former pathway leads mainly to activation of mitogen-activated protein kinases (MAPKs) and the transcription factor NF-κB to induce inflammatory cytokines and chemokines, the latter additionally activates the transcription factor IFN-regulatory factor 3 (IRF3) to induce expression of type I interferons, like IFN-β. The fifth, most evolutionary conserved member of the TIR adaptor family is sterile α and HEAT/Armadillo motif containing protein (SARM), which is unique among the adaptors as it does not activate the transcription factors NF-κB or IRF3, when overexpressed (43). Instead, SARM was shown to negatively regulate TRIF-dependent TLR signalling (44), besides its more recently discovered functions in the nervous system (described in 1.4).

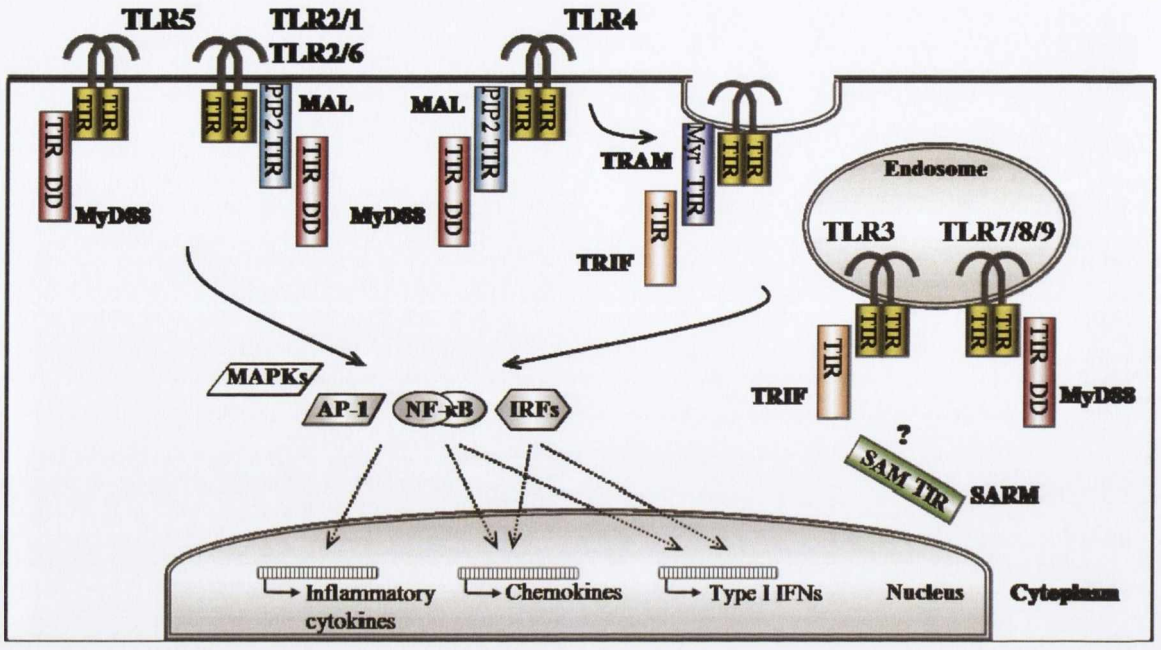


Figure 1.1: Subcellular localisation of TLRs and their selective usage of TIR adaptors

While TLR1, 2, 4, 5 and 6 are found on the plasma membrane, the nucleic acid-sensing TLR3, 7, 8 and 9 are exclusively expressed in endocytic compartments. After ligand binding, TLRs dimerise and engage with different TIR adaptor proteins to initiate signalling cascades that lead to activation of transcription factors, such as AP-1, NF-κB and IRFs, and expression of proinflammatory cytokines, chemokines and type I IFNs. MyD88 is the key signalling adaptor used by all TLRs, except TLR3, that uses TRIF instead. While most TLRs recruit MyD88 directly, TLR2 and TLR4 require MAL as a bridging TIR adaptor. TLR4 is specific in that, after initiating the MyD88-dependent pathway from the plasma membrane, it gets internalised and recruits TRIF to the endosomal membrane via the bridging adaptor TRAM.

Following pathogen recognition, MyD88 signalling is initiated by homotypic binding of MyD88-TIR domain to the TIR domain interface of the TLR receptor dimer or the bridging adaptor MAL in the case of TLR2 and TLR4. This releases the N-terminal death domain (DD) of MyD88, leading to the recruitment of DD-containing IL-1 receptor associated kinase (IRAK) family members (45). A multiprotein signalling complex is formed, and by using the death domains the crystal structure has recently been resolved and demonstrated the sequential assembly of DDs of 6 MyD88, 4 IRAK4 and 4 IRAK2 into a stable superhelical structure, called the Myddosome (46). The specific and stable assembly is mediated by molecular complementarity and electrostatic interactions and its importance for signal transduction was illustrated by the analysis of single nucleotide polymorphisms (SNPs) in human MyD88. Two natural occurring SNPs in the DD of MyD88, S34Y and R98C, showed highly impaired NF-κB activation due to instability of

the homotypic MyD88 and heterotypic MyD88-IRAK4 interactions (47). Those mutations affected MyD88-dependent responses differently depending on the TLR, indicating that TLRs might have maintained receptor-specific signalling via the formation of distinct Myddosome complexes. Before the Myddosome structure was resolved it was well established that IRAK4 was essential in the MyD88-dependent pathways (48), but the exact role of IRAK2 was less clear and it was thought to have a redundant role with IRAK1 (49). Upon recruitment to the receptor, IRAK4 most likely phosphorylates both, IRAK1 and IRAK2, initiating their auto- and cross-phosphorylation. IRAK1 is further modulated by Pellino-mediated K63-ubiquitination (50). Both IRAKs subsequently interact with the E3 ligase TNF receptor-associated factor 6 (TRAF6), where IRAK2 promotes TRAF6 polyubiquitination (51). The crucial role of IRAK2 is also indicated by its targeting by a poxviral protein A52 and by recent studies in human cells showing its requirement in proinflammatory gene expression by regulating transcriptional and posttranscriptional events (52, 53). Activated TRAF6 in conjunction with the E2 ubiquitin-conjugating enzymes Ubc13 and Uev1A synthesises K63-polyubiquitin chains, which subsequently recruit the regulatory factors TAK binding proteins 2 and 3 (TAB2/3), leading to autophosphorylation and activation of TGF-β-activated kinase 1 (TAK1) (54, 55). It was recently shown that this activation process is mediated by unanchored, free polyubiquitin chains that are not conjugated to any protein (56). Similarly, the IκB kinase (IKK) complex consisting of IKKγ/NEMO, IKKα and IKKβ gets recruited to polyubiquitin chains via NF-κB essential modulator (NEMO). These polyubiquitin chains are also most likely unanchored and generated by TRAF6 and the E2 enzyme UbcH5c (56). The close proximity of both complexes allows phosphorylation of IKKβ by TAK1, which then phosphorylates the inhibitor of NF-κB (IκB) leading to its ubiquitination and proteasomal degradation (57, 58). This allows the transcription factor NF-κB to translocate to the nucleus. The MAPK pathway is also initiated downstream of MyD88. TAK1 activates the MAPK kinases MKK3/6 and MKK4/7, which subsequently phosphorylate p38 and JNK MAPKs, respectively (57). The MAPKs extracellular signal-regulated kinases 1 and 2 (ERK1/2), on the other hand, are activated via the IKK complex, which phosphorylates p105, a negative regulator of tumor progression locus 2 (Tpl2) (59). Released Tpl2 then activates MKK1/2, the upstream kinases of ERK1/2. Finally, these MAPKs lead to activation of transcription factors, such as activator protein 1 (AP-1) and cAMP response element-binding (CREB) (60). These transcription factors together with NF-κB

subsequently induce the expression of inflammatory cytokines and chemokines. In contrast to the cell surface MyD88-dependent TLRs, endosomal TLR7 and 9, which are also restricted to MyD88, additionally trigger the expression of type I IFNs, mainly IFN-α. In this case, MyD88 forms a complex with IRAK4, TRAF6, TRAF3, IRAK1 and IKKα, where the latter two kinases phosphorylate the transcription factor IRF7, causing its nuclear translocation (61-63). Similar to the other TLRs, NF-κB and AP-1 are activated by the MyD88/IRAK4/TRAF6 signalling axis. IRF5 was also shown to be implicated in inflammatory gene induction downstream of MyD88 and TRAF6 (64).

The TRIF pathway used by TLR3 and TLR4 differs from the MyD88 pathway in signalling molecules that are initially recruited to activate NF-κB and MAPKs, and TRIF activates an additional signalling arm to induce IFN-β expression through the transcription factor IRF3. Interestingly, TRIF initiates two separate pathways to activate TAK1. On the one hand, TRIF recruits TRAF6 directly via its N-terminal TRAF6-binding motif, which activates TAK1 and subsequently NF-κB and MAPKs by a similar mechanism as described for the MyD88-dependent pathway. On the other hand, TAK1 activation is mediated by receptor-interacting protein 1 (RIP1), which is recruited to the C-terminus of TRIF through a RIP homotypic interaction motif (RHIM) (65). This activation requires K63-polyubiquitination of RIP1, which involves the adaptor TNF-receptor 1-associated death domain (TRADD) and the E3 ligase Pellino-1 (66-68). For activating the IRF3 pathway, TRIF initially recruits TRAF3, which activates the noncanonical IKKs, TBK1 and IKKε (IKKi), leading to phosphorylation and nuclear translocation of IRF3 (69). (reviewed in (70))

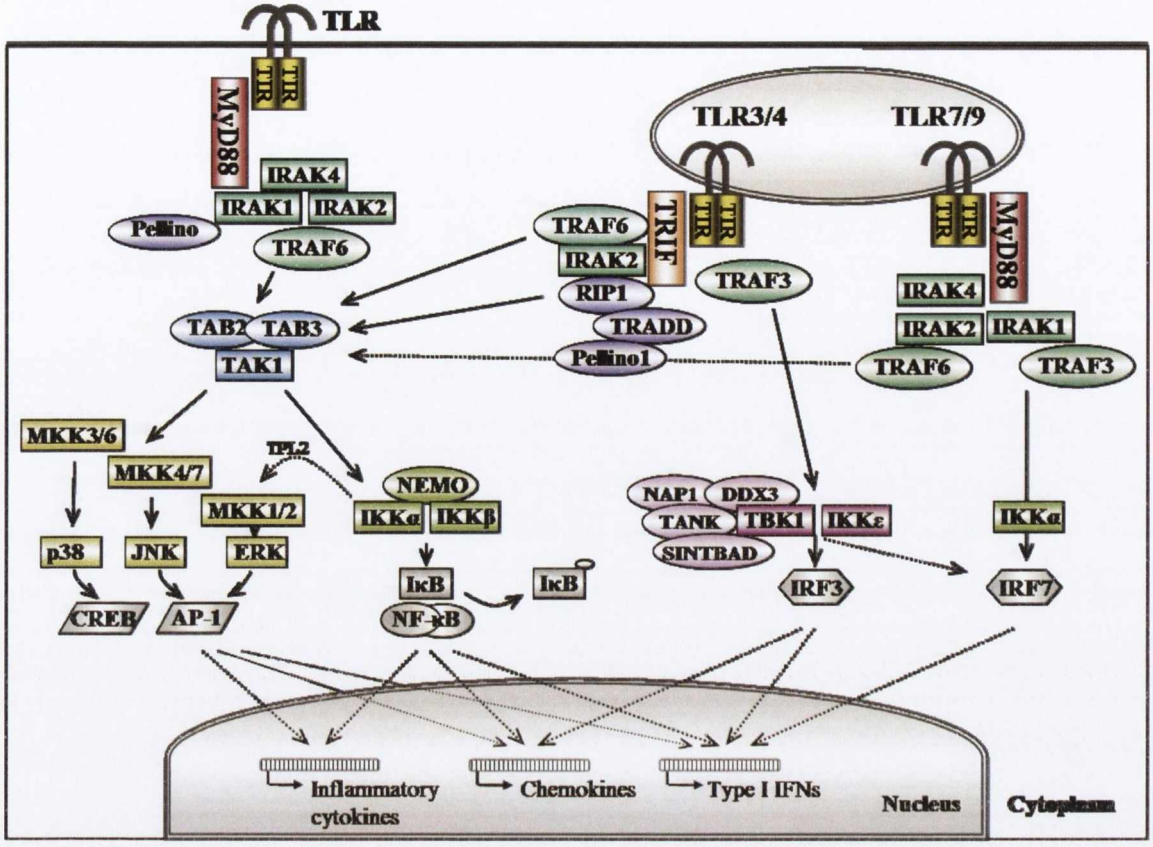


Figure 1.2: Overview of TLR signalling pathways

After the recruitment of MyD88 to the TIR domain interface of the receptor, IRAK4, 1 and 2 get recruited and subsequently activate TRAF6, which synthesises K63-polyubiquitin chains. TAB2/3 in complex with TAK1 and NEMO in complex with IKKα and IKKβ get recruited to most likely free ubiquitin chains, followed by activation of the IKKs by TAK1. IKKs then induce phosphorylation and degradation of IκB, which releases NF-κB to translocate into the nucleus and induce proinflammatory cytokines. TAK1 also activates p38 and JNK MAPKs via MKK3/6 and MKK4/7, respectively. The MAPKs ERK1/2 are activated by the IKK complex via TPL2 and MKK1/2. MAPKs then activate the transcription factors AP-1 and CREB. Besides the common TRAF6-mediated TAK1 activation, the TRIF-pathway can activate TAK1 also via ubiquitinated RIP1. Specific to endosomal TLRs is the ability to initiate IRF pathways and the expression of type I IFNs. This involves TRAF3, which in the case of TRIF-dependent TLR3 and TLR4 activates the noncanonical kinases TBK1 and IKKε to activate IRF3 and IRF7, or in the MyD88-dependent TLR7, 8 and 9 signalling activates IRF7 by IRAK1- and IKKα-mediated phosphorylation.

A general theme has emerged, that besides the selective PAMP/TLR and TLR/TIR adaptor interaction, the subcellular localisation of TLRs also determines the specific signalling cascade that is initiated (71). Endolysosomal compartments in particular seem to provide a specific platform for signalling to IRF transcription factors to induce the expression of type I IFNs. At the same time cell surface TLRs are unable to transduce a

signal for IFN expression. Only the internalisation of plasma membrane-associated TLR4 allows its signalling to IRF3 via the TRAM/TRIF-TRAF3 pathway (38). The current explanation for this phenomenon is the restricted accessibility of TRAF3 at endosomal compartments and not at the plasma membrane. A similar mechanism seems to apply for TLR2, which was recently described to secrete low amounts of IFN-β after internalisation and signalling via the MyD88-IRF1/7 pathway (72).

Even though TLRs are widely expressed among immune cells, there is some cell type specificity. Endosomal TLRs in particular are differently expressed among DC subsets; plasmacytoid DCs (pDCs), for example, express TLR7 and 9, but not TLR3 or 8, and produce high amounts of type I IFNs upon activation, which is related to their important role in antiviral immunity (73). Interestingly, TLR7 and TLR9 activation in conventional DCs and macrophages favours the induction of inflammatory cytokines, rather than type I IFNs, which relies on the spatiotemporal signalling from endolysosomal compartments (74).

1.2.2 C-type lectin receptors (CLRs)

The C-type lectin receptors (CLRs) are a group of PRRs also found on the plasma membrane, which belong to a superfamily of proteins containing the characteristic C-type lectin-like domain (CTLD) (75). The C-type lectin domain was originally described in Ca^{2+}-dependent (C-type), carbohydrate-binding (lectin) proteins; however a similar domain structure was soon identified in proteins that recognised other ligands, such as proteins and lipids. According to domain architecture and phylogeny the superfamily was soon divided into 17 groups, with members performing highly diverse functions as soluble and transmembrane proteins. Some signal-generating, type II transmembrane CLRs emerged to have important roles in innate and adaptive immunity. In response to specific pathogens they activate signalling pathways leading either to gene expression directly or to modulation of other PRR-induced responses (76). These CLRs are predominantly expressed on myeloid cells and specialised to sense fungal infection, but also have a role in detecting viruses, mycobacteria and helminths. Most of the recognised PAMPs are carbohydrates, such as mannose, glucan and fucose. Some receptors also sense endogenous ligands and are implicated in homeostasis (77).

The CLRs which are able to induce gene expression independently of other PRRs signal via specific cytoplasmic immunoreceptor tyrosine-based activation motifs (ITAMs) that consist of dual YxxL sequences to recruit the adaptor spleen tyrosine kinase (Syk). Most of these CLRs, like DC-associated C-type lectin 2 (Dectin2), macrophage-inducible C-type lectin (Mincle) and myeloid DAP12-associating lectin-1 (MDL-1), lack their own cytoplasmic signalling domain and instead associate with ITAM-containing adaptor proteins, like the Fc receptor γ (FcRγ) chain and DNAX-activating protein (DAP10/12). Upon ligand recognition, the ITAM gets phosphorylated at two tyrosines by Src kinases, which creates a docking platform for Syk. In contrast, the CLR Dectin1 itself contains a single tyrosine ITAM-like motif in its cytoplasmic tail, referred to as hemITAM. In this case, Syk likely binds to a dimer of two monophosphorylated Dectin1 proteins (78). Different signalling pathways are activated downstream of Syk, which vary depending on the receptor and the cell type.

Nevertheless, Dectin1 signalling has become a paradigm for Syk-coupled CLRs (Figure 1.3). Dectin1 specifically recognises β-1,3-linked glucans of fungal cell walls, as well as mycobacteria (79, 80). One major pathway downstream of Syk leads to activation of canonical NF-κB via a complex containing caspase recruitment domain-containing protein 9 (CARD9), B cell lymphoma 10 (Bcl10) and mucosa-associated lymphoid tissue lymphoma translocation protein 1 (Malt1) (81). This complex subsequently activates the IKK complex, which leads to IκB phosphorylation and release of NF-κB. Syk also initiates a noncanonical NF-κB pathway independently of CARD9 via NF-κB-inducing kinase (NIK) and IKKα to induce RelB-p52 dimer nuclear translocation (82). This RelB-p52 dimer inhibits transcription of certain cytokines, such as IL1-β. In addition, Syk mediates the activation of MAPKs, phosphoinositide 3-kinase (PI3K) and nuclear factor of activated T cells (NFAT) (83-85), and is implicated in reactive oxygen species (ROS) production that also activates the NLRP3 inflammasome (86). Finally, Dectin1 couples to a Syk-independent pathway through the kinase Raf-1 to modulate NF-κB activity. Raf-1 leads to Ser276-phosphorylation of the Syk-activated NF-κB subunit p65, which promotes binding of the acetyltransferases CREB-binding protein (CBP) and p300 followed by acetylation of p65 and enhanced transcriptional activity. P65 also forms a dimer with RelB, which cannot bind DNA, hence sequesters RelB from the functional RelB-p52 complex. Overall, this modulates Syk-dependent cytokines expression and shapes T_h1/T_h17 adaptive immune responses (82, 87). In fact, Syk-coupled CLRs, such as Dectin1 and Dectin2, were shown

to be non-redundant for the induction of T_h17 responses to fungal infections like *Candida*, which has emerged to be an essential response for antifungal immunity (85, 88, 89). But they also induce T_h1 responses and in cooperation with other PRRs (e.g. TLRs) lead to effective clearance of the pathogen.

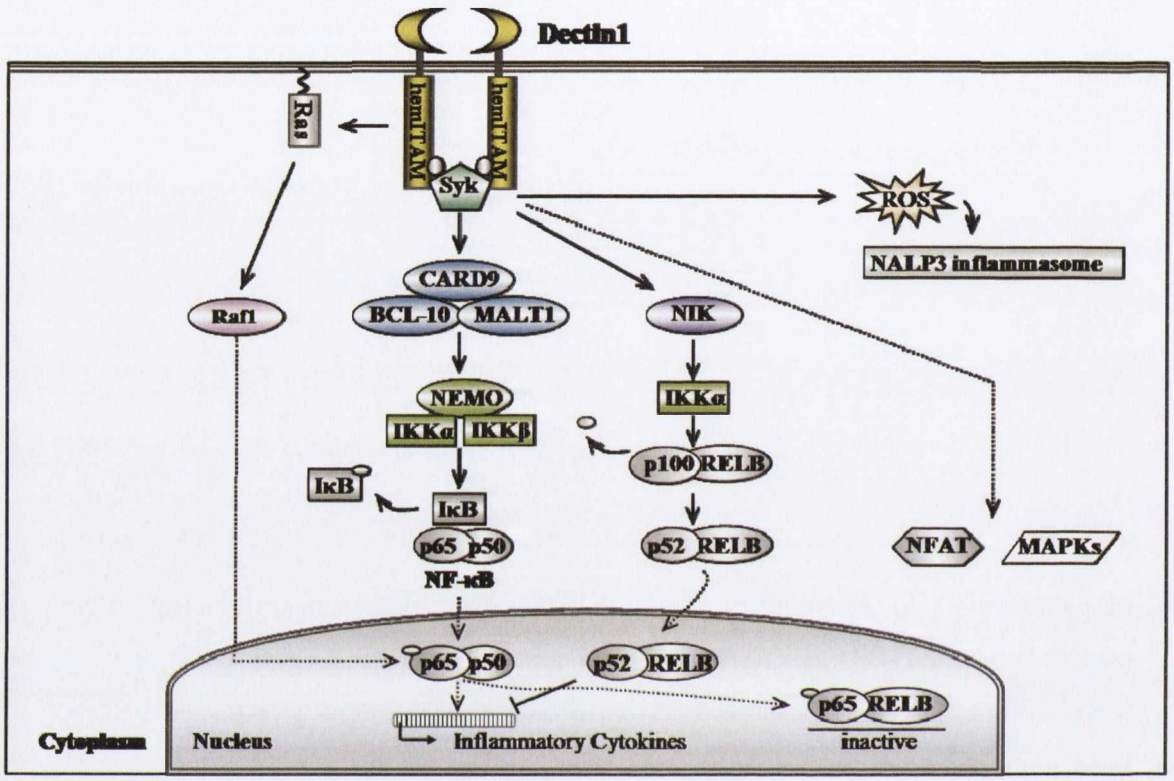


Figure 1.3: Dectin1 signalling

Upon ligand recognition, Dectin1 forms homodimers and gets monophosphorylated at its hemITAM motif, which recruits the kinase Syk that subsequently activates a complex of CARD9, BCL-10 and MALT1. This leads to activation of the IKK complex NEMO/IKKα/IKKβ, followed by phosphorylation and degradation of IκB and the release of NF-κB to the nucleus to induce proinflammatory cytokines. In parallel Syk activates a noncanonical NF-κB pathway, where NIK and IKKα induce processing of p100 to p52, forming a p52-RelB dimer that inhibits the transcription of some cytokines. Syk is also implicated in the activation of the NALP3 inflammasome via the induction of ROS. A Syk-independent, Ras/Raf1-dependent pathway leads to Ser276-phosphorylation of active p65, which enhances its transcriptional activity and impairs RelB activity by interacting with it.

A different group of signal-generating CLRs is unable to induce gene expression by themselves, but rather modulates the responses of other PRRs. These CLRs include DC-specific ICAM3-grabbing non-integrin (DC-SIGN), DC immunoreceptor (DCIR), myeloid C-type lectin-like receptor (MICL) and blood DC antigen 2 protein (BDCA2), which

mostly initiate a Syk-independent signalling cascade directly through their cytoplasmic domain. The exception is BDCA2, which similar to Dectin2 and Mincle couples to the FcRγ chain and Syk and causes inhibition of TLR-induced cytokines possibly via a mechanism involving Ca^{2+}/calcineurin (90). DC-SIGN was shown to modulate TLR4-induced immune responses via the Raf1/p65 axis, as described for Dectin1. In this case, Raf1 activation was mediated by small GTPase proteins and various kinases (91). The two CLRs DCIR and MICL contain a specific inhibitory cytoplasmic domain, immunoreceptor tyrosine-based inhibitory motif (ITIM), which gets phosphorylated after ligand binding to recruit the phosphatases SH2-domain-containg protein tyrosine phosphatase 1 or 2 (SHP1/2). This subsequently inhibits other PRR-induced cytokine responses (92, 93).

CLR	Signalling motif	Major ligand
CLRs, that directly induce gene expression (Syk-dependent)		
Dectin1	hemITAM	**β-1,3-glucan**: fungi, mycobacteria
Dectin2	ITAM (FcRγ)	**High mannose, α-mannans**: fungi, mycobacteria, house dust mite allergen, helminth *S. mansonii* egg extract
Mincle	ITAM (FcRγ)	**α-mannose** (fungi), **glycolipid** trehalose-6,6-dimycolate (mycobacteria), endogenous ribonucleoprotein SAP130 (dead cells)
MDL-1	ITAM (DAP10/12)	Dengue virus
CLRs, that modulate immune responses of other PRRs		
DCIR	ITIM	**Mannose, fucose**: virus HIV-1
MICL	ITIM	?
DC-SIGN	?	**High mannose, fucose**: fungi, mycobacteria, virus (HIV-1, measles virus, dengue virus, SARS coronavirus, filoviruses), helminth *S. mansonii* egg antigen, peanut allergen Ara h1, Tick saliva protein Salp15
BDCA-2	ITAM (FcRγ)	**Mannose, fucose**

Table 1.2: Selection of signal-generating CLRs relevant in innate and adaptive immunity

Another important function of CLRs is the induction of phagocytosis and effective antigen presentation. The selective expression of CLRs by DC subsets and their ability to dictate MHC class I and class II presentation and adaptive immune responses makes them interesting targets for vaccination strategies (94, 95).

1.2.3 RIG-I-like receptors (RLRs)

Since almost all cell types can potentially be infected by intracellular pathogens like viruses and bacteria that enter the cytosol and use the host cell machinery for their replication, cells have also evolved a broad cytosolic detection system. A family of cytosolic receptors, that specifically recognises microbial RNA, are the RIG-I-like receptors (RLRs). They are mostly activated during viral infection hence they are potent inducers of antiviral immune responses via the expression of type I IFNs. The RLR family consists of three members: retinoic acid-inducible gene I (RIG-I), melanoma differentiation-associated gene 5 (MDA5) and laboratory of genetics and physiology 2 (LGP2) (96). They are ubiquitously expressed and also further inducible by IFNs. RIG-I and MDA5 share a similar domain structure, composed of two N-terminal caspase activation and recruitment domains (CARDs) required for downstream signalling, a central DExD/H-box RNA helicase domain with the capacity to hydrolyse ATP and a C-terminal domain (CTD). LGP2, however, lacks the CARD domains and therefore the signalling function.

Unlike nucleic acid-sensing TLRs, which are sequestered in the endosomal compartment, RLRs are cytosolic and surrounded by various host RNAs, which raises the question how RLRs discriminate between self- and nonself-RNA. Intense studies revealed that RIG-I and MDA5 indeed sense specific molecular features of nonself, microbial RNA that are usually absent in host RNA. Both receptors exhibit ligand specificity and complement each other by sensing a distinct set of RNA viruses, besides some overlap. RIG-I was initially identified due to its IFN response to cytosolic Poly(I:C), however later studies found that MDA5 was more responsive to Poly(I:C) (97, 98). This was later explained by the fact that both receptors respond to dsRNA, such as Poly(I:C), but with different dependency on length (99). While MDA5 recognises long dsRNA molecules, RIG-I detects small dsRNA fragments preferential blunt-ended and as short as 23bp (100). This preference might also explain the specificities in ssRNA virus detection. MDA5, for example, senses picornaviruses like EMCV, Mengo virus and Theiler's virus, whereas RIG-I detects members of the Paramyxoviridae (e.g. Sendai virus, RSV), Rhabdoviridae (e.g. VSV), Orthomyxoviridae (influenza A/B) and many others. However, a subset of viruses is sensed by both, like the Flaviviruses dengue virus, WNV and Japanese

encephalitis virus (JEV) and reovirus. Short, uncapped 5'-triphosphate (5'ppp) ssRNA with small regions of base pairing present in some viruses and in vitro-transcribed RNA serves as a potent RIG-I ligand. This provides self/nonself discrimination, as host transcripts are usually "capped" with a 7-methyl-guanosine group at the 5'end (101-103). Also some sequence compositions, like PolyU-rich motifs, probably mark the viral RNA as nonself (104). During infection, further RIG-I ligands are generated by RNA polymerase III (Pol III), which converts intracellular pathogenic AT-rich dsDNA into 5'ppp dsRNA (105, 106), and by endoribonuclease RNase L, which cleaves microbial and endogenous RNA to trigger MDA5 and RIG-I (107). The third member, LGP2, is also able to bind RNA however the functional consequences are still not fully understood. While LGP2 was originally thought to negatively regulate RLR signalling by sequestering viral dsRNA or inhibiting RIG-I multimerisation (108, 109), it was later demonstrated that LGP2 facilitated viral RNA recognition by RIG-I and MDA5 through its ATPase domain, while it was dispensable for the detection of synthetic RNA ligands, such as Poly(I:C) (110). A different role for LGP2 was recently described in promoting antigen-specific $CD8^+$ T cell survival during RNA virus infection (111).

It was long unclear how RLRs bind their ligands, as none of the helicases contain a classical RNA-binding motif. The CTD was shown to be involved in RNA recognition, and in the case of RIG-I a large, positively charged cleft in the CTD was required for 5'ppp dsRNA-binding (112, 113). Recent structural analysis provided detailed insights on the ligand-binding and activation mechanism of RIG-I (114). In the absence of a RNA ligand, RIG-I is held in an autorepressed conformation with the CARDs sequestered by the helicase subdomains and not available for signalling. Initial binding of RNA to CTD is followed by cooperative tight binding of ATP and RNA to the helicase domain, which leads to a conformational change pushing the CARDs out of the complex, allowing subsequent modifications and downstream signalling. It was previously shown that the ATPase activity of RIG-I was dependent on dsRNA-binding (115). The now accessible CARDs are subsequently modified by K63-linked polyubiquitin chains via the E3-ligase tripartite motif-containing 25 (TRIM25), and free ubiquitin chains were required for RIG-I activity and the recruitment of the signalling adaptor mitochondrial antiviral signalling (MAVS, also known as IPS-1, VISA, Cardif), leading to homotypic CARD-CARD interaction with the RLR (116, 117). The protein 14-3-3ε is also involved in the stable RIG-I-TRIM25 interaction and the redistribution to the mitochondrial membrane (118).

Although the overall regulatory mechanism of MDA5 might differ and probably involve LGP2, it was recently shown that unanchored K63 polyubiquitin chains also played a role in MDA5 activation (112, 119). This study also demonstrated that the ubiquitin chains induced oligomerisation of RIG-I, which might mediate the aggregation of MAVS at the mitochondrial membrane (120).

The adaptor protein MAVS is anchored with its C-terminus to the outer membrane of mitochondria and peroxisomes, while the N-terminal CARD domain is accessible for the recruitment of activated RLRs (121, 122). Similar to endosomal TLRs, the location provides a platform for the accumulation of distinct signalling molecules leading to formation of the "MAVS signalosome". Binding of RIG-I or MDA5 to mitochondrial MAVS initiates different signalling pathways that, similar to TLRs, activate the key transcription factors NF-κB and IRFs to induce cytokines, chemokines and type I IFNs (Figure 1.4). A recent study suggested that particularly the mitochondrial MAVS is essential for establishing an antiviral state by inducing a strong type I IFN response, while the peroxisomal MAVS specifically functions in the early expression of IFN-independent viral defence genes, possibly involving the transcription factor IRF1 (122). Signalling of mitochondrial MAVS involves the adaptor TNF receptor 1-associated death domain protein (TRADD). TRADD initiates the IRF3 pathway by recruiting TRAF3 to activate TBK1- and IKKε-containing complexes, which consist also of the adaptor proteins TRAF family member-associated NF-κB activator (TANK), NF-κB-activating kinase-associated protein 1 (NAP1), similar to NAP1 TBK1 adaptor (SINTBAD) and DEAD box protein 3 (DDX3) to finally activate IRF3 and IRF7 and the expression of type I IFNs (123, 124). Only recently it was shown that NEMO is involved in recruiting TBK1 to MAVS via binding to K63 polyubiquitin associated with TBK1 (125). TRADD, alongside with TRAFs like TRAF6, 2 and 5, also initiate the proinflammatory NF-κB pathway by assembling Fas-associated death domain protein (FADD) and RIP1, leading to activation of the IKK complex, consisting of NEMO, IKKα and IKKβ and subsequent nuclear translocation of NF-κB due to phosphorylation and degradation of the inhibitor IκB. Further signalling modules were described to be involved in NF-κB activation, such as a complex formed of FADD and caspase-8/10 and a signalling axis mediated by MAVS-CARD9-Bcl10 (126, 127). Recently, several membrane-associated regulators of RLR signalling were identified. Among them, the transmembrane protein stimulator of IFN genes (STING, also known as MPYS, MITA) was shown to interact with RIG-

I/MAVS/IRF3 and to be important in the RIG-I pathway, while it was dispensable for MDA5-mediated responses (128). STING is preferentially expressed in the ER membrane, but its exact subcellular location is controversial and STING may also be present at the outer mitochondrial membrane. Also the mitochondrial membrane protein translocase of outer membrane 70 (TOM70) was reported to link TBK1 and IKKε to MAVS (129). Finally, it is worth mentioning, that RNA virus-activated RIG-I is also able to form an inflammasome with apoptosis-associated speck-like protein containing a CARD (ASC) to activate casapase-1-dependent maturation of the cytokines IL-1β and IL-18, thus triggering an important pathway of the inflammatory response (see 1.2.5 for details) (127).

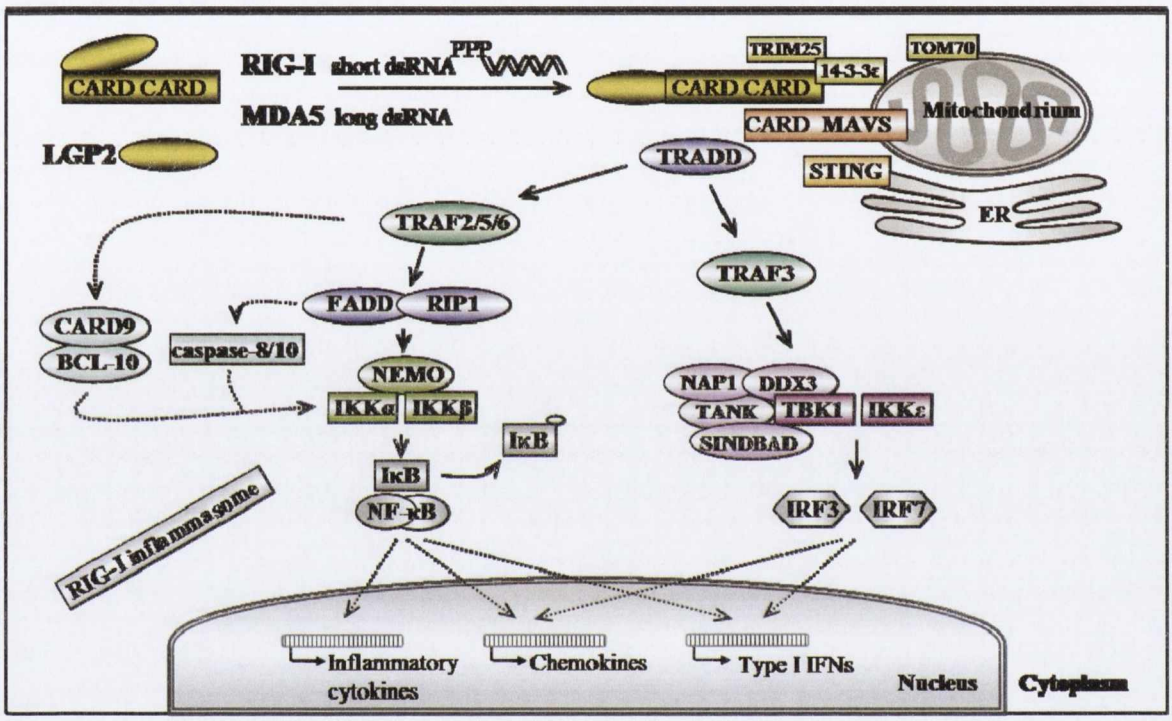


Figure 1.4: RLR signalling

Upon ligand recognition, RIG-I and MDA5 bind via homotypic CARD-CARD interaction to MAVS localised at the outer mitochondrial membrane. This induces the recruitment of TRADD and initiates the NF-κB pathway via TRAF proteins, including TRAF6, to subsequently activate the IKK complex and NF-κB translocation. The transcription factors IRF3 and IRF7 are activated via the TRAF3-dependent TBK1/IKKε-axis. The RIG-I-induced IRF3 pathway also requires the ER protein STING. RIG-I is also able to form an inflammasome to initiate a robust inflammatory response.

Other cytosolic dsRNA-binding proteins have also been implicated in type-I IFN production, but their role as true receptors is questionable, as they might possess more

auxiliary functions in RLR-mediated responses. The dsRNA-dependent protein kinase (PKR) amplifies IFN-β expression during viral infection, but it is not clear whether this is mediated via the RIG-I-MAVS-dependent complex (130). It was recently revealed that PKR enhanced NF-κB activity indirectly by phosphorylating eukaryotic translation initiation factor eIF-2α, which subsequently inhibits translation and thus resynthesis of the NF-κB inhibitor IκB (131). Members of the DExD/H-box family were also implicated in cytosolic responses to dsRNA in myeloid DCs. DHX9 was shown to bind Poly(I:C) and mediated downstream signalling via MAVS (75), while a complex composed of DDX1, DDX21 and DHX36 was demonstrated to initiate type I IFN expression via the adaptor TRIF (132). Their role in relation to RLRs needs to be defined, but as they are constitutively expressed it is possible that they mediate the initial IFN production, before the IFN-induced RLRs come into play.

1.2.4 Cytosolic DNA receptors

Alongside the above described cytosolic RNA receptors, many immune and non-immune cells also express a complementary system of DNA sensing molecules in the cytosol. Both types of nucleic acid sensors are particularly important to recognise infection with RNA and DNA viruses and to establish an effective antiviral defence programme mainly via expression of type I IFNs and subsequent induction of IFN-stimulated genes (ISGs). But they also mount proinflammatory immune responses and are involved in detecting intracellular bacteria. In immune cells, this cytosolic nucleic acid detection system exists in parallel to the endosomal TLRs, although the expression of the proposed DNA sensors varies depending on the cell type. It has long been known that cytosolic delivery of dsDNA can trigger immune responses, independent of the endosomal TLR9 (133, 134). However, only recently these cytosolic DNA sensors are being identified. Up to now, several cytosolic DNA receptors have been implicated in triggering type I IFN production (see Figure 1.5): DNA-dependent activator of IRFs (DAI, ZBP1), RNA Polymerase III (Pol III), leucine-rich repeat flightless-interacting protein 1 (LRRFIP1), the ALRs IFNγ-inducible protein 16 (IFI16) and the related murine protein p204, Ku70 and proteins of the DExD/H-box helicase superfamily, including DHX9, DHX36 and DDX41 (135). On the other hand, two members of the ALR family are involved in DNA-mediated inflammasome activation, absent in melanoma 2 (AIM2) and IFI16 (136). In contrast to

RLRs, DNA sensors seem to be less selective regarding the type of DNA and mainly require a certain length of the dsDNA molecule. But they are expressed in a cell type-specific manner, where they activate distinct pathways and responses, and not all are directly involved in gene expression. Before identification of the first DNA sensor, it was shown that most cytosolic DNA-induced type I IFN responses required TBK1 and IRF3 (134, 137). Later the endoplasmic reticulum-resident, transmembrane protein STING was identified as a crucial adaptor in the cytosolic DNA response upstream of the TBK1-IRF3 axis (128). In addition to its adaptor function, STING was recently found to directly sense and respond to cyclic diguanylate monophosphate (c-di-GMP), which is a second messenger molecule specific to bacteria (138). The first identified DNA receptor upstream of STING was DAI, which mediated IFN-β gene expression in L929 cells following dsDNA detection via its Z-DNA and putative B-DNA binding domains (139). DAI was found to interact with TBK1 and IRF3 and recruited RIP1/3 via additional RHIM domains to activate NF-κB (140, 141). However, *Dai*-knockout mice and knockout cells, such as mouse embryonic fibroblasts (MEFs) and macrophages, responded normally to DNA, which suggested a redundant and possibly cell type-specific function of DAI (142). IFI16 and its related mouse protein p204 were discovered as critical DNA receptors for induction of IFN-β in response to viral DNA and HSV-1 infection in human and murine immune cells (143). IFI16 is a member of the PYHIN protein family, containing a pyrin and two HIN domains. The HIN domain was shown to directly bind viral DNA via non-sequence-specific, electrostatic interactions (143, 144). IFI16 colocalised with transfected 70bp-dsDNA from vaccinia virus in the cytosol, recruited STING and initiated IRF3 and NF-κB nuclear translocation and gene induction. However, during HSV-1 infection the mainly nuclear protein IFI16 detected pathogenic DNA in the nucleus, and it was shown that IFI16 cellular distribution is controlled by acetylation of its nuclear localisation signal (145). Two members of the DExD/H-box helicase family, DHX9 and DHX36, were also proposed as cytosolic DNA sensors which mediated NF-κB and IRF7 activation, respectively, in response to CpG DNA in plasmacytoid DCs (pDCs) (146). Both receptors initiated downstream signalling through interaction with the TIR domain of MyD88, which was consistent with the previous observation that DNA responses in pDCs were entirely MyD88-dependent, including the endosomal TLR9. DDX41 was recently identified as another member of the DExD/H-box helicase family that played a role in cytosolic DNA detection and gene induction in myeloid DCs and human monocytes (147). Similar to

IFI16, DDX41 induced NF-κB and IRF3 transcription factors via the adaptor STING. The constitutively expressed DDX41 may regulate the early burst of type I IFN expression, but requires amplification by IFN-induced IFI16 later on in the response. A different pathway is activated following DNA detection by Ku70, which activates the transcription factors IRF1 and IRF7 leading to induction of type III IFN (IFN-λ1), rather than type I IFNs (148). Two other cytosolic DNA-sensing molecules were found to be more indirectly involved in gene expression. LRRFIP1 contributed to IFN-β gene induction in response to cytosolic dsDNA and dsRNA by initiating a β-catenin-dependent coactivator pathway (149). LRRFIP1 was not required for NF-κB and IRF3 activation, but triggered β-catenin phosphorylation, which subsequently recruited p300 to the IFN-β enhanceosome via IRF3. Furthermore, the DNA-sensing molecule Pol III did not directly initiate downstream signalling, but rather generated a ligand for RIG-I by converting AT-rich dsDNA, such as Poly(dA:dT), into 5'-triphosphate-containing dsRNA (105, 106). This explains why the adaptor MAVS was found to be involved in some DNA responses, as observed for Poly(dA:dT)-stimulated human embryonic kidney (HEK) 293 cells (134). It was noted that besides the transcriptional response, dsDNA also triggered maturation of the inflammatory cytokines IL-1β and IL-18, which is known to be mediated by caspase-1-dependent inflammasomes (150) (described in 1.2.5). AIM2 was identified as the DNA sensor that subsequently interacted with the adaptor ASC followed by caspase-1 recruitment to form an "AIM2 inflammasome" (151-154). AIM2 belongs like IFI16 and p204 to the PYHIN protein family. Crystallographic studies recently proposed that AIM2 forms an autoinhibitory complex between its pyrin and HIN domain in the basal state, which gets released after dsDNA-binding to the HIN domain, facilitating homotypic interaction of the pyrin domain with ASC (144). Also the DNA receptor IFI16, which mediates cytokine and type I IFN gene expression (as described above) was shown to have the potential of forming an inflammasome. IFI16 interacted with ASC and caspase-1 after detecting DNA of Kaposi's sarcoma-associated herpesvirus (KSHV) in the nucleus of endothelial cells (155). The "IFI16 inflammasome" was initially detected in the nucleus, but relocated to the perinuclear area later on in the response. The DNA-sensing PYHIN proteins, including AIM2, IFI16 and p204, form a new family of PRRs, termed AIM2-like receptors (ALRs) (135).

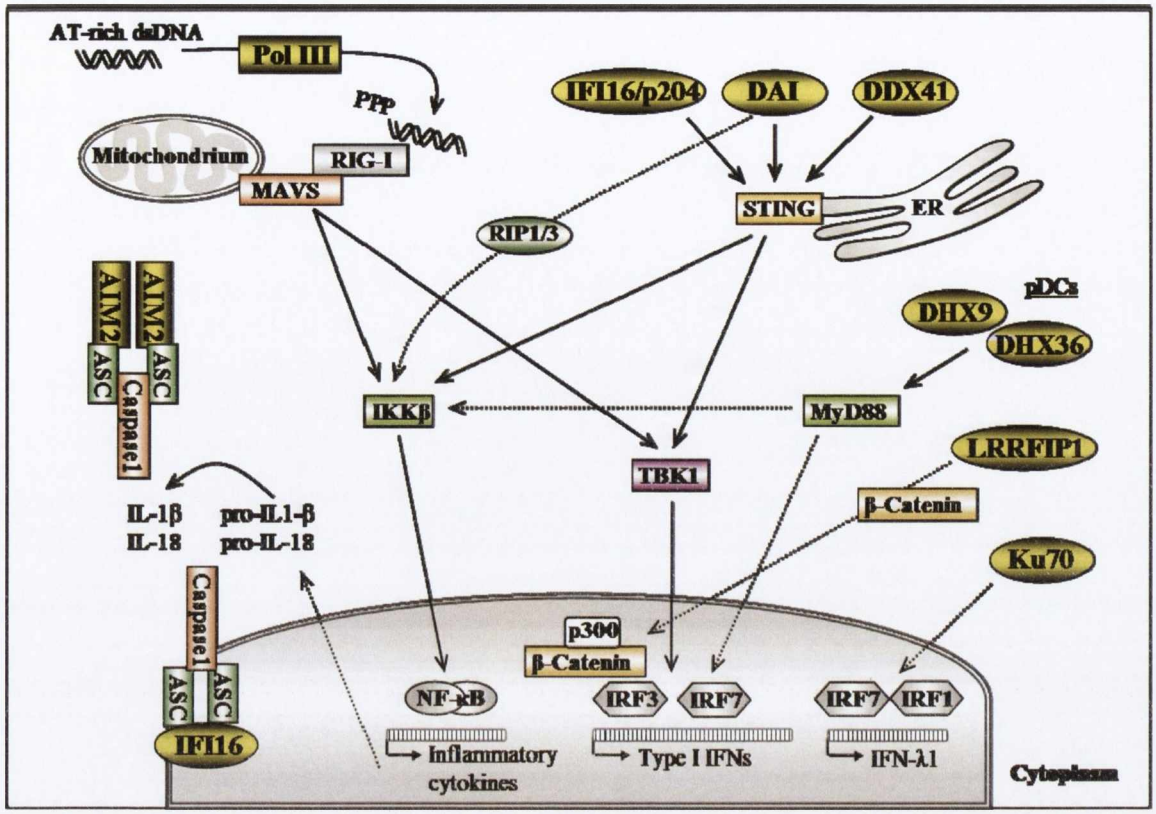


Figure 1.5: Overview of cytosolic DNA receptors and their signalling pathways

The expression profile of DNA sensors is highly cell type-specific. Upon DNA recognition, DAI, IFI16 and the mouse protein p204 and DDX41 signal via STING to trigger TBK1/IRF3-dependent type I IFNs. They also induce a proinflammatory response through the transcription factor NF-κB, which in the case of DAI is mediated via RIP1/3. In pDCs, cytosolic DNA is sensed by DHX9 and DHX36, which subsequently signal via MyD88 to activate NF-κB and IRF7, respectively. The coactivator pathway LRRFIP1 enhances type I IFN responses by activating β-catenin and facilitating p300 recruitment to IRF3. Ku70 selectively drives IFN-λ1 expression via activation of IRF1 and IRF7. Pol III does not directly induce signalling, but converts AT-rich dsDNA into 5'-triphosphate dsRNA, which signals through RIG-I to activate TBK1 and NF-κB. Cytosolic, DNA-activated AIM2, on the other hand, forms an inflammasome with ASC and caspase-1 to convert inactive pro-IL1-β and pro-IL-18 into their bioactive forms. IFI16 is also implicated in inflammasome formation in the nucleus.

It is worth mentioning, that unlike most other PRRs which are selectively activated by microbial ligands, cytosolic DNA sensors potentially respond to self and non-self DNA. Compartmentalisation is probably one mechanism to avoid autoimmune reactions, as the cytoplasm is usually DNA-free and only infection or tissue damage would result in the appearance of cytosolic DNA and initiate a response. Thus cytosolic DNA receptors are probably more sensors of "danger" (any mislocated, naked DNA) rather than "stranger"

(microbial DNA) (135). As IFI16 also responds to foreign DNA in the nucleus, it is likely that specific control mechanisms prevent detection of genomic DNA, such as the formation of DNA-protein complexes in chromatin. A second mechanism is provided by deoxyribonucleases (DNases), which are present at various locations to avoid accumulation of DNA from apoptotic and necrotic cells. DNase I, for example, is found in the extracellular space and serum, while DNase II degrades DNA in lysosomes and thus has an important role in clearance of engulfed DNA in macrophage phagosomes. A cytosolic ER-associated DNase III, termed three prime repair exonuclease 1 (TREX1), was shown to be important to digest reverse-transcribed ssDNA intermediates from endogenous retroelements (156). Mutations in these enzymes are linked to autoimmune diseases, such as systemic lupus erythematosis (SLE) and Aicardi-Goutières syndrome (AGS), which are driven by self-DNA recognition and massive type I IFN production (157-159).

1.2.5 NOD-like receptors (NLRs)

The nucleotide-binding-and-oligomerisation domain (NOD)-like receptors (NLRs) are a family of cytosolic proteins that drive inflammation in response to various microbial molecules (PAMPs) or endogenous danger signals following tissue damage (DAMPs) (see Table 1.3). Therefore, they are also implicated in various human inflammatory disorders. Up to now, 22 NLR genes have been identified in the human genome and at least 34 in mouse (160). They display a tripartite domain structure with a C-terminal LRR domain, a central nucleotide binding domain (NBD) consisting of a NACHT and a NACHT-associated domain (NAD) and an N-terminal effector domain (161). The LRRs are believed to bind directly to specific ligands, which would justify the term "receptor"; however, so far no receptor-ligand interaction has been shown for any NLR. Furthermore some NLRs, like NLRP3 (described below), are activated by such a broad spectrum of stimuli that activation is more likely mediated by an intermediate signalling molecule rather than the specific PAMP or DAMP directly. Engagement of an NLR with its ligand probably induces a conformational change and oligomerisation via the NBD in conjunction with ATP hydrolysis (162). Downstream signalling molecules are then recruited by the N-terminal domain, which differs among NLRs dividing them in subfamilies: NLRAs contain an N-terminal acidic activation domain (AD), NLRBs a baculovirus inhibitor repeat (BIR) domain, NLRCs a CARD and NLRPs a pyrin domain (PYD); with the latter two

representing most NLRs. Also there are some NLRs with an undefined domain, grouped in the NLRX subfamily.

Some NLRs were intensely studied due to their role in the posttranslational inflammatory response (163). NLRP1, NLRP3 and NLRC4 form a large protein complex, known as the "inflammasome", into which inactive pro-caspase-1 is recruited via homotypic CARD-CARD interaction and activated by proximity-induced autoproteolytic cleavage. NLRP1 contains a CARD in addition to its PYD, thus NLRP1 and NLRC4 are able to activate caspase-1 directly. Other inflammasome initiators with a PYD use the adaptor molecule ASC, which consists of a PYD and a CARD domain, to recruit pro-caspase-1. This includes the recently described non-NLRs, PYD-containing proteins AIM2 and in certain cases also IFI16, which form an inflammasome following dsDNA detection (see 1.2.4). Also the RNA sensor RIG-I, which belongs to the RLR family, was shown to assemble an inflammasome, which required ASC even though RIG-I has N-terminal CARD domains (see 1.2.3). The inflammasome-induced active caspase-1 then processes the precursor cytokines pro-IL-1β and pro-IL-18 into their active forms, which are subsequently secreted by a nonclassical pathway that is not completely understood. IL-1β expression requires a priming step, where the pro-form is transcriptionally induced by NF-κB downstream of a different PRR or cytokine pathway. Thus, this two-step activation process allows a tight control of IL-1β secretion to avoid accidental release of the very potent inflammatory mediator, which activates lymphocytes, endothelial cells and recruits immune cells into tissue. Pro-IL-18, on the other hand, is constitutively expressed and its mature form mainly activates NK cells to produce IFN-γ (164). Some inflammasomes require additional NLR proteins. The NLR NOD2 for example was shown to interact with the NLRP1 inflammasome and was required for the response to bacterial muramyl dipeptide (MDP) and lethal toxin of *Bacillus anthracis* in vivo (165). Naip proteins on the other hand were shown to provide a link between bacterial PAMPs with a type III or IV secretion system and NLRC4 activation (166). Naip5 for example binds flagellin of *Legionella pneumophila* and mediates the formation of the NLRC4 inflammasome (167). Many studies focused on the NLRP3 (also known as NALP3) inflammasome due to a broad range of activating stimuli, including many DAMPs, and its role in adjuvanticity. High extracellular ATP concentrations released from dying cells function as a potent endogenous DAMP, which bind to pannexin-1 channel-associated receptor P2X7 leading to potassium (K^+)-efflux and NLRP3 activation (168). K^+-efflux might also mediate the

sensing of microbes with pore-forming toxins or influenza A virus M2 ion channel (169). Also nonmicrobial, crystalline materials were found to activate NLRP3 resulting in inflammatory diseases, such as monosodium uric acid (MSU) crystals in gout, asbestos fibers causing asbestosis and amyloid-beta sensing in Alzheimer's (170-172). Here, crystals probably lead to lysosomal disintegration and cytosolic entry of potential NALP3 activators like cathepsins (173). Also the vaccine adjuvant aluminium hydroxide (alum) is now known to activate NALP3, but as it also increases antigen uptake by DCs, the exact mechanism of promoting adaptive immunity is still under investigation (174). Reactive oxygen species (ROS) were specifically discussed as a common signalling intermediate in NALP3 activation, but this requires further investigation (175). It became apparent that a crucial step prior to NALP3 activation by cellular stress or damage is the NF-κB-dependent transcriptional upregulation of NALP3 in a priming process initiated by receptors, such as TLRs, RLRs, NLRs and cytokine receptors (176). This incorporates an additional control mechanism of IL-1β release.

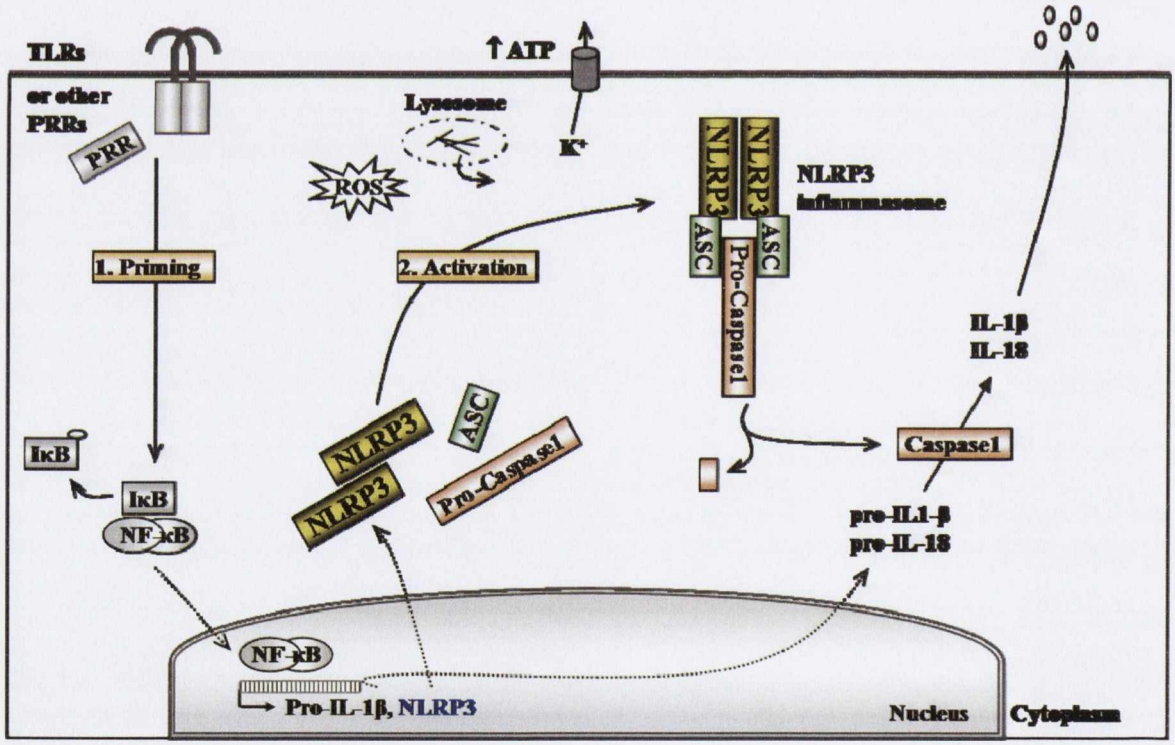


Figure 1.6: Activation process of the NLRP3 inflammasome

The upregulation of NLRP3 in an initial priming step mediated by PRR-induced NF-κB is crucial for its function. This priming also induces the expression of the inactive proinflammatory cytokine pro-IL-1β. NALP3 is activated by various stimuli, such as K^+-efflux caused by high concentration of extracellular ATP or pore-forming toxins, lysosomal disintegration followed by the release of cathepsins and the presence of

ROS. Activated NALP3 oligomerises and recruits the adaptor ASC, which subsequently binds pro-caspase-1, leading to its cleavage and activation. Active caspase-1 catalyses the processing of pro-IL-1β and pro-IL-18 into their bioactive forms that are subsequently secreted.

Besides the posttranscriptional inflammasome activity of some NLRs, other NLRs perform immune functions by inducing gene expression directly. This group includes the NOD1 and NOD2 proteins, which formally belong to the CARD-containing subfamily NLRCs (177). Early after their identification, mutations in NOD2 were associated with familial cases of Crohn's disease and Blau syndrome (178). NOD1 and NOD2 respond to the bacterial peptidoglycan components meso-diaminopimelic acid (DAP) and MDP, respectively, but similar to other NLRs no direct ligand-binding could be demonstrated so far. Both induce a signalling cascade leading to NF-κB and MAPKs activation and subsequent expression of cytokines, chemokines and antimicrobial peptides, such as α/β-defensins (179). Upon stimulation, NOD1 and NOD2 oligomerise and localise to the plasma membrane, where they engage with receptor interacting protein-2 (RIP2) via homotypic CARD-CARD interaction. The subsequent K63-linked polyubiquitination of RIP2 by the E3 ubiquitin ligases inhibitor of apoptosis (IAP) cIAP1 and cIAP2 allows the recruitment of the TAK1-TAB2/3 complex and activation of NF-κB via the IKK complex (180, 181). CARD9 was found to be required for MAPK p38 and JNK activation downstream of NOD2 (182). Also an interaction of NOD2 with the RLR adaptor MAVS was demonstrated, as well as binding to 2'-5'-oligoadenylate synthase type 2 (OAS2), which triggers generation of RIG-I RNA ligands via RNaseL (183, 184). Thus, NOD2 possibly participates in antiviral immune responses via various pathways. NOD1 was also shown to induce type I IFNs in a mouse model of *Helicobacter pylori* infection (185). In contrast, the mitochondria-associated NLRX1 was proposed as a negative regulator of viral RNA-induced IFN responses by interacting with MAVS and preventing RIG-I-binding (186). Another report described a role for NLRX1 in mitochondrial ROS production and amplification of NF-κB and MAPK responses (187).

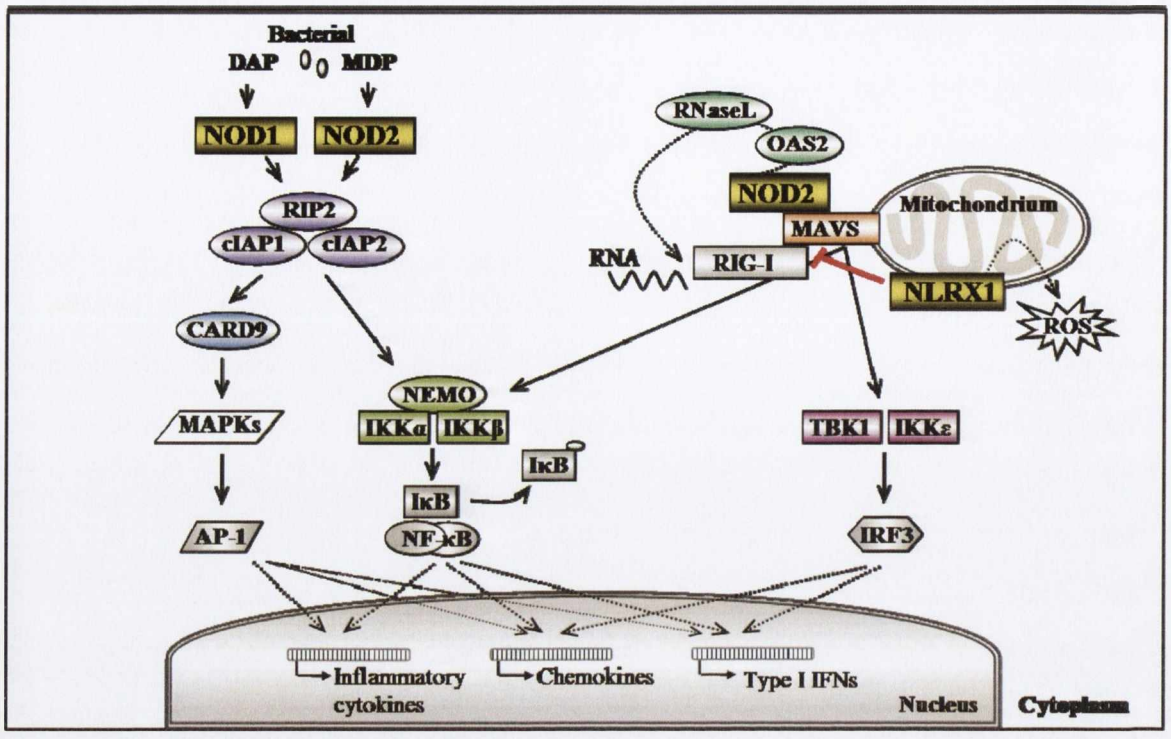


Figure 1.7: NOD1 and NOD2 signalling

After ligand recognition, NOD1 and NOD2 translocate to the plasma membrane, where they engage with RIP2. The E3 ubiquitin ligases cIAP1 and cIAP2 get recruited leading to K63-polyubiquitination of RIP2 and subsequent activation of the IKK complex, followed by phosphorylation and degradation of IκB and the release of NF-κB to the nucleus. CARD9 was found to be involved in p38 and JNK MAPK activation downstream of NOD2. NOD2 was also involved in antiviral immune responses by interacting with MAVS and OAS2. The latter interaction possibly triggers RIG-I signalling indirectly by generating RNA ligands through activation of RNaseL. In contrast, the mitochondrial NLRX1 binds MAVS to inhibit binding of RIG-I and subsequent signal transduction. Also a role for NLRX1 in ROS production was proposed.

Sensor	Stimulus
Inflammasome-forming NLRs	
NLRP1	Peptidoglycan component MDP from bacteria, anthrax lethal toxin of *Bacillus anthracis*
NLRP3	Pore-forming agents (e.g. streptolysin), ion channel (e.g. ATP-binding to P2X7, Influenza virus M2 channel), phagocytosed crystals/particles/protein aggregates (e.g. MSU, hemozoin and cholesterol crystals, asbestos fibers, aluminium salts, amyloid-beta)
NLRC4	Flagellin, components of the type III secretion system (T3SS) of bacteria
Other inflammasome-forming receptors	
AIM2	dsDNA (bacterial, viral, mammalian, synthetic) in the cytosol

IFI16	dsDNA (during KSHV infection) in the nucleus
RIG-I	5'-triphosphate RNA, RNA viruses
Non-inflammasome NLRs	
NOD1	Peptidoglycan component DAP from bacteria
NOD2	Peptidoglycan component MDP from bacteria (also mycobacteria and actinomycetes)

Table 1.3: Inflammasome-forming receptors and a selection of non-inflammasome NLRs

1.3 The IFN system

An important arm of PRR-induced immune responses is mediated by the induction of interferons (IFNs) and their subsequent signalling via IFN receptors, leading to the expression of a wide range of IFN-stimulated genes (ISGs) with immunomodulatory potential. IFN was the first cytokine identified in 1957 by Isaacs and Lindenmann as the secreted factor responsible for the long known phenomenon of "viral interference" (188). Apart from their potent antiviral role, IFNs have also various immunomodulatory functions on the adaptive immune system, on apoptosis and on cell cycle and on many other physiological processes (189). IFNs are divided into three classes: type I IFNs (12 IFN-α subtypes, IFN-β, IFN-ε/κ/ω), type II IFN (IFN-γ) and type III IFNs (IFN-λ1, -λ2, -λ3), which signal via different receptors each composed of two subunits, namely the IFNAR (IFNAR1 and IFNAR2), the IFNGR (IFNGR1 and IFNGR2) and the IFNLR (IFNLR1, IL-10R2), respectively. Type I IFNs are induced by most virally infected cells mainly through nucleic acid-sensing PRRs and modulate many processes via the broadly expressed IFNAR. IFN-γ, on the other hand, is primarily induced by activated T cells and NK cells and activates macrophages to effectively respond to intracellular microbes, but also modulates T cell development. Type III IFNs are a relatively new family that emerged to be functionally related to type I IFNs (190). They are upregulated in a similar manner by TLR agonists and viruses involving the transcription factors IRF3 and IRF7 and induce the same signalling pathways and ISGs. However, the expression of the IFNLR is mainly restricted to epithelial cell types; hence the IFN-λ-mediated responses are not separately discussed here. IFN receptors signal mainly via JAK-STAT pathways, but several STAT-

independent signalling pathways have been described in recent years (ref (191), Figure 1.8).

Upon IFN-binding, the receptor dimerises, which initiates autophosphorylation and activation of the receptor-associated Janus activated kinases (JAKs). JAKs subsequently phosphorylate signal transducer and activator of transcription (STAT) proteins that once activated form homo- and heterodimers, translocate to the nucleus and selectively induce ISGs by binding to distinct promoter elements. The main transcriptional complex formed downstream of the IFNAR is composed of STAT1, STAT2 and IRF9, also termed the ISGF3 complex, which specifically binds to IFN-stimulated response elements (ISRE) in the promoter. The IFNGR mainly activates STAT1 homodimers, known as IFN-γ-activated factor (GAF), which target IFN-γ-activated site (GAS) elements to initiate transcription. The JAK-mediated tyrosine phosphorylation of STATs, such as tyrosine 701-STAT1, is crucial for dimer formation, but also other modifications are required for optimal gene expression. In this regard, Serine 727-phosphorylation of STAT1 was shown to be important for type I and type II IFN-induced responses due to the recruitment of p300 and CBP coactivators, which regulate chromatin remodelling. Various kinases have been implicated in Ser727-phosphorylation, such as protein kinase C (PKC) isoforms and calcium/calmodulin-dependent protein kinase II (CaMKII). IFN receptors also induce the formation of other STAT-dimers, involving STAT1 to STAT6, which mainly bind (GAS) elements. Apart from the JAK-STAT pathways, other signalling cascades were shown to be required for optimal IFN responses, such as MAPK and phosphatidyl-inositol 3-kinase (PI3K) cascades (191). The p38 MAPK cascade mainly regulates IFNAR-mediated ISG expression, independent of STAT activation (192). The IFNAR activates p38 likely via the GTPase RAC1 and the MAPK kinases MKK3/6, which might initiate downstream effectors such as MAPK-activated protein kinase 2 (MK2) and mitogen- and stress-activated kinase 1 (MSK1), implicated in transcriptional and posttranscriptional regulation. The role of p38 in IFNGR signalling is controversial, but the receptor was shown to engage with MyD88 to mediate *Tnf-α* and *IP-10* mRNA stability via the MLK3-MKK3-p38-MK2 axis (193). In contrast the ERK MAPKs were activated by different pathways in response to IFN-γ, and also IFN-α/β. They play a role in IFN-γ-dependent transcription by CCAAT-enhancer binding protein-β (C/EBP-β) and c-Jun/AP-1 (194), and also regulate ISG translation (195). Also the PI3K-AKT-mTOR pathway regulates ISG mRNA translation downstream of the IFNAR and IFNGR. Furthermore PI3K-dependent activation of PKC

isoforms, particularly PKC-δ, leads to Ser727-phosphorylation of STAT1. Also activation of the NF-κB pathway has been reported in response to type I and type II IFNs, and implicated the PI3K-AKT-axis in classical p65/p50 NF-κB activation and TRAF2/NIK to activate the alternative NF-κB p65/p52 (196). However, the exact role of NF-κB in ISG expression is less clear and was shown to be partially inhibitory (197). IFNGR signalling also leads to the expression of transcription factors such as IRF1 and IRF8, which subsequently cooperate with STAT1 to upregulate a subset of IFNγ-stimulated genes (194). IRF8 often cooperates with the transcription factors PU.1 and IRF1. It emerges that the combination of multiple STAT-dependent and -independent pathways possibly defines the selective expression of ISGs in response to a distinct type of IFN.

It is important to mention, that cells constitutively express and secrete low amounts of type I IFNs, which induce weak signalling of the IFNAR and therefore prime the cell for many processes partially by establishing a specific transcriptional profile (198). The IFN priming is also essential for an effective immune response following microbial stimulation, as it ensures the basal expression of signalling molecules, such as IRF7 (199-201).

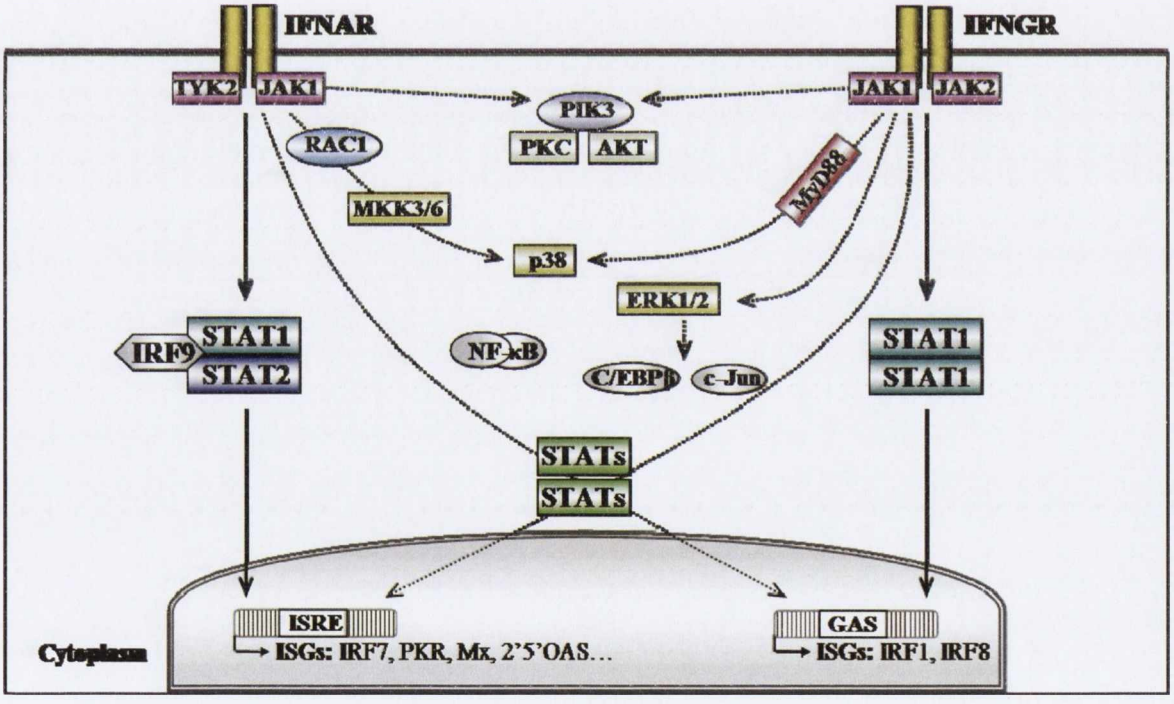


Figure 1.8: Type I and type II IFN signalling

The binding of type I IFNs, i.e. IFN-α and IFN-β, to the IFNAR initiates receptor dimerisation and activation of JAKs, leading to tyrosine phosphorylation of STAT1 and STAT2 that subsequently form a transcriptional complex with IRF9, known as the ISGF3 complex. ISGF3 translocates to the nucleus and binds to ISRE

promoter elements to initiate transcription of certain ISGs. The type II IFN, IFN-γ, on the other hand signals via the IFNGR, which mainly leads to the formation of STAT1 homodimer formation and the induction of genes containing GAS elements. Both IFN pathways also induce other STAT homo- and heterodimers that mostly bind GAS elements. Besides this classical JAK-STAT pathway, IFNs activate alternative STAT-independent pathways including MAPKs, PI3K and NF-κB.

1.4 SARM

SARM (sterile α and HEAT/Armadillo motif containing protein) was identified by Mink et al. in 2001 as the fifth member of the mammalian TIR domain-containing adaptor protein family, which also includes MyD88, MAL, TRIF and TRAM (described in 1.2.1) (34, 202). SARM is the most evolutionary conserved member of the family, as it is found in lower organisms such as nematodes (*Caenorhabditis elegans*) and arthropods (*Drosophila melanogaster*), and is preserved in chordates like amphioxus, fish (*Danio rerio*) and mammals (203, 204). Apart from the characteristic C-terminal TIR domain, SARM additionally exhibits two central sterile α motif (SAM) domains and HEAT/Armadillo repeats at its N-terminus (Figure 1.9). This unique combination of protein-protein interaction motifs may allow SARM to perform distinct functions compared to the other TIR adaptors (205, 206). SARM is also the only TIR adaptor protein that is mainly localised at the mitochondria due to its N-terminal 27 amino acids (aa) hydrophobic and polybasic signal sequence (207). Two main isoforms of human SARM have been described, a 690aa and a 724aa form, which vary at their N-terminus, hence only the longer version contains the mitochondria target sequence. The 724aa SARM is also present in mouse with 94% amino acid identity to its human counterpart, including the highly conserved leader sequence. In addition, a 764aa mouse SARM has been reported that harbours an extended region between the second SAM domain and the C-terminal TIR domain.

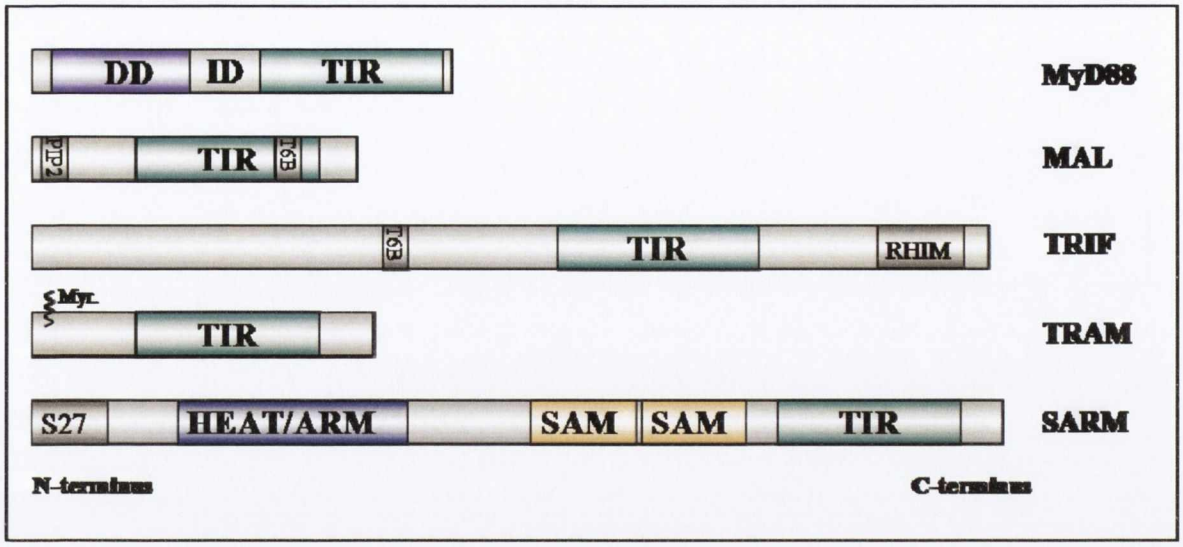


Figure 1.9: Schematic of protein domains and motifs found in the human TIR adaptor family

All TIR adaptor proteins consist of the characteristic TIR domain at their C-terminus. MyD88 also contains a N-terminal death domain (DD) and an intermediary domain (ID). MAL and TRIF both harbour a putative TRAF6-binding motif (T6B) and TRIF additionally exhibits a RIP homotypic interaction motif (RHIM). MAL and TRAM are targeted to the membrane by a PIP2-binding motif or myristoylation, respectively. SARM contains additionally to the characteristic TIR domain two central SAM domains and HEAT/Armadillo repeats at the N-terminus, including a 27aa leader sequence that targets 724aa SARM to mitochondria. Adapted from (33).

It was surprising that unlike the other TIR adaptors, SARM overexpression did not lead to activation of NF-κB- and IRF3-dependent reporter gene constructs (43, 44). First reports on a function of SARM came from studies in *C. elegans*, where the homologous TIR-1 mediated immune responses to pathogenic bacteria and fungi independent of the sole TLR homologue, TOL-1 (43, 208). TIR-1 is the only cytosolic TIR domain-containing protein in worms, but five isoforms are known that differ at the N-terminus. It was demonstrated that TIR-1 functions upstream of the conserved NSY-1-SEK-1-PMK-1 MAPK cascade, which is orthologous to the mammalian ASK1-MKK3/6-p38 MAPK pathway (209). Following exposure to pathogens, PMK-1 leads to upregulation of various antimicrobial peptides partially by activating the conserved transcription factor ATF-7, the orthologue of mammalian ATF-2 (208, 210, 211). The receptor upstream of TIR-1 remains unknown, but different signalling molecules have been implicated in TIR-1 activation, such as the protein kinase C-δ homologue TPA-1 (ref. in (212)). Interestingly, the TIR-1-NSY-1-SEK-1 axis is also functional in the nervous system. In chemosensory neurons the TIR-1-mediated MAPK cascade (independent of PMK-1) leads either to aversive behaviour in response to

pathogenic bacteria or stimulates reproductive egg laying after sensing nutrient-providing microbes (213). Furthermore, this pathway is operational in the postsynapse of olfactory neurons in *C. elegans*, where TIR-1 regulates the asymmetric expression of odorant receptors during development (214). TIR-1 functioned downstream of a voltage-gated calcium channel and interacted with UNC-43, a homologue of human calcium-calmodulin-dependent protein kinase II (CaMKII).

The first report on a function of mammalian SARM was published by Carty et al. from my laboratory in 2006 (44). SARM inhibited TRIF-dependent TLR3 and TLR4 signalling when overexpressed in HEK293 cells via direct interaction with TRIF. And knockdown of endogenous SARM using siRNA enhanced LPS-induced TNF-α production in human peripheral blood mononuclear cells (PBMCs). Another study of human SARM showed inhibition of TRIF- and MyD88-induced AP-1-regulated reporter genes, and suppression of basal p38 phosphorylation (215). The inhibitory role of SARM was subsequently reported for several other SARM homologues mainly by overexpression in HEK293 cells, including SARM of the ancient horseshoe crab, amphioxus and porcine SARM (216-218). Amphioxus is devoid of TRIF and IRF orthologues, but amphioxus SARM could interact with MyD88 and TRAF6 and inhibit the activation of NF-κB-dependent reporter genes. Interestingly in adult amphioxus, SARM was predominantly expressed in the digestive system, which is a primary line of defence, while during embryogenesis it was found in neural cells, thus highlighting its possible dual function in immunity and neural development as seen in *C. elegans*. The inhibitory function was also demonstrated for endogenous SARM in the murine cell line RAWs, where the intracellular bacterium *Burkholderia pseudomallei* circumvented host defense mechanism by upregulating SARM, which suppressed IFN-β and iNOS expression and IκB degradation, while TNF-α induction was mostly unaffected (219).

However, recent studies on *Sarm*-knockout mice questioned the TLR-inhibitory function of SARM. The analysis of SARM-deficient bone marrow-derived macrophages (BMDMs) showed normal cytokine (TNF-α) and chemokine (MCP-1) production in response to various TLRs, including TLR3 and TLR4 (220). It was also demonstrated that murine and human myeloid cells expressed very low levels of SARM compared to a high abundance in the brain. The brain-restricted tissue expression profile of murine SARM was subsequently confirmed by two other reports (221, 222), whereas the initial study on human tissue detected SARM predominantly in liver and kidney (202). Since then,

different functions have been assigned to SARM in the nervous system. Kim et al. demonstrated that SARM localised to mitochondria and recruited JNK3 to mediate neuronal cell death after oxygen and glucose deprivation, presumably via an apoptotic pathway (220). Also in *C. elegans*, anoxic conditions were shown to activate the TIR-1-dependent MAPK cascade leading to anoxic death (171). Furthermore, SARM is currently discussed to mediate apoptosis in T lymphocytes (Panneerselvam (207), unpublished). More recently it was discovered that *Drosophila* and murine SARM function in a new death pathway that actively promotes axon destruction following injury, previously known as Wallerian degeneration (223). Interestingly, *C. elegans* TIR-1 and SEK-1 were also implicated in a nonapoptotic cell death pathway in a linker cell during male gonad development (224). Apart from the role in cell death, murine SARM was found to regulate neuronal morphology. SARM interacted with transmembrane syndecan-2 (Sdc2) at synapses and controlled dendritic aborisation via the MKK4-JNK pathway (222). SARM also mediated dendritic and axonal outgrowth independently of Sdc2 by stabilising microtubules through tubulin acetylation. This indicated that the SARM-MAPKs module described for olfactory neurons in *C. elegans* might also be operational at mammalian synapses. Another study found SARM in a membrane-associated complex with retinoschisin and Na/K ATPase in photoreceptors and bipolar cells of retina tissue and postulated a role for SARM in maintaining the photoreceptor-bipolar synaptic structure (225). The first and so far only report of an immune function of SARM in the brain was given by Szretter et al. in 2009 (221). *Sarm*-knockout mice showed enhanced mortality after infection with neurotropic WNV, which was associated with increased neuronal cell death and viral replication in the brainstem, and linked to reduced microglia activation and TNF-α production in this specific brain region.

Regarding the role of SARM in immune responses it became apparent that SARM activity might be controlled via its expression level, as SARM mRNA and protein were up- and/or downregulated following microbial stimulation. While some studies showed enhanced SARM mRNA and/or protein levels in response to immune stimulation (44, 219, 226), others reported a decrease in *Sarm* mRNA (218, 227). Also a bidirectional regulation was described with an increase of *Sarm* mRNA early after stimulation, followed by suppression at later times (215-217).

Overall, these studies demonstrated that SARM exhibits multiple functions depending on the cell type and the model system used, with emerging roles in immunity and the

nervous system; two areas in which SARM function is preserved from *C. elegans* to humans (Figure 1.10). However, particularly for mammalian SARM, data had been conflicting and more work is needed to understand the exact function and mechanism in the different systems.

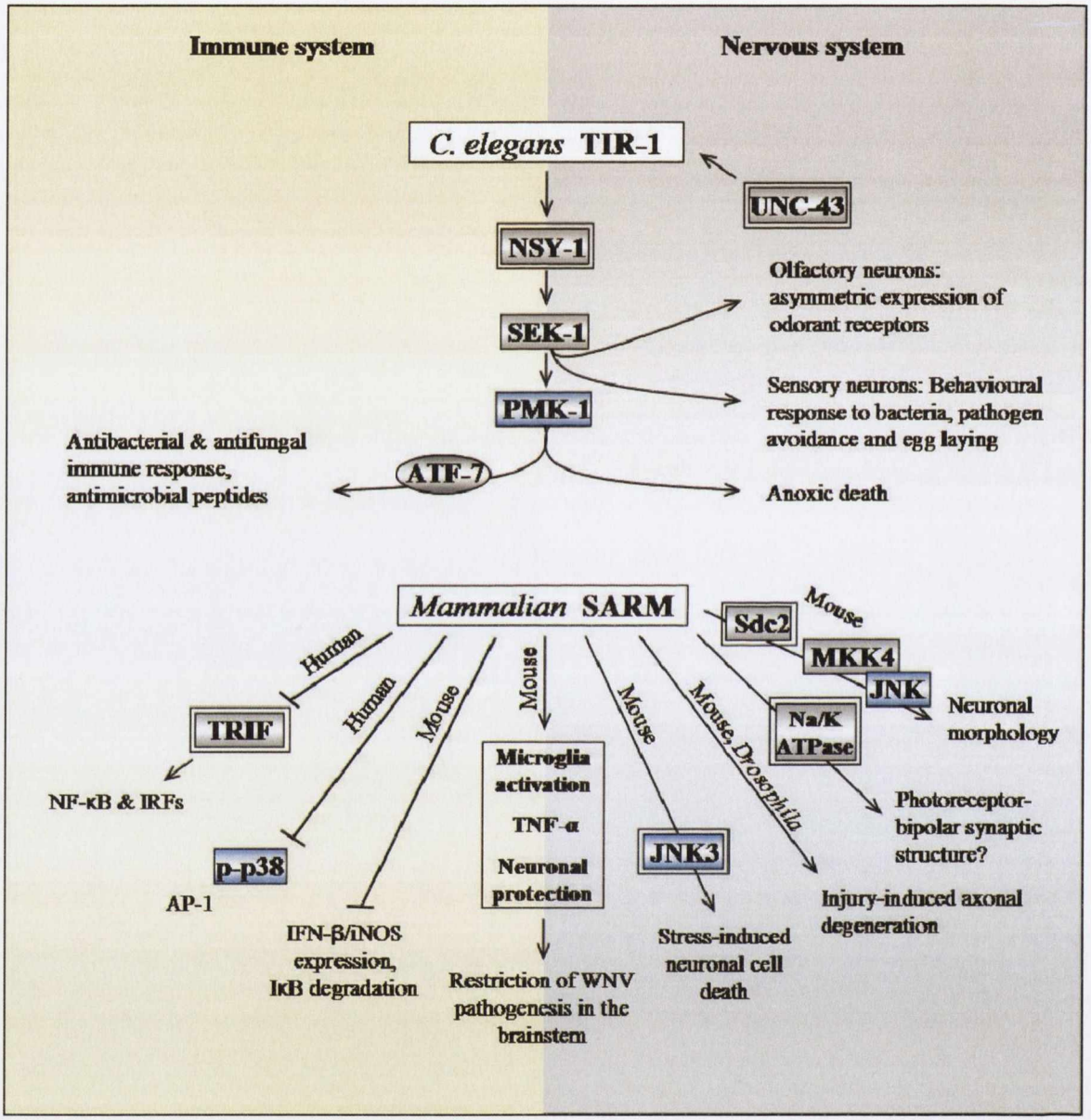


Figure 1.10: Overview of SARM functions in *C. elegans* and mammals

To date, SARM functions have been described in the immune and the nervous system and emerged to be highly cell type-specific. In *C. elegans* TIR-1 functions upstream of a MAPK cascade consisting of NSY-1-SEK-1-PMK-1 and is essential for host defence to pathogenic bacteria and fungi. Part of this cascade is also operational in neurons mediating behavioral responses to bacteria or the development of olfactory neurons. The *C. elegans* MAPK cassette is evolutionary conserved in mammals represented by the orthologous ASK1-MKK3/6-p38 MAPK cascade, but an upstream role of SARM in this exact pathway has not been reported so

far. However, mammalian SARM is implicated in activating MAPKs (indicated by blue boxes), particularly in the central nervous system, where it is highly expressed and has roles in neuronal development, homeostasis and cell death. In contrast to *C. elegans*, the functions of mammalian SARM in immunity are less understood, and depending on the system SARM positively or negatively regulated immune responses. Refer to the text for further details. Double boxes indicate the known interaction partners of SARM/TIR-1.

1.5 Aims

The immune functions of mammalian SARM are still poorly understood, and conflicting data emerged from studies of human and murine SARM (described in 1.4). SARM was found to negatively regulate TRIF-dependent TLR signalling in human cells, including PBMCs, but murine SARM-deficient BMDMs showed normal cytokine responses to a range of TLR agonists (44, 220). Furthermore it was demonstrated that human and murine myeloid cells expressed very low levels of SARM compared to its high expression in the brain, where it performed non-immune functions in regulating neuronal cell death after oxygen and glucose deprivation. Due to these discrepancies, I sought to explore the immune function of murine SARM in more detail.

- First, I wanted to investigate the mRNA and protein expression of SARM in primary immune cells, such as human PBMCs and murine BMDMs. Additionally I assessed if SARM expression in these cells was modulated by TLR stimulation, as this would indicate a role for SARM in TLR-dependent immune responses. Furthermore, I performed a direct comparison of SARM expression in various murine tissues and BMDMs.
- In the second part of this project, I characterised the cytokine profile of murine wild-type and SARM-deficient BMDMs and BMDCs in more detail, with a particular focus on TNF-α and CCL5/RANTES expression. As TNF-α is mainly induced by the transcription factor NF-κB, while CCL5 induction additionally requires IRF3 activation. In the TLR4 response both genes are selectively regulated by the MyD88- and TRIF-dependent pathway, which is interesting in light of the known SARM-TRIF interaction. Furthermore, I investigated a role for SARM in other TRIF-dependent immune functions, such as endotoxin tolerance and DC maturation.

SARM is the most ancient member of the TIR adaptor family with a key immune function in host defence in *C. elegans*, in addition to its role in the nervous system. The conservation of SARM throughout the animal kingdom up to mammals highlights its important functions, such as its role in immunity, which requires further investigations and might lead to novel therapies for immune-related diseases.

2 Materials & Methods

2.1 Materials

Cell culture plastics were from Corning Life Sciences and Greiner bio-one supplied by Fisher Scientific (Ireland). All generic laboratory chemicals were purchased from Sigma-Aldrich (Ireland) unless stated otherwise.

2.1.1 Cells and cell culture reagents

Cell type	Description	Medium
PBMCs	• primary human cells • peripheral blood mononuclear cells	• RPMI • 10% FCS (v/v) • 2mM L-Glutamine • Gentamycin [50µg/ml]
pBMDCs (wt, *Sarm*$^{-/-}$)	• primary murine cells • bone marrow-derived dendritic cells	• RPMI • 10% FCS (v/v) • 2mM L-Glutamine • Pen/Strep [50µg/ml] (GM-CSF [20ng/ml])
pBMDMs (wt, *Sarm*$^{-/-}$)	• primary murine cells • bone marrow-derived macrophages	• DMEM • 10% FCS (v/v) • Ciprofloxacin [10µg/ml] (10-20% M-CSF (v/v))
iBMDMs (various knockouts)	• immortalised murine cells • bone marrow-derived macrophages • a gift from K. Fitzgerald (173)	• DMEM • 10% FCS (v/v) • Ciprofloxacin [10µg/ml]
MEFs (wt, *Sarm*$^{-/-}$)	• mouse embryonic fibroblasts • a gift from MS. Diamond (221)	• DMEM • 10% FCS (v/v) • Ciprofloxacin [10µg/ml]
NIH3T3	• mouse embryonic fibroblast cell line	• DMEM • 10% FCS (v/v) • Ciprofloxacin [10µg/ml]

L929	• murine fibroblast cell line • a gift from K. Fitzgerald	• RPMI • 10% FCS (v/v) • 2mM L-Glutamine • Ciprofloxacin [10µg/ml]
J558	• plasmacytoma cell line • containing a GM-CSF expression vector • a gift from E. Lavelle	• RPMI • 10% FCS (v/v) • 2mM L-Glutamine • Ciprofloxacin [10µg/ml]
HEK293T	• human embryonic kidney cell line • expressing SV40 large T-antigen	• DMEM • 10% FCS (v/v) • Ciprofloxacin [10µg/ml]
HEK293-TLR4	• human embryonic kidney cell line • expressing TLR4, MD2, CD14	• DMEM • 10% FCS (v/v) • Ciprofloxacin [10µg/ml] • HygroGold [50µg/ml] • Normocin [100µg/ml] • Blasticidin [10µg/ml]

Table 2.1: Cell types

Cell culture reagent	Company
Dulbecco's Modified Eagle Medium (DMEM GlutaMAX)	Gibco Invitrogen
RPMI-1640 medium (R0883)	Sigma-Aldrich
Foetal Bovine Serum (FBS, FCS)	Biosera
L-Glutamine [200mM], #G7513	Sigma-Aldrich
Penicillin/Streptomycin [5000µg/ml]	Invitrogen
Ciprofloxacin	Sigma-Aldrich
Gentamycin [50mg/ml]	Sigma-Aldrich
HygroGold [100mg/ml]	InvivoGen
Normocin [50mg/ml]	Sigma-Aldrich
Blastocidin [10mg/ml]	Sigma-Aldrich
Trypsin/EDTA Solution 10x, #T4174	Sigma-Aldrich
EDTA 0.02% Solution, #E8008	Sigma-Aldrich

Dulbecco's phosphate buffered saline (PBS)	Sigma-Aldrich
Trypan Blue Solution (0.4%)	Sigma-Aldrich
Lipofectamine 2000 Transfection Reagent	Invitrogen
Red Blood Cell Lysis Solution (10x)	Miltenyi Biotec
HyClone HyPure Cell Culture water	Thermo Scientific
Dimethyl sulfoxide (DMSO)	Fisher Scientific
Lymphoprep	Axis-Shield
Actinomycin D [5mg/ml], #9415	Sigma-Aldrich
Cycloheximide (CHX)	Sigma-Aldrich
Anti-mouse IFNAR1 antibody, MAR1-5A3, #16-5945	eBioscience

Table 2.2: Cell culture reagents

2.1.2 Cell receptor ligands and siRNA

Receptor ligand	Description	Company
LPS	• Lipopolysaccharide from *E. coli* Serotype EH100	Alexis Biochemicals
Poly(I:C)	• Polyinosinic-polycytidylic acid, #P0913	Sigma-Aldrich
CLO75	• thiazoloquinoline compound	InvivoGen
ds70mer	• from VACV 5'CCATCAGAAAGAGGTTTAATATTTTTGTGAGACCATCGAAGAGAGAAAGAGATAAAACTTTTTTACGACT-3' • complementary strands were annealed by boiling for 5min at 98°C and slow cooling at RT	Eurofins MWG Operon
SeV	• Sendai virus • a gift from I. Julkunen (University of Aarhus, Denmark)	
IFN-α	• recombinant murine IFN-α, #130093131 • some as a gift from C. O'Farrelly (TCD)	Miltenyi Biotec
IFN-γ	• recombinant murine IFN-γ, #12343536	ImmunoTools

Table 2.3: Cell receptor ligands

siRNA	Target sequence	Company
Control siRNA	5'-AATTCTCCGAACGTGTCACGT-3'	Qiagen
SARM S1	5'-AACGCCTGGTTTCCTACTCTA-3'	Qiagen
SARM S2	5'-AAGGCAAGACCAAGGTGTTCA-3'	Qiagen

Table 2.4: siRNA

2.1.3 Antibodies

Antibody (anti-)	Company
β-actin	Sigma-Aldrich
SARM, rabbit [1mg/ml], #3295	ProSci
SARM (C-20), rabbit, #sc-130620	Santa Cruz
SARM, chicken, unpurified, a gift from A. Ding (USA) (220)	
FLAG, mouse [1mg/ml]	Sigma-Aldrich
IκBα, mouse, a gift from Ron Hay (Dundee University, UK)	
p-38, rabbit, #9212	CellSignaling
p-p38 (Tyr180/182), rabbit, #9211	CellSignaling
JNK, rabbit, #9252	CellSignaling
p-JNK (Tyr183/185), rabbit, #44-682G	Biosource
p44/42 MAPK (Erk1/2), mouse, #4696	CellSignaling
Phospho-p44/42 MAPK (Erk1/2), rabbit, #4377S	CellSignaling
IRF3, rabbit, #51-3200	invitrogen
p-IRF3 (Ser396), rabbit, #07-582	upstate
NF-κB p65, mouse, #sc-8008	Santa Cruz
STAT1, #9172	CellSignaling
p-STAT1 (Tyr701), #9171S	CellSignaling
viperin, mouse, a gift from K. Fitzgerald (UMass, USA)	
IRF1 (M-20), rabbit [2mg/ml], #sc-640x	Santa Cruz
IRF8/ICSBP (C-19), goat [2mg/ml], #sc-6058x	Santa Cruz
Pol II (N-20), rabbit [2mg/ml], #sc-899x	Santa Cruz
IgG, rabbit polyclonal serum [12.5mg/ml]	Sigma-Aldrich

IRDye® 680LT anti-mouse secondary antibody for Odyssey Imag.	LI-COR
IRDye® 800CW anti-rabbit secondary antibody for Odyssey Imag.	LI-COR
IRDye® 680/800 anti-goat secondary antibody for Odyssey Imag.	LI-COR
Anti-rabbit Alexa 488 secondary antibody [2mg/ml]	invitrogen
Anti-mouse Alexa 647 secondary antibody [2mg/ml]	invitrogen
Anti-mouse CD80-FITC	BD Pharmingen
Anti-mouse CD86-PE	BD Pharmingen
Anti-mouse CD40-FITC	BD Pharmingen
Anti-mouse I-A/I-E (MHCII)-PE	BD Pharmingen
Anti-mouse CD11c-APC	BD Pharmingen
Anti-mouse IFNAR1 antibody, MAR1-5A3, #16-5945	eBioscience

Table 2.5: Antibodies

2.1.4 Primers

Primer	Forward primer	Reverse primer
• **mRNA** (quantitative real-time PCR)		
β-actin (h)	5'-CGCGAGAAGATGACCCAGATC-3'	5'-GCCAGAGGCGTACAGGGATA-3'
SARM (h)	5'-GGGTGCATAAGGAGATTGTGAC-3'	5'-GTGGGACCACTTGATACCGTT-3'
CCL5 (h)	5'-CCCATATTCCTCGGACACCA-3'	5'-GGTGACAAAGACGACTGCTG-3'
IFN-β (h)	5'-CTGCATTACCTGAAGGCCAAG-3'	5'-TTGAAGCAATTGTCCAGTCCC-3'
β-actin (m)	5'-TCCAGCCTTCCTTCTTGGGT-3'	5'-GCACTGTGTTGGCATAGAGGTC-3'
Sarm (m)	5'-GGTGCACAAGGAGATTGTGAC-3'	5'-CATGGGACCATTTGATGCCGTT-3'
Tnf-α (m)	5'-TCCCCAAAGGGATGAGAAGTT-3'	5'-GTTTGCTACGACGTGGGCTAC-3'
Ccl5 (m)	5'-CTCACCATATGGCTCGGACA-3'	5'-ACAAACACGACTGCAAGATTGG-3'
Ifn-β (m)	5'-ATGGTGGTCCGAGCAGAGAT-3'	5'-CCACCACTCATTCTGAGGCA-3'
Ifit2 (m)	5'-GACTTAGAGGTGCTGCACAG-3'	5'-CTCGTTGTACTCATGACTGCTG-3'
Irf3 (m)	5'-TGAGTTTGTGACTCCAGGGG-3'	5'-GTAGGTTTTCCTGGGAGTGAG-3'
Irf7 (m)	5'-TTGGATCTACTGTGGGCCCA-3'	5'-CTTGCCAGAAATGATCCTGGG-3'
• **genomic DNA** (*Sarm*$^{-/-}$ genotyping) (m)		
wt E3-I4	5'-ACGCCTGGTTTCTTACTCTACGA-3'	5'-GCTGGGGCCTCCTTACCTCTT-3'

Neo	5'-CAGGTAGCCGGATCAAGCGTATGC-3'	5'-CCTGTCCGGTGCCCTGAATGAACT-3'
• **genomic DNA** (sequencing the 927bp 5'-*Ccl5* gene region) (m)		
Ccl5-927bp	5'-GGGAATCAGGATTACCTGGC-3'	5'-GGCACCAGTTCACAATAAGGAG-3'
• **genomic DNA** (ChIP assay) (m)		
Ccl5-prom.	5'-GCAGTTAGAGGCAGAGTCATAC-3'	5'-CCAGGGTAGCAGAGGAAGTG-3'
β-actin-prom.	5'-GGAGGGGAGAGGGGGTAAA-3'	5'-CACTCGAGCCATAAAAGGCAAC-3'
• **Cloning** (m)		
mSARM-C-Flag	5'GACTAGTATGGTCCTGACGCTGCTCT TCTCCGCCTACAAACTGTG-3'	5'GCTCGAGTTACTTATCGTCGTCATCC TTGTAATCAGGCAGACCCATTGGCG-3'
Ccl5-luc. (+190/-57)	5'GCTCGAGCAGTTAGAGGCAGAGTCA TAC-3'	5'-ACCATGGTACCCGCGGCAGAGGCT-3'
Ccl5-luc. (+120/-57)	5'GCTCGAGTGACAGCAACAAGTGTTT GGT-3'	5'-ACCATGGTACCCGCGGCAGAGGCT-3'

Table 2.6: Primer pairs

The primer pairs were directed against human (h) or murine (m) gene sequences, and were purchased from Eurofins MWG Operon.

2.1.5 Method-specific materials

PCR (conventional)	**Company**
Herculase II Fusion Enzyme with dNTPs Combo, #600677	Agilent Technologies
5x Green GoTaq Flexi Buffer, #M891A	Promega
GoTaq DNA Polymerase, #M830B	Promega
Deoxynucleotide Mix [10mM]	Sigma-Aldrich
$MgCl_2$ [25mM], #A351H	Promega
2-Log DNA Ladder (0.1-10.0kb), #N3200L	NewEngland BioLabs
Real-time PCR (quantitative)	**Company**
RNeasy Mini Kit	Qiagen
High Pure RNA Isolation Kit, #11828665001	Roche

Random Hexamer	Eurofins MWG Operon
dATP, dTTP, dCTP, dGTP, each [100mM]	NewEngland BioLabs
M-MLV RT 5x Buffer	Promega
M-MLV Reverse Transcriptase, #M1705	Promega
RNase Out Recombinant Ribonuclease Inhibitor	Invitrogen
GoTaq® qPCR Master Mix, #A6001	Promega
ELISA	**Company**
Murine TNF-α, #DY410E	R&D systems
Murine CCL5/RANTES, #DY478	R&D systems
Human CCL5/RANTES, #DY278	R&D systems
• Murine IFN-β Coating Antibody, rat, #sc-57201 • Murine recombinant IFN-β • Murine IFN-β Detection Antibody, rabbit, #32400-1 • anti-rabbit HRP	• Santa Cruz • Alpha Technologies • PBL InterferonSource • Sigma-Aldrich
Murine M-CSF, #DY416	R&D systems
Murine GM-CSF, #DY415	R&D systems
TMB Substrate Reagent Set, #555214	BD Biosciences
Western Blotting	**Company**
Protogel (30% Acrylamide : 0.8% Bis-acrylamide) Stock 37.5:1	Biosciences
N'Tetramethylethylenediamine (TEMED), #T7024	Sigma-Aldrich
Prestained Protein Marker, Broad Range, #7708	NewEngland BioLabs
Immobilon PVDF Membranes, 0.2μm	Fisher Scientific
Bovine Serum Albumin (BSA), #A8022	Fisher Scientific
ChIP	**Company**
Formaldehyde solution, 36.5-38%, #8775	Sigma-Aldrich
Salmon Sperm DNA Solution, [10mg/ml], #15632-011	invitrogen
Proteinase K, #19131	Qiagen
Protein A-Sepharose 4B, #P9424	Sigma-Aldrich

Chelex 100 Resin	Bio-Rad
Cloning	
NovaBlue Singles™ Competent Cells, #70181-3	Clontech
LB BROTH, LB AGAR (pronadisa)	Chromatrin Ltd.
Novagen Clonables™ Ligation/Transformation Kit, #70526	Clontech
QuickLyse Miniprep Kit, #27406	Qiagen
EndoFree Plasmid Maxi Kit, #12362	Qiagen
Agarose GelExtract Mini Kit, #2300510	5 Prime
QIAquick PCR Purification Kit	Qiagen
Restriction Enzymes and 10x NEB Buffers (1-4)	New England BioLabs

Table 2.7: Method-specific materials

2.1.6 Buffers

Buffer	Composition
10x PBS	• 1.45M NaCl • 39mM NaH_2PO_4 • 227mM Na_2HPO_4
10x TBS	• 250mM Tris • 1.37M NaCl • 27mM KCl
WB Lysis buffer	• 50mM Tris pH 7.4 • 150mM NaCl • 30mM NaF • 5mM EDTA • 10% Glycerol (v/v) • 40mM β-Glycerophosphate • 1% Triton X100 → store at 4°C, add fresh: • 0.1mM PMSF • 1mM Sodium Orthovanadate (Na_3VO_4) • 5µl/ml Aprotonin

3x WB Sample buffer	• 187mM Tris pH 6.8 • 30% Glycerol (v/v) • 6% SDS (w/v) • 0.3% Bromophenol Blue (w/v) → add fresh: 150mM DTT
10x WB Running buffer	• 250mM Tris • 1,9M Glycine • 10% SDS (w/v)
10x WB Transfer buffer	• 250mM Tris • 1,9M Glycine
1x WB Transfer buffer	• 10% 10x WB Transfer buffer (v/v) • 20% Methanol (v/v) → store at 4°C
5x RT buffer	• 250 mM Tris-HCl (pH 8.3) • 375mM KCl • 15mM $MgCl_2$ → prepare RNase-free, autoclave, then add • 50mM DTT (RNase-free) → store aliquots at -20°C
Carbonate buffer	• 10mM $NaHCO_3$ • 3.4mM Na_2CO_3 → pH 9.4-9.6
Luciferase assay mix	• 20mM Tricine • 1.07mM $(MgCO_3)_4Mg(OH_2)\cdot 5H_2O$ • 2.67mM $MgSO_4$ • 0.1M EDTA • 33.3mM DTT • 270mM coenzyme A • 470mM Luciferin (Biosynth) • 530mM ATP

ChIP Lysis buffer	• 50mM Tris-HCl (pH 7.5) • 150mM NaCl • 5mM EDTA • 0.5% NP-40 (v/v) • 1% Triton X-100 (v/v) → store at 4°C, add fresh: • 0.1mM PMSF • 1mM Sodium Orthovanadate (Na_3VO_4) • 5µl/ml Aprotonin

Table 2.8: Buffers

2.2 Methods

2.2.1 Cell handling

Cells were handled under aseptic conditions in a sterile laminar flow hood or a microbiological safety cabinet and all materials and reagents were sterile.

2.2.1.1 Resuscitation of frozen cell lines

The frozen cells in cryovials were taken from the liquid nitrogen storage and quickly thawed in a 37°C water bath until only small ice crystals remained. The cell suspension was transferred into a 50ml Falcon tube containing 10ml prewarmed medium supplemented with the appropriate constituents (complete medium, c.medium, see 2.1.1). Cells were centrifuged at 260g for 5min and cell pellet was resuspended in c.medium and transferred into a 75cm^2 flask. Cells were cultured in a humidified incubator at 37°C with 5% CO_2 until reaching 80% confluency and subcultured using the appropriate method. After two passages, cells were used for experiments.

2.2.1.2 Cell culture

Cells were cultured in a humidified incubator at 37°C with 5% CO_2 in 75cm^2 or 175cm^2 flasks with 17-20ml or 25-30ml, respectively, of the appropriate c.medium (see 2.1.1). Cells were subcultured every three to four days, when they reached around 80% confluency.

To subculture the adherent immortalised BMDMs (iBMDMs) and HEK293-TLR4 cells, cells were directly scraped into the medium, transferred to a 50ml Falcon tube and centrifuged at 180g for 5min. After the supernatant was discarded, the cell pellet was resuspended in 10ml prewarmed c.medium (37°C) and 0.5-1ml cell suspension was transferred to a new 75cm^2 flask containing c.medium (1:10-1:20 v/v). The adherent HEK293Ts, NIH3T3 and MEFs were split by trypsinisation. Medium was removed and the cell layer was washed with 10ml prewarmed 1x PBS, that was subsequently discarded. Then 5ml prewarmed 1x Trypsin solution in PBS was added to the cell layer and incubated for approximately 2min until cells detached. The reaction was terminated by adding 10ml prewarmed c.medium and cells were centrifuged and reseeded as described above. The generation and culture conditions of the primary cells are described in 2.2.4 for pBMDMs and pBMDCs and in 2.2.6 for PBMCs. The generation of iBMDMs is described in 2.2.5.

The excess of cells was used for experiments. Cells were counted using a hemocytometer under a light microscope. To exclude dead cells, the cell suspension was diluted 1:10 in Trypan Blue solution and 9µl were transferred to the hemocytometer. Depending on the experiment, cells were seeded at densities ranging from 1-5x10^5 cells/ml in c.medium, except PBMCs, which were seeded at 1.5x10^6 cells/ml. Cells were incubated over night and treated as required the next day.

- 96 well plates at 200µl/well (for ELISA)
- 24 well plates at 500µl/well (for quantitative real-time PCR, confocal)
- 12 well plates at 1ml/well (for quantitative real-time PCR of PBMCs)
- 6 well plates at 2ml/well (for Western Blotting)
- 10cm dishes at 10ml/dish (for Western Blotting)
- 15cm dishes at 30ml/dish (for ChIP)

All ligands for cell stimulation were diluted in serum-free medium (SFM) before adding to the cells. The infection with SeV was performed at a dilution of 1:200-1:1000, which was determined to potently induce IFN-β expression while not affecting cell viability. The cytoplasmic delivery of Poly(I:C) and ds70mer was achieved using Lipofectamine 2000 transfection (see 2.2.2.3).

2.2.1.3 Freezing cells

A cell pellet was reconstituted in FCS containing 10% DMSO (v/v) to obtain a cell suspension of 1x10^6 cells/ml. 1ml cell suspension was immediately transferred to a cryovial and placed in a freezing container Nalgene® "Mr. Frosty" and kept at -80°C overnight before permanent storage in liquid nitrogen.

2.2.2 Cell transfection using Lipofectamine 2000

Cells were seeded the day before in the appropriate tissue culture plate. The protocol is given for each well of cells seeded in 500µl c.medium in 24 well plates, but was adjusted depending on the volume of the tissue culture dish. Two mixtures were prepared. Mix A contained the plasmid or oligonucleotide in 25µl SFM. Mix B was prepared in a separate tube and was composed of 0.6µl Lipofectamine diluted in 24.4µl SFM and incubated for

5min at RT. Both solutions were mixed, incubated for 20min at RT and 50µl were added to each well of the 24 well plates.

2.2.2.1 Plasmid transfection

For confocal microscopy, NIH3T3 cells were seeded at $1x10^5$ cells/ml on coverslips in 24 well plates. The next day, each well was transfected with 0.5µg plasmid DNA using 0.8µl Lipofectamine according to the protocol described above (2.2.2). 50µl of total mix was added to the cell and cells were placed in the incubator for 48h before harvesting.

2.2.2.2 siRNA transfection

Cells were usually seeded at $1x10^5$ cells/ml in 24 well plates. On two consecutive days, cells of each well were transfected with 12.5-50pmol siRNA using 0.6µl Lipofectamine according to the protocol described above (2.2.2). 24h after the last transfection, cells were stimulated with the appropriate ligands depending on the experiment.

2.2.2.3 Oligonucleotide transfection

Cells were seeded at $3\text{-}5x10^5$ cells/ml in 24 well plates. The next day, the ligands Poly(I:C) and ds70mer were transfected for cytoplasmic delivery according to the protocol described above (2.2.2) and incubated for 6h before harvesting for quantitative real-time PCR analysis.

2.2.3 Generation of M-CSF- and GM-CSF-conditioned medium

2.2.3.1 M-CSF-conditioned medium

To generate macrophage colony-stimulating factor (M-CSF)-containing medium, L929 cells were seeded in $175cm^2$ flasks at $2x10^7$cells/40ml c.medium/flask and cultured for 7 days without changing the medium. Then the supernatant was transferred to a 50ml Falcon tube, centrifuged at 260g for 10min and filtered into a new Falcon tube using a 0.45µM filter. The L929 supernantant was stored at -80°C. The presence of M-CSF was analysed by ELISA (optional), although exact quantification was not required, as the activity was tested in BMDM cultures using various amounts of L929 supernatant (5, 10, 15, 20%). Medium supplemented with 10-20% L929 supernatant was found to be efficient for generating BMDMs.

2.2.3.2 GM-CSF-conditioned medium

Granulocyte-macrophage colony-stimulating factor (GM-CSF)-containing medium was generated using J558 cells stably transfected with a GM-CSF expression vector. Cells were cultured for 2 passages in selection medium using 1mg/ml G418 in c.medium and seeded at $1x10^6$ cells/ml. To generate the J558-conditioned supernatant, cells were washed twice in c.medium and cultured in c.medium without G418. First, cells were plated at $1x10^6$ cells/ml and grown until they reached 50% confluency, then cells were seeded at $0.25x10^6$ cells/ml for further passages (maximum 9 passages). Supernatants were harvested, centrifuged and stored at -20°C. The supernatants were not filtered as this would affect activity. GM-CSF concentration was quantified by ELISA and used at 20ng/ml in BMDC cultures.

2.2.4 Generation of pBMDMs and pBMDCs

Wt and *Sarm*$^{-/-}$ hind legs were obtained from our collaborator A. Ding (Weill Cornell Medical College, USA) and later also from K. Fitzgerald (University of Massachusetts Medical School, USA) shipped in c.medium in 50ml Falcon tubes on cold packs. At day 0, the femur and tibiae were cleaned from the surrounding muscles using a dissection kit, previously sterilised with 70% ethanol. The bones were separated and the ends were cut open with scissors. The bone marrow (BM) was flushed with c.medium without growth factors (see 2.1.1) into a sterile petri dish using a 20ml syringe with a 27G needle attached (BRAUN). Aggregates within the BM suspension were disintegrated by passing the cells through a 20ml syringe with a 19G needle attached. The cell suspension was then transferred into a 50ml Falcon tube and centrifuged at 260g for 5min. The pellet was resuspended in 5ml 1x RBL buffer and incubated for 3-4min at RT to lyse the red blood cells. Then 15ml c.medium were added to stop the reaction and the cells were centrifuged. The pellet was resuspended in 10ml c.medium for counting.

2.2.4.1 Generation of pBMDMs

To generate primary BMDMs (pBMDMs), cells were seeded in 10cm dishes at a density of $5\text{-}7x10^5$ cells/ml in 10ml of c.medium supplemented with 15-20% L929 supernatant (containing M-CSF, see 2.2.3.1). On day 3, 1ml prewarmed L929 supernatant was added per dish. On day 5, medium was replaced with fresh 10ml prewarmed c.medium

containing 10-15% L929 supernatant. If cells were already 100% confluent on day 5, they were split in 15cm dishes by trypsinisation (described below). At day 7-9, the differentiated cells were harvested by trypsinisation and plated for experiments. First the medium was removed, the adherent cells were washed gently with 6ml prewarmed 1x PBS and then incubated with 5ml prewarmed 1x Trypsin solution in PBS for 3 minutes at 37°C. The cells were flushed in the Trypsin solution using a 5 or 10ml pipette and immediately transferred into a 50ml Falcon tube containing 10ml c.medium to stop the reaction. After centrifugation at 260g for 5min the cell pellet was resuspended in 10ml c.medium, cells were counted and seeded for the experiments at 4-5x10^5 cells/ml in c.medium without growth factors.

2.2.4.2 Generation of pBMDCs

To generate primary BMDCs (pBMDCs), BM cells were seeded in 10cm dishes at 4x10^5 cells/ml in 10ml of c.medium containing 20ng/ml GM-CSF (J558 supernatant, see 2.2.3.2). On day 3, 10ml prewarmed c.medium with 20ng/ml GM-CSF were added per dish. On day 6, 10ml medium were removed and replaced with fresh 10ml prewarmed c.medium with 20ng/ml GM-CSF. On day 8-10, the cells were harvested by resuspending the loosely-adherent pBMDCs in the medium that the cells were grown in. The cell suspension was transferred to a 50ml Falcon tube and centrifuged at 260g for 5min. Cell pellets were resuspended in 10ml c.medium, counted and seeded for experiments at a density of 5x10^5 cells/ml in c.medium containing 10ng/ml GM-CSF.

Another protocol used to generate pBMDCs was performed in 175cm^2 flasks. Here, the cells were seeded at 4x10^5 cells/ml (C57BL/6) in 30-38ml c.medium containing 20ng/ml GM-CSF. On day 3, 30ml of prewarmed c.medium with 20ng/ml GM-CSF were added per flask. On day 6, the loosely-adherent pBMDCs were separated from the granulocytes and macrophages. First, the supernatant containing the non-adherent granulocytes was gently removed by pipetting and discarded. Then 30ml prewarmed 1x PBS were added to each flask and the loosely-adherent pBMDCs were resuspended by pipetting the PBS solution gently against the cells. The suspension was transferred in a 50ml Falcon tube containing 10ml of c.medium. Then 30ml of prewarmed EDTA 0.02% solution was added to each flask and incubated at 37°C for 10min. The cells were flushed in the solution and transferred into a 50ml Falcon tube containing 10ml of c.medium. Cells were centrifuged at 260g for 5min and resuspended in 10ml of c.medium for counting. The cells were seeded at 4x10^5 cells/ml in 30-38ml c.medium with 20ng/ml GM-CSF in 175cm^2 flasks.

On day 8, 30ml of prewarmed c.medium with 20ng/ml GM-CSF was added per flask. On day 10, the loosely-adherent cells were collected by resuspending them in the medium that the cells were grown in and transferred to a 50ml Falcon tube. After centrifugation and resuspension in 10ml of c.medium, the cells were counted and plated in 96 well plates at a density of $6.2x10^5$ cells/ml in c.medium containing 10ng/ml GM-CSF.

2.2.5 Generation of iBMDMs

The immortalised BMDM cell lines (iBMDMs) were generated by K. Fitzgerald (University of Massachusetts Medical School, USA) using a J2 recombinant retrovirus carrying *v-myc* and *v-raf/mil* oncogenes (173, 228). Primary BM cells were cultured for 3-4 days in L929-conditioned medium (similar to the protocol described in 2.2.4.1). Subsequently the cells were infected with J2 recombinant retrovirus and cultured for 3-6 months with reducing concentrations of L929-supernatant until the immortalised BMDMs were growing without L929-conditioned medium. The maintenance of the iBMDM cell line is described in 2.2.1.2.

2.2.6 Isolation of human PBMCs

Human PBMCs were isolated from buffy coats of heparinised blood provided by the Irish blood transfusion service at St. James's Hospital (Dublin). The buffy coat was diluted 1:7 with 1x PBS and 35ml were slowly layered over 15ml lymphoprep in a 50ml Falcon tube. The tubes were centrifuged at 350g for 30min at RT in a swing-out rotor with the break off. After centrifugation the PBMCs were collected from the lymphoprep/serum interface using a transfer pipette and transferred to a 50ml Falcon tube containing 15ml c.medium. The cells were centrifuged at 350g for 8min, washed again in c.medium, centrifuged and resupended in 8ml 1x RBL solution and incubated for 8min at RT to lyse the red blood cells. After incubation the Falcon tube was filled up with c.medium, centrifuged and the cell pellet was resuspended in an appropriate volume of c.medium for counting. The PBMCs were plated at $1.5x10^6$ cells/ml for experiments.

2.2.7 Murine tissue RNA and protein preparation

Mice were sacrificed by cervical dislocation and the organs were immediately removed, transferred into a zipper-top poly bag (Sigma) and snap-frozen in liquid nitrogen and stored at -80°C until processed for RNA and protein analysis.

2.2.7.1 Tissue RNA extraction

Tissue RNA extraction was performed using the RNeasy Mini Kit. Approximately 42mg frozen tissue were transferred into a 7ml tube containing 1ml ice-cold Qiagen RLT lysis buffer supplemented with 20µl 2M DTT (on ice). The tissue was disrupted and homogenised in the buffer at 15000-30000rpm using a rotor-stator homogeniser (Polytron PT1600E, Kinematica AG) and lysates were stored at -80°C until RNA isolation. The frozen lysates were thawed at 37°C in a water bath, centrifuged for 3min at 15700g and 600µl lysate (corresponding to 25mg tissue) were transferred to a new eppendorf tube for processing, while the rest was stored at -80°C. The RNA was purified according to the manufacturer's protocol. Briefly, 600µl of 70% ethanol were added to the lysate before it was applied to a column, where the total RNA bound to a membrane. After several washing steps the RNA was eluted in 40µl RNase-free water.

2.2.7.2 Tissue protein extraction

For tissue protein analysis using Western Blotting, approximately 50mg frozen tissue was placed in a 7ml tube containing 1ml of 1x PBS (on ice). The tissue was disrupted at 5000-10000rpm using the rotor-stator homogeniser. The cell suspension was transferred into an eppendorf tube and centrifuged at 800g for 7min. The pellet was lysed in 200µl 3x WB Sample buffer, boiled for 8min at 99°C and stored at -20°C until analysed by Western Blotting.

2.2.8 Quantitative real-time PCR

2.2.8.1 RNA isolation

To quantify target mRNA expression via real-time PCR analysis, RNA was first isolated from the cells using the High Pure RNA Isolation Kit. The medium was removed from the adherent cells that were usually grown in 24 well plates and 200µl of lysis buffer and 100µl of 1x PBS were added directly into the well. The plates were stored at -80°C

until further processed for RNA isolation according to the manufacturer's protocol. Briefly, the RNA was bound to the membrane, the genomic DNA was removed by on-column digestion using DNase and after several washes the RNA was eluted into an eppendorf tube with 50µl elution buffer and stored at -80°C until used for cDNA synthesis.

2.2.8.2 cDNA synthesis

Complementary DNA (cDNA) was synthesised from isolated RNA in a reaction catalysed by the enzyme reverse transcriptase (from M-MLV). A negative control sample was also prepared by replacing the reverse transcriptase with water to control for any remaining genomic DNA amplified in the real-time PCR reaction. The reactions were prepared on ice and also the RNA samples were kept on ice. 5µl RNA (approximately 0.5-1µg RNA) were mixed with 5µl cDNA reaction mix (Table 2.9) in tubes of 8-tube PCR strips, mixed and centrifuged at 240g for 10sec to remove air bubbles. The reaction was applied to a Thermo Hybaid PxE 0.2 thermal cycler using the thermal protocol described in Table 2.9. The cDNA was later diluted 1:2 by adding 10µl water and stored at -20°C until real-time PCR analysis.

cDNA reaction mix	Volume [µl]
Random hexamer [1µg/µl]	0.5
Home-made 5x RT buffer	2
dNTPs [2.5mM each]	2
RNase Out	0.25
Reverse Transcriptase M-MLV	0.25

Temperature [°C]	Time [min]
25	10
42	50-60
95	3
4	hold

Table 2.9: cDNA synthesis protocol

2.2.8.3 Real-time PCR

Real-time PCR was performed using the GoTaq® qPCR Master Mix and the 7500 Fast Real-time PCR System (Applied Biosystems), which allowed detection and quantification of amplified DNA in "real time". 9µl of real-time PCR reaction mix containing the specific primers of the target gene (Table 2.6) were added per well of a Thermo-Fast 96 well PCR plate and 1µl cDNA sample was added (or to reduce the pipetting error, 8µl of PCR reaction mix were added per well and 2µl diluted cDNA sample was added). In a separate well, each sample was also analysed for expression of the housekeeping gene *β-actin*. The

plate was sealed with adhesive film (Thermo Scientific) and centrifuged 240g for 10sec to remove air bubbles. The plate was applied to the 7500 Fast Real-time PCR machine (Applied Biosystems) using the following PCR cycle conditions (Table 2.10).

Real-time PCR reaction mix	Volume [µl]
Forward primer [5pmol/µl]	0.5
Reverse primer [5pmol/µl]	0.5
GoTaq qPCR Master Mix	2.5
Mol.biol. water	5.5
ROX dye	1:200 of total mix

Temperature [°C]	Time [sec]	Cycle number
95	120	1
95	3	40
60	30	

Table 2.10: Real-time PCR protocol

Relative quantification (RQ) was performed using the Applied Biosystems 7500 Fast System Software v.1.3.1 and the comparative C_t method. Calculations are based on comparing the cycle numbers, where fluorescence crossed a certain threshold (C_t). Low C_t values represent a high expression of target mRNA. To eliminate variations in cDNA input sample concentration, each target sample was normalised to the reference gene *β-actin* as an internal control using the following equation:

$$\Delta C_t = C_t target - C_t \beta\text{-}actin$$

Next, the expression of the target gene was determined relative to the mean of the control sample (e.g. unstimulated cells):

$$\Delta C_t \text{mean control} = (\Delta C_t \text{control1} + \Delta C_t \text{control2} + \Delta C_t \text{control3}) / 3$$

$$\Delta\Delta C_t = \Delta C_t - \Delta C_t \text{mean control}$$

$$RQ = 2^{-\Delta\Delta Ct}$$

The mean RQ values were calculated from three biological replicates and presented as fold induction relative to the control sample (set to 1). The standard deviation was displayed by the error bar and was calculated by the GraphPad Prism 5 software.

2.2.9 Genomic DNA extraction

$2x10^5$ cells were harvested in an eppendorf tube and centrifuged at 800g for 5min at 4°C. The cell pellet was resuspended in 100µl QuickExtract Solution (epicentre), vortexed for 15sec and incubated at 65°C for 6min. The sample was vortexed again and incubated at 98°C for 2min. 2-4µl DNA solution were used in PCR reactions. DNA was stored at -20°C.

2.2.10 Genotyping of *Sarm*$^{-/-}$ cells

Genomic DNA was isolated from cells using the protocol described in 2.2.9. The wild-type *Sarm* locus was analysed using a primer pair binding to Exon 3 and Intron 4 of the *Sarm* gene (wt E3-I4, Table 2.6), which were absent from the mutated *Sarm* locus (see Figure 2.1), generating an approximately 500bp PCR product. The mutated *Sarm* locus was identified with primers directed against the neomycin cassette (Neo, Table 2.6), amplifying an approximately 200bp DNA-fragment. The primer sequences were kindly provided by K. Fitzgerald. The PCR was performed according to the protocol described in Table 2.11.

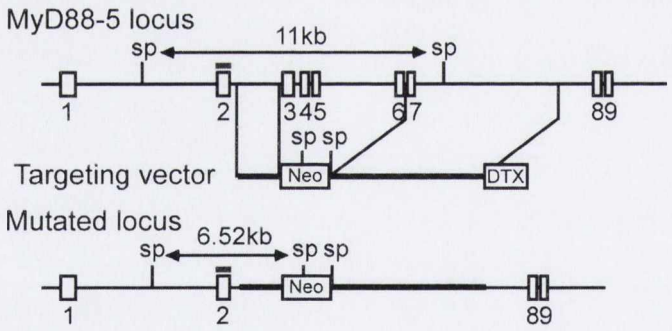


Figure 2.1: Schematic of the mutated *Sarm* locus in *Sarm*$^{-/-}$ mice (by A. Ding)

The schematic shows the strategy for homologous recombination used by Kim et al. (A. Ding) to generate the *Sarm*-knockout mouse (220). The top schematic illustrates the 9 exons of the wild-type *Sarm* gene (termed MyD88-5 locus), while the bottom displays the mutated *Sarm* locus, where Exon 3-7 were replaced with a neomycin resistance gene in reverse orientation. The remaining gene parts are out of frame, precluding expression of a truncated SARM protein.

PCR reaction mix [20µl]	Volume [µl]
mol. biol. H_20	10.1
5x Green GoTaq Buffer	4
$MgCl_2$ [25mM]	2
dNTPs [10mM]	0.4
Forward primer [5µM]	1.2
Reverse primer [5µM]	1.2
GoTaq DNA Polymerase	0.1
DNA template	1

Temperature [°C]	Time [sec]	Cycle number
95	120	1
95	20	35
62	20	
72	30	
72	300	1
4	hold	

Table 2.11: PCR protocol for *Sarm*$^{-/-}$ genotyping

2.2.11 PCR for sequencing the 5'-*Ccl5* gene locus

Primers were designed (Table 2.6) to PCR amplify a 927bp DNA-fragment from genomic DNA isolated as described in 2.2.9. The PCR was performed as shown in Table 2.12 using the Herculase II Fusion Enzyme PCR Kit. The PCR product was controlled by resolving 10µl on a 1% agarose gel together with a DNA ladder. The DNA was visualised by ethidium bromide staining and UV illumination. The remaining 40µl of PCR product were purified using the QIAquick PCR Purification Kit and sent for sequence analysis to Source BioScience.

PCR reaction mix [50µl]	Volume [µl]
mol. biol. H_20	30
5x Reaction Buffer	10
dNTPs [25mM each]	0.5
Forward primer [5µM]	2.5
Reverse primer [5µM]	2.5
DNA Polymerase	0.5
DNA template	4

Temperature [°C]	Time [sec]	Cycle number
95	120	1
95	20	35
55	20	
72	30	
72	300	1
4	hold	

Table 2.12: PCR protocol to amplify a 5'-*Ccl5* gene DNA-fragment for sequencing

2.2.12 Enzyme-linked immunosorbent assay (ELISA)

Cells were stimulated in 96 well plates and cell-free supernatants were harvested by centrifuging the plate at 240g for 2min and transferring the supernatant into a new 96 well plate. The plate was stored at -20°C until cytokine analysis was performed using ELISA.

2.2.12.1 TNF-α and CCL5 ELISA

The antibodies were reconstituted according to the manufacturer's protocol (R&D ELISA kits), but only half the amount of recommended antibody was used for each step of the protocol. High-binding 96 well plates (Greiner bio-one) were coated with 50µl capture antibody diluted in 1x PBS and incubated at 4°C over night. Then the plates were washed 4 times with 1x PBS/0.05%Tween 20 and blocked for 2h at RT with 200µl 1% BSA in PBS. The blocking solution was removed and 1:2 serial dilutions of the respective standard in triplicates were applied starting at 4 or 8ng/ml using 40µl/well diluted in 1% BSA/PBS. Also 40µl sample supernatant diluted approximately 1:4 for TNF-α and 1:5-1:20 for CCL5 were added to each well and incubated at 4°C over night. The following day the plates were washed 4 times in PBS/0.05%Tween 20 and incubated for 2h at RT with 50µl/well of detection antibody diluted in 1% BSA/PBS. After washing again 4 times, the plates were incubated for 30min with 50µl/well of Streptavidin-HRP diluted 1:200 in 1% BSA/PBS. The plates were washed again 4 times and incubated with 50µl/well of TMB Substrate (solution A mixed 1:2 with solution B). The reaction was stopped by adding 25µl 1N H_2SO_4 to each well and the optical density (absorbance) was measured at 450nm (540nm subtracted) using the VersaMax ELISA microplate reader (Molecular Devices). The cytokine concentrations of the samples were interpolated from the standard curve using SoftMax Pro4.8 Software.

2.2.12.2 IFN-β ELISA

The high-binding 96 well plates were coated with 50µl capture antibody diluted 1:1000 in Carbonate buffer and incubated at 4°C over night. The plates were washed as described above and blocked for 2h at 37°C with 200µl 10% FCS/PBS. The blocking solution was removed and 40µl of recombinant IFN-β standard in triplicates and 1:2 serial dilutions in 10% FCS/PBS starting at 20U/ml was applied to the plate. 40µl sample supernatant (undiluted or diluted 1:2 with 10% FCS/PBS) were added to each well and incubated at 4°C over night. The following day the plates were washed and incubated over night with 50µl/well of detection antibody diluted 1:2000 in 10% FCS/PBS. After washing, the plates

were incubated for 2h with 50µl/well of anti-rabbit HRP diluted 1:2000 in 10% FCS/PBS. The plates were washed again and developed with TMB Substrate as described above.

2.2.13 Western Blotting

For protein analysis using Western Blotting, cells were mostly grown in 6 well plates. Adherent cells were harvested by removing the medium, washing the cell layer gently with 1x ice-cold PBS and after the PBS was removed completely, the cells were freeze-thawed by incubating the plate for at least 1h at -80°C. After thawing, cells were scraped into 80µl/well WB Lysis buffer, transferred to an eppendorf tube and incubated for 45min on ice with intermitting vortexing. Cell debris were removed by centrifugating for 10min at 15700g at 4°C. Lysates were transferred to a new eppendorf tube and mixed with the appropriate Sample buffer either for SDS- or Native-PAGE.

2.2.13.1 SDS-polyacrylamide gel electrophoresis (SDS-PAGE)

80µl lysates were mixed with 40µl 3x WB Sample buffer and boiled for 10min at 99°C. WB samples were stored at -20°C until Western Blot analysis. Samples were reboiled before 15-20µl sample were applied to a 10% SDS polyacrylamide gel. During SDS-PAGE the proteins were separated according to their molecular weight using 100V for 2-3h, the Mini-Protean Tetra cell system (Bio-Rad) and 1x Running buffer. In addition 7µl prestained protein marker were loaded to determine the molecular weight of the proteins of interest. The 10% SDS gels were made up one day before use and stored at 4°C in wet tissue. They consist of a stacking gel that was casted over a resolving gel (Table 2.13).

2x 10% SDS gels (1.5mm)	**6ml Stacking gel [µl]**	**15ml Resolving gel [µl]**
Protogel	1000	5000
Tris-HCl	750 (1M, pH 6.8)	3800 (1.5M, pH 8.8)
10% SDS	60	150
10% APS	60	150
Water	4100	5900
TEMED	6	6

Table 2.13: Composition of 10% SDS gels

2.2.13.2 Native-PAGE

Native gels were used for the IRF3 dimerisation assay. Cell lysates were mixed gently with native 3x WB Sample buffer (without SDS and DTT) and the samples were not boiled. Samples were stored at -20°C. 8% native gels were prepared the day before use. They had a similar composition as the SDS gels, but without SDS (Table 2.14). The gel chamber was put on ice. 2 gels were pre-run for 30min in pre-cooled 1x Native Running buffer (similar to 1x Transfer buffer, but without methanol) at 40mA (25mA for one gel). Then 1% deoxycholate (DOC) was added to the upper chamber (approximately 14ml of 10% DOC) and pre-run for another 30min. 20µl sample were loaded and run for 1h at 40mA. Transfer and immunoblotting for total IRF3 was performed as for SDS gels.

2x 8% native gels (1.5mm)	**8ml Stacking gel [µl]**	**15ml Resolving gel [µl]**
Protogel	1300	4000
Tris-HCl	1000 (1M, pH 6.8)	3800 (1.5M, pH 8.8)
10% APS	80	150
Water	5500	7000
TEMED	8	9

Table 2.14: Composition of 8% native gels

2.2.13.3 Transfer

The transfer of the separated proteins from the gel to a PVDF membrane was done by electroblotting using the Semi-Dry apparatus (Biometra). The membrane was first activated in methanol and then immersed in 1x Transfer buffer. Three sheets of whatman paper soaked in 1x Transfer buffer were placed on the semidry blotter and the membrane was placed on top. The gel was placed on top of the membrane and covered by 3 sheets of soaked whatman paper. Air bubbles were removed by rolling a 10ml pipette over the transfer sandwich. After blotting for 2h at 75mA/membrane, the membrane was washed in 1x TBS/0.05%Tween.

2.2.13.4 Immunoblotting

The membrane was first incubated in 3% BSA in TBS/0.05%Tween for 1h at RT to block nonspecific binding sites. Then the membrane was incubated overnight at 4°C in a Falcon tube with the primary antibody diluted 1:1000 in 4.5ml 3% BSA in

TBS/0.05%Tween. The next day, the membrane was washed 6 times for 5-10min in TBS/0.05%Tween before incubating for 1h with the fluorescent-labeled secondary antibody anti-rabbit 800CW (1:7000) or anti-mouse 680LT (1:10000) (LI-COR) in 4.5ml 3% BSA in TBS/0.05%Tween covered with tin foil. After 6 washes, the proteins were detected using the Odyssey Imaging system (LI-COR Biosciences).

2.2.14 Luciferase reporter gene assay

HEK293, HEK293-TLR4 and NIH3T3 cells were seeded at $1.5x10^5$, $2x10^5$ and $1x10^5$ cells/ml, respectively, in 96 well plates. The next day, plasmid DNA was transfected using GeneJuice Transfection Reagent. Each treatment was performed in triplicate (x3.5 wells). Per well, 60ng firefly luciferase reporter plasmid (pGL3-*Ccl5* promoter luc.) and 20ng *Renilla* luciferase plasmid (pRL-TK, Promega) were added to a V-bottomed 96 well plate. A GeneJuice transfection mixture was prepared by mixing 0.8µl GeneJuice with 9.2µl SFM per well. The mixture was vortexed and incubated for 5min at RT before adding to the DNA. The GeneJuice/DNA mixture was incubated for 15min at RT and 10µl/well were added to the cells. Approximately 19h after transfection, cells were stimulated and then harvested 12h later.

The supernatant was completely removed by pipetting and 50µl 1x Passive Lysis Buffer (made up in H_2O from 5x, Promega) were added per well and the plate was incubated for 20min at RT with vigorous shaking. 20µl of the lysates were transferred into two different white 96 well plates. The plates were analysed for either firefly or *Renilla* luciferase activity by adding 40µl Luciferase assay mix or 40µl coelenterazine (2µg/ml in 1x PBS) as a substrate, respectively. The samples were analysed spectrophotometrically using a microplate luminometer (Luminoskan, Thermo Scientific) and Ascent Software v2.6. Firefly luciferase activities were normalised to *Renilla* activities to account for differences in transfection efficiency and data were presented as fold induction compared to an untreated control.

2.2.15 Chromatin immunoprecipitation (ChIP) assay

2.2.15.1 Cell preparation -ChIP

1.5-2 x10^7 cells (BMDMs) were seeded in 30ml c.medium in 15cm dishes. The next day, cells were stimulated (e.g. 30min-3h LPS) and harvested. Cross-linking was performed by adding 27µl 37% formaldehyde per 1ml of medium (810µl/30ml) directly to the medium of the dish (final conc. 1% formaldehyde), while the dish was slowly shaking for 10min at RT under the fume hood. Formaldehyde was quenched by adding 141µl 1M glycine per 1ml of medium (4.2ml/30mls) incubated for 5min at RT. The dish was placed on ice and in the case of adherent cells the supernatant was removed and discarded. Adherent cells were washed twice gently with 10ml ice-cold 1x PBS, then cells were scraped into 5ml PBS and transferred into a 15ml conical tube. The remaining cells were transferred with another 5ml PBS. The pooled cell suspension was centrifuged at 1500g for 5min at 4°C. The cell pellet was resuspended in 1ml ice-cold PBS, transferred to an eppendorf tube and centrifuged. Cell pellets were stored at -80°C, if required. Cells were lysed in 1-1.5ml ChIP Lysis buffer (ChIP-b.) (optimal 1x10^7cells/1ml Lysis buffer) by resuspending the pellet and pipetting up and down several times. Lysates were centrifuged at 12000g for 1min at 4°C and supernatants were discarded. The nuclear pellets were resuspended and washed with 1ml ChIP-b./+inhibitors, followed by centrifugation. For sonication, the pellets were resuspended in approximately 1ml ChIP-b./+inh. per 1x10^7 cells. For optimal sonication efficiency the volume per eppendorf tube did not exceed 1ml. Sonication conditions were determined empirically using the Branson Sonifier 250 with a microtip. For BMDMs, 10 cycles of 15x 1sec pulses with 1min rest on ice between each cycle was found to generate optimal DNA fragment sizes ranging from 200-1000bp. The power output was 3 and 90% duty cycle. During the sonication, the microtip was kept only a few millimeters from the bottom of the tube to avoid foaming of the sample. The sheared chromatin lysates were cleared by centrifugation at 12000g for 10min at 4°C and the supernatant (sheared chromatin) was transferred to a new eppendorf tube. The sample was centrifuged once more and sheared chromatin was transferred to a new tube and stored at -80°C or directly applied to immunoprecipitation. A 50µl aliquot was transferred to an extra tube and stored at -80°C. This aliquot was used to analyse chromatin shearing efficiency on an agarose gel and also served as "Input DNA" control sample in the PCR analysis, after cross-links were reversed and DNA purified (described below).

2.2.15.2 *Immunoprecipitation (IP) -ChIP*

The following steps were performed on ice. Aliquots of 200µl sheared chromatin were used per IP (equivalent of approximately $2x10^6$ cells/IP) and diluted by adding 100-200µl ChIP-b./+inh.. The relevant antibody was added to the lysate (2µg of Pol II, IRF1 or IgG and 1µg of IRF3) and the sample was incubated overnight at 4°C while rotating. As mock IP served nonimmune IgG from the same species in which the specific antibodies were produced (here rabbit). The following day, Protein A-Sepharose beads were prepared by washing the beads 3 times with 1ml ChIP-b. with centrifugation at 1500g for 2min at 4°C. Then according to the volume of the 100% bead pellet the same volume of ChIP-b/+inh. was added to make a 50% bead slurry. To block nonspecific binding sites, beads were incubated with 1µg BSA (from 20mg/ml Stock solution) and 200ng salmon sperm DNA (10mg/ml Stock) per 1µl of 100% bead pellet for 30-40min at RT while rotating. After incubation, beads were washed once with ChIP-b. and a 50% bead slurry was aliquoted into eppendorf tubes as 40µl bead slurry/ IP. The overnight-incubated chromatin/antibody sample was centrifuged at 12000g for 10min at 4°C and the top 90% of cleared chromatin were transferred to the beads and rotated for 1h at 4°C. Beads were washed 5 times with 1ml ChIP-b. (without inh.) and centrifuged at 1500g for 2min at 4°C.

2.2.15.3 *DNA Isolation and PCR -ChIP*

100µl 10% Chelex slurry (w/v in mol. biol. H_20) were added to the washed bead pellet with the tip cut off. Sample was vortexed for 10sec and incubated at 99°C for 10min, while shaking. The sheared chromatin aliquot taken previously as "DNA Input" sample was precipitated using 3 volumes of 100% ethanol, centrifuged at 15700g for 10min at 4°C and washed with 70% ethanol. The dried pellet was dissolved in 100µl 10% Chelex slurry, vortexed and boiled similar to the beads. Once the "Input" and IP samples had cooled after boiling, 1µl Proteinase K (Stock 20µg/µl) was added, vortexed and incubated at 55°C for 30-40min, while shaking. Samples were boiled again for 10min to inactivate Proteinase K and centrifuged at 12000g for 1min at 4°C. 70µl supernatant were transferred to a fresh eppendorf tube, while avoiding taking any Chelex resin. Then, 70µl mol. biol. H_2O were added to the beads, vortexed 10sec and centrifuged. The 70µl supernatant was pooled with the previous 70µl. The DNA samples were centrifuged for 2min at 15700g at 4°C and 90% DNA solution was transferred to a fresh eppendorf tube to clear the sample from any resin

contamination. DNA was stored at -20°C until PCR analysis. "Input" DNA sample was dilute 1:10 or 1:20 before use.

Semi-quantitative PCR was performed according to the protocol depicted in Table 2.15 using primer pairs directed against the *Ccl5* promoter and *β-actin* promoter (see Table 2.6). The PCR products were resolved on a 1.2% agarose gel together with a DNA ladder. The DNA was visualised by ethidium bromide staining and UV illumination. The ChIP protocol is currently optimised for quantitative real-time PCR detection, which might require better DNA quality achieved by using a DNA isolation kit (Wizard® SV Gel and PCR Clean-up system, #A9282) instead of the Chelex DNA extraction.

PCR reaction mix [20µl]	Volume [µl]
5x Green GoTaq Buffer	4
$MgCl_2$ [25mM]	2
dNTPs [10mM]	0.4
Forward primer [5µM]	1.2
Reverse primer [5µM]	1.2
GoTaq DNA Polymerase	0.1
mol. biol. H_20	9.9
DNA template	1.2

Temperature [°C]	Time [sec]	Cycle number
95	120	1
95	30	35
59	30	
72	30	
72	300	1
4	hold	

Table 2.15: PCR protocol for semi-quantitative ChIP analysis

2.2.16 Fluorescence activated cell sorting (FACS) staining

2.2.16.1 Intracellular staining

$1x10^6$ PBMCs were collected in FACS tubes and the cell pellet was resuspended in 100µl 1x PBS/5%FCS. Cells were fixed and permeabilised using the IntraStain Kit (Dako). First, cells were fixed by diluting the cell suspension 1:2 with Reagent A and incubating for 15min at RT. After a wash in 1x PBS/5%FCS and centrifugation at 260g for 5min, the cells were incubated for 7min at 4°C with permeabilising Reagent B diluted 1:2 in 1x PBS/5%FCS. As a blocking reagent goat serum was used at 1:100 dilution. 16µg/ml primary anti-SARM antibody (rabbit) or an isotype control (rabbit IgG) was added and

incubated for 20min at 4°C. After two washing steps, the sample was incubated for 20min with 10µg/ml secondary anti-rabbit 488 antibody. The cells were washed twice and resuspended in 500µl 1x PBS/3%FCS for analysis on a CyAn flow cytometer (Dako).

2.2.16.2 *Cell surface staining*

Approximately $0.2x10^6$ cells were resuspended in 100µl FACS buffer (1x PBS/2%FCS with 0.15µM sodium azide) and incubated with 1:200 diluted F_c blocking reagent (purified rat anti-mouse CD16/CD32) for 10min at 4°C. Then 20µl of the fluorescent-labeled antibody dilution was added and incubated for 30min at 4°C (Table 2.16). Cells were washed twice with FACS buffer, resuspended in 250µl FACS buffer and applied to a CyAn flow cytometer (Dako). The analysis was performed using the FlowJo software (TreeStar).

Surface protein	Fluorescent label	Concentration [mg/ml]	Dilution
CD80	FITC	0.5	1:200
CD40	FITC	0.5	1:200
CD86	PE	0.2	1:500
I-A/I-E (MHCII)	PE	0.2	1:660
CD11c	APC	0.2	1:660

Table 2.16: Fluorescent-labeled antibodies used in DC maturation assay (FACS)

2.2.17 Confocal microscopy

Glass coverslips were immersed in 70% ethanol, air-dried and placed into the wells of a 24 well plate. NIH3T3 cells and BMDMs were seeded on glass coverslips at $1x10^5$ or $3x10^5$ cells/ml and treated the next day as required. For harvesting, the plate was placed on ice, medium was removed, adherent cells were gently washed with 500µl ice-cold 1x PBS and fixed in 200µl 4% paraformaldehyde (v/v in PBS) for 12min at RT. After 3 washes with PBS, the cells were permeabilised in 0.5% Triton X-100 in PBS for 15min. Coverslips were incubated with 400µl 5% BSA in PBS/0.05%Tween for 1h to block nonspecific binding sites. Then cells were stained with primary antibody diluted in 180µl blocking solution/coverslip in a humid chamber in 24 well plates overnight at 4°C (Table 2.17). After 3 washes with ice-cold PBS, coverslips were incubated with 180µl diluted secondary antibody for 3h at RT in a humid chamber in 24 well plates covered with tin

foil. Coverslips were washed 3 times in PBS and each coverslip was mounted with 3µl Mowiol 4-88 (Calbiochem) containing 1µg/ml DAPI. After 30min, the edges of the coverslips were sealed using nail polish and dried at least for 1h before images were obtained with an Olympus FV1000 scanning confocal microscope.

Primary antibody	Dilution
p65 (mouse)	1:200
IRF3 (rabbit)	1:200
FLAG (mouse)	1:300

Secondary antibody	Dilution
Anti-mouse Alexa 647	1:500
Anti-rabbit Alexa 488	1:500
Anti-mouse Alexa 647	1:500

Table 2.17: Antibody concentrations used in confocal microscopy

2.2.18 Amplification and purification of plasmid DNA

2.2.18.1 Transformation

NovaBlue Singles™ Competent Cells *E. coli* were thawed on ice, mixed gently and 10µl were transferred into a new eppendorf tube. Up to 500ng plasmid DNA (approximately 1µl) was added directly to the cells, mixed and incubated for 5min on ice. Tubes were placed for 40sec at 42°C and incubated on ice for another 2mins. 80µl SOC medium was added, mixed and the cell suspension was added on LB agar plates containing the selective antibiotic, here 100µg/ml ampicillin. The suspension was streaked over the agar plate using a yellow tip and plates were incubated overnight upside down at 37°C in a bacterial incubator. The next day, a single bacterial colony was picked to inoculate LB medium for Miniprep or Maxiprep purification. The agar plates were stored at 4°C.

2.2.18.2 Miniprep

A single bacterial colony was picked from the agar plate using a yellow tip and inoculated with 3-5ml LB medium containing 100µg/ml ampicillin in a 20ml tube. Bacteria were grown at 37°C with vigorous shaking in a bacterial shaker overnight (9-16h). The next day, 2ml bacterial culture were centrifuged at 5000g for 5min and plasmid DNA was isolated using the QuickLyse Miniprep Kit according to the manufacturer's instructions. Plasmid DNA was eluted in 50µl Buffer QLE and used for further restriction enzyme digestions and sequence analysis and stored at -20°C.

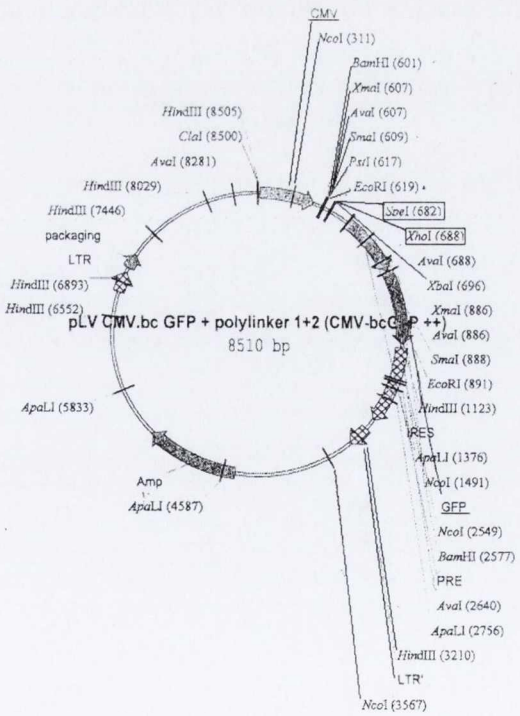
2.2.18.3 *Maxiprep*

As a starter culture, a single bacterial colony was inoculated with 3ml LB medium containing 100µg/ml ampicillin in a 20ml tube and incubated for 8h at 37°C with vigorous shaking in a bacterial shaker. 1ml starter culture was then transferred into an Erlenmeyer flask containing 100ml LB medium with 100µg/ml ampicillin and incubated overnight in the bacterial shaker. The next day, the bacterial suspension was transferred into 50ml Falcon tubes and centrifuged at 2500g for 15min at 4°C. Plasmid DNA was isolated using the EndoFree Plasmid Maxi Kit according to the manufacturer's protocol. The plasmid DNA pellet was redissolved in 500µl TE buffer and DNA concentration was determined spectophotometrically at 260nm using the NanoDrop (Thermo Scientific). Plasmid DNA was used for cell transfections and cloning and stored at 4°C and -20°C.

2.2.19 Cloning of mSARM-C-Flag into pLV-CMV

The pGW1-CMV vector encoding the 724aa isoform of murine SARM was a gift from Yi-Ping Hsueh (Taiwan) (119). The pLV-CMV-GFP was a gift from S. Keating (TCD, Dublin) originally obtained from P. Moynagh (Maynooth). Murine SARM was subcloned into pLV-CMV lentiviral vector using the restrictrion enzymes *Spe*I and *Xho*I, as depicted in the vecor map (

Figure 2.2).



To subclone murine SARM into pLV-CMV vector, primers were designed with *Spe*I and *Xho*I restriction enzyme sites that bound to the 5'- and 3'-end of the *Sarm* gene, respectively (see Table 2.6). The reverse primer (3'-end) additionally contained a Flag sequence (5'-3': GAT TAC AAG GAT GAC GAC GAT AAG) before the stop codon to create the C-terminal Flag-tag (DYKDDDDK). The new mSARM-C-Flag insert was generated using the Herculase II Fusion Enzyme PCR Kit according to the following protocol (Table 2.18):

Figure 2.2: pLV-CMV-GFP vector map

PCR reaction mix [50µl]	Volume [µl]
mol. biol. H_20 (to final vol.)	x
5x Reaction Buffer	10
dNTPs [25mM each]	0.5
pGW1 DNA template (50ng)	x
Forward primer [5µM]	2.5
Reverse primer [5µM]	2.5
DNA Polymerase	1

Temperature [°C]	Time [sec]	Cycle number
95	120	1
95	20	35
69	20	
72	80	
72	300	1
4	hold	

Table 2.18: PCR protocol to generate the mSARM-C-Flag insert

The expected size of the PCR product was 2213bp, which was controlled by resolving 10µl on a 1% agarose gel together with a DNA ladder (Figure 2.3). The DNA was visualised by ethidium bromide staining and UV illumination.

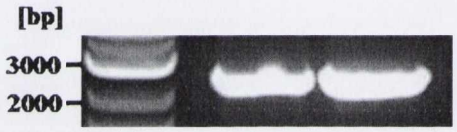


Figure 2.3: PCR product mSARM-C-Flag insert

The remaining 40µl PCR product were purified using the QIAquick PCR Purification Kit according to the manufacturer's instructions. The purified PCR product and 1µg target pLV-CMV expression vector were digested in separate tubes overnight at 37°C in the bacterial incubator using *Spe*I and *Xho*I restriction enzymes (Table 2.19).

PCR product digestion mix	Volume [µl]
DNA: mSARM-C-Flag	40
*Spe*I	0.5
*Xho*I	0.5
10x NEBuffer 4	4.5
100x BSA	0.45

Plasmid digestion mix	Volume [µl]
mol. biol. H_2O (to final 20µl)	x
DNA: pLV-CMV (1µg)	x
*Spe*I	0.5
*Xho*I	0.5
10x NEBuffer 4	2
100x BSA	0.2

Table 2.19: Digestion protocols of mSARM-C-Flag insert and pLV-CMV plasmid

Digested DNA products were gel purified from a 1% agarose gel using the Agarose GelExtract Mini Kit. The digested mSARM-C-Flag insert and pLV-CMV vector were ligated using the Clonables™ Ligation/Transformation Kit (see Table 2.20). The ligation mix was incubated for 15min at 16°C in a PCR machine.

Ligation reaction mix	Volume [µl]
2x Ligation mix	2.5
Digested vector	0.5
Digested insert	1.5

Table 2.20: Ligation reaction mix

The ligated plasmid (1µl) was transformed into competent bacteria (10µl) as described in 2.2.18.1. The next day, 9 single colonies were picked and individual bacterial cultures were inoculated for miniprep plasmid isolation according to the protocol 2.2.18.2. Then, 24µl of eluted plasmid were digested with *Spe*I and *Xho*I similar to the protocol given in Table 2.19 and clones were analysed on a 1% agarose gel and compared to an undigested control (Ctrl.) (Figure 2.4). Some of the plasmids that contained an insert of expected size were sent for sequencing (here clone 1 and 3). The expected mSARM-C-Flag sequence was encoded in clone 3, which was used in subsequent experiments. Maxiprep was performed to generate a highly pure plasmid preparation for cell transfections (2.2.18.3). The protein expression of mSARM-C-Flag was confirmed by analysing lysates of cells transfected with either pLV-mSARM-C-Flag or pLV-empty vector control using Western Blotting and anti-Flag antibody.



Figure 2.4: Screening of minipreps for pLV-mSARM-C-Flag following *Spe*I/*Xho*I-digest

2.2.20 Cloning of murine *Ccl5* promoter constructs into pGL3

The pGL3-Control Vector was purchased from Promega (Figure 2.5). It contained the SV40 promoter upstream of the firefly luciferase gene. *Xho*I and *Nco*I restriction enzymes were used to clone two different lengths of the murine *Ccl5* promoter that also contained the 5'UTR (+1/+57) into the pGL3-luciferase vector, replacing the SV40 promoter. The longer -190/+57 construct contained the ISRE and NF-κB elements, while the shorter -120/+57 construct lacked the ISRE. Forward and reverse primer pairs were designed containing *Xho*I and *Nco*I restriction enzyme recognition sites, respectively (see Table 2.6). The *Ccl5* promoter constructs were PCR amplified from a 927bp-DNA fragment generated earlier from wt and *Sarm*$^{-/-}$ pBMDMs, as described in 2.2.11. Thus, three PCR reactions were performed for each construct using either the wt or *Sarm*$^{-/-}$ 927bp-DNA fragment as a template and a no-template control, where the DNA template was replaced by water. The PCR reagents used were from the Herculase II Fusion Enzyme PCR Kit (Table 2.21).

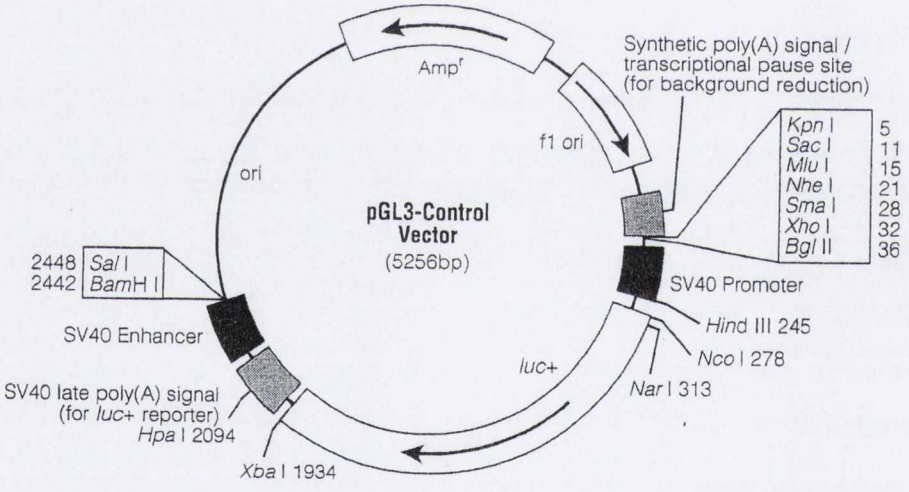


Figure 2.5: pGL3-luciferase vector map

PCR reaction mix [50µl]	Volume [µl]
mol. biol. H_20	32
5x Reaction Buffer	10
dNTPs [25mM each]	0.5
Forward primer [5µM]	2.5
Reverse primer [5µM]	2.5

Temperature [°C]	Time [sec]	Cycle number
95	120	1
95	20	35
63	20	
72	30	
72	300	1

DNA Polymerase	0.5	4	hold
DNA: 927bp-DNA fragment	2		

Table 2.21: PCR protocol to generate the *Ccl5* promoter constructs

The expected sizes of the -190/+57 and -120/+57 PCR products including the restriction sites were 258bp and 189bp, respectively, which was controlled by resolving 10µl on a 1% agarose gel together with a DNA ladder (Figure 2.6).

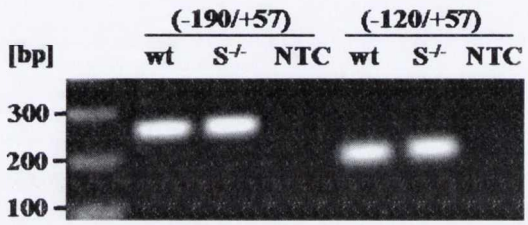


Figure 2.6: PCR products *Ccl5* promoter constructs

The remaining 40µl PCR products were purified using the QIAquick PCR Purification Kit according to the manufacturer's protocol. The purified PCR products and 1µg target pGL3-luciferase vector were digested with *Xho*I and *Nco*I in separate tubes overnight at 37°C in the bacterial incubator, similar to the protocol given in Table 2.19. Digested DNA products were gel purified from a 1% agarose gel using the Agarose GelExtract Mini Kit. The digested *Ccl5* promoter inserts and pGL3 vector were ligated as described above using the Clonables™ Ligation/Transformation Kit according to Table 2.20. Similar to 2.2.19, after bacterial transformation and culture, several minipreps were screened for inserts and positive clones were sent for sequencing. Plasmids that contained the correct sequence of the wt and *Sarm*$^{-/-}$ *Ccl5* promoter fragment were amplified using maxiprep and subsequently used for luciferase reporter gene assays (2.2.14).

2.2.21 Statistical analysis

The graphs were generated following data transfer into GraphPad Prism v.5.02 software. Statistical analysis was performed using the two-tailed unpaired student *t* test.

3 SARM expression in human and murine cells and implications for immune responses

3.1 Introduction

Shortly after the engagement of a TLR with its specific microbial ligand, the receptor selectively recruits TIR domain-containing adaptor proteins to mediate downstream signalling. The specific signalling cascade depends on the TIR adaptor used and finally leads to selective or combinatorial transcription factor activation, including NF-κB, AP-1 and IRF3. They in turn induce the gene expression of inflammatory cytokines, chemokines and type I interferons (IFNs) to initiate the appropriate immune response. The four TIR adaptor proteins MyD88, MAL, TRIF and TRAM are well known for their essential positive function in different TLR signalling pathways, shown extensively in overexpression and knockout mouse studies. However, the immunological function of the fifth, most evolutionarily conserved TIR adaptor SARM is not fully understood. Differences from the other family members emerged in overexpression studies, where SARM failed to activate transcription factor NF-κB- or IRF3-dependent reporter constructs, usually selectively driven by the other TIR adaptors (43). Instead a study by Carty et al. from my laboratory demonstrated that human SARM had a negative regulatory role in TRIF-dependent TLR signalling (44). Human SARM was shown to directly interact with TRIF and inhibit TLR3- and TLR4-mediated gene induction, when overexpressed. Likewise knockdown of endogenous SARM using siRNA enhanced LPS-induced TNF-α production in human PBMCs. Also an increase in SARM protein was observed almost immediately after LPS stimulation, most likely due to stabilisation of the protein by its N-terminus. However, studies of SARM knockout mice have recently questioned the immunological function of SARM in murine immune cells. Analysing SARM-knockout bone marrow-derived macrophages (BMDMs), Kim et al. observed normal cytokine (TNF-α) and chemokine (MCP-1) responses to a range of TLR agonists, including the TLR3 and TLR4 ligands Poly(I:C) and LPS, respectively (220). They demonstrated that among human and mouse immune cells, myeloid cells barely expressed SARM, while it was detectable in lymphocytes. However, the highest expression of SARM was found in neurons of the brain, where it associated with mitochondria, microtubules and JNK3 and mediated stress-induced neuronal cell death following deprivation of oxygen and glucose.

Nevertheless, given the immunological function of SARM in lower organisms such as *C. elegans* (as described in 1.4) and its high degree of conservation among species throughout evolution, additional functions for murine SARM in immunity are likely to emerge. The hypothesis of an immunological role of SARM in the brain was recently addressed by Szretter et al. in a study where they infected SARM knockout mice with neurotrophic WNV (221). Mice lacking SARM showed enhanced mortality upon infection. Surprisingly, the pathogenic phenotype was mainly restricted to the brainstem, where SARM-deficient mice displayed a reduced TNF-α level, decreased microglia activation and increased neuronal cell death accompanied by higher viral replication. This observation indicated a positive regulatory function of SARM in the immune response in mammals, which might have been conserved throughout evolution. However the mechanism was not further elucidated in this study. So far, the reported differences between the function of SARM in human PBMCs compared to the murine brain may be explained by a cell type- and/or species-specific function. But differences also emerged regarding the tissue expression profile of human and mouse SARM. An early study demonstrated a liver- and kidney-restricted expression of SARM in human tissue, while the murine studies revealed a more brain-restricted expression profile (202, 220, 221). However Szretter et al. also detected a weak expression of murine SARM in the liver but not in the kidney. Interestingly, the latter study also indicated a weak expression in BMDMs. In light of these human-mouse functional discrepancies and the questioned SARM expression in myeloid cells, it was reasonable for the first part of the project to characterise SARM in human and murine immune cells and murine tissues in more detail. Besides evaluating its expression, I also gained insights into the subcellular localisation of SARM. Furthermore, I investigated a possible modulation of SARM expression by TLR stimulation, as this would emphasise its role in immune responses. Then, to follow up on the study by Carty et al. and to further investigate the negative role of SARM, I examined cytokine responses in human cells after siRNA-mediated reduction of SARM.

3.2 Results

3.2.1 SARM expression and its downregulation following immune stimulation

Conflicting functional data regarding SARM emerged from human and murine studies. The TRIF-inhibitory function of SARM was observed in human HEK293 cells and PBMCs, including a TLR4-mediated upregulation of SARM protein (44). However a more recent study questioned the SARM expression in myeloid cells and the use of the commercially available SARM antibody (220). Hence, I sought to investigate SARM expression in PBMCs in more detail. Therefore PBMCs were isolated from buffy coats using Ficoll density centrifugation and the whole population was stained for intracellular SARM protein. SARM was detected using the commercially available antibody raised against human SARM (from ProSci), followed by Alexa 488-conjugated secondary antibody and analysis by flow cytometry. The dot blot revealed three subpopulations due to the different sideward scatter (SSC) representing the granularity/complexity of a cell and the strength of autofluorescence detected in the Alexa 488 channel (Figure 3.1a, top panel). In an independent experiment I identified the subpopulations of the scatter using cell type-specific surface markers (data not shown). The population with the low SSC and the absence of autofluorescence represented B and T lymphocytes, while monocytes shifted to the right due to their autofluorescence. These cell types are known as the main constituents of PBMCs. The third population with a high and elongated SSC represented granulocytes, which can appear in the PBMC preparation as contaminants. Analysing SARM fluorescence compared to the control, I observed a shift of the whole PBMC population (98%), displayed in the histogram (Figure 3.1a, lower panel). The shift was similar in all three subpopulations (Figure 3.1a, top panel), indicating equal expression of SARM protein in lymphocytes, monocytes and granulocytes. To prove the specificity of the SARM antibody and to confirm SARM protein expression in human PBMCs, immunoblot analysis was performed. Lysates of PBMCs were resolved on a 10% SDS-Polyacrylamide gel followed by Western Blotting using the same SARM antibody. The blot was also probed for β-actin as a loading control. To control for antibody specificity, PBMCs treated with two different SARM-specific siRNA oligonucleotides, hS1 and hS2, to knockdown endogenous SARM protein were included in the analysis, as well as a nontargeting control siRNA. The immunoblot revealed only one band of the expected molecular weight of 75-

79kD, which was reduced by the SARM-specific siRNA in a dose-dependent manner, but not by control siRNA (Figure 3.1b), confirming the specific detection of SARM in PBMCs. Two main isoforms of human SARM have been described, a 690aa and a 724aa form with expected molecular weight of 75 and 79kD, respectively. I suspect that the band detected in PBMCs represents the 690aa SARM, as it ran at a similar height as overexpressed 690aa SARM in HEK293 cells (data not shown).

Previous studies in our laboratory showed that LPS treatment of human PBMCs enhanced SARM protein level almost immediately (44). To further elucidate the TLR4-mediated regulation of SARM, I analysed the effect of TLR stimulation on *SARM* mRNA. Therefore human PBMCs were isolated and stimulated with LPS and CLO75 for 4 and 24h. The TLR7 agonist CLO75 was included in the analysis as a control, given that it activated a TRIF-independent, MyD88-dependent TLR signalling pathway. Quantitative real-time PCR analysis was performed in order to assess *SARM* mRNA expression. The mRNA was normalised to the housekeeping gene *β-actin* and the results of four donors are presented in percentage relative to each untreated control. In contrast to the known stabilising effect of LPS on SARM protein, the mRNA expression was significantly reduced following stimulation with both TLR ligands (Figure 3.1c). The reduction of *SARM* mRNA was already apparent 4h after TLR stimulation and decreased further at 24h. Surprisingly, TLR7 signalling was particularly potent in downregulating *SARM* mRNA, reflected in a 85% reduction 24h after CLO75 treatment. 24h LPS also reduced the *SARM* expression by 64%. The opposite TLR-mediated effect on SARM message compared to protein indicated a complex regulatory mechanism of SARM expression. Altogether it suggested a role for SARM in TLR-dependent responses and that its function might be regulated by its expression level.

Nevertheless, the study by Kim et al. using *Sarm*-knockout mice has questioned the TLR-related function of SARM, as BMDMs showed normal cytokine and chemokine expression in response to a range of TLRs, including TLR4 and TLR7 (220). Also they demonstrated that myeloid immune cells expressed low level of SARM compared to its high expression in the brain. To address this discrepancy to the human PBMC data, I evaluated SARM expression in primary and immortalised BMDMs (named pBMDMs and iBMDMs) and different murine tissues. I obtained femurs of wild-type (wt) and *Sarm*$^{-/-}$ mice from A. Ding and later K. Fitzgerald and generated pBMDMs using the growth factor M-CSF. The iBMDM cell line of both genotypes were generated and provided by K.

Fitzgerald. First, I verified the wt and *Sarm*-knockout genotype of these cells by PCR analysis of the genomic *Sarm* locus. The knockout mouse had Exon 3-7 of the *Sarm* gene replaced with a neomycin resistance gene in reverse orientation to preclude any production of truncated proteins (220). Hence the PCR primer pair to detect the mutated *Sarm* locus was directed against the neomycin cassette, which was only present in the knockout genotype, and expected to generate a PCR product of approximately 200bp. The wt *Sarm* locus was analysed using primers spanning a 500bp DNA region from Exon 3 to Intron 4, which was absent in *Sarm*-knockout genomic DNA. The PCR products amplified in the two different PCR reactions were resolved on a 1% agarose gel and visualised by ethidium bromide staining and UV illumination. The genomic DNA analysis of wt and $Sarm^{-/-}$ pBMDMs and iBMDMs confirmed the expected genotypes (Figure 3.2a). Next I attempted to investigate SARM protein expression in these cells. Lysates of pBMDMs and iBMDMs were subjected to immunoblot analysis and different SARM antibodies were used due to the concerns regarding antibody specificity. β-actin served as a loading control. The SARM antibodies were either purchased from Santa Cruz and ProSci or were a gift from A. Ding. The commercially available antibodies were most likely identical, except that the Santa Cruz antibody was less concentrated than the one purchased from ProSci. In addition to wt cells the analysis also included $Trif^{-/-}$ iBMDMs and as a negative control $Sarm^{-/-}$ p/iBMDMs. Two isoforms of murine SARM are reported. Similar to humans, mice express a 724aa SARM with expected molecular weight of 79kD, but also a longer 764aa form (84kD) that harbours an additional region between the second SAM domain and the C-terminal TIR domain. All SARM antibodies revealed a protein band of the expected molecular weight in iBMDMs (Figure 3.2b), which ran at a comparable height to overexpressed 724aa murine SARM (data not shown). However, this protein band was also present in SARM-deficient iBMDMs, but with significantly reduced intensity compared to wt, using the less concentrated Santa Cruz antibody or the non-commercial antibody from A. Ding. This demonstrated that besides SARM, the antibodies nonspecifically detected another murine protein of the same molecular weight as SARM that was apparent in the knockout cells. The nonspecific detection was particularly pronounced using the higher concentrated ProSci SARM antibody. Nevertheless, the reduction in the protein band of $Sarm^{-/-}$ compared with wt iBMDMs was evidence for SARM protein expression in this cell type. Of note is, that this protein band was absent in pBMDMs, where also no second nonspecific protein was detected (Figure 3.2b). This indicated that SARM protein

expression in pBMDMs was lower than in iBMDMs and possibly fell below the detection limit. Overall, these observations limit the usefulness of the antibody in murine cells and with it any reliable SARM protein analysis. As a different approach to assess SARM expression in BMDMs, I analysed its mRNA level using quantitative real-time PCR. I was able to detect *Sarm* transcripts in wt pBMDMs and not in SARM-deficient cells, confirming the specificity of detection (Figure 3.2c). Given the TLR-mediated modulation of SARM expression in human PBMCs (shown in Figure 3.1c), I asked if a similar regulatory mechanism was present in murine BMDMs. As the effect in PBMCs was observed with TLR ligands independent of TRIF, I decided to include IFN-α as a non-TLR agonist, in addition to the TLR4 agonist LPS. IFN-α binds to the type I IFN receptor and activates a totally different signalling cascade compared to TLR and other PRR pathways. Interestingly, also in pBMDMs I observed a dramatic downregulation of *Sarm* mRNA 6h after LPS treatment, with only 2% remaining on average in three independent experiments (Figure 3.2c). Unexpectedly, the TLR-independent stimulus IFN-α also significantly reduced *Sarm* levels. This suggested that SARM may play a role in the immune response of human and murine immune cells, as its expression is detectable and modulated by immune stimulation in these cells.

Next, I wanted to evaluate SARM expression in immune cells compared to other murine tissues, especially because recent studies claimed that its main expression is found in the brain (220, 221). Hence I examined SARM mRNA and protein levels in various murine tissues and compared them to the level observed in BMDMs. Organs such as liver, brain, lung, kidney and intestine were isolated from two mice and processed for quantitative real-time PCR and immunoblot analysis. As known from the previous experiment, the protein detection using the SARM antibody has to be interpreted with caution due to nonspecific reactions. Therefore I performed the immunoblot analysis again with two SARM antibodies, the commercial SARM antibody from ProSci and the non-commercial antibody from A. Ding. Consistent with published work, I observed the highest SARM mRNA and protein expression in the brain (Figure 3.3a, b). Also liver and lung expressed some *Sarm* mRNA, but to a much weaker extent, and the protein was barely detectable in these organs. No SARM mRNA and protein were detectable in kidney and intestine. Direct comparison of the *Sarm* mRNA levels in pBMDMs with the brain revealed 300-fold higher levels of *Sarm* in brain tissue (Figure 3.3b, lower panel). The comparison of SARM protein level in iBMDMs with the brain was more difficult (Figure

3.3a), because the previous analysis has shown that the detected protein band in wt iBMDMs represented SARM, but also another protein nonspecifically detected by the SARM antibody. However, the SARM-specific siRNA S1 reduced the amount of detected protein in iBMDMs, suggesting that a relevant amount of SARM protein is expressed in these cells compared to the brain.

In addition to analysing the cell type-specific expression profile, insights into the potential function of a protein can also be gained by characterising its subcellular localisation. Confocal microscopy is a suitable technique to delineate the localisation of a protein within a cell, but the lack of a reliable SARM antibody precluded the analysis of endogenous SARM protein. Therefore I generated a construct to overexpress 724aa mouse SARM tagged with Flag at its C-terminus to allow detection using an anti-Flag antibody. Murine NIH3T3 cells were transiently transfected with mSARM-C-Flag and confocal microscopy was performed after staining for Flag. Nuclei were visualised with the DNA-intercalating dye DAPI. I found that murine SARM associated with punctuate structures in the cytosol (Figure 3.4). The higher magnification revealed a clear circular assembly of SARM, as if it covered the outside of a cytosolic structure. This observation coincided well with the report by Kim et al., where the punctuate structures were identified as mitochondria and SARM appeared to be more located to the outside of these organelles (220).

3.2.2 Divergent effects of siRNA-mediated SARM knockdown on PRR-induced cytokine responses

After having established that human and murine immune cells expressed SARM and regulated SARM expression upon TLR and type I IFN stimulation, I sought to assess its potential function in TLR and non-TLR pathways. Following up on the study by Carty et al., which showed the TRIF-inhibitory role of SARM in TLR3 and TLR4 signalling mainly in human HEK293 cells, I choose this cell type for the analysis (44). Most of the reported data were based on overexpression studies, but siRNA-mediated knockdown of endogenous SARM confirmed the negative function on TLR3-induced CCL5 protein. Hence I decided to use *CCL5* mRNA expression as readout for SARM function in the following experiments, also because it was induced by a combination of transcription factors, including NF-κB and IRF3 (229). To first investigate a TRIF-dependent TLR

pathway, I examined LPS-induced CCL5 expression in HEK293-TLR4 cells treated with two different SARM-specific siRNA oligonucleotides, h_S1 and h_S2, to suppress endogenous SARM level. Due to the lack of a reliable SARM antibody, I evaluated SARM knockdown using quantitative real-time PCR. Both siRNAs were effective in downregulating *SARM* mRNA more than 50% (Figure 3.5a). S1 was more potent and reduced *SARM* levels by 65%, compared to a 53% reduction with S2, whereas mock-transfected or cells transfected with nontargeting control siRNA showed little effect on *SARM* expression. I noted that LPS stimulation slightly reduced *SARM* mRNA levels in general, which was in agreement with the previously observed TLR-mediated modulation on SARM expression. Analysing CCL5 mRNA and protein following LPS stimulation revealed impaired CCL5 production in cells treated with S1 siRNA, but not S2 (Figure 3.5b, c). S1-mediated SARM knockdown reduced CCL5 mRNA and protein expression by 50% compared to the control, and the effect was even more prominent using a lower concentration of siRNA (Figure 3.5c). However, no impairment in CCL5 production was observed in S2-treated cells, even though some SARM knockdown was achieved. It is possible that the better knockdown with S1 reduced the SARM level below a threshold necessary to elicit an effect. The result of a potential requirement of SARM in TLR4-mediated CCL5 induction was unexpected, as SARM was shown previously to inhibit TRIF-dependent pathways, like TLR4, in these cells. To determine if the observed effect was TLR- and TRIF-restricted I repeated the siRNA experiment in normal HEK293 cells lacking TLRs and stimulated CCL5 induction via the cytosolic RLR pathway. Transfected Poly(I:C) and Sendai virus served as ligands to activate the cytosolic MDA5 and RIG-I receptor, respectively, which signal in a TRIF-and MyD88-independent manner to induce genes such as *CCL5* and *IFN-β*. A successful downregulation of *SARM* mRNA was achieved using both siRNA oligonucleotides (Figure 3.6a). The knockdown was even more significant than seen previously, with 77 and 67% reduction after S1 and S2 siRNA treatment, respectively. Surprisingly, the experiment revealed that the non-TLR-mediated *CCL5* expression was also impaired in samples treated with SARM-specific siRNA compared to control (Figure 3.6b, c). Likewise, the induction of *IFN-β* mRNA was suppressed in these samples (Figure 3.6d, e). Consistent with the experiment in HEK-TLR4 cells, the defective cytokine production was only observed following S1-mediated SARM knockdown and not S2, even though S2 was almost as effective as S1 in reducing *SARM* mRNA level. As described above, the small difference in SARM expression level

may account for this divergent effect. Another explanation could be the immunostimulatory potential of some siRNAs, which in turn might mask the real effect caused by the protein knockdown. This hypothesis was supported by the observation that cells treated with nontargeting siRNA showed a slight enhancement of cytokine expression compared with mock-transfected cells, also basally (Figure 3.6b-e). To test the immunostimulatory potential of the siRNAs used, I treated HEK293 cells with three different doses of nontargeting control, S1 and S2 siRNA. A similar *SARM* mRNA knockdown was achieved with all three doses, leading to significant 70% reduction using S1 siRNA and 58% reduction with S2 (Figure 3.7, top graph). Analysing *CCL5* induction in response to transfected Poly(I:C) exhibited the same S1/S2 siRNA-mediated divergence observed previously (Figure 3.7, bottom graph). Interestingly, the S1-dependent *CCL5* inhibition was most significant at the lowest dose of siRNA and gradually became less prominent with increasing doses of siRNA, even though *SARM* mRNA level were equally reduced with all three doses. This clearly indicated an immunostimulatory side effect of S1 siRNA at higher doses. In light of this it was surprising that S2 siRNA did not provoke a similar stimulation, as I would have predicted from the divergence with S1. Also the nontargeting control siRNA was inert in this experiment. This illustrated that the unwanted immunostimulatory capacity of siRNAs varies between different oligonucleotides, possibly due to differences in the nucleotide sequence and their putative binding to immunoreceptors.

In summary, the analysis revealed that human and murine immune cells clearly expressed SARM, and that its expression was regulated following immune stimulation. This indicated a role for SARM in immune responses in myeloid cells, even though its predominant expression was found in the brain. Furthermore I determined that murine SARM was mainly located at punctuate structures in the cytosol. An initial approach to further investigate SARM function in human HEK293 cells was inconclusive due to divergent effects of the SARM-specific siRNA.

3.3 Discussion

The function of the fifth, highly conserved TIR-adaptor SARM is still not fully understood and conflicting data emerged from studies of human and mouse SARM, as described in 1.4. That its function might diverge from the other four TIR adaptors was already demonstrated in 2004 by Liberati et al., as it did not activate NF-κB and IRF3 reporter constructs, when overexpressed (43). Furthermore its unique domain architecture and its high conservation during evolution suggested a fundamental, possibly divergent role in immunity. A function of mammalian SARM was first discovered by Carty et al. in 2006, elucidating human SARM as an inhibitor of TRIF-dependent TLR3 and TLR4 signalling in HEK293 cells and PBMCs (44). However this function was questioned with the generation of SARM-knockout mice. First, murine SARM-deficient BMDMs responded normally to a range of TLR agonists, including Poly(I:C) and LPS. Second, SARM expression was mainly restricted to the brain, while barely detectable in myeloid cells (220). Due to this discrepancy it was important for the first part of the project to assess SARM expression in primary human and murine immune cells more rigorously and also to evaluate its expression in comparison to murine tissues, such as the brain. The characterisation of protein expression in different cells and tissues is often informative and might provide some clues regarding its function.

The expression study revealed that murine SARM mRNA and protein was indeed predominantly expressed in the brain, compared with other tissues and primary BMDMs, which is in agreement with published reports (220, 221). Besides the brain, only liver and lung expressed some *Sarm* mRNA, but much weaker, while it was not detectable in kidney and intestine. This concurred with a study by Szretter et al., which showed also a weak expression in murine liver, and also data on human SARM, where it was predominantly found in liver and kidney (202, 221). On a cautionary note it should be mentioned that all *Sarm* mRNA levels were normalised to the housekeeping gene *β-actin*, which may vary between different tissue cell types, representing a limitation of the method. However, confidence was gained by the fact that the *Sarm* mRNA data in murine tissues correlated with the protein detection. In addition to the pronounced expression in the brain, I was able to detect SARM also in immune cells, such as murine BMDMs and human PBMCs. This was interesting, as the presence in those cell types was recently questioned by Kim et al. (220). They also raised concerns of using the commercially available SARM antibody due

to detection of a protein at similar molecular weight as SARM in SARM-deficient cells. This nonspecific reaction of the SARM antibody was also observed in my study. However I detected a reduction of the putative SARM protein band in *Sarm*-knockout iBMDMs compared to wt, as well as in wt iBMDMs treated with SARM-specific siRNA. This was revealed by using a more diluted solution of the commercial SARM antibody and the non-commercial antibody provided by A. Ding, and gave evidence for some SARM protein expression in those cells. Unfortunately, no SARM protein was detected in pBMDMs. But given the presence of *Sarm* transcript in pBMDMs and the detection of the protein in iBMDMs, this was most likely caused by low antibody sensitivity, meaning that the SARM protein level in pBMDM probably fell below the detection limit. In contrast to iBMDMs, the primary cells and the murine tissues did not display any nonspecific protein at the molecular weight of SARM. This suggested the specific detection of SARM in the brain, further emphasised by its correlation with the mRNA data. Due to the different approaches of SARM detection at the mRNA and protein level, I am confident that SARM is expressed in murine BMDMs and the brain. However the nonspecific reaction of the SARM antibody in murine cells limits the execution of further protein studies. The development of a new, more specific SARM antibody has not been successful so far.

With regard to human immune cells I was also able to confirm SARM expression. The nonspecificity of the SARM antibody was here less of a concern, as SARM-specific siRNA almost completely abrogated SARM protein in PBMCs. FACS analysis of the whole PBMC population revealed that SARM was likely expressed to a similar extent in the different PBMC subpopulations, including T and B lymphocytes, monocytes and granulocytes. This was confirmed in an independent experiment on FACS-separated PBMC subpopulations and analysis of SARM mRNA and protein by quantitative real-time PCR and immunoblot, respectively (data not shown). The latter experiment gave evidence for a slightly elevated expression in lymphocytes compared with monocytes, which correlated with published work (220).

After having established that SARM is expressed in human and murine immune cells, I next investigated a potential TLR-mediated impact on SARM expression in these cells, which might provide further insights into its function. Previously, Carty et al. had shown an increase of SARM protein almost immediately after LPS stimulation in human PBMCs, possibly due to stabilisation of its N-terminus (44). Due to the concerns regarding the SARM antibody, I decided to examine regulation of *SARM* mRNA. Surprisingly, the

mRNA analysis revealed a dramatic downregulation of *SARM* message following TLR4 and TLR7 stimulation. The reduction of *SARM* mRNA was already observed 4h after stimulation, but became much more significant at 24h. The TLR7 ligand CLO75 was especially potent in suppressing *SARM* mRNA expression, which was unexpected given the TRIF-independent signalling of this pathway. A similar observation was reported from an in vivo study in humans, where SARM mRNA and protein levels in blood leukocytes decreased 4-8h after LPS injection and slowly returned to basal level at 24h (227). During this time period cells were refractory to restimulation with LPS, but also to other TLR ligands that used MyD88-dependent and -independent signalling pathways; a phenomenon known as LPS tolerance and cross-tolerance, respectively. This could not be explained in light of the TRIF-inhibitory role of SARM. In contrast, another study on endotoxin tolerance reported an increase of *SARM* mRNA 3-20h after LPS treatment in human monocytes (226). Thus the TLR-mediated regulation of SARM expression might be quite complex. Accordingly, my study and the data from Carty et al. revealed a divergence in SARM mRNA and protein regulation (44). While the *SARM* mRNA level slowly decreased, the protein was immediately elevated 1h after LPS treatment and persisted up to 24h. For the protein expression this suggested a translational or posttranslational mechanism, which are often used in immune responses to rapidly modulate gene expression, as opposed to the more long term regulation via transcription (230). Control of translation is often mediated by proteins binding to the 5' and 3' untranslated regions (UTRs) of target mRNAs. However, in the case of SARM protein the TLR4-induced upregulation was also seen with overexpressed SARM, that lack UTRs, hence the increase was most likely caused by stabilisation of the protein itself. This was supported by analysing an N-terminal truncated form of SARM protein, which was more stable and expressed independently of LPS stimulation (44). Thus SARM protein might be inherently unstable due to motifs in its N-terminus, which is subsequently reversed by TLR4 signalling. Preliminary data indicated that basal ubiquitination of the N-terminus might target SARM protein for proteasomal degradation (M. Carty personal communication, (231)).

As the immune function of SARM was specifically questioned in murine macrophages, I was curious to examine pBMDMs for the TLR-mediated modulation of SARM expression observed in human PBMCs. Due to the unspecificity of the SARM antibody in murine cells, it was not possible to assess SARM protein. However, the mRNA analysis

revealed, consistently with human immune cells, a dramatic downregulation of *Sarm* following TLR4 activation. In fact, *Sarm* levels were almost completely abrogated 6h after stimulation, exhibiting an even more rapid and pronounced phenotype than observed in PBMCs. In PBMCs, this effect was not restricted to TRIF-dependent pathways and also elicited by the MyD88-dependent TLR7. Hence, to further specify *Sarm* regulation, I used the PRR-independent stimulus IFN-α. IFN-α signals via the type I IFN receptor (IFNAR) and activates different signalling molecules and transcription factors to finally induce a specific set of IFN-stimulated genes (ISGs). Surprisingly, the IFN-α stimulation also led to a significant reduction of *Sarm* message. Given that TLR4 and TLR7 signalling also induce the expression of type I IFNs, such as IFN-α and IFN-β, it is possible that SARM might be regulated by the type I IFN pathway in a secondary response rather than the TLR pathway directly. The mechanism mediating the downregulation of *SARM* message in human and murine immune cells could be either transcriptional suppression or an acceleration of mRNA decay. The latter is controlled by various proteins and miRNAs that bind the 3' UTR of target mRNAs (230). Regulation of gene expression by miRNAs is an emerging field in immunity and TLR and IFN signalling pathways have been shown to induce certain immunoregulatory miRNAs (232, 233). Thus, detailed analysis is required to elucidate the mechanism of the complex SARM regulation, including the relation of mRNA and protein expression. The fact that *SARM* mRNA expression is significantly downregulated by TLR and probably IFNAR stimulation in human and murine immune cells indicated a crucial role for SARM in immune responses in these cells. However, it is difficult to explain the modulation in light of the TRIF-inhibitory function of SARM, as also TRIF-independent pathways, like TLR7 and IFNAR, were strong mediators of SARM suppression. One can speculate that the rapid enhancement of SARM protein is required for its immediate function in immunity, while the subsequent decrease of *SARM* mRNA restores homoeostasis later on in the response. Negative regulators of immune signalling pathways are generally transcriptionally upregulated in a feedback loop to avoid excessive immune responses with detrimental consequences to the host (234). However, the rapid stabilisation of SARM protein and the downregulation of the message by TLRs and IFNAR might suggest a positive immune function of SARM, maybe independent of TLRs and TRIF. This hypothesis is supported by the immune function of SARM in lower organism, such as *C. elegans*, where the SARM homologue TIR-1 exerts a positive role in immunity independent of the sole TLR homologue TOL-1 (see 1.4).

To gain further insights as to where SARM might be functionally active within a cell, I next assessed the subcellular localisation of SARM. Due to the concerns regarding the SARM antibody, I overexpressed Flag-tagged SARM in murine NIH3T3 cells and examined the cellular localisation following staining of Flag and confocal microscopy. The analysis clearly revealed an association of SARM with punctate structures in the cytosol. This was in agreement with the literature, where the structures were identified as mitochondria (220). In line with the data presented by Kim et al., SARM seemed to assemble more at the outside of the cytosolic structure. Also a recent, more detailed study on SARM localisation demonstrated the specific targeting of SARM to mitochondria (207). The N-terminal 27aa of SARM were identified as a mitochondria-targeting sequence with an inherent ability to bind lipids. Furthermore it was suggested that SARM translocates into the mitochondria, as observed with EGFP fused to the C-terminus of the 27aa-leader sequence. The current proposed function at the mitochondria implicates SARM in the apoptotic pathway. SARM was shown to recruit JNK3 to mitochondria and induce neuronal death after oxygen and glucose deprivation (220). Furthermore, a role in apoptosis in T cells is discussed (207). It will be interesting to investigate more direct immune functions of SARM from the mitochondria, given that these organelles provide an essential and highly diverse platform for various immune responses, including MAVS and STING signalling (235).

Following up on the study by Carty et al. (44) and to gain further insights into a possible function of SARM in TLR- and TRIF-independent pathways, I analysed immune responses in HEK293 cells after siRNA-mediated knockdown of SARM. Using two different SARM-specific siRNA oligonucleotides, S1 and S2, I observed an effect on immune responses only with one oligonucleotide, whereas the other was mostly inert. The analysis of the TRIF-dependent TLR4 pathway in HEK293-TLR4 cells revealed a requirement of SARM for CCL5 mRNA and protein induction using S1 siRNA, but this was not observed with S2. Apart from the divergence of the two siRNAs, this result was unexpected given the reported TRIF-inhibitory function of human SARM (44). A similar observation was made investigating the TRIF-independent, RLR-mediated cytokine response. Stimulating the MDA5 or RIG-I pathway with transfected Poly(I:C) or Sendai virus, respectively, induced *CCL5* and *IFN-β* expression in HEK293 cells, that were impaired in S1-treated cells, while unaffected following S2-mediated knockdown. The divergent effect was difficult to explain, as both siRNA oligonucleotides significantly

downregulated *SARM* mRNA, with 70 and 60% reduction using S1 and S2 siRNA, respectively. However it is possible that the slightly better knockdown using S1 reduced the SARM level below a threshold necessary to suppress SARM function, which was then only revealed by S1 and not S2 siRNA. Another explanation could be the known immunostimulatory capacity of some siRNAs, which in consequence may affect cytokine readouts. Especially the RNA-sensing endosomal TLRs, TLR3, 7 and 8, and the cytosolic RLRs, mainly RIG-I, have been implicated in detecting siRNAs depending on the sequence and structure of the RNA molecule (reviewed in (236)). Therefore, if S2 siRNA was slightly more immunostimulatory than S1 in HEK293 cells, which express cytosolic RLRs, but lack TLRs, this might have masked the inhibitory effect on CCL5 expression seen in S1-treated cells. Some initial experiments showed indeed an enhanced cytokine response in cells treated with nontargeting control and S2 SARM-specific siRNA. However a detailed siRNA dose response experiment showed an inert phenotype of those siRNAs, thus negating this hypothesis. Instead a stimulatory potential was observed with high doses of S1, which subsequently diminished the *CCL5* inhibitory effect seen with low S1 siRNA treatment. Thus the reason for the different phenotypes caused by the SARM-specific siRNA oligonucleotides remains elusive and questions the reliability of the observed impaired CCL5 response seen in S1-treated cells. It is of concern that S1 might have caused an off-target effect by targeting other unintended transcripts. Hence a siRNA-independent approach was required to confirm and further investigate the potential positive role of SARM in PRR-mediated CCL5 induction. Given that *SARM* mRNA expression was regulated in a similar manner in murine BMDMs as it was in human PBMCs, and that a *Sarm*-knockout mouse was available, it was feasible to pursue further analysis on SARM function in knockout BMDMs (see 4.2).

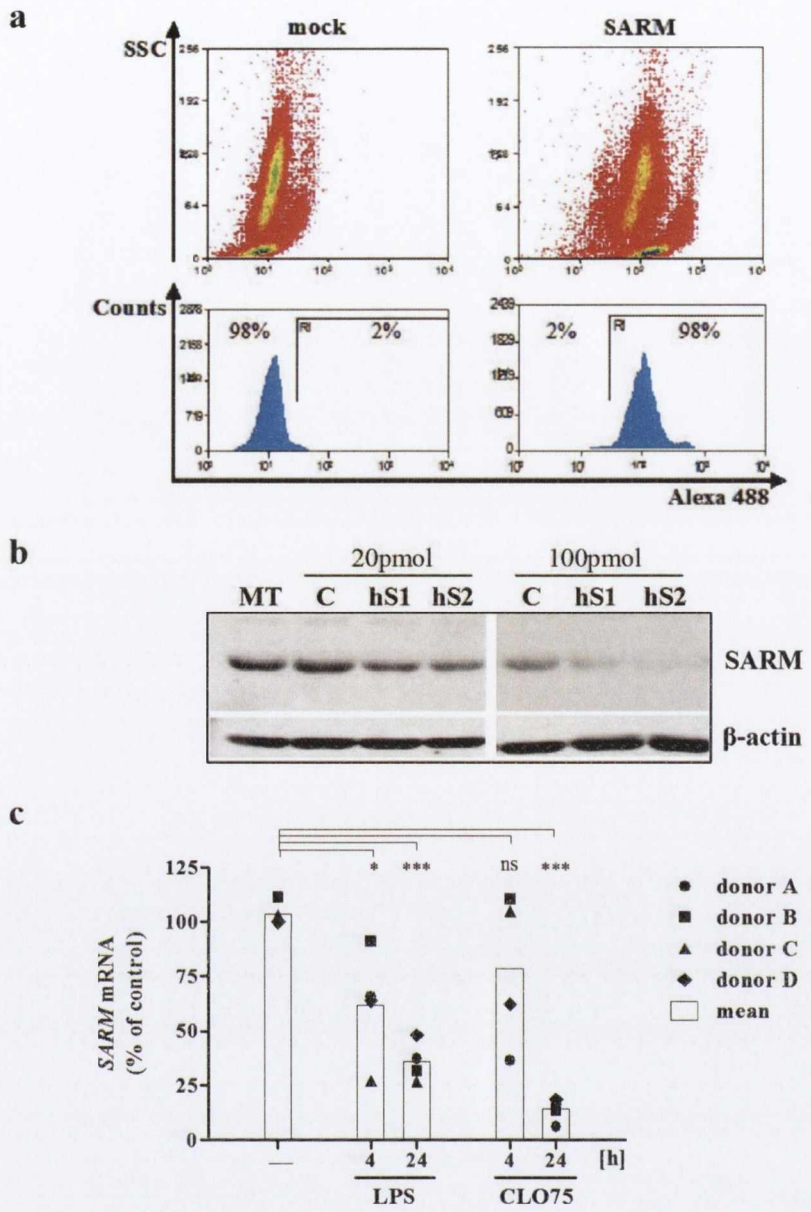


Figure 3.1: SARM is expressed in human PBMCs and *SARM* mRNA is downregulated following TLR stimulation

(a) Flow cytometry analysis of human PBMCs stained for intracellular SARM protein using a SARM-specific antibody (SARM) or an isotype-control antibody (mock) followed by Alexa Fluor 488-conjugated secondary antibody. Dot-blots show sideward scatter (SSC) versus log fluorescence (Alexa 488). The histograms display the percentage of PBMCs expressing SARM protein according to their fluorescence. (b) Immunoblot analysis of SARM protein in human PBMCs. PBMCs were seeded in 12 well plates at $1.2x10^6$ cells/ml and transfected for 24h with control siRNA (C) or two different human SARM-specific siRNA oligonucleotides (hS1, hS2) at 20 and 100pmol/ml or mock-transfected (MT). Lysates were subjected to SDS-PAGE followed by Western blotting using specific antibodies to detect SARM and β-actin as a loading control. (c) Human PBMCs were seeded in 6 well plates at $1.5x10^6$ cells/ml and stimulated for 4 and 24h with LPS [100ng/ml], CLO75 [2.5µg/ml] or medium as control (—). *SARM* mRNA expression was determined by quantitative real-time PCR and normalised to the housekeeping gene *β-actin*. Data are presented as the percentage of the level in untreated controls of each donor. The open bar represents the average *SARM* mRNA level of all donors. The experiment was performed in four different donors as single treatments. The experiments in (a,b) were performed once. Not significant (ns), * $P<0.05$, ** $P<0.01$, *** $P<0.001$ compared with control (Student's *t*-test).

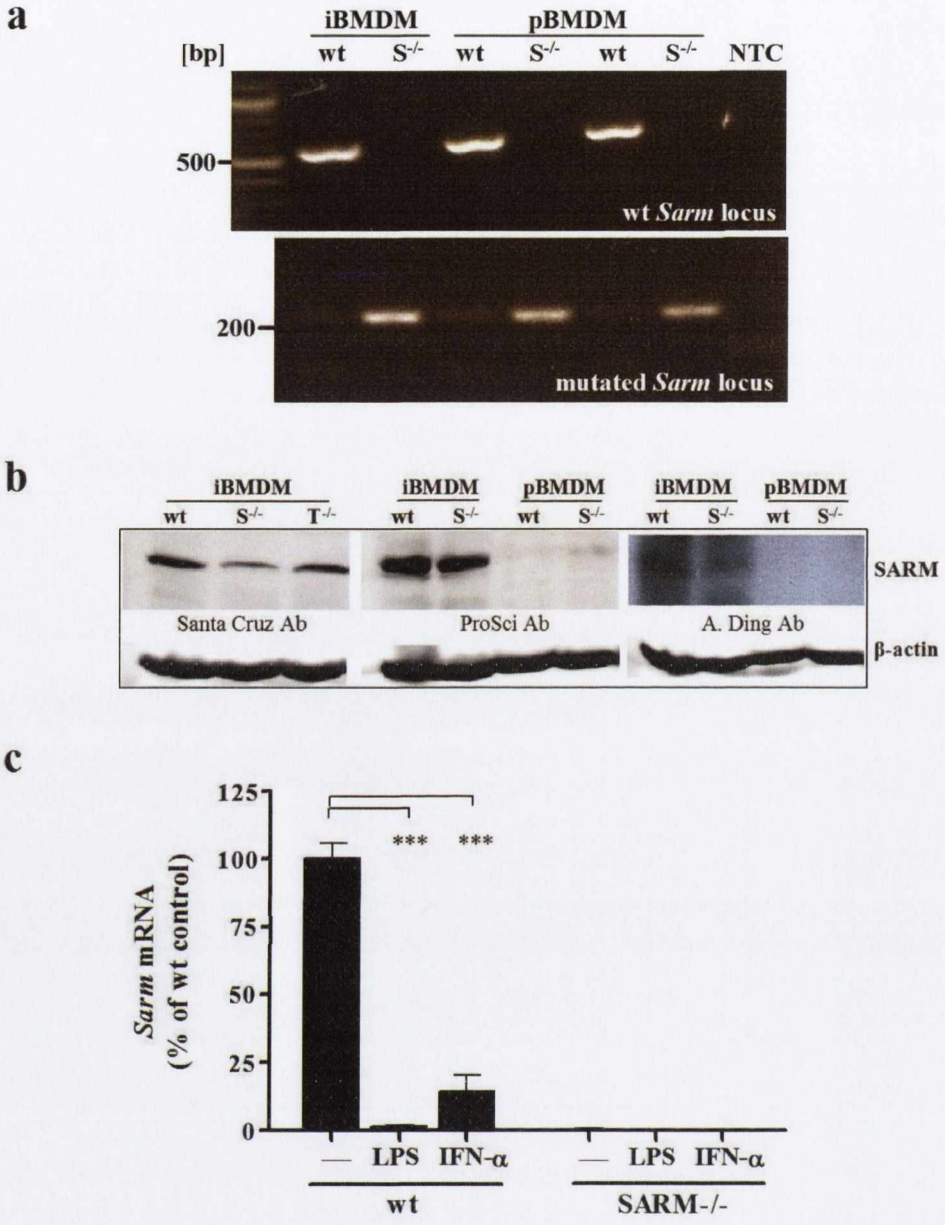


Figure 3.2: SARM detection in murine BMDMs and the downregulation of *Sarm* mRNA following TLR4 and IFNAR stimulation

(a) PCR analysis verified the wild-type (wt) and *Sarm*$^{-/-}$ ($S^{-/-}$) genotype in immortalised and primary BMDMs (iBMDM, pBMDM). Genomic DNA was extracted from cells and the wt and mutated *Sarm* locus were PCR amplified with specific primer pairs generating a 500bp or 200bp PCR product, respectively. PCR products were resolved on a 1% agarose gel and visualised by ethidium bromide staining and UV illumination. (b) The available SARM antibodies nonspecifically detected a protein of same molecular weight as SARM in *Sarm*$^{-/-}$ iBMDMs. Immunoblot analysis of SARM protein in lysates of wt and *Sarm*$^{-/-}$ ($S^{-/-}$) i/pBMDMs and *Trif*$^{-/-}$ ($T^{-/-}$) iBMDMs using the commercial anti-SARM antibodies from Santa Cruz (left) and ProSci (middle) or an unpurified chicken anti-SARM antibody (right, a gift from A. Ding). β-actin serves as a loading control. Data represent one of two or three independent analysis. (c) LPS- and IFN-α-mediated downregulation of *Sarm* mRNA in pBMDMs. wt and *Sarm*$^{-/-}$ pBMDMs were stimulated for 6h with LPS [100ng/ml], IFN-α [1000U/ml] or medium as control (—). *Sarm* mRNA expression was determined by quantitative real-time PCR, normalised to the housekeeping gene *β-actin* and is presented as the percentage of the level in untreated controls. Data include three independent experiments (mean ± s.e.m). *** $P<0.001$ compared with untreated control (Student's *t*-test).

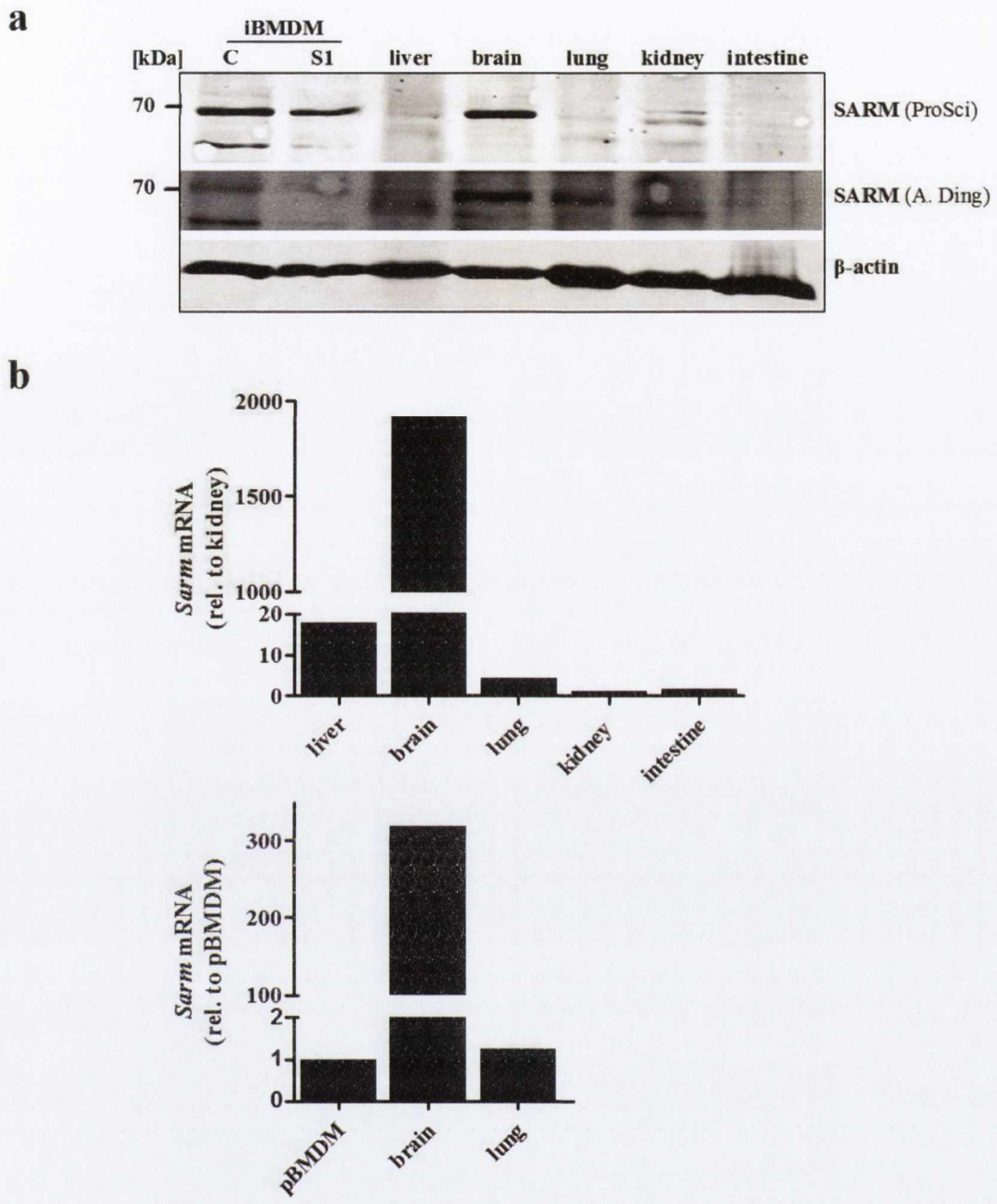


Figure 3.3: SARM is predominantly expressed in murine brain compared with other murine tissues and BMDMs

(a) Immunoblot analysis of SARM protein in murine tissues and iBMDMs. Lysates of various murine tissues and wt iBMDMs treated for 48h with control siRNA (C) or SARM-specific siRNA (S1) at 200pmol/ml were subjected to SDS-PAGE. Western Blotting was performed to detect SARM using the commercial anti-SARM antibody (ProSci) or an unpurified chicken anti-SARM antibody (a gift from A. Ding). β-actin was used as a loading control. The tissue lysates are from one mouse representative of two from one experiment. (b) Relative quantification of *Sarm* mRNA in murine tissues and pBMDMs using real-time PCR. *Sarm* mRNA was normalised to the housekeeping gene *β-actin* and is presented relative to the average level detected in kidney (top graph) or pBMDMs (bottom graph). The data of the murine tissues present the average level detected in two mice from one experiment.

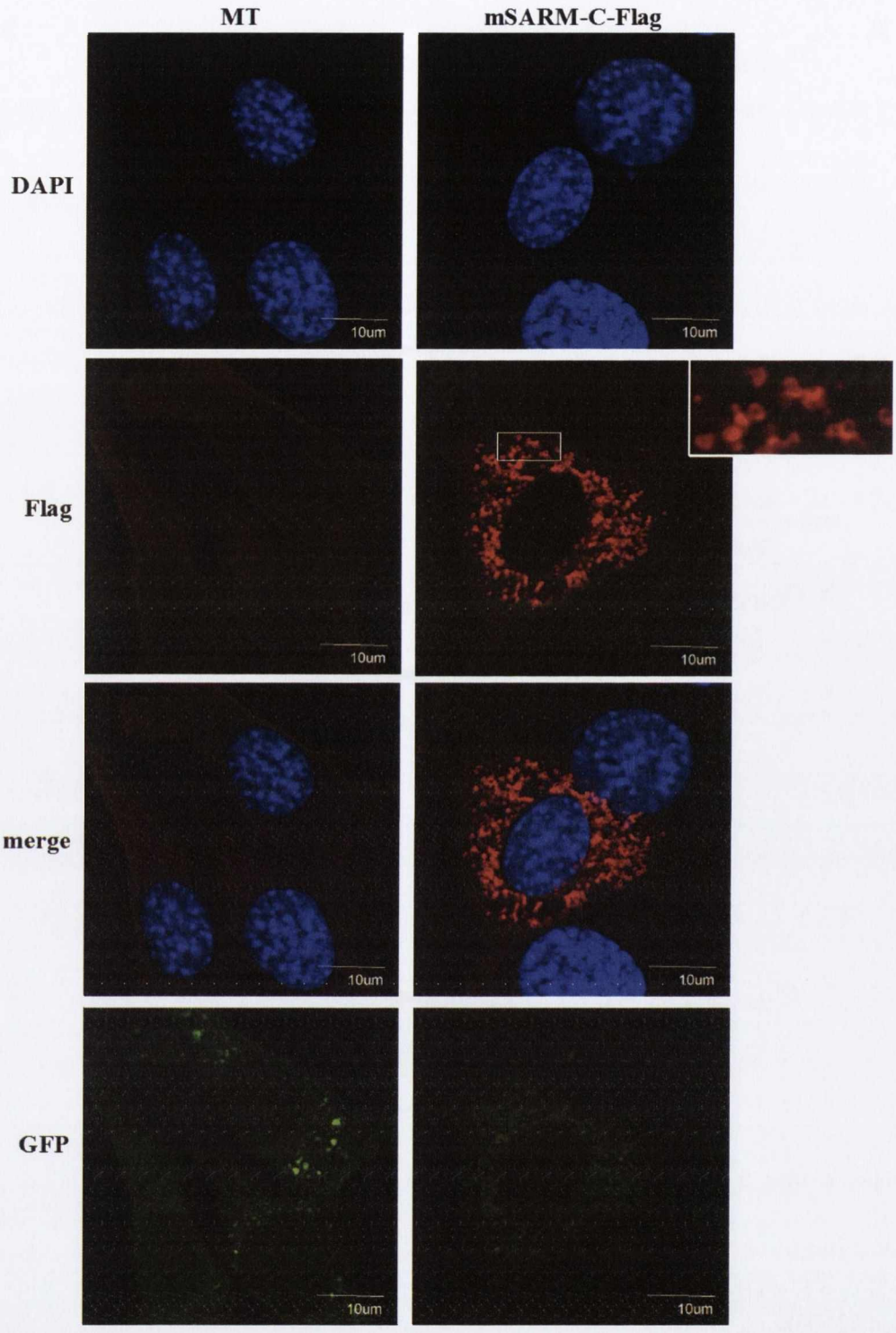


Figure 3.4: Overexpressed mSARM-C-Flag localises to punctate structures in the cytoplasm of murine NIH3T3 cells

Confocal microscopy of NIH3T3 cells grown on coverslips and transiently transfected with a pLV-CMV-GFP expression plasmid encoding mSARM-C-Flag or mock-transfected with empty vector as control (MT). After 48h, cells were fixed and stained for SARM using an anti-Flag antibody followed by Alexa Fluor 647-conjugated secondary antibody (red). Nuclei were visualised with the DNA-intercalating dye DAPI (blue). The plasmid also expressed GFP as a marker of transfection (green). Merge shows an overlay of the DAPI and Flag staining. The magnified image on the right displays the boxed area to illustrate the circular pattern of SARM. The scale bar indicates 10μm. Data are from one experiment representative of three.

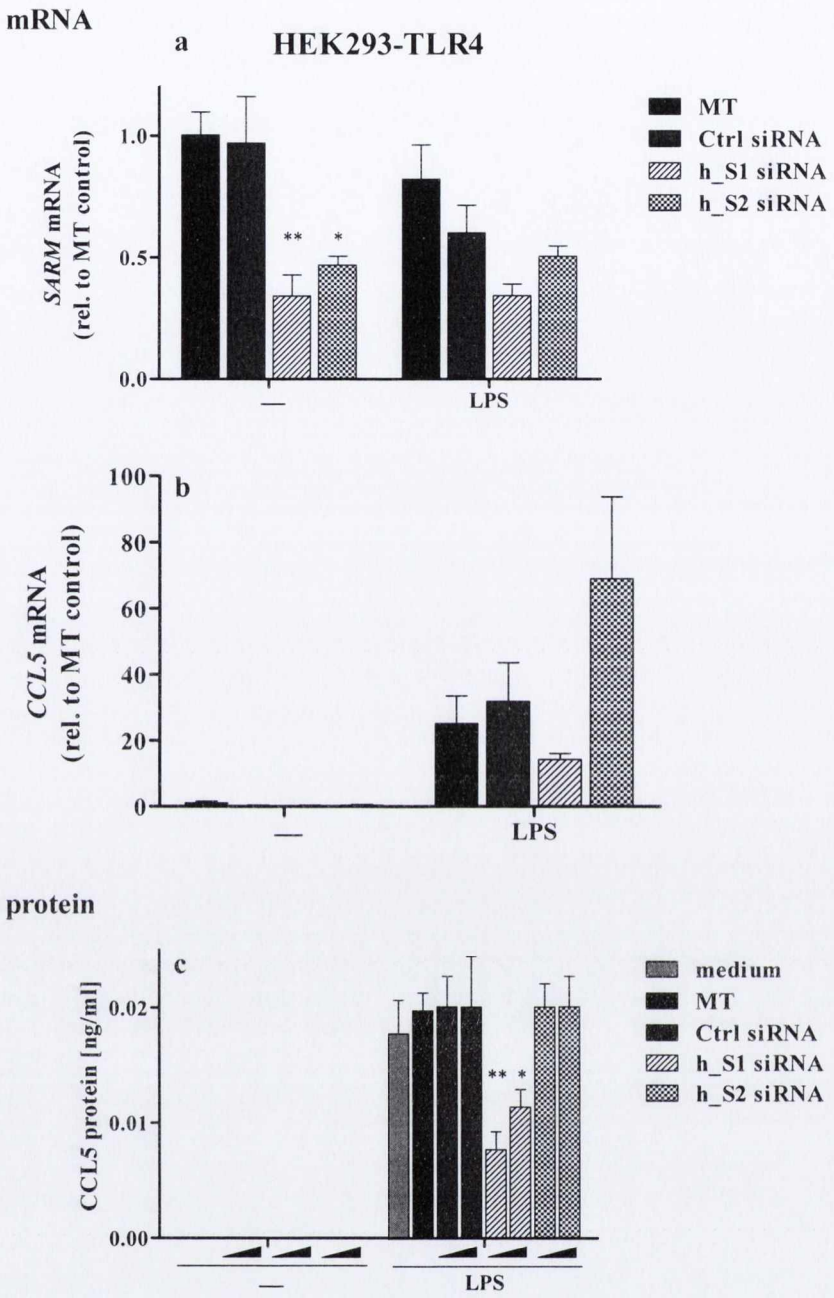


Figure 3.5: Effect of SARM siRNA on TLR4-induced CCL5 expression in human HEK293-TLR4 cells

(a,b) HEK293-TLR4 cells were seeded in 24 well plates at $2x10^5$ cells/ml and treated on two consecutive days with control siRNA (Ctlr siRNA) or two different human SARM-specific siRNA oligonucleotides (h_S1, h_S2 siRNA) at 50pmol/ml. Mock-transfected cells served as control (MT). 24h after the last siRNA transfection, cells were stimulated for 8h with LPS [100ng/ml] or medium as control (—). *SARM* and *CCL5* mRNA expression were determined by quantitative real-time PCR, normalised to the housekeeping gene *β-actin* and are presented relative to the MT control. (c) HEK293-TLR4 cells were seeded in 96 well plates at $2x10^5$ cells/ml and treated as described in (a) with 25 and 50pmol/ml siRNA, indicated by the filled triangle. Medium and mock-transfected (MT) cells served as control. 24h after the last siRNA transfection, cells were stimulated for 24h with LPS [100ng/ml] or medium as control (—). Supernatants were collected and assayed for CCL5 protein by ELISA. Data are from one experiment representative of three (a,b) or one (c) (mean ± s.d.). * $P<0.05$, ** $P<0.01$, *** $P<0.001$, compared with control siRNA (Student's *t*-test).

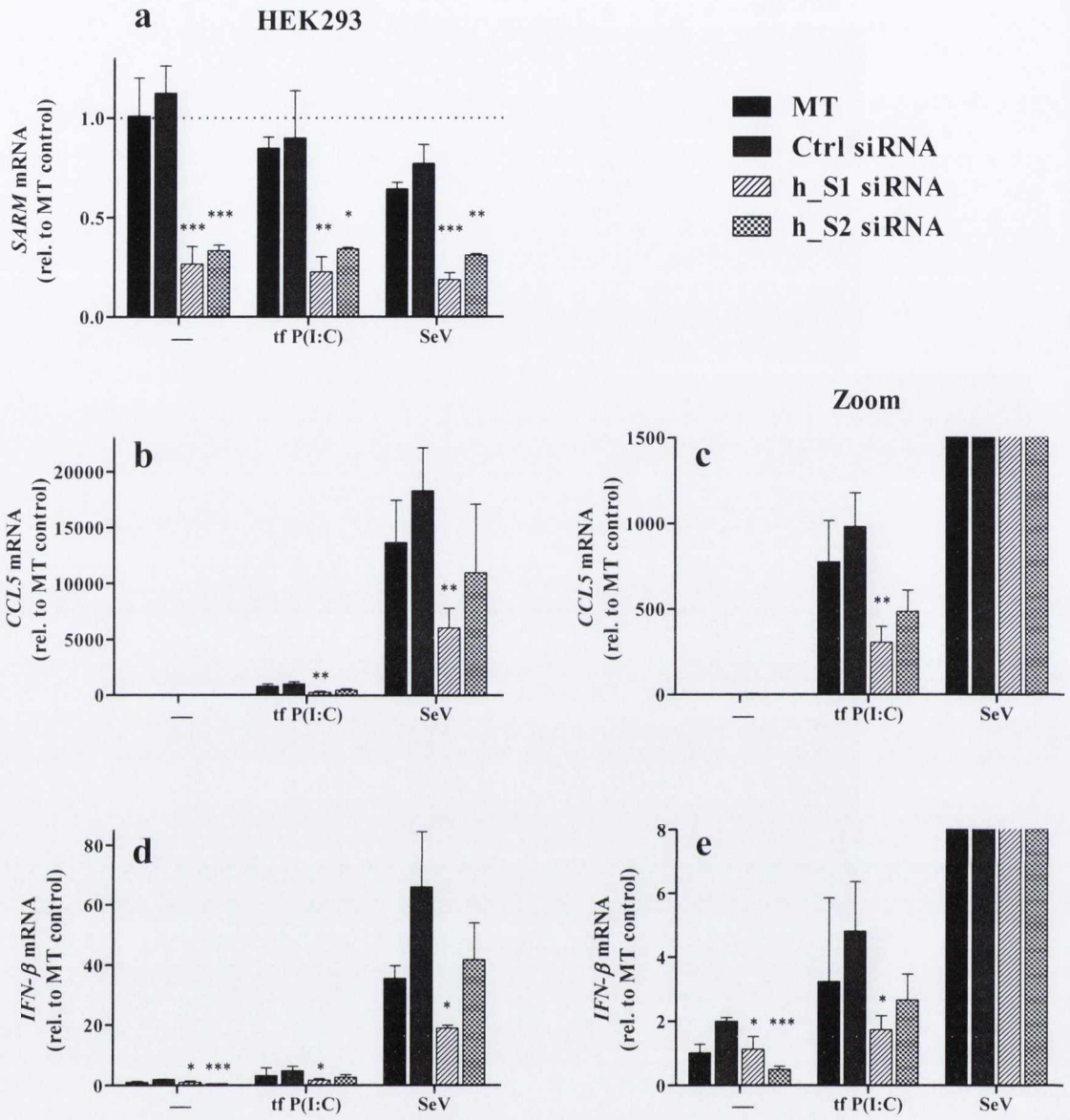


Figure 3.6: Effect of SARM siRNA on RLR-induced CCL5 expression in human HEK293 cells

HEK293 cells were seeded in 24 well plates at $1x10^5$ cells/ml and treated on two consecutive days with control siRNA (Ctlr siRNA) or two different human SARM-specific siRNA oligonucleotides (h_S1, h_S2 siRNA) at 50pmol/ml. Mock-transfected cells served as control (MT). 24h after the last siRNA transfection, cells were stimulated for 8h with transfected Poly(I:C) [2μg/ml], Sendai virus (SeV) or medium as control (—). *SARM*, *CCL5* and *IFN-β* mRNA expression were determined by quantitative real-time PCR, normalised to the housekeeping gene *β-actin* and are presented relative to the MT control. Data are from one experiment representative of three (mean ± s.d.). * $P<0.05$, ** $P<0.01$, *** $P<0.001$, compared with control siRNA (Student's *t*-test).

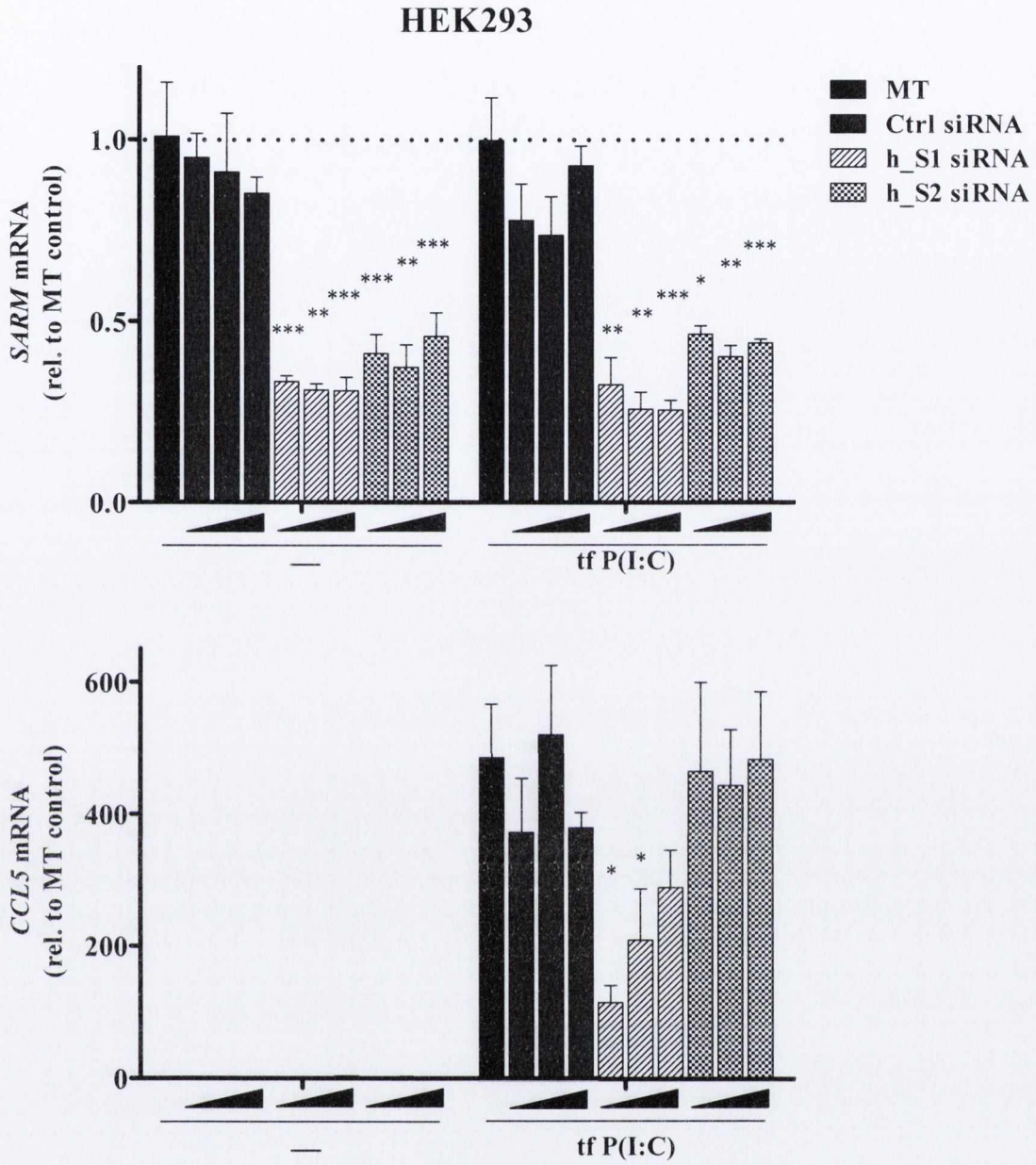


Figure 3.7: Divergent effects of SARM siRNA on RLR-induced CCL5 expression in human HEK293 cells

HEK293 cells were seeded in 24 well plates at $1x10^5$ cells/ml and treated on two consecutive days with control siRNA (Ctlr siRNA) or two different human SARM-specific siRNA oligonucleotides (h_S1, h_S2 siRNA) with the increasing concentrations 25, 50, 100pmol/ml, indicated by the filled triangle. Mock-transfected cells served as control (MT). 24h after the last siRNA transfection, cells were stimulated for 8h with transfected Poly(I:C) [2μg/ml] or medium as control (—). *SARM* and *CCL5* mRNA expression were determined by quantitative real-time PCR, normalised to the housekeeping gene *β-actin* and are presented relative to the MT control. Data are representative of one experiment (mean ± s.d.). * $P<0.05$, ** $P<0.01$, *** $P<0.001$, compared with control siRNA (Student's *t*-test).

4 Characterising SARM function in murine BMDCs and BMDMs

4.1 Introduction

As described in detail in 1.4, the function of SARM, the most ancient member of the TIR adaptor family, is still controversial. Previously my group revealed that human SARM negatively regulated TRIF-dependent TLR signalling and knockdown of endogenous SARM using siRNA enhanced TLR3- and TLR4-induced CCL5 and TNF-α in human HEK293-TLR3 cells and PBMCs, respectively (44). In contrast, a study by Kim et al. on murine SARM knockout BMDMs did not confirm this inhibitory role for SARM, as these cells showed normal cytokine (TNF-α) and chemokine (MCP-1) responses to a range of TLR agonists, such as LPS, Poly(I:C), Pam3Cys and CpG (220). Also they demonstrated that myeloid cells expressed relatively low level of SARM compared with its high abundance in the brain, which was confirmed in my expression analysis. Nevertheless SARM was also detectable in immune cells, including human PBMCs and murine BMDMs. Further evidence for an immunological role of SARM in these cell types was given by its regulation following immune stimulation. *SARM* mRNA was dramatically downregulated in response to TLR4, TLR7 and also IFNAR signalling, indicating that SARM might possess other, TRIF-independent, immune functions. This hypothesis was supported by the function of SARM in lower organisms. In *C. elegans*, the homologue of mammalian SARM, TIR-1, has a positive antibacterial and antifungal immune role, independent of the sole TLR homologue, TOL-1, and independent of any other TIR adaptor, as TIR-1 is the only TIR homologue present in worms (43, 208). Several studies indicated that TIR-1 functions upstream of the MAPK signalling cascade NSY-1-SEK-1-PMK-1, which is conserved in mammals by the orthologous ASK1-MKK3-p38 MAPK pathway (209). Also the siRNA-mediated knockdown study of SARM in HEK293 cells suggested a potential requirement of SARM in TLR4-, but also non-TLR-induced cytokine responses (shown in 3.2.2). The TRIF-independent, cytosolic RLR pathways were analysed, which showed impaired CCL5 induction in cells with significantly reduced *SARM* mRNA. However, this effect was only observed with one of the two SARM-specific siRNAs, raising concern about a potential off-target effect. Hence, it was important to further investigate SARM function using a siRNA-independent approach. Given that a

Sarm-knockout mouse was available and that murine BMDMs showed a similar regulation of *SARM* expression in response to immune stimulation than human PBMCs, BMDMs seemed a good cell type to pursue the analysis. Furthermore, studying immune responses in BMDMs, the cell type where Kim et al. did not observe any TRIF-inhibitory or TLR-regulatory function of SARM would help to elucidate the current discrepancy of SARM in the human and murine system. Nevertheless, it is still conceivable that SARM might exhibit cell type- and/or species-specific functions. To gain insights into a possible immune function of SARM in murine cells, I first characterised the cytokine profile of wt and SARM-deficient BMDMs. I included bone marrow-derived dendritic cells (BMDCs) in the study as another important innate immune cell type, also because it was reported previously that splenic DCs expressed slightly more SARM protein than macrophages (220). The cytokine profile of wt and *Sarm*$^{-/-}$ primary BMDMs (pBMDMs) was subsequently compared with that obtained in immortalised BMDMs (iBMDMs) in order to establish the latter cell line as a model for more detailed SARM analysis. Given the previous result of TLR- and non-TLR-dependent SARM modulation and implication in immune responses, I expanded the cytokine analysis also to non-TLR, cytosolic receptor pathways. The various PRR pathways differ mainly in the upstream usage of adaptor proteins, but most of the signalling cascades converge further downstream to activate the common transcription factors NF-κB, AP-1 and IRFs. To allow discrimination of the distinct transcription factor activation pathways during cytokine analysis, I examined cytokines differently regulated by the transcription factors. TNF-α is an inflammatory cytokine mainly induced by NF-κB, while the expression of CCL5 and IFN-β is additionally controlled by IRFs, such as IRF3 and IRF7 (229, 237). In the TLR4 response, the analysis of both types of cytokines also distinguishes between the MyD88 and the TRIF signalling pathway. While MyD88 mediates the induction of NF-κB-dependent genes, TRIF, the known interaction partner of SARM, is required for the IRF3-dependent gene induction and late activation of NF-κB (238). Furthermore, the analysis of CCL5 expression was particularly interesting in light of the previously observed impairment in SARM siRNA-treated HEK293 cells.

4.2 Results

For the study of murine primary immune cells, femurs from wt and *Sarm*$^{-/-}$ mice were obtained from A. Ding, who originally generated the *Sarm*-knockout mouse, and later also from K. Fitzgerald. BMDMs and BMDCs were generated using the growth factors M-CSF and GM-CSF, respectively. A source of these growth factors was supernatant from M-CSF- or GM-CSF-producing cell lines. After approximately 8 days of culture, the differentiated cells were plated at $5x10^5$ cells/ml in 6, 24 or 96 well plates and stimulated with various PAMPs and virus to elicit cytokine responses. To quantify cytokine mRNA expression, cells of the 24 well plates were harvested 1-6h after stimulation. RNA was extracted, reverse transcribed into cDNA and applied to quantitative real-time PCR analysis. The mRNA of the target gene was normalised to the housekeeping gene *β-actin* and expressed relative to the untreated wt control, thus representing the fold induction in wt cells following stimulation. Calculating also the *Sarm*$^{-/-}$ values relative to the wt control allowed a direct comparison of the relative mRNA level between wt and SARM-deficient cells. ELISA was performed to analyse protein expression in culture supernatants mostly 24h after stimulation of cells in 96 well plates. All other analysis are described in detail later, where required.

4.2.1 Role for SARM in TLR4-induced CCL5 and IFN-β expression in primary BMDCs

Analysing TLR4-mediated cytokine responses in primary BMDCs stimulated with LPS, I observed that *Ccl5* and *Ifn-β* mRNA induction were impaired in SARM-deficient cells compared to wt (Figure 4.1b, c). The defect in CCL5 expression was also confirmed at the protein level (Figure 4.1e), while IFN-β protein was not analysed. In contrast, *Tnf-α* mRNA induction was mostly unaffected in BMDCs lacking SARM (Figure 4.1a). Surprisingly, the LPS-induced TNF-α protein was slightly reduced in *Sarm*$^{-/-}$ BMDCs, which might suggest a translational role for SARM in TNF-α production (Figure 4.1d). Overall the effect on CCL5 and IFN-β expression were more significant, and even though this observation was a bit inconsistent throughout the experiments, it suggested a role for SARM in optimal induction of these cytokines. Interestingly, TLR4 mediates the upregulation of both genes via the TIR adaptor TRIF, the known interaction partner of

SARM, while the mostly unaffected TNF-α is induced by the MyD88-dependent TLR4 pathway. To determine if the SARM-mediated effect was restricted to TRIF signalling, I next examined other TRIF-dependent and -independent TLR responses. The endosomal TLR3 signals solely via TRIF, while the TLR7 pathway is TRIF-independent and uses MyD88 to signal. The activation of those pathways with the corresponding ligands Poly(I:C) and CLO75, respectively, led to upregulation of TNF-α independently of SARM, which was consistent with the previous result (Figure 4.2a). The impact of SARM on *Ccl5* expression was difficult to analyse, as both pathways barely induced the chemokine CCL5. In contrast, a requirement for SARM in the TLR7-mediated *Ifn-β* response was observed, while the preliminary data obtained with TLR3 showed no dependency on SARM (Figure 4.2c). This indicated that the role of SARM in IFN-β, and possibly CCL5, regulation may be TRIF-independent. To further define the pathways regulated by SARM, I investigated the *Ccl5* and *Ifn-β* response of TLR-independent, cytosolic receptors that use different adaptor proteins to initiate downstream signalling. The cytosolic, RNA-sensitive receptor RIG-I signals via the adaptor protein MAVS and was activated by infecting BMDCs with Sendai virus. The cytosolic DNA sensors in contrast use the adaptor STING and were activated by transfecting dsDNA 70mer. This ligand was originally derived from VACV genome and is mainly detected by the DNA receptor p204 in murine cells (143). As expected, both pathways induced a significant upregulation of *Ifn-β* mRNA, whereas *Ccl5* expression was much weaker (Figure 4.2e, f). However, the induction of *Ccl5* and *Ifn-β* were not found to be dependent on SARM following cytosolic receptor stimulation. In agreement with a predominant IRF activation, rather than NF-κB, these pathways barely induced the inflammatory cytokine *Tnf-α* (Figure 4.2d). Overall, the cytokine data obtained in this study were quite variable; nevertheless I gained evidence for a potential immune function of SARM in this cell type (Table 4.1). SARM was found to be required for optimal CCL5 and IFN-β induction in the TLR4 response, while it was dispensable for *Tnf-α* mRNA expression. A similar phenotype was observed for TLR7-induced responses, albeit less significantly. Furthermore, this regulatory role of SARM was specific to the TLR pathway, as cytokine responses of non-TLR, cytosolic receptors were unaffected by SARM ablation. In addition, I obtained evidence for a function of SARM in TLR4-mediated TNF-α translation.

4.2.2 SARM has no role in TLR-induced DC maturation and endotoxin tolerance

Due to the observation described in 4.2.1 that SARM might particularly promote the TLR4-induced IFN-β expression in BMDCs and given the known SARM-TRIF interaction, I sought to investigate two processes in dentritic cells (DCs) that were recently demonstrated to be mainly TRIF- and IFN-β-dependent. One of them was DC maturation, which is a process initiated in antigen-presenting cells, such as DCs, after sensing a pathogen via PRRs, especially TLRs. It involves characteristic phenotypical changes within the cell, such as the upregulation of costimulatory molecules (e.g. CD40, CD80, CD86) and MHC class I and class II proteins (239). The expression of these molecules on DCs is essential to activate T lymphocytes and thereby linking innate and adaptive immune responses (see 1.1). The LPS/TLR4-induced DC maturation was shown to be partly TRIF-dependent, mainly due to IFN production and subsequent signalling via the type I IFN receptor (IFNAR) (240, 241). Also the MHC class II upregulation was demonstrated to be TRIF-dependent following LPS stimulation (242). Hence it was reasonable to examine a possible role for SARM in DC maturation. Wt and *Sarm*-knockout BMDCs were seeded in 96 well plates and stimulated for 24h with LPS, Poly(I:C) and R848 in order to activate TLR4, 3 and 7, respectively, and to induce maturation. The surface expression of CD80, CD86, CD40 and MHC class II were analysed in the $CD11c^+$ cell population, which represented BMDCs, using specific fluorescent-labeled antibodies and flow cytometry. The induction of DC maturation was assessed by comparing TLR-stimulated BMDCs with an untreated control. All three TLR agonists enhanced the expression of the costimulatory molecules and MHC class II protein indicating successful activation of the maturation process (Figure 4.3). Among them, LPS was most potent in inducing DC maturation, and in particular the upregulation of CD40 was stronger with LPS compared to other ligands. However, no significant differences were observed in the expression profile between wt and SARM-deficient cells, which excluded an essential role for SARM in DC maturation. Only the LPS-induced CD86 expression was slightly impaired in $Sarm^{-/-}$ BMDCs, which was interesting, as the TRIF-pathway was described to be particularly required for the sustained upregulation of this molecule (241). However a repeat of this experiment did not confirm the result. I also noted a minor difference in MHC class II expression between both genotypes, but this effect was not significant and probably caused by interstaining variations, rather than a SARM-specific role in this process.

Another important immune process that was interesting to investigate in BMDCs in light of the discovered SARM function in TLR4-induced IFN-β expression and the known interaction with TRIF was endotoxin tolerance. Endotoxin tolerance is a phenomenon, where exposure to low doses of LPS results in hyporesponsiveness to subsequent LPS challenge, mirrored in the repressed expression of proinflammatory cytokines, like TNF-α (243). One mechanism to establish the tolerant state of the cell is the upregulation of TLR inhibitors. Furthermore, the TRIF-pathway was shown to actively promote endotoxin tolerance by inducing IFN-β and the subsequent activation of the IFNAR pathway (244). Thus I hypothesised that SARM might mediate endotoxin tolerance either via its known interaction with TRIF and/or by promoting IFN-β induction, according to the cytokine study in BMDCs (4.2.1). Apart from BMDCs, I also included BMDMs in the analysis as a cell type critical in mediating endotoxin tolerance and homoeostasis (245). To induce tolerance, cells were plated in 96 well plates and pretreated for 24h with increasing concentrations of LPS (0.01, 1 and 100ng/ml) or left untreated as control. Then cell supernatants were replaced by fresh medium and the cells were challenged with 100ng/ml LPS or control medium. 24h later, the supernatant was harvested and assayed for secreted TNF-α and CCL5 protein using ELISA. Comparing the cytokine expression of wt and *Sarm*-knockout cells, I was able to determine if SARM had a role in tolerising these cells. I observed that cells pretreated with LPS produced less TNF-α and CCL5 following LPS challenge than cells that were only medium-pretreated (Figure 4.4). The cytokine release was suppressed in a dose-dependent manner by LPS pretreatment reflecting tolerisation of the cells, especially at 1 and 100ng/ml LPS. Also both cell types, BMDMs and BMDCs, were equally tolerisable following LPS pretreatment. In agreement with the literature, particularly the secretion of the proinflammatory cytokine TNF-α was strongly inhibited in tolerant cells (Figure 4.4a, c). Also CCL5 expression was found to be tolerisable, although the reduction was less dramatic than for TNF-α (Figure 4.4b, d). Nonetheless, the degree of TNF-α and CCL5 suppression was comparable in wt and SARM-deficient cells, excluding a role for SARM in establishing endotoxin tolerance in these cells. However, the difference in cytokine expression observed between wt and *Sarm*$^{-/-}$ cells was interesting. In line with the previous cytokine study in BMDCs, I observed significantly impaired LPS-induced CCL5 protein in *Sarm*-knockout cells, whereas TNF-α protein was only slightly reduced (Figure 4.4). This was independent from the tolerisation state of the cell and the cell type. I noted that the requirement for SARM to induce CCL5 protein was even more pronounced

in primary BMDMs, than BMDCs. This was interesting and gave a first indication that the role of SARM in selectively regulating cytokine expression might be even more fundamental in BMDMs.

4.2.3 Role for SARM in TLR- and non-TLR-induced CCL5 expression in primary and immortalised BMDMs

From previous experiments I gained several lines of evidence that SARM had an immune function in primary BMDMs (pBMDMs). First, pBMDMs expressed SARM and significantly downregulated *Sarm* mRNA following immune stimulation (3.2.1). Second, preliminary data revealed a role for SARM in TLR4-induced CCL5 expression in BMDMs (4.2.2). Hence I next performed a more detailed cytokine expression analysis in BMDMs. The analysis of TLR4 responses in pBMDMs revealed that CCL5 mRNA and protein expression were significantly impaired in the absence of SARM with a particular strong reduction at the protein level (Figure 4.5b, d). In contrast, the LPS-induced *Tnf-α* mRNA was unaffected by SARM ablation; however a slight reduction was observed at the protein level (Figure 4.5a, c). This mirrored the observation made in BMDCs and suggested an additional role for SARM in TNF-α translation. I next analysed other TLR and non-TLR ligands to define if SARM function was TRIF- and/or TLR-specific. Surprisingly, and different from the result in BMDCs, SARM was found to mediate CCL5 expression in response to all PRR pathways tested (Figure 4.6b, d). This included the TRIF-dependent and -independent TLR pathways TLR3 and TLR7, respectively, as well as the cytosolic RNA and DNA receptor pathways MDA5, RIG-I and p204. MDA5 is, like RIG-I, a RNA sensitive receptor of the RLR family, that was activated by transfected Poly(I:C). In contrast, SARM was not found to be required for TNF-α induction, which was mainly upregulated by TLR stimulation and only poorly by cytosolic receptors (Figure 4.6a, c). This illustrated again the selective regulatory role of SARM on CCL5 expression, which surprisingly was not restricted to TRIF- and TLR-dependent pathways in pBMDMs. Furthermore, the data indicated that the potential translational role of SARM on TNF-α was restricted to TLR4.

In order to pursue analysis of this newly discovered SARM function it was crucial to establish the immortalised wt and *Sarm*$^{-/-}$ BMDM cell line (iBMDM) as a reliable model system and constant source of cell material. The immortalisation of primary *Sarm*-

knockout BMDMs was performed by K. Fitzgerald (UMass Medical School/USA) using J2 retrovirus containing oncogenes (228). First, I characterised the TNF-α and CCL5 cytokine responses of SARM-deficient iBMDMs in comparison with the wt iBMDM cell line previously established in our laboratory. This would evaluate if the effects observed in pBMDMs were preserved in the immortalised cell line. Consistent with the pBMDMs, the LPS-induced *Tnf-α* mRNA expression was unaffected by SARM ablation (Figure 4.7a). Unexpectedly, the protein expression of TNF-α was enhanced in SARM-deficient iBMDMs following LPS stimulation, which was opposed to the slightly reduced level observed in pBMDMs (Figure 4.7c). Additionally, I noted elevated basal TNF-α mRNA and protein level in *Sarm*$^{-/-}$ iBMDMs, an effect that was not detected in primary cells. Analysing the TLR4-mediated CCL5 expression revealed a complete abrogation of CCL5 mRNA and protein in iBMDMs lacking SARM (Figure 4.7b, d). The effect on CCL5 coincided with the primary cell data; however the dependency on SARM was much more pronounced in the immortalised cell line, as SARM was absolutely required for CCL5 expression. Next I assessed *Tnf-α* and *Ccl5* mRNA expression following stimulation of other TLRs like TLR3 and TLR7 and the cytosolic, TLR-independent receptors MDA5, RIG-I and p204. Consistent with previous observations, the cytosolic receptors elicited only low level of *Tnf-α*, but were able to significantly upregulate *Ccl5* mRNA. As in primary cells, *Tnf-α* mRNA induction was unaffected by SARM ablation following activation of the various PRRs (Figure 4.8, top graph). In regard to *Ccl5*, a dependency on SARM was observed following the cytosolic receptor pathways, whereas the low *Ccl5* induction following Poly(I:C)- and CLO75-activated TLR3 and TLR7, respectively, did not require SARM (Figure 4.8, bottom graph). Thus the positive role of SARM in PRR-induced CCL5 expression was mostly preserved in the iBMDM cell line. However the evidence for an additional role of SARM in TLR4-mediated TNF-α translation was not sustained in immortalised cells and therefore was not pursued in further analysis of these cells.

4.2.4 SARM is additionally required for IFN-β expression in immortalised, but not in primary BMDMs

The data reported so far demonstrated a selective role of SARM in gene expression of CCL5, but not TNF-α. The fact that SARM mediated CCL5 expression of all receptor

pathways tested, TLR-dependent and -independent, suggested a more downstream regulation in the pathway. In this regard it was interesting that TNF-α and CCL5 use different transcription factors for their expression. In addition to NF-κB, which is sufficient for TNF-α upregulation, CCL5 is also dependent on the transcription factor IRF3 (229). Hence to further define SARM function it was reasonable to analyse another IRF3-dependent gene. IFN-β was a good candidate because preliminary data in BMDCs indicated a SARM-regulatory function also for IFN-β expression (4.2.1). Activation of TLR4, 3 and 7 induced *Ifn-β* mRNA was slightly reduced in *Sarm*$^{-/-}$ pBMDMs. This was also observed at the protein level following TLR4 stimulation (Figure 4.9a-c). However this effect was inconsistent and less significant compared to the previously observed CCL5 regulation. Furthermore, I could exclude a role for SARM in *Ifn-β* expression induced by the non-TLR, RNA-dependent cytosolic receptors MDA5 and RIG-I, which was in line with the BMDC data (Figure 4.9c). Only the cytosolic DNA pathway showed an effect on *Ifn-β* expression, reflected in an enhanced level of mRNA in SARM-deficient BMDMs (Figure 4.9c). Although this observation was consistent throughout several experiments, it did not persist at the protein level (data not shown). Next, I analysed IFN-β responses in immortalised BMDMs, which revealed an unexpected, much more dramatic phenotype. SARM-deficient iBMDMs had a complete defect in IFN-β expression following all PRR ligands tested (Figure 4.9d-f). The absolute requirement for SARM to express IFN-β, even basally, differed significantly from the data obtained in primary BMDMs and BMDCs. Although primary cells exhibited a slight reduction of TLR-induced IFN-β, it was evident that the role of SARM on IFN-β expression was less crucial than in immortalised cells.

Nevertheless, in light of the profound immunomodulatory functions of IFNs, it was feasible to assess the potential role of SARM in IFN-β regulation by an independent approach. PRR-induced type I IFNs, mainly IFN-α and IFN-β, can subsequently signal via the type I IFN receptor (IFNAR) in an autocrine/paracrine manner. This consequently activates a signalling cascade that results in the induction of a wide range of IFN-stimulated genes (ISGs), as illustrated in the schematic (Figure 4.12, described later). Thus as an indirect readout of TLR4-induced type I IFN production, I examined the activation of the IFN-dependent transcription factor STAT1 and the induction of the ISGs viperin and IRF7 following LPS treatment. One important step in STAT1 activation is its phosphorylation on tyrosine 701, termed p-STAT1. I assessed the appearance of p-STAT1 and the induction of viperin using immunoblot analysis. Wt and *Sarm*$^{-/-}$ BMDMs were

stimulated for various times with LPS, Sendai virus or medium as control. Lysates were then resolved on a 10% SDS-Polyacrylamide gel followed by Western Blotting using specific antibodies to p-STAT1 (Tyr701) and viperin. Additionally, the blot was probed for β-actin as a loading control. The induction of *Irf7* mRNA was examined using quantitative real-time PCR. First I analysed primary BMDMs, where SARM was shown to be mostly dispensable for PRR-induced IFN-β. This was confirmed by the immunoblot analysis. TLR4 and RIG-I stimulation triggered STAT1 phosphorylation 3h and 6h after LPS and Sendai virus treatment, respectively (Figure 4.10a). *Sarm*$^{-/-}$ pBMDMs exhibited only a minimal reduced pSTAT1 level 3h after LPS treatment, while Sendai virus-induced p-STAT1 was equal in both genotypes. This coincided with the previous cytokine study, which revealed slightly impaired LPS-induced IFN-β in some experiments. P-STAT1 then subsequently decreased at 6h, while the antiviral protein viperin was upregulated at this time point to a similar extend in both genotypes. Also the induction of the ISG *Irf7* was mostly unaffected by SARM ablation (Figure 4.10c, left graph). Thus the results demonstrated indirectly that primary BMDMs were able to upregulate TLR4- and RIG-I-induced type I IFNs independently of SARM, which was consistent with the cytokine data. In contrast the previous cytokine analysis of immortalised BMDMs revealed that SARM was absolutely required for IFN-β expression in this cell type. This dramatic defect in IFN-β production was also visible when analysing the IFN-dependent responses. While wt iBMDMs induced p-STAT1 and viperin 3h after LPS treatment, these responses were completely inhibited in SARM-deficient cells (Figure 4.10b). Even 24h after stimulation, viperin was barely expressed in the knockout iBMDMs as opposed to its persistent and significant upregulation in the wt cells. The inability of *Sarm*$^{-/-}$ iBMDMs to induce IFN-dependent genes in response to LPS was further demonstrated by the completely abrogated *Irf7* expression (Figure 4.10c, right graph). Also basal *Irf7* mRNA level were dramatically impaired in the absence of SARM, which was an indication of the defective IFN system and the lack of IFN priming. These data confirmed the essential role of SARM in IFN-β production in iBMDMs. Together with the cytokine study, these observations clearly demonstrated a difference in the requirement for SARM in IFN-β expression in primary and immortalised BMDMs (Figure 4.11b).

4.2.5 TLR4-induced CCL5 is a primary response gene in BMDMs

The previous results revealed a consistent regulatory function of SARM in PRR-induced CCL5 expression in primary and immortalised BMDMs. PRR stimulation initiates a signaling cascade that leads to activation of several transcription factors, including NF-κB, AP-1 and IRF3/7 (Figure 4.12). A combination of these factors finally induces the upregulation of a set of primary response genes (PRGs) independent of new protein synthesis, like the cytokines TNF-α and IFN-β (246). Those upregulated proteins themselves mediate further responses and may also induce another set of genes, referred to as secondary response genes (SRGs). Particularly type I IFNs induced by the PRR pathways are known for their extensive immunomodulatory potential by subsequently upregulating numerous IFN-stimulated genes (ISGs) by signalling via the IFNAR. CCL5 was reported to belong to a class of genes that showed some IFN-dependency (247). Thus it was of importance to determine if PRR-stimulated BMDMs induced CCL5 solely as a PRG or if its expression was further regulated by IFNs in a secondary response. This would on the one hand define the transcription factor complex involved in CCL5 regulation and also elucidate if a potential SARM modulation of IFN-β expression could have affected CCL5 expression indirectly. As an approach to distinguish primary from secondary response genes I compared LPS-induced cytokine expression in primary and immortalised wt BMDMs (p/iBMDMs) either pretreated for 1h with the protein synthesis inhibitor cycloheximide (CHX) or left untreated. The cells were subsequently stimulated for 3h with LPS and quantitative real-time PCR was applied to analyse cytokine mRNA expression of *Ccl5* and several control genes. The analysis of *Tnf-α* mRNA served as control for a classical PRG, which should be unaffected by CHX, while *Ifit2* was known to be also IFN-dependent, hence should show some sensitivity to inhibition of protein synthesis (246, 248). As expected, *Tnf-α* mRNA expression was not impaired in the presence of CHX, in fact treatment with the inhibitor caused an enhanced mRNA level in p/iBMDMs (Figure 4.13a, b). In contrast the expression of the IFN-dependent gene *Ifit2* was completely abolished in CHX-treated cells, indicating the successful inhibition of protein synthesis. Similar to *Tnf-α*, I observed an accumulation of *Ccl5* and *Ifn-β* mRNA in LPS-stimulated p/iBMDMs treated with the inhibitor. This indicated that TLR4-mediated *Ccl5* upregulation in BMDMs, just as *Ifn-β*, was directly induced by the primary signal transduction pathway and did not require protein synthesis. Nevertheless, it was interesting to examine the impact of secreted type I IFNs on LPS-induced *Ccl5* expression. Thus the

IFNA receptor signalling was blocked using a specific antibody against the IFNAR1 subunit. The optimal anti-IFNAR1 antibody concentration was determined in an initial experiment by treating wt iBMDMs overnight with various concentrations of the blocking antibody followed by 3h LPS stimulation to elicit IFN-β production. Cell lysates were analysed by immunoblot for activation of STAT1, a component of the IFN signalling pathway. In control cells that were not pretreated with the blocking antibody, LPS induced tyrosine 701-phosphorylation of STAT1. This was significantly inhibited in cells treated with anti-IFNAR1 antibody, demonstrating the successful neutralisation of the IFNA receptor (Figure 4.13c). The suppression of IFN signalling was comparable among all antibody concentrations tested, though I decided to use 5μg/ml in the following experiment, a concentration which was also described in the literature (249). Using this protocol, wt p/iBMDMs were pretreated overnight with the anti-IFNAR1 antibody or left untreated as control. Cells were then stimulated for different times with LPS or medium and mRNA of the various cytokines was analysed using quantitative real-time PCR. Comparing cytokine induction in the presence or absence of the blocking antibody revealed the contribution of secreted IFNs on gene induction. In line with the previous experiment, LPS-induced *Tnf-α* expression was independent of a secondary factor and thus unaffected by inhibiting the IFN response in p/iBMDMs (Figure 4.13 d, e). As control for IFNAR blocking, I analysed the highly IFN-dependent gene *Irf7* (200). The expression of *Irf7* mRNA was completely abrogated in anti-IFNAR1 antibody-treated cells, even basally, which confirmed the successful block of the IFN signal. In agreement with the CHX experiment, the immediate upregulated *Ifn-β* expression in iBMDMs was independent of secreted IFNs, however at later time points it showed some dependency on subsequent IFN signalling (Figure 4.13e IV). In contrast, pBMDMs required an intact IFN pathway already for the immediate *Ifn-β* production even 1h after LPS stimulation (Figure 4.13d IV). This was surprising, given that *Ifn-β* was clearly identified as a PRG in the CHX study, hence independent of a newly synthesised factor. This suggested that pBMDMs, in contrast to iBMDMs, may require a specific factor for *Ifn-β* expression that was dependent on basal IFN priming. Nevertheless the experiment in pBMDMs needs to be repeated in order to confirm the result. Analysing *Ccl5*, I observed that its expression was mainly unaffected by blocking the secondary IFN pathway in p/iBMDMs (Figure 4.13d, e III). Thus LPS-induced CCL5 was a PRG in BMDMs and also independent of IFN signalling.

4.2.6 SARM is also required for type I and type II IFN-induced CCL5, while it is dispensable for most other IFN-dependent responses

The previous experiment demonstrated the crucial role of SARM in TLR- and non-TLR-induced CCL5 expression. The fact that TLR4-induced CCL5 was upregulated as a primary response gene, independent of a secondary induced factor, was evident for a direct function of SARM in the PRR pathways. To determine if SARM-mediated regulation was restricted to PRR signalling and their specific transcription factors, such as NF-κB, AP-1 and IRF3/7, I sought to assess CCL5 expression of other, PRR-independent pathways. CCL5 expression is also known to be induced by type I and type II IFNs that signal via the IFNAR or IFNGR, respectively, to classically activate the JAK-STAT pathways (Figure 4.12). IFNAR signalling leads mainly to formation of a transcriptional complex composed of STAT1, STAT2 and IRF9, also known as IFN-stimulated gene factor 3 complex (ISGF3), whereas IFNGR more strongly activates STAT1 homodimer formation. Both complexes then initiate a specific set of ISGs, controlled either more by ISRE or GAS promoter elements, respectively (191). Also in those pathways some responses can be more secondary, for example due to upregulated transcription factors such as IRF1 or IRF8. Given that the signalling molecules and transcription factors involved in the IFN pathway differed significantly from the ones used by PRRs, I investigated if SARM would also regulate IFN-induced CCL5 expression, and additionally also examined other IFN-mediated responses. Wt and *Sarm*$^{-/-}$ p/iBMDMs were directly stimulated with recombinant IFN-α or IFN-γ in order to activate IFNAR or IFNGR pathways, respectively. To my surprise, the analysis of IFN-α-induced CCL5 protein in primary BMDMs revealed a strong SARM dependency (Figure 4.14a). To confirm equal activation of the IFN pathway and to test for an upstream inhibition by SARM, I performed immunoblot analysis of tyrosine 701-phosphorylated STAT1 (p-STAT1), as an indicator for transcription factor activation. Total STAT1 protein and β-actin served as loading control. However, wt and *Sarm*$^{-/-}$ pBMDMs showed similar kinetics of STAT1 activation in response to IFN-α treatment, and the induction of the ISG viperin was unaffected by SARM ablation (Figure 4.14b). Immunoblot analysis of IFN-γ-stimulated pBMDMs also excluded a role for SARM in IFN-γ-mediated p-STAT1 activation and induction of viperin (Figure 4.14c). A similar phenotype was observed in iBMDMs. Analysing several ISGs using quantitative

real-time PCR, I found that the upregulation of *Ccl5* mRNA was significantly impaired in SARM-deficient iBMDMs stimulated with IFN-α (Figure 4.15a I,II). This was confirmed at the protein level (Figure 4.15b). In contrast, the IFN-α-mediated fold induction of other ISGs, such as *Ifit2* and *Irf7*, were unaffected by SARM ablation (Figure 4.15a IV,VI). Only the relative mRNA level of *Irf7* was reduced in SARM-deficient iBMDMs, probably caused by the lack of IFN priming (Figure 4.15a V). As shown earlier, *Sarm*$^{-/-}$ iBMDMs had a significant defect in basal IFN-β production, which consequently attenuated the expression of IFN-dependent genes, in the basal state as well as after stimulation. The analysis of fold induction of mRNA, which set the different basal expression levels of both genotypes as one, revealed a SARM-dependency only for *Ccl5* (as described above). The impaired viperin expression in response to IFN-α in iBMDMs, was possibly also an effect of the defective IFN-β priming (Figure 4.15c). In agreement with the primary cell data, p-STAT1 activation was comparable between wt and *Sarm*$^{-/-}$ iBMDMs. Next I assessed CCL5 mRNA and protein production in response to IFN-γ. Consistent with the type I IFN pathway, the IFNGR was unable to upregulate CCL5 in the absence of SARM, although p-STAT1 activation was unaffected (Figure 4.15d-f). Again, viperin induction was attenuated in *Sarm*$^{-/-}$ iBMDMs, which was most likely an indirect effect due to defective IFN priming. Overall the analysis of type I and type II IFN-mediated responses demonstrated that SARM had no direct role in the IFN signalling pathways, but rather elucidated that the selective regulatory role of SARM in CCL5 induction was not restricted to the PRR pathway and also valid for the IFN transduction pathways (Figure 4.16).

4.3 Discussion

Given the initial observation that SARM was detectable in murine BMDMs and that its expression was regulated upon TLR and IFNAR stimulation, it was interesting to perform a detailed analysis on the role of SARM in immune responses in these cells. This might also help to explain the discrepancy in SARM function that emerged from human and murine studies. While human SARM was found to interact with TRIF and negatively regulate TRIF-dependent TLR signalling, a study on murine *Sarm*-knockout BMDMs could not confirm a TLR-regulatory function of SARM (44, 220). Here, the cytokine study in primary and immortalised BMDMs (p/iBMDMs) revealed that SARM played a significant and selective role in promoting CCL5 expression (Figure 4.16). Unexpectedly, this function was not restricted to TRIF-dependent TLR pathways, as might have been suggested by the SARM-TRIF interaction, and SARM was positively involved as opposed to its known inhibitory role in the human system (44). Also the MyD88-dependent TLR pathways, like TLR7, required SARM for CCL5 expression. In this regard, an interaction of SARM with the TIR adaptor MyD88 had also been observed for amphioxus (217) and human SARM (M. Carty, personal communication). However, further analysis revealed that SARM also regulated optimal CCL5 expression in TLR-independent pathways. The cytosolic RNA- and DNA-sensitive PRR pathways showed a strong dependency on SARM for CCL5 induction, even though they signal independently of the TIR adaptors MyD88 and TRIF. The RNA receptors of the RLR family MDA5 and RIG-I signal via the adaptor protein MAVS, whereas the DNA receptors, such as p204, highly depend on STING. However, the signalling cascades initiated by the various PRRs converge further downstream leading to activation of common transcription factors, including AP-1, NF-κB and IRF3/7. Thus SARM might act at this downstream level to regulate CCL5 expression. Interestingly, I observed that SARM was dispensable for the mRNA upregulation of the NF-κB-dependent gene *Tnf-α* following all PRR pathways tested. As CCL5 is additionally controlled by IRF transcription factors, such as IRF3, this suggested a role for SARM in the IRF pathway. However, IFN-β, a gene like CCL5 mainly controlled by NF-κB and IRF transcription factors, was mostly unaffected by SARM-deficiency following PRR stimulation of primary BMDMs. Only TLR pathways, like TLR4 and TLR7, showed a slight dependency on SARM, which was more prominent in BMDCs than BMDMs. A more recent experiment suggested that the effect on IFN-β in primary cells was most likely

caused by a delay in IFN-β expression in the absence of SARM, rather than a profound dysfunction (data not shown). Nevertheless, due to the potential function of SARM in TLR4-mediated IFN-β expression in primary BMDCs and the known SARM-TRIF interaction, I investigated if SARM played a role in DC maturation and endotoxin tolerance, but found that these processes were independent of SARM. In contrast to the subtle IFN-β regulation in primary BMDMs, immortalised BMDMs showed an absolute requirement for SARM for IFN-β expression in all PRR pathways tested. The dramatic difference in IFN-β expression of *Sarm*$^{-/-}$ primary and immortalised BMDMs was confirmed by an independent approach. Instead of directly analysing IFN-β expression following LPS stimulation, I assessed IFN-dependent responses elicited by secreted IFNs and their subsequent signalling via the type I IFN receptor (IFNAR). As expected, SARM-deficient iBMDMs had a complete defect in activating IFN-dependent STAT1 or inducing the IFN-stimulated genes (ISGs) viperin and *Irf7*. This coincided with the lack of IFN-β production in these cells. Even the basal expression of *Irf7* was abrogated in *Sarm*$^{-/-}$ iBMDMs, indicating the additional defect of IFN priming. "IFN priming" is usually mediated by the constitutive production of low amounts of IFNs and their signalling via the IFNAR, which establishes the basal gene expression profile of resting BMDMs and is also critical for the unique cytokine response upon stimulation (247). Therefore the lack of IFN priming in *Sarm*$^{-/-}$ iBMDMs was likely to have affected many other genes, apart from *Irf7*, which needs to be considered when interpreting the results. On the contrary, the IFN-dependent responses in pBMDMs were mostly unaffected by SARM ablation, which correlated with the intact IFN-β production in these cells following LPS and Sendai virus stimulation. This highlighted again the different requirement for SARM in IFN-β expression in primary and immortalised BMDMs. Furthermore it suggested that iBMDMs may require SARM for IRF3-dependent genes in general, while in primary cells SARM function was more restricted to CCL5 regulation. The iBMDMs were originally generated using a J2 retrovirus carrying oncogenes to induce the transformation of the primary cell to a "tumor-like" cell line (173, 228). It is conceivable that in the setting of a tumor cell, SARM may have acquired different functions, which might explain the divergence between the two BMDM cell types (further discussed in 5.3).

Evaluation CCL5 induction in response to type I and type II IFN pathways then further defined that SARM-mediated regulation was not restricted to the transcription factors activated by PRRs, as IFN receptors mainly initiate the formation of STAT-containing

transcriptional complexes to upregulate IFN-stimulated genes (ISGs) (191). The ISGF3 complex composed of STAT1, STAT2 and IRF9 is mainly activated by the IFNAR and targets genes with ISRE promoter elements, such as *Irf7*, *Ifit2*, *viperin* and potentially *Ccl5* (Figure 4.16). The IFN-γ-stimulated type II IFN receptor (IFNGR) on the other hand activates mostly STAT1 homodimer formation to induce genes controlled by GAS elements. Many of those genes are transcription factors, such as *Irf1* and *Irf8*, which in turn participate in the next wave of gene induction. In fact, IFN-γ-induced CCL5 expression was shown to be mediated by those IRFs (250, 251), while STAT1 was directly implicated in IFNAR-mediated CCL5 induction (252). Most surprisingly, also in the type I and type II IFN response, SARM selectively regulated CCL5 mRNA and protein induction, while the expression of other ISGs, such as *Irf7*, *Ifit2* and viperin, were mostly independent of SARM. Accordingly, no SARM-dependency was observed for the activation of the common transcription factor STAT1.

It is known that after PRR stimulation a huge number of genes are not directly upregulated by the primary pathway, but instead induced in a secondary response by secreted type I IFNs and their subsequent signalling via the IFNAR (201, 253). For CCL5 it was reported that IFNs may contribute to its expression (201). Thus to exactly define the pathway regulated by SARM, I assessed if PRR-induced CCL5 expression in BMDMs was dependent on IFNs or other secondary responses, using an IFNAR blocking antibody and the protein synthesis inhibitor cycloheximide (CHX), respectively. The analysis revealed that *Ccl5*, like *Tnf-α* and *Ifn-β*, was a primary response gene (PRG) following TLR4 activation in primary and immortalised BMDMs. In fact the mRNA of all three genes actually accumulated in the presence of the protein synthesis inhibitor. The CHX-mediated accumulation of certain mRNAs, also basally, is a well documented phenomenon and most likely caused by enhanced mRNA stability (254). The mRNAs of proinflammatory molecules, such as *Tnf-α*, are usually highly unstable in the basal state due to the binding of destabilising proteins to AU-rich elements (ARE) in the 3' untranslated region (UTR) (255). The inhibition of protein synthesis might have reduced the abundance of these proteins and in turn increased mRNA stability. This also explains why *Ccl5* was only marginally enhanced in CHX-treated cells, as its mRNA is known to be inherently stable and devoid of any ARE sequences (256). Consistent with the induction of *Ccl5* as a PRG, its expression was mainly independent of a secondary IFN signal. Only at later time points, IFNs might slightly contribute to *Ccl5* expression, which was overall in agreement with the

literature (201). Thus, in addition to the IFN pathway, SARM also selectively regulated CCL5 expression directly in the PRR pathway in the context of the constitutively expressed signalling molecules, transcription factors and coactivators. But the mechanism had to differ from the other TLR4-induced PRGs, TNF-α and IFN-β, as they were mostly unaffected by SARM-deficiency in pBMDMs. TNF-α regulation clearly differs from CCL5, as it is mainly controlled by NF-κB (257). But referring to the literature, the transcriptional regulation of CCL5 and IFN-β is more similar, as they both require the cooperative assembly of NF-κB, AP-1 and IRF transcription factors at the promoter to form an enhanceosome for optimal gene induction (258, 259). Interestingly, the analysis of the IFNAR blocking experiment revealed a clear regulatory difference between both genes. While TLR4-induced *Ccl5* expression was mostly independent of IFNs, the *Ifn-β* expression showed some dependency on intact IFN signalling. It is well established that TLR4-induced IFN-β is initially mainly upregulated by constitutive IRF3, but requires IFN-induced IRF7 later on in the response to amplify the expression (237, 260). This positive IFN feedback loop was also operational in iBMDMs, where I observed that IFNs were dispensable for the initial *Ifn-β* peak, but required for the sustained *Ifn-β* expression at later times. Surprisingly, pBMDMs required an intact IFN signal already for the immediate-early expression of *Ifn-β*. This was most likely caused by the complete loss of basal IRF7 due to the blocking of the IFNAR and the lack of IFN priming (201). Thus the data elucidated a different regulatory mechanism of CCL5 and IFN-β, in that IFN-β was more reliant on IRF7 or another IFN-induced factor, while CCL5 expression was completely independent of IFN-mediated regulation. Furthermore, I noted that the kinetics of *Ccl5* expression were delayed compared to the immediate-early upregulation of *Ifn-β*, which suggested that additional control mechanisms were in place to decelerate *Ccl5* induction. More recently, new concepts of the selective transcriptional regulation of gene expression have emerged whereby particularly chromatin and its modifications play a key role in controlling the accessibility of transcription factor binding sites and the recruitment of regulatory proteins to the promoter (261). Further CCL5 was shown to belong to a group of PRGs that is tightly controlled by chromatin remodelling processes and even actively suppressed at the basal state, which might explain the delayed expression in comparison to IFN-β (246, 262-264). IRF molecules in particular, which interact with other transcription factors and coactivators, seem to play a crucial role in initiating chromatin remodelling by SWI/SNF complexes on selective, tightly regulated genes, including *Ccl5 (246).*

Interestingly, all the investigated pathways, namely PRRs, IFNAR and IFNGR, potentially use an IRF family member as a central means to upregulate CCL5. The fact that SARM selectively regulated CCL5 expression of all these different pathways, suggested a more downstream regulatory role of SARM, independent of the different transcription factors of the individual pathways. Thus it is intriguing to speculate that SARM might be involved in a *Ccl5*-specific remodelling process at the promoter level. Another possibility may be that SARM acts more upstream in an alternative pathway common to PRR and IFN receptors, which would function more as a coactivator pathway to enhance the response. This hypothesis was particularly attractive in light of the role of SARM in *C. elegans*, where the homologue TIR-1 functioned independent of the TLR pathway upstream of a p38 MAPK cascade to mediate immune responses (see 1.4, (212)). As the p38 MAPK pathway was also implicated in IFNAR- and IFNGR-mediated gene induction, independent of STAT1 activation, it will be interesting to investigate if SARM regulated CCL5 expression via activating this evolutionary conserved pathway (191, 194). Accordingly, SARM might play a role in the expression of a specific set of genes, a question which is currently under investigation.

Furthermore, I noted that the role of SARM in CCL5 expression was more apparent in cell types and pathways with an inherent high CCL5 induction capacity. Thus SARM played only a minor role in CCL5 expression in BMDCs, which generally induced much lower levels of CCL5 compared to BMDMs. A slight dependency on SARM was mainly observed in the TLR pathways, while the cytosolic receptors showed no requirement for SARM to express CCL5. Explanations for the different potential of BMDCs and BMDMs to upregulate CCL5 can be found in more recent studies. The corresponding growth factors GM-CSF and M-CSF, respectively, have been shown to polarise monocytic cells towards a M1- and M2-like macrophage phenotype with a specific cytokine profile (247). GM-CSF-treated cells exhibited a more proinflammatory phenotype with stronger activity of the NF-κB pathway, in contrast to the more IFN- and IRF-dominated profile present in M-CSF-derived BMDMs. This might explain the enhanced CCL5 induction in BMDMs compared to BMDCs. The transcription factors IRF5 and IRF4 are currently discussed as key mediators of the macrophage polarisation process (265, 266). That SARM possessed more an enhancing function in CCL5 expression was also indicated by the fact that SARM-deficiency attenuated, but did not completely abrogate CCL5 expression.

During the cytokine study I also noted that, even though SARM was dispensable for *Tnf-α* mRNA induction, the TNF-α protein expression was slightly modulated by SARM. This would suggest an additional role for SARM in TNF-α translation, but the effects were conflictive in primary and immortalised BMDMs. Primary *Sarm*$^{-/-}$ BMDMs and BMDCs showed slightly reduced TNF-α protein levels, while immortalised knockout cells exhibited elevated basal and stimulated protein levels. The latter phenotype was likely caused by the basally enhanced *Tnf-α* mRNA expression in *Sarm*$^{-/-}$ iBMDMs. Subsequently, I examined if SARM played a role in *Tnf-α* mRNA stability, but could exclude a function for SARM in this process (data not shown). I rather suspect that the basally enhanced *Tnf-α* mRNA levels in immortalised *Sarm*$^{-/-}$ cells were a side effect of the defective IFN system, as it was proposed that the lack of IFN priming could cause a more NF-κB-related phenotype and lead to elevated levels of proinflammatory cytokines, such as TNF-α (247). However a different study showed that constitutive IFN-β was also required for the basal expression of TNF-α (201). Thus the cause of the enhanced TNF-α mRNA and protein in resting *Sarm*$^{-/-}$ iBMDMs remains elusive and was not further investigated due to the divergence to primary cells. On the contrary, in primary BMDMs and BMDCs, SARM might play a subtle role in promoting TNF-α translation following TLR4 activation. Interestingly, a recent in vivo study on *Sarm*-knockout mice also revealed a dependency on SARM to upregulate TNF-α in response to neurotropic WNV (221). However this effect was restricted to the brainstem and included a regulation of *Tnf-α* mRNA, which was unaltered in my study in BMDMs. Thus, SARM-mediated TNF-α regulation may depend on the cell type, the environment and the immune stimulus; and might be more pronounced in an immune cell type of the brain, where SARM is highly expressed. It is well documented that due to the potent proinflammatory functions, TNF-α expression is highly controlled at the transcriptional and posttranscriptional level. Proteins that bind AREs in the 3' UTR of *Tnf-α* mRNA play a major role in regulating its stability and translation (267). It is intriguing that particularly the p38 MAPK pathway and its downstream kinases MNK1 and MK2 mediate the TLR4-induced enhanced TNF-α translation (268, 269), as there might be several possibilities as to how SARM may regulate this process. As the TLR4-induced prolonged activation of MK2 was shown to be TRIF-dependent, I examined a role for SARM in this pathway, but preliminary data indicated a normal phosphorylation of MK2 in the absence of SARM (data not shown). Also interesting was, that IRAK2, a newly identified interaction partner of SARM, was

involved in MNK1 activation and TNF-α translation (270, 271). And as described above, the homologue of mammalian SARM in *C. elegans*, TIR-1, was already shown to function upstream of such a MAPK cascade to mediate immune responses (see 1.4, (212)). However, the effects on TNF-α translation were only subtle and not as significant as the role of SARM in CCL5 expression, which was consistent in primary and immortalised BMDMs and which will be the focus of the following mechanistic studies.

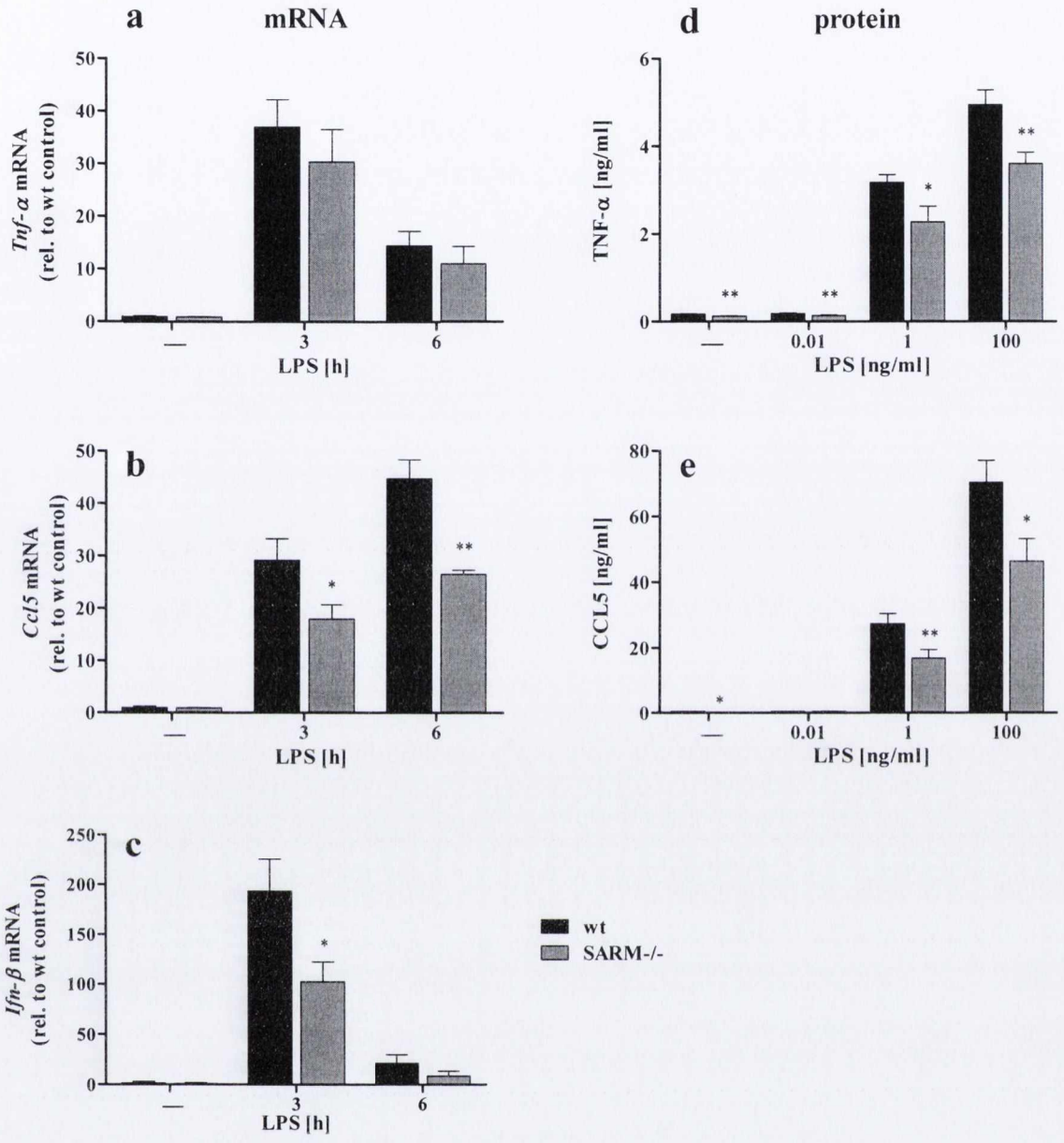


Figure 4.1: Role for SARM in TLR4-induced CCL5 and IFN-β expression in primary BMDCs

Analysis of TNF-α, CCL5 and IFN-β mRNA and protein expression in primary wt and *Sarm*$^{-/-}$ BMDCs. (a-c) Cells were seeded in 24 well plates at 5x10^5 cells/ml and stimulated for 3 and 6h with LPS [100ng/ml] or medium as control (—). *Tnf-α*, *Ccl5* and *Ifn*-β mRNA expression were determined by quantitative real-time PCR, normalised to the housekeeping gene *β-actin* and presented relative to the control of wt BMDCs. (d,e) Cells were seeded in 96 well plates at 5x10^5 cells/ml and stimulated for 24h with the indicated concentrations of LPS or medium as control (—). Supernatants were collected and assayed for TNF-α and CCL5 protein by ELISA. Data are from one experiment representative of at least three (mean ± s.d.). * P<0.05, ** P<0.01, *** P<0.001, compared with wt (Student's *t*-test).

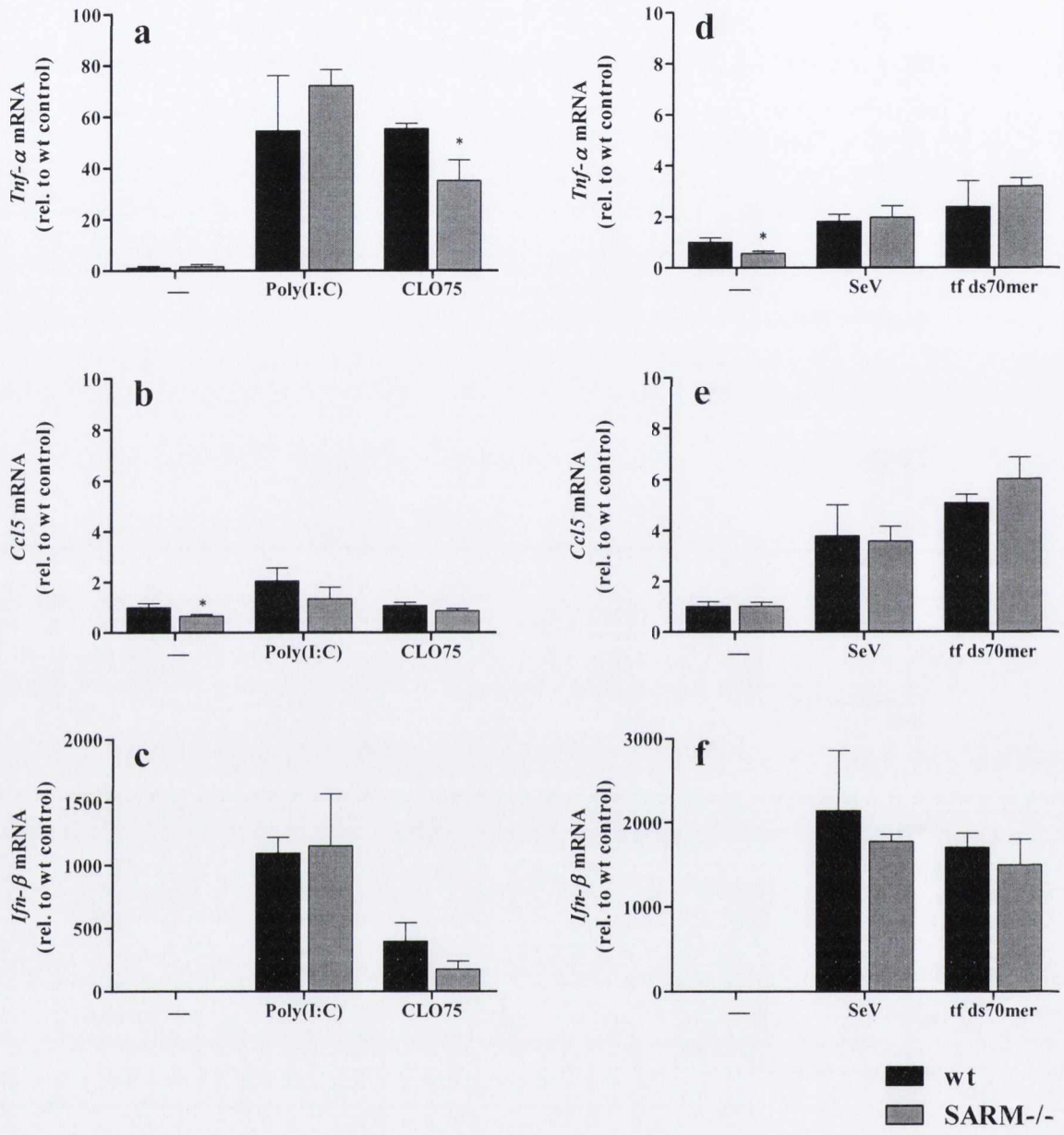


Figure 4.2: SARM is dispensable for non-TLR-induced CCL5 and IFN-β expression in primary BMDCs

Analysis of *Tnf-α*, *Ccl5* and *Ifn-β* mRNA expression in primary wt and *Sarm*$^{-/-}$ BMDCs. Cells were seeded in 24 well plates at 5x10^5 cells/ml and stimulated for 2h with Poly(I:C) [25μg/ml] and CLO75 [2.5μg/ml] or for 6h with Sendai virus (SeV) and transfected ds70mer [1μg/ml]. Medium-treated cells served as control (—). *Tnf-α*, *Ccl5* and *Ifn*-β mRNA expression were determined by quantitative real-time PCR, normalised to the housekeeping gene *β-actin* and are presented relative to the wt control. Data are from one experiment representative of three (mean ± s.d.). * P<0.05, ** P<0.01, compared with wt (Student's *t*-test).

Receptor	TLR4	TLR7	TLR3	RIG-I	DNA sensor
Ligand	LPS	CLO75	Poly(I:C)	SeV	tf ds70mer
TNF	0 (0/--)	0 (0/-)	0/n.d.	0	0
CCL5	-/0	-/0	0/n.d.	0	0
IFN-β	---/0	--/0	0	0	0

Sarm$^{-/-}$ BMDCs compared to wt	
0	no difference
-	< 25% reduction
--	25-49% reduction
---	≥ 50% reduction
n.d.	not detectable

Table 4.1: Overview of the effect of SARM-deficiency on TLR- and non-TLR-induced cytokines in primary BMDCs

The table summarises the TLR- and non-TLR-induced TNF-α, CCL5 and IFN-β expression in *Sarm*$^{-/-}$ primary BMDCs compared to the corresponding wt. The overview is based on the mRNA data of three or more individual experiments. The protein data mostly showed a similar trend, except were brackets display a divergent effect at the protein level. Slash (/) separates different phenotypes observed to a similar extend in the experiments.

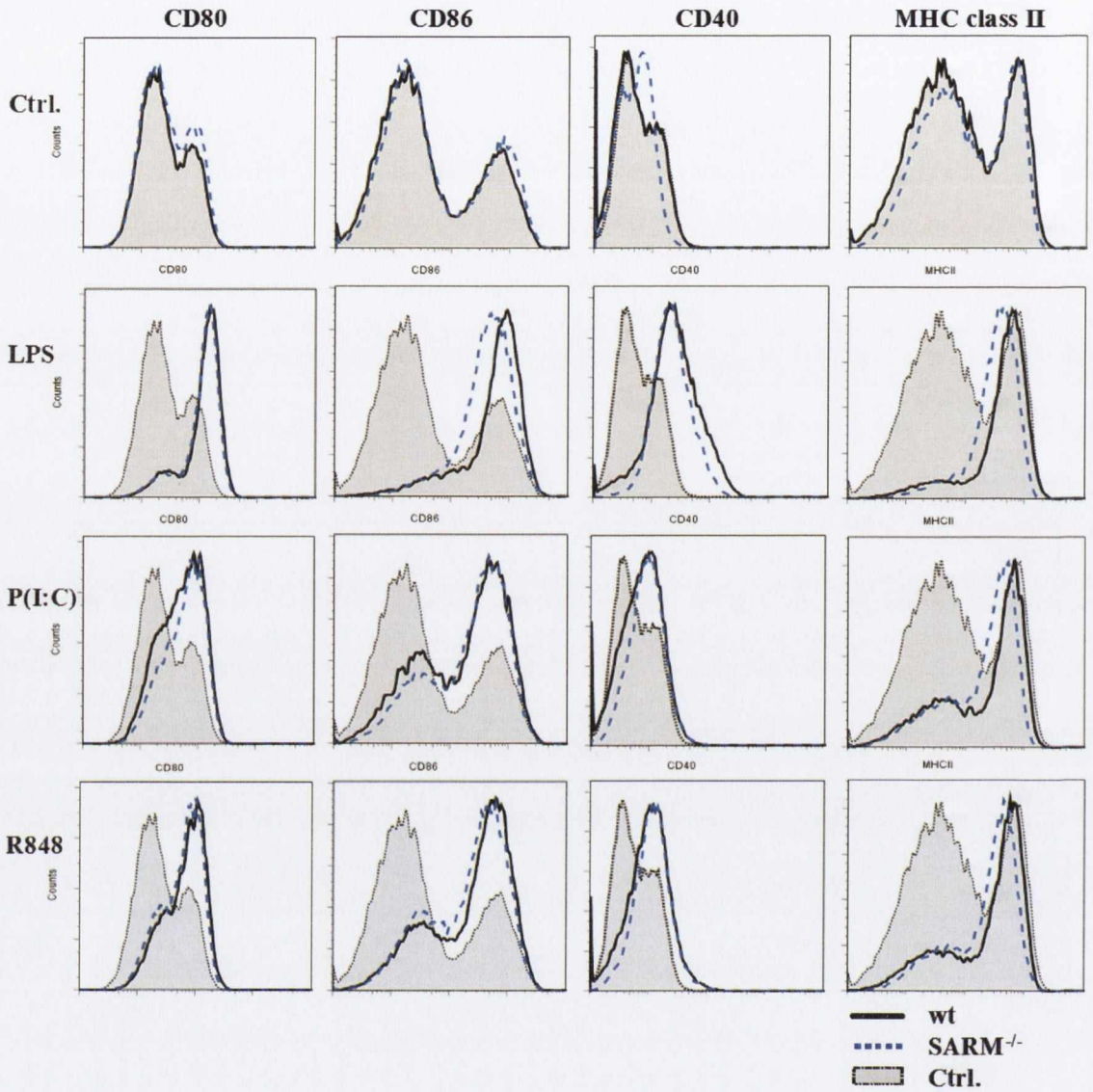


Figure 4.3: SARM is dispensable for TLR-induced maturation of primary BMDCs

Primary wt and *Sarm*$^{-/-}$ BMDCs were seeded in 96 well plates at 6x10^5 cells/ml and stimulated for 24h with LPS [100ng/ml], Poly(I:C) [10µg/ml], R848 [5µg/ml] or medium as control (Ctrl.). Then cells were analysed for surface expression of the costimulatory molecules CD80, CD86 and CD40 or MHC class II using fluorescent-labeled specific antibodies and flow cytometry. Cells were gated on the CD11c$^+$ population, representing BMDCs. The histograms present the changes in surface molecule expression comparing treated wt (bold black lines) and treated *Sarm*$^{-/-}$ (dashed blue lines) BMDCs with untreated control (shaded histograms). The data are from one experiment representative of three.

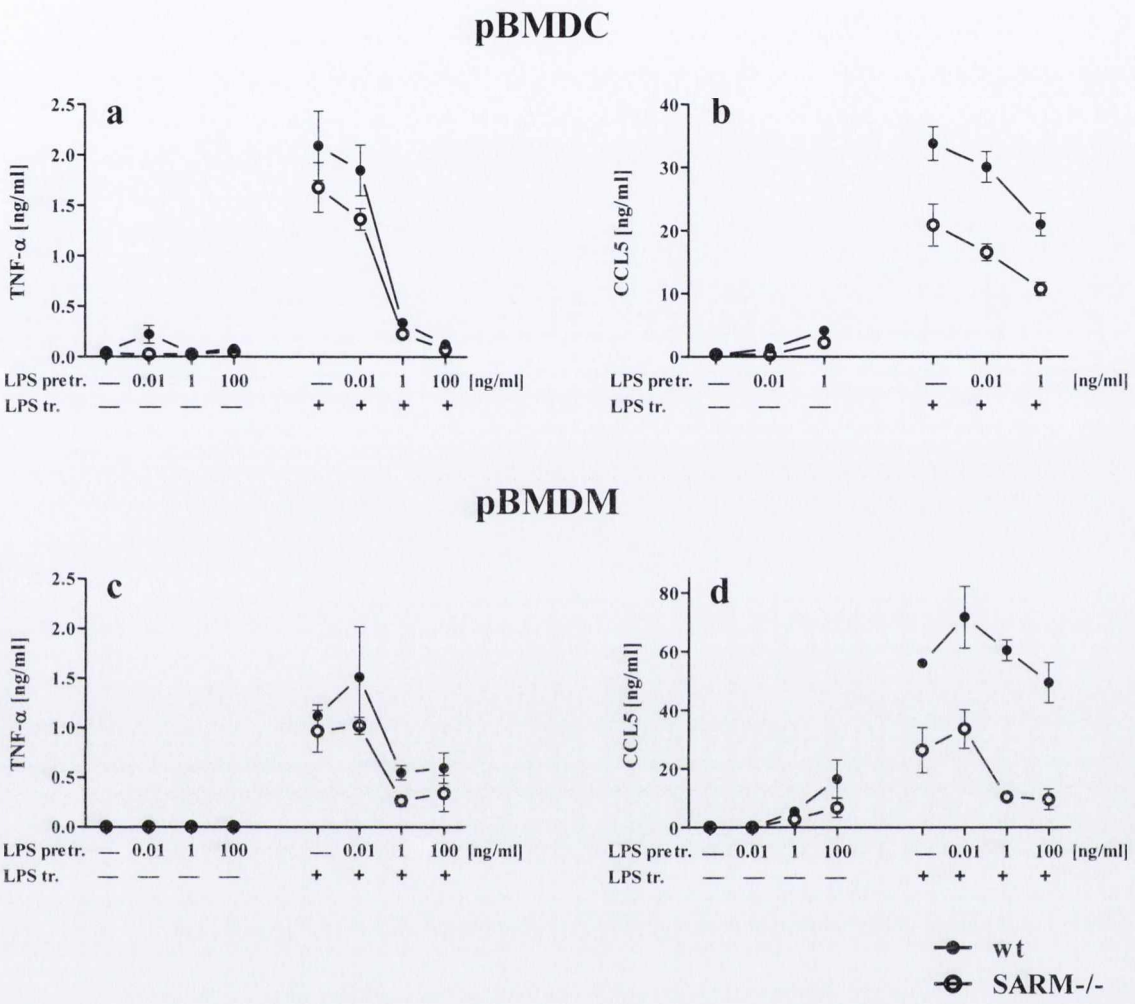


Figure 4.4: SARM has no role in endotoxin tolerance in primary BMDCs and BMDMs

Analysis of endotoxin tolerance in wt and *Sarm*$^{-/-}$ pBMDCs and pBMDMs. Cells were seeded in 96 well plates at $5x10^5$ cells/ml and pretreated with the indicated concentrations of LPS or medium as control (—) (LPS pretr.). After 24h the medium was replaced by fresh medium and 1-2h later the cells were treated with LPS [100ng/ml] or medium as control (—) (LPS tr.). After 24h, supernatants were collected and assayed for TNF-α and CCL5 protein by ELISA. pBMDC TNF-α and CCL5 data are from one experiment representative of three or two, respectively. The experiment in pBMDMs was performed once (mean ± s.d.).

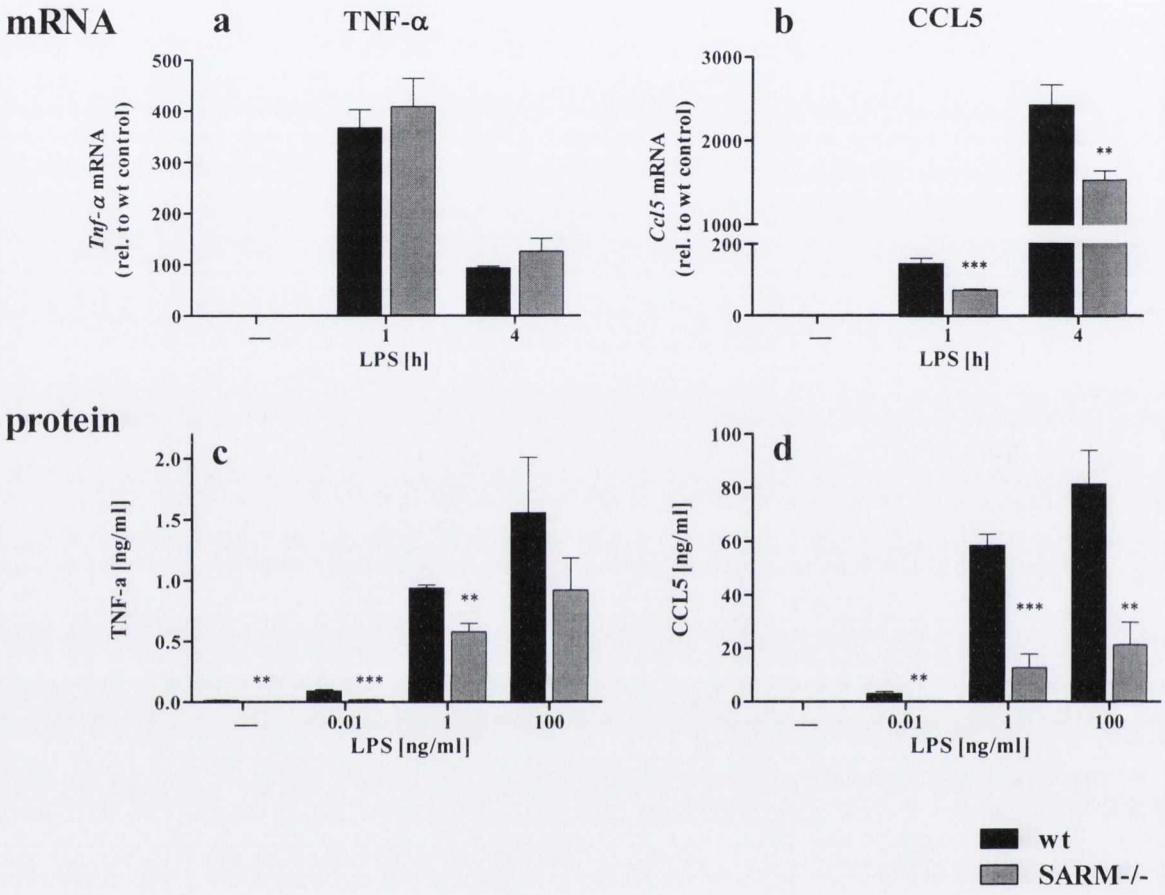


Figure 4.5: SARM is required for TLR4-induced CCL5 expression in primary BMDMs

Analysis of TNF-α and CCL5 mRNA and protein expression in primary wt and *Sarm*$^{-/-}$ pBMDMs following LPS stimulation. (a,b) Cells were seeded in 24 well plates at 5x10^5 cells/ml and stimulated with LPS [100ng/ml] for 1 and 4h or medium as control (—). *Tnf-α* and *Ccl5* mRNA expression were determined by quantitative real-time PCR, normalised to the housekeeping gene *β-actin* and are presented relative to the control of wt BMDMs. (c,d) Cells were seeded in 96 well plates at 5x10^5 cells/ml and stimulated with 0.01, 1 and 100ng/ml LPS or medium as control (—). After 24h, supernatants were collected and assayed for TNF-α and CCL5 protein by ELISA. Data are from one experiment representative of three (mean ± s.d.). * P<0.05, ** P<0.01, *** P<0.001, compared with wt (Student's *t*-test).

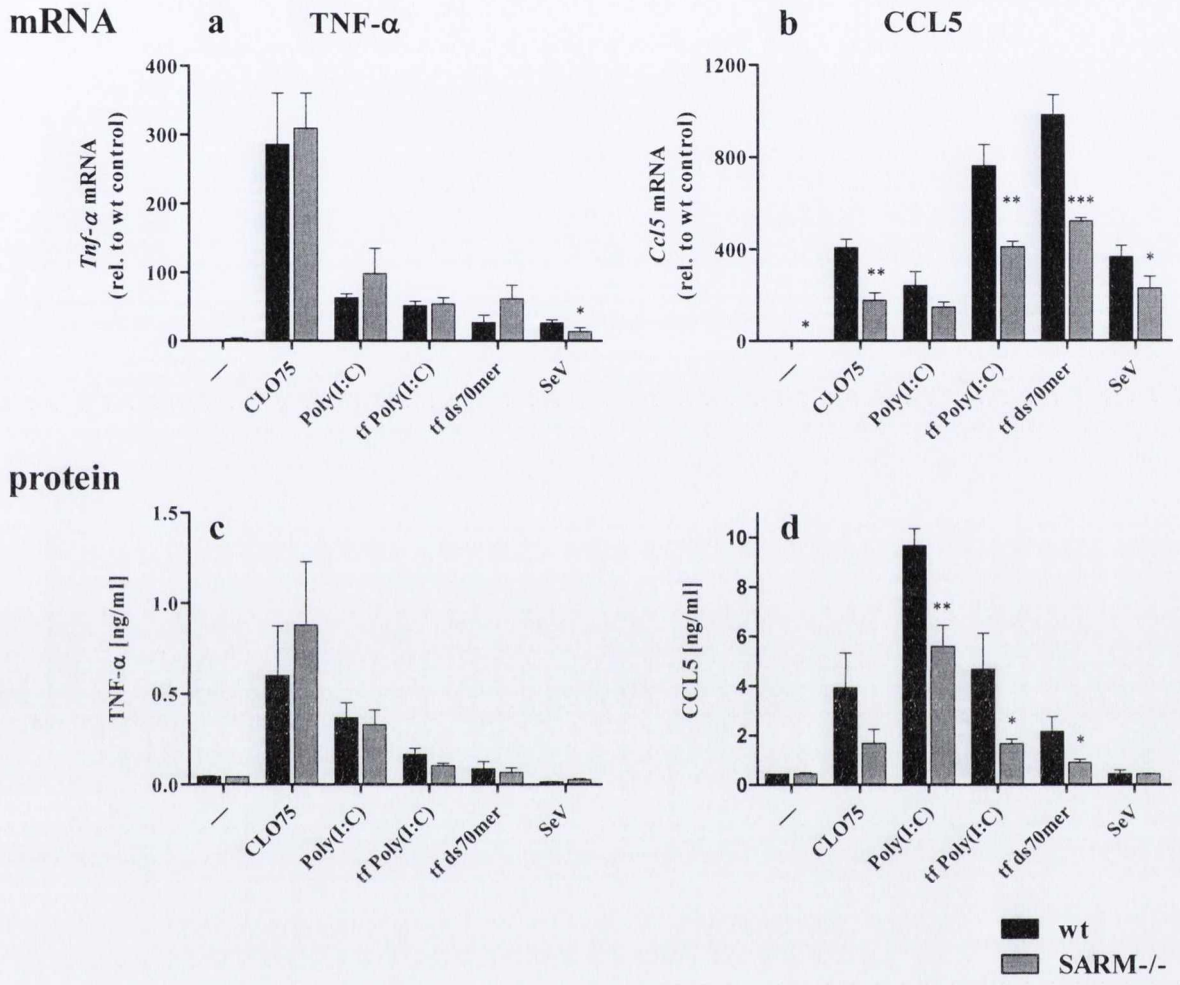


Figure 4.6: SARM promotes TLR- and non-TLR-induced CCL5 expression in primary BMDMs

Analysis of TNF-α and CCL5 mRNA and protein expression in wt and *Sarm*$^{-/-}$ pBMDMs following stimulation with CLO75 [5μg/ml], Poly(I:C) [25μg/ml], transfected Poly(I:C) [2μg/ml], transfected ds70mer [1μg/ml] and Sendai virus (SeV). (a,b) Cells were seeded in 24 well plates at 5x10^5 cells/ml and stimulated for 3h with CLO75 and Poly(I:C) or for 6h with tf Poly(I:C), tf ds70mer and SeV. Medium-treated cells served as control (—). *Tnf-α* and *Ccl5* mRNA expression were determined by quantitative real-time PCR, normalised to the housekeeping gene *β-actin* and are presented relative to the wt control. (c,d) Cells were seeded in 96 well plates at 5x10^5 cells/ml and stimulated with the various ligands for 10h or medium as control (—). Supernatants were collected and assayed for TNF-α and CCL5 protein by ELISA. Data are from one experiment representative of three (mean ± s.d.). * P<0.05, ** P<0.01, *** P<0.001, compared with wt (Student's *t*-test).

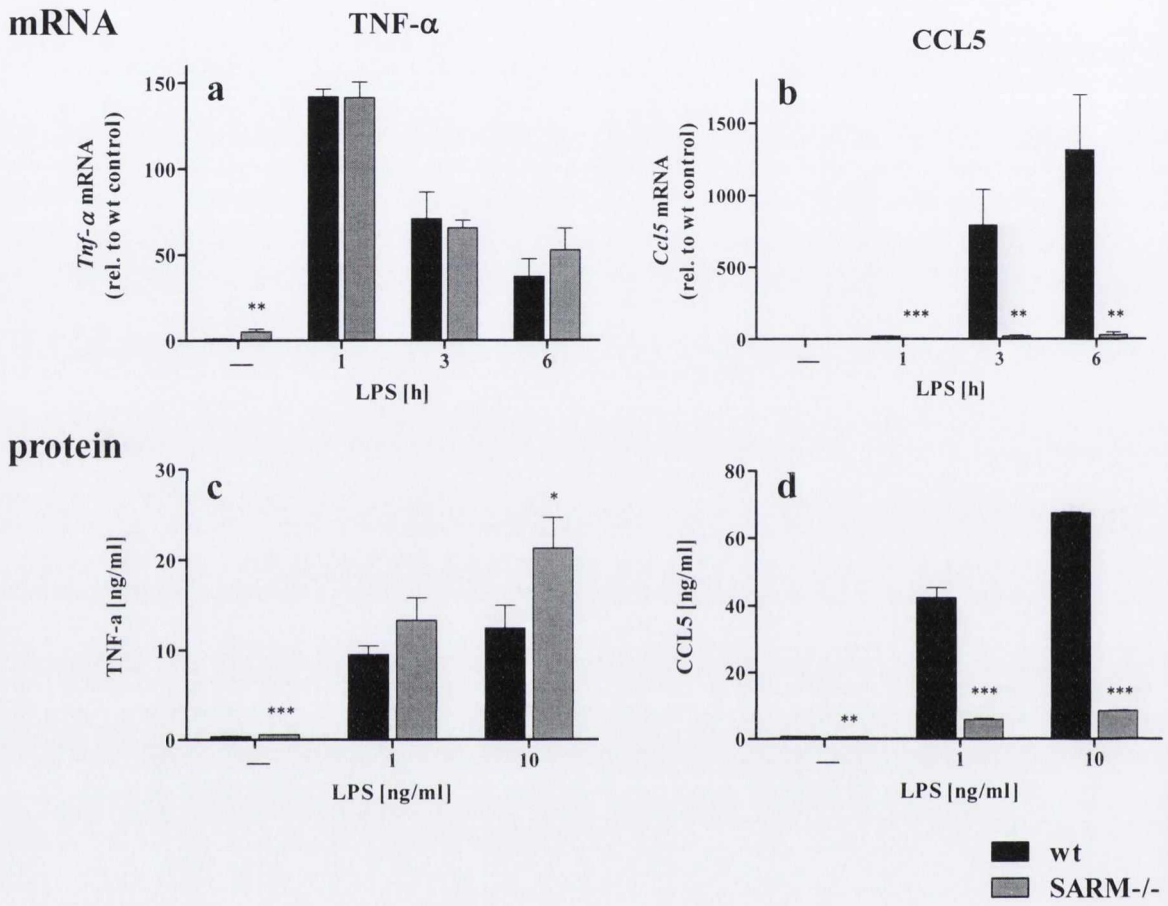


Figure 4.7: SARM is required for TLR4-induced CCL5 expression in immortalised BMDMs

Analysis of TNF-α and CCL5 mRNA and protein expression in immortalised wt and *Sarm*$^{-/-}$ BMDMs (a,b) Cells were seeded in 24 well plates at 5x10^5 cells/ml and stimulated for 1, 3 and 6h with LPS [100ng/ml] or medium as control (—). *Tnf-α* and *Ccl5* mRNA expression were determined by quantitative real-time PCR, normalised to the housekeeping gene *β-actin* and are presented relative to the wt control. (c,d) Cells were seeded in 96 well plates at 5x10^5 cells/ml and stimulated for 24h with 1 and 10ng/ml LPS or medium as control (—). Supernatants were collected and assayed for TNF-α and CCL5 protein by ELISA. Data are from one experiment representative of three (mean ± s.d.). * P<0.05, ** P<0.01, *** P<0.001, compared with wt (Student's *t*-test).

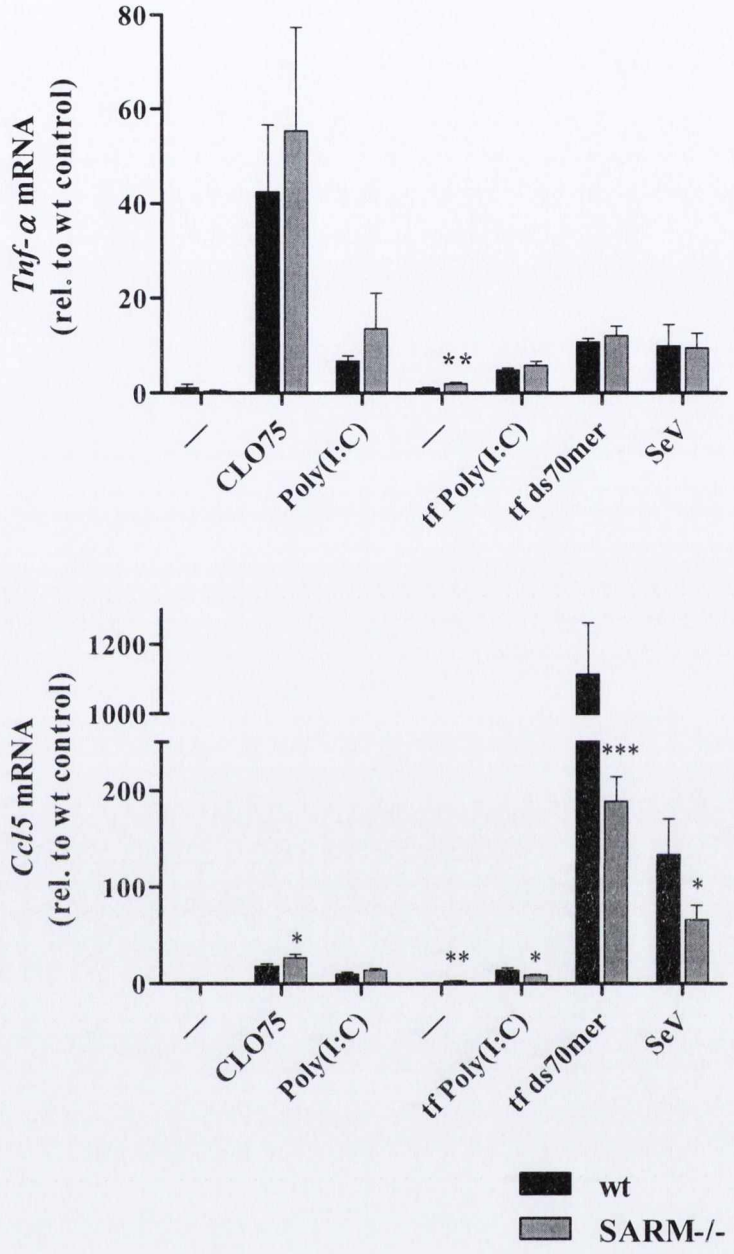


Figure 4.8: SARM promotes non-TLR-induced CCL5 expression in immortalised BMDMs

Wt and *Sarm*$^{-/-}$ iBMDMs were seeded in 24 well plates at 5x10^5 cells/ml and stimulated for 4h with CLO75 [5μg/ml] and Poly(I:C) [25μg/ml] or for 6h with transfected Poly(I:C) [2μg/ml], transfected ds70mer [1μg/ml] and Sendai virus (SeV). Medium-treated cells served as control (—). *Tnf-α* and *Ccl5* mRNA expression were determined by quantitative real-time PCR, normalised to the housekeeping gene *β-actin* and are presented relative to the wt control. The TLR- and PRR-stimulated cells are from independent experiments, shown with the corresponding control. Data are from one experiment representative of three (mean ± s.d.). * P<0.05, ** P<0.01, *** P<0.001, compared with wt (Student's *t*-test).

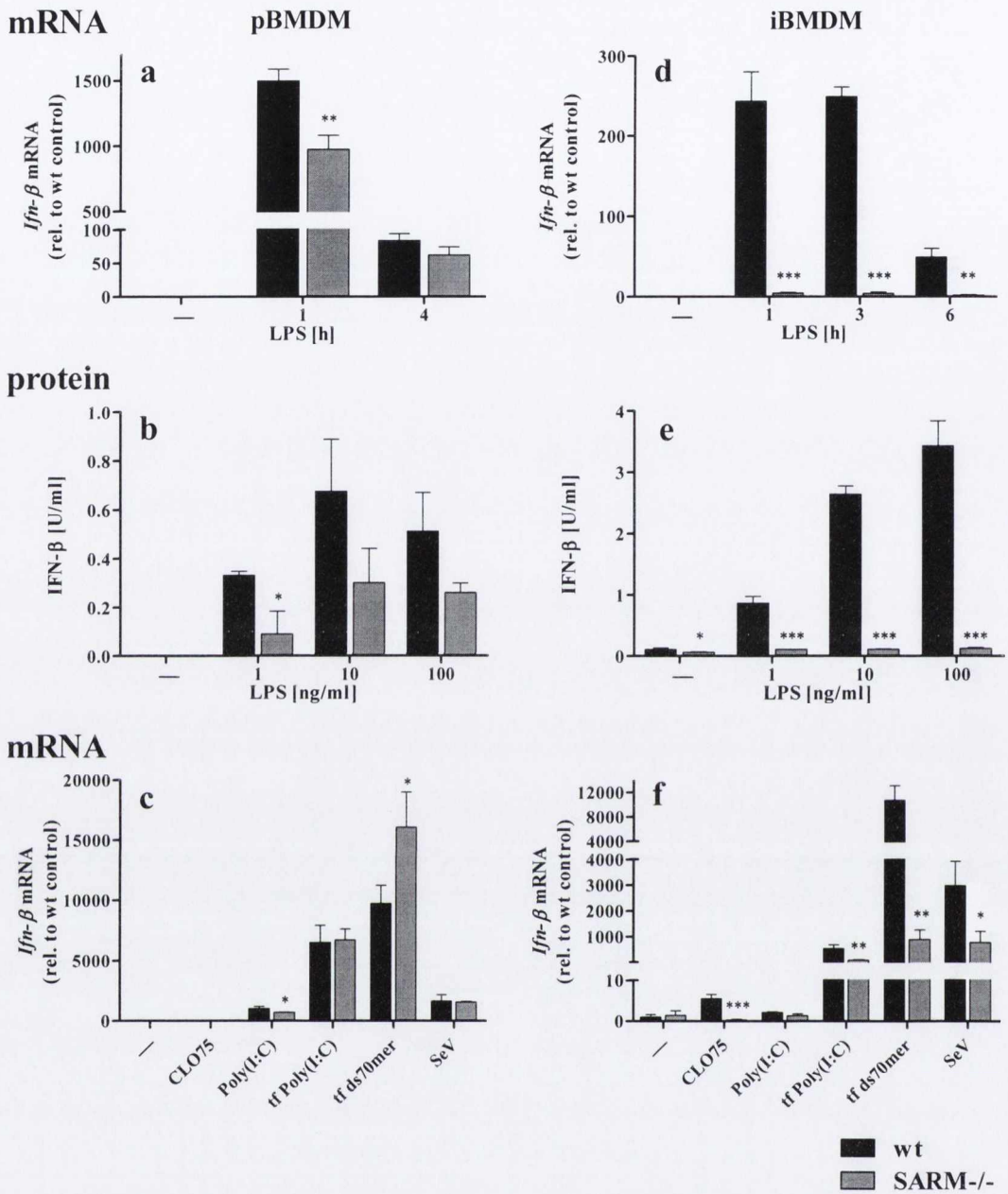


Figure 4.9: SARM is required for TLR- and non-TLR-induced IFN-β expression in immortalised, but not in primary BMDMs

Comparison of IFN-β mRNA and protein expression in wt and *Sarm*$^{-/-}$ pBMDMs and iBMDMs. (a,c,d,f) Quantitative real-time PCR analysis of *Ifn-β* mRNA expression. Cells were seeded in 24 well plates at $5x10^5$ cells/ml and stimulated for the indicated time points with LPS [100ng/ml], for 3h (c) or 4h (f) with CLO75 [5μg/ml] and Poly(I:C) [25μg/ml] or for 6h with transfected Poly(I:C) [2μg/ml], transfected ds70mer [1μg/ml] and Sendai virus (SeV). Medium-treated cells served as control (—). *Ifn-β* mRNA was normalised to the housekeeping gene *β-actin* and is presented relative to the wt control. Data are from one experiment representative of three (mean ± s.d.). (b,e) Cells were seeded in 96 well plates at $5x10^5$ cells/ml and stimulated for 24h with the indicated concentrations of LPS or medium as control (—). Supernatants were collected and assayed for IFN-β protein by ELISA. The experiment was performed once (but (b) was repeated with 6h LPS stimulation) (mean ± s.d.). * $P<0.05$, ** $P<0.01$, *** $P<0.001$, compared with wt (Student's *t*-test).

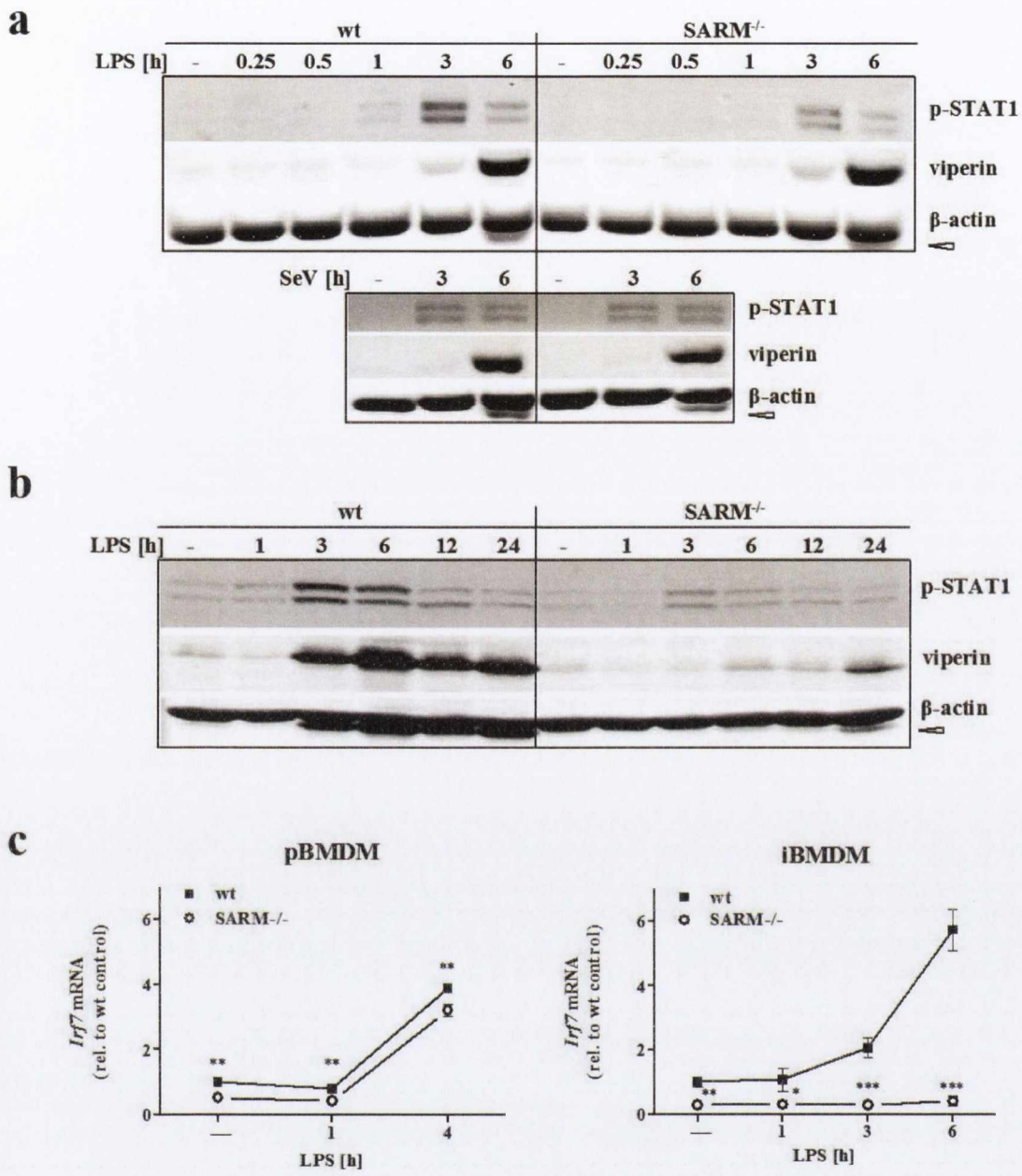


Figure 4.10: SARM is required for TLR4-mediated IFN-dependent responses in immortalised, but not in primary BMDMs

Immunoblot analysis of phosphorylated STAT1 and viperin induction in wt and *Sarm*$^{-/-}$ pBMDMs (a) and iBMDMs (b). Cells were seeded in 6 well plates at 5x10^5 cells/ml and stimulated with LPS [100ng/ml] (a,b) and SeV (a) for the indicated time points or medium as control (—). Lysates were subjected to SDS-PAGE followed by Western Blotting using specific antibodies to detect tyrosine 701-phosphorylated STAT1 (p-STAT1), viperin and β-actin as a loading control. The open arrowhead indicates the detection of viperin on the β-actin blot again. (c) Analysis of *Irf7* mRNA expression in wt and *Sarm*$^{-/-}$ pBMDMs (left) and iBMDMs (right). Cells were seeded in 24 well plates at 5x10^5 cells/ml and stimulated with LPS [100ng/ml] for the indicated time points or medium as control (—). *Irf7* mRNA was determined by quantitative real-time PCR, normalised to the housekeeping gene *β-actin* and is presented relative to wt control (mean ± s.d.). Data are from one experiment representative of one or three for pBMDMs and iBMDMs, respectively. * P<0.05, ** P<0.01, *** P<0.001, compared with wt (Student's *t*-test).

a

Receptor		TLR4	TLR7	TLR3	MDA5	RIG-I	DNA sensor
Ligand		**LPS**	**CLO75**	**P(I:C)**	**tf P(I:C)**	**SeV**	**tf ds70mer**
pBMDM	**TNF**	**0 (0/-)**	**0**	**0**	**0**	**0**	**0/++**
iBMDM		**0 (+)**	**0**	**0**	**0**	**0**	**0**
pBMDM	**CCL5**	**--**	**---**	**--**	**--**	**--**	**--**
iBMDM		**---**	**0**	**0**	**--**	**---**	**---**
pBMDM	**IFN-β**	**--/0**	**-**	**-/0**	**0**	**0**	**+++ (---)**
iBMDM		**---**	**---**	**---**	**---**	**---**	**---**

***Sarm*$^{-/-}$ BMDMs compared to wt**	
0	no difference
-/+	< 25% reduction/enhancement
--/++	25-49% reduction/enhancement
---/+++	≥ 50% reduction/enhancement

b

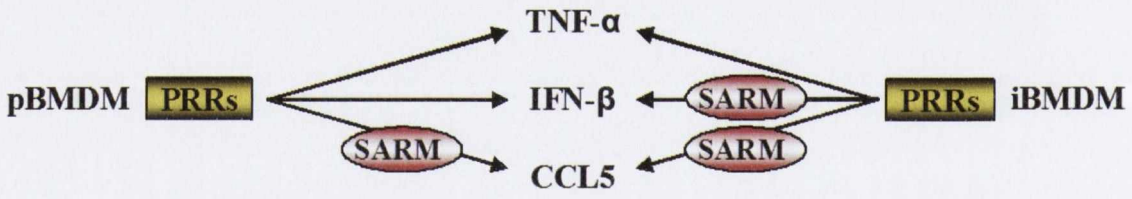


Figure 4.11: Overview of the effect of SARM-deficiency on TLR- and non-TLR-induced cytokines in primary and immortalised BMDMs

(a) The table summarises the TLR- and non-TLR-induced TNF-α, CCL5 and IFN-β expression in *Sarm*$^{-/-}$ primary and immortalised BMDMs (p/iBMDMs) compared with the corresponding wt. The overview is based on the mRNA data of all experiments performed, which mostly correlated with the protein level, except where brackets indicate a stronger or divergent effect seen at the protein level. Slash (/) separates two effects seen to a similar extend in all experiments. The conclusions are based on three or more individual experiments. (b) The simplified cartoon highlights the genes that were positively regulated by SARM in response to PRR stimulation in pBMDMs and iBMDMs.

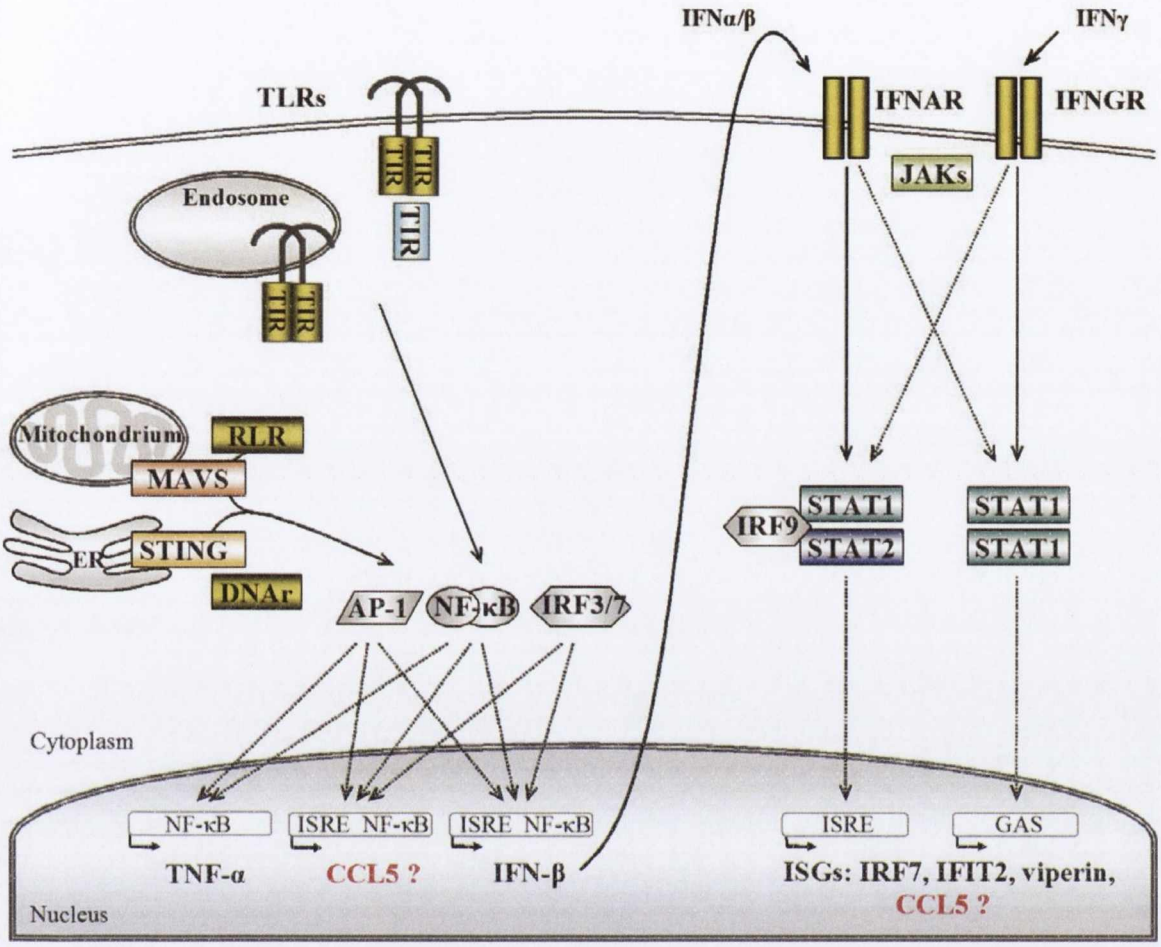
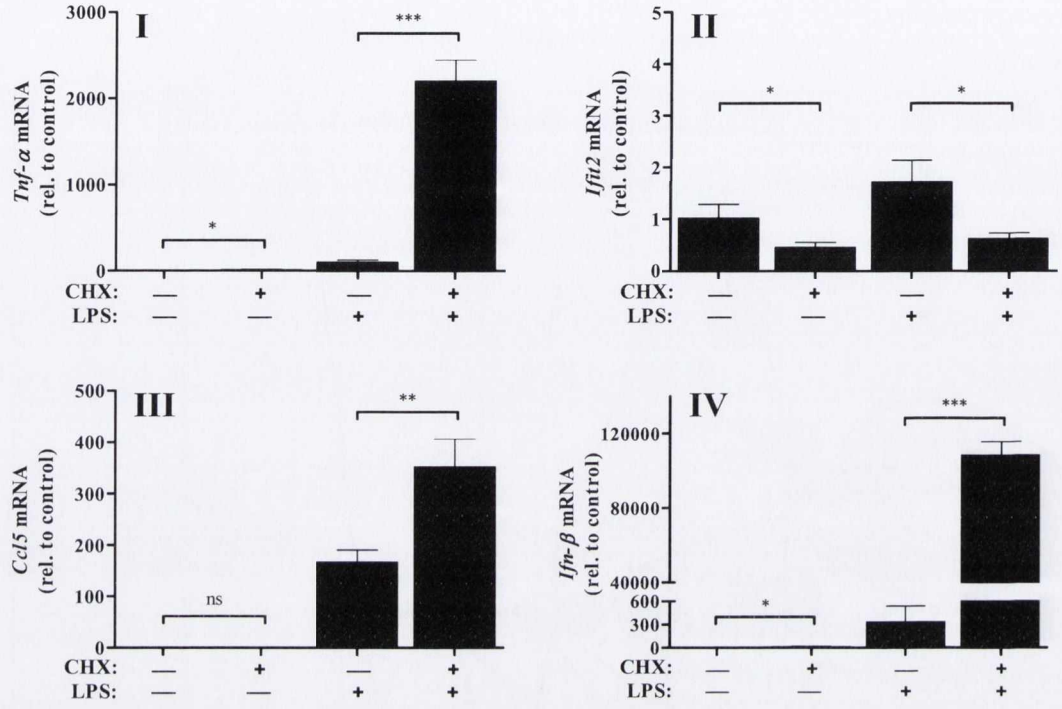


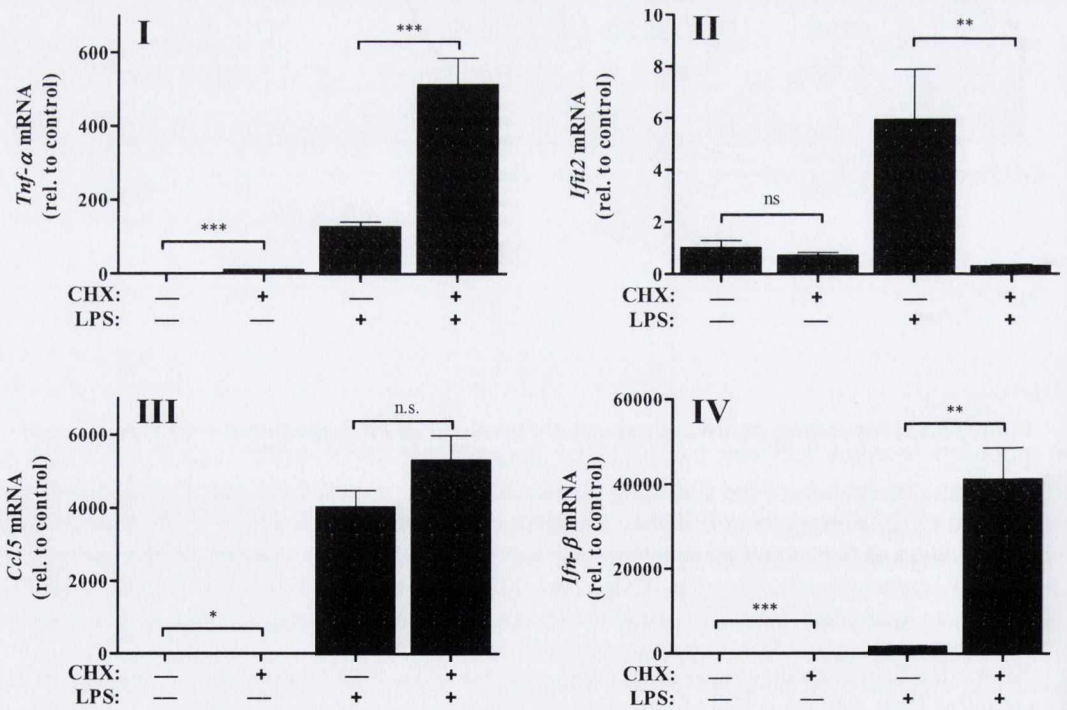
Figure 4.12: Signalling pathways potentially involved in PRR-mediated CCL5 expression

Schematic illustration of the signalling pathways possibly involved in pattern recognition receptors (PRR)-induced CCL5 expression in BMDMs. Stimulation of PRRs, such as TLRs, RLRs and DNA receptors, leads to activation of the transcription factors AP-1, NF-κB and IRF3/7, resulting in the upregulation of a set of primary response genes, including TNF-α and IFN-β. Once secreted, IFN-β can act in an autocrine/paracrine manner to induce numerous IFN-stimulated genes (ISGs) by signalling via the type I IFN receptor (IFNAR). The main transcription factor complex activated by the IFNAR pathway is composed of STAT1, STAT2 and IRF9, also known as ISG factor 3 (ISGF3) complex. Also STAT1 homodimers are known to upregulate a subset of ISGs following IFNAR stimulation. The latter transcriptional complex is typically involved in the type II IFN receptor (IFNGR) pathway that is activated by exogenous IFN-γ stimulation. The following investigations analyse immune responses of these three signalling pathways to further define the role of SARM in CCL5 expression.

a pBMDM



b iBMDM



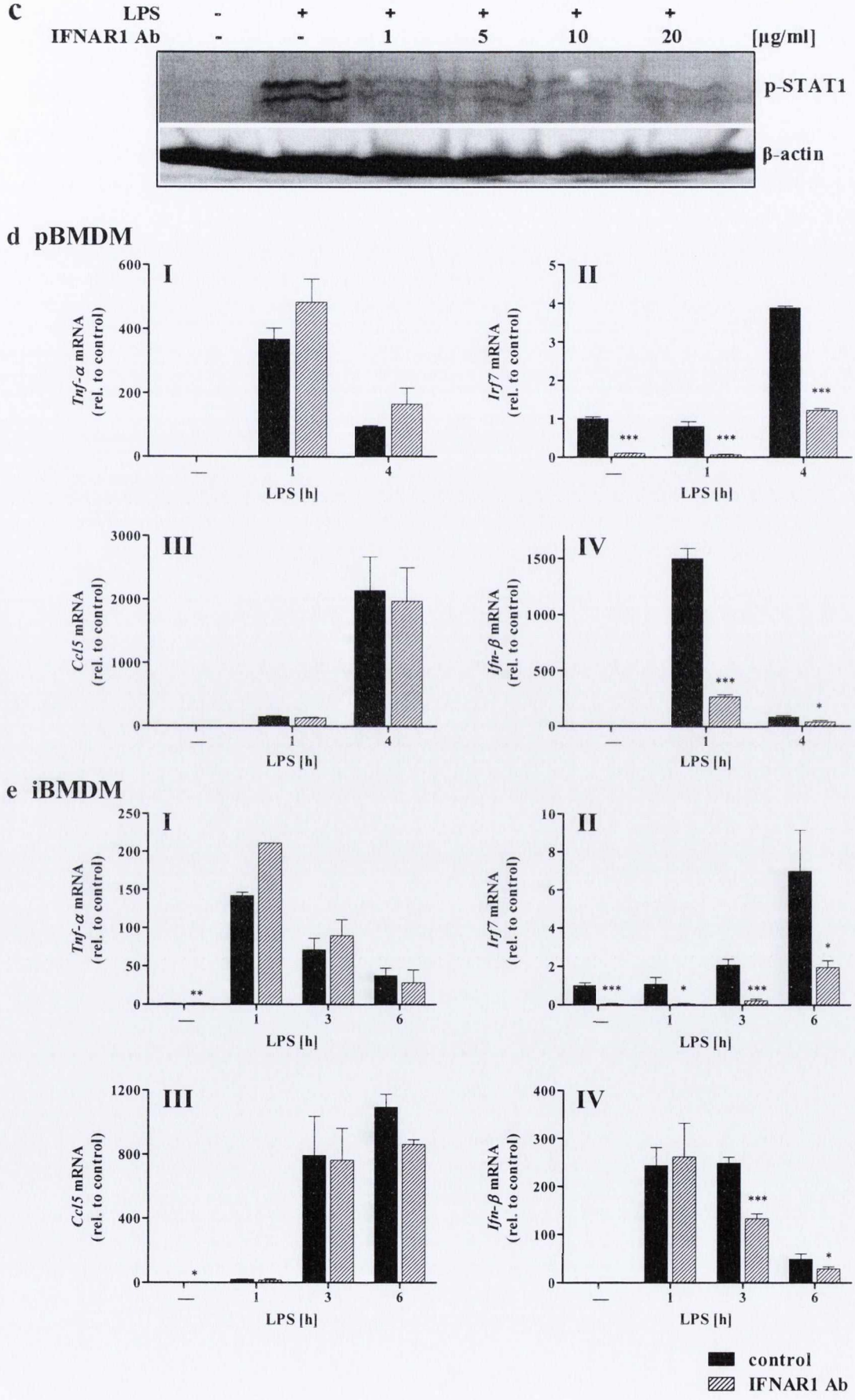

c
LPS - + + + + +
IFNAR1 Ab - - 1 5 10 20 [µg/ml]
p-STAT1
β-actin
d pBMDM
I
Tnf-α mRNA (rel. to control)
II
Irf7 mRNA (rel. to control)
III
Ccl5 mRNA (rel. to control)
IV
Ifn-β mRNA (rel. to control)
LPS [h]
e iBMDM
control
IFNAR1 Ab

Figure 4.13: TLR4-induced TNF-α, CCL5 and IFN-β are primary response genes in BMDMs

(a,b) The protein synthesis inhibitor cycloheximide (CHX) was used to distinguish primary from secondary response genes. wt pBMDMs (a) and iBMDMs (b) were seeded in 24 well plates at $5x10^5$ cells/ml and treated with CHX [5μg/ml] or medium (–) 1h before stimulation with LPS [100ng/ml] or medium (–) for 3h. *Tnf-α*, *Ifit2*, *Ccl5* and *Ifn-β* mRNA were determined by quantitative real-time PCR, normalised to the housekeeping gene *β-actin* and are presented relative to the medium-treated control. (c) Immunoblot analysis to control the blocking of the type I IFN receptor using the IFNAR1 antibody (IFNAR1 Ab). wt iBMDMs were seeded in 12 well plates and incubated overnight with the indicated concentrations of IFNAR1 Ab. The next day, cells were stimulated for 3h with LPS [100ng/ml] and lysates were subjected to SDS-PAGE followed by Western Blotting using specific antibodies to detect tyrosine 701-phosphorylated-STAT1 and β-actin as a loading control. (d,e) The IFNAR1 Ab was used to distinguish LPS-induced IFN-dependent from IFN-independent gene expression. wt pBMDMs (d) and iBMDMs (e) were seeded as described in (a) and incubated overnight with IFNAR1 Ab [5μg/ml] or medium as control. Then cells were stimulated with LPS [100ng/ml] for the indicated time points or medium as control (—). *Tnf-α*, *Irf7*, *Ccl5* and *Ifn-β* mRNA expression were determined as in (a). The data are from one experiment representative of one or two for pBMDMs or iBMDMs, respectively (mean ± s.d.). ns = not significant, * $P<0.05$, ** $P<0.01$, *** $P<0.001$, compared with each control (Student's *t*-test).

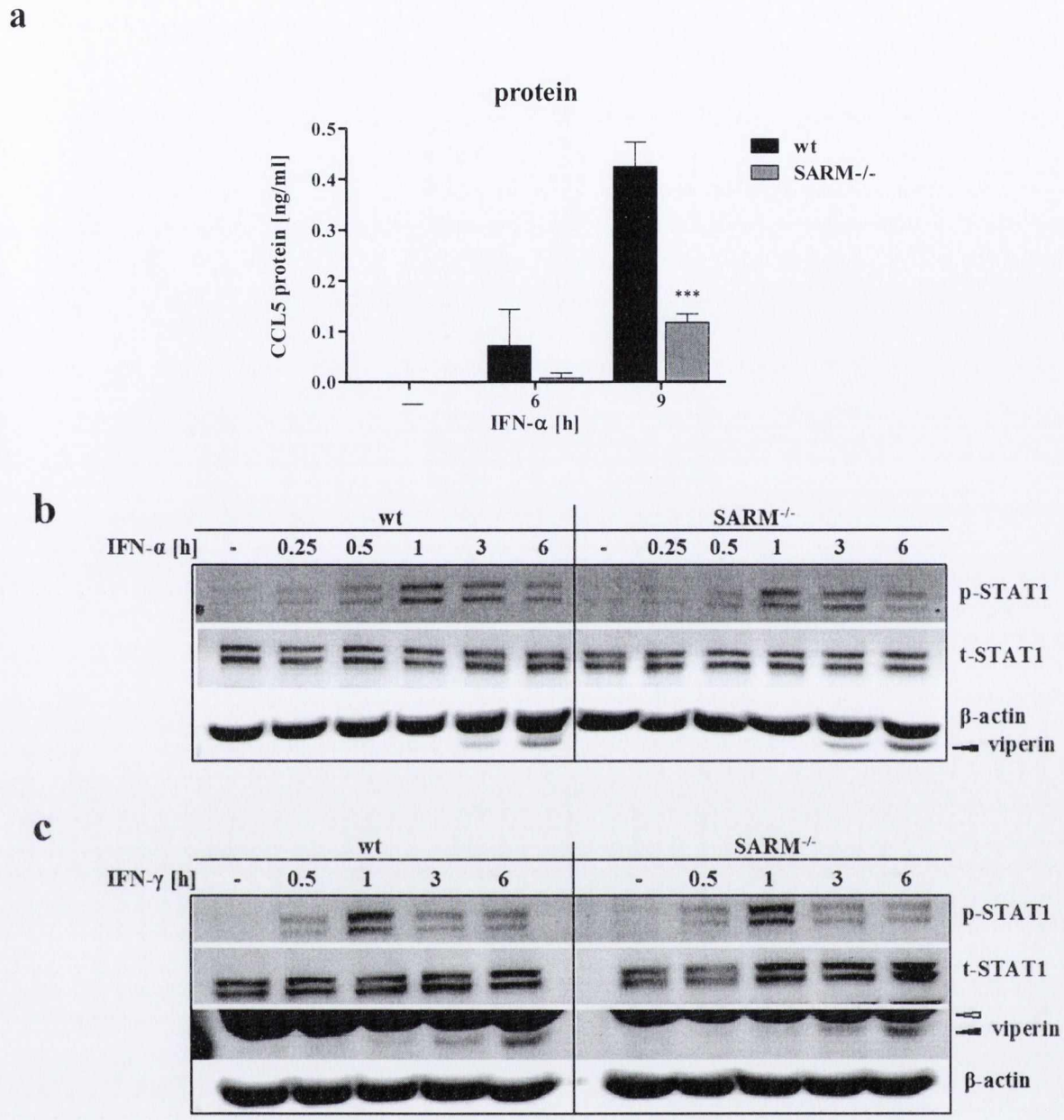
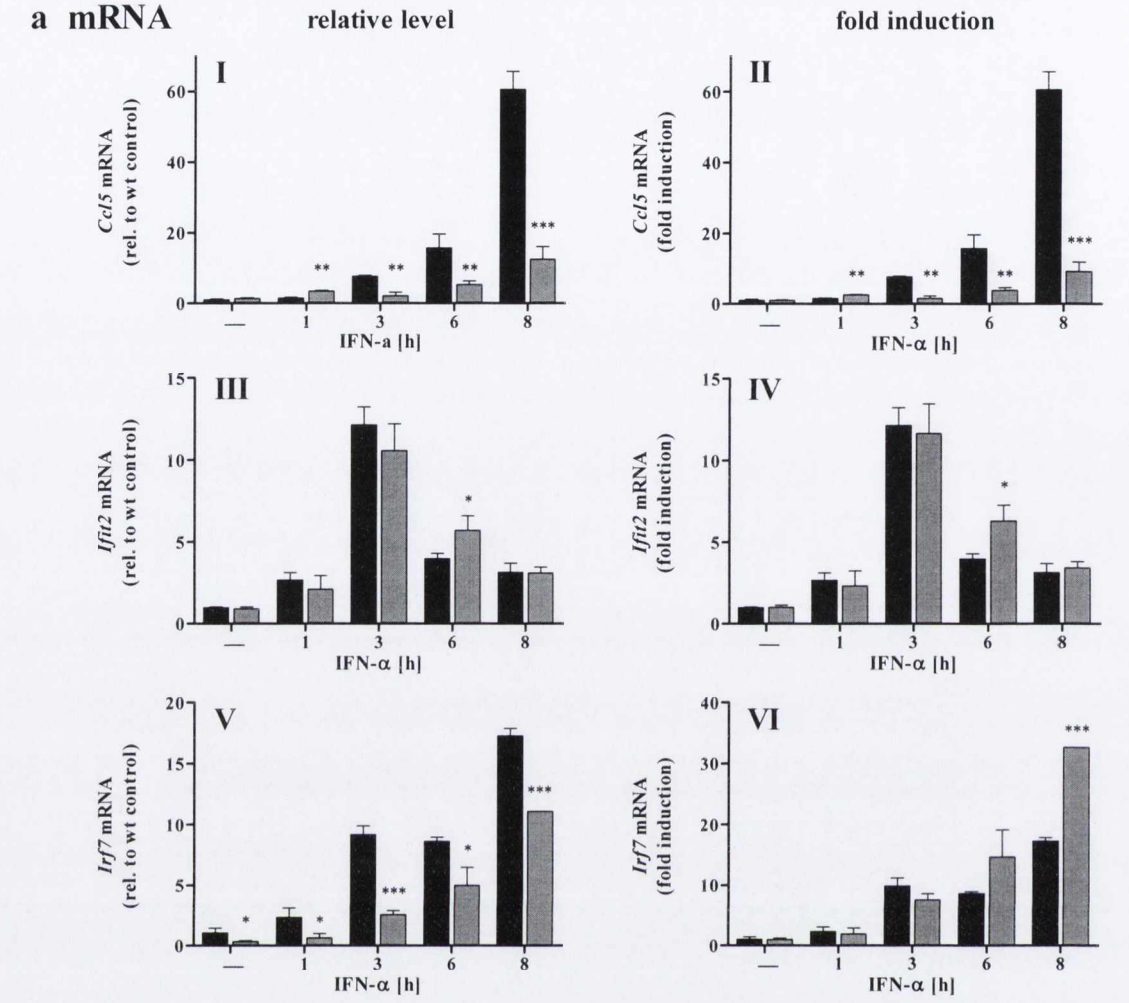
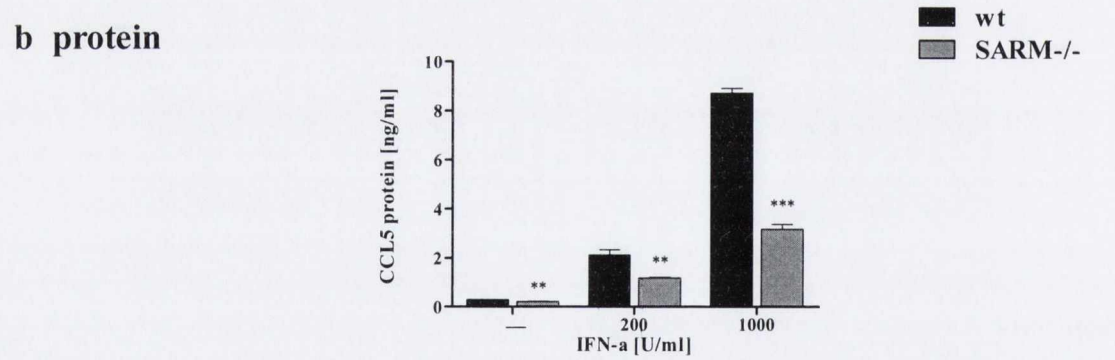
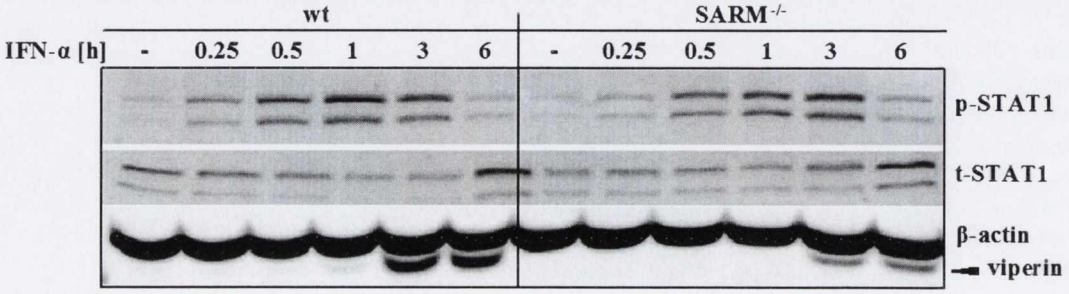


Figure 4.14: SARM is required for IFNAR-induced CCL5 expression, but dispensable for other IFN-mediated responses in primary BMDMs

(a) Analysis of CCL5 protein expression in wt and *Sarm*$^{-/-}$ pBMDMs. Cells were seeded in 24 well plates at $5x10^5$ cells/ml and stimulated with IFN-α [1000U/ml] for 6 and 9h or medium as control (—). Supernatants were collected and assayed for CCL5 protein by ELISA (mean ± s.d.). (b,c) Immunoblot analysis of the induction of p-STAT1 and viperin in wt and *Sarm*$^{-/-}$ pBMDMs. Cells were seeded in 6 well plates at $5x10^5$ cells/ml and stimulated with IFN-α [1000U/ml] (b) and IFN-γ [10ng/ml] (c) for the indicated time points or medium as control (—). Lysates were subjected to SDS-PAGE followed by Western Blotting using specific antibodies to detect tyrosine 701-phosphorylated STAT1 (p-STAT1), t-STAT1, viperin (filled arrowhead) and β-actin as a loading control. The open arrowhead in (c) indicates the detection of β-actin on the viperin blot. Data are from one experiment representative of one (a,c) or two (b). * $P<0.05$, ** $P<0.01$, *** $P<0.001$, compared with wt (Student's *t*-test).


a mRNA
relative level
fold induction
I
II
III
IV
V
VI
Ccl5 mRNA (rel. to wt control)
Ccl5 mRNA (fold induction)
Ifit2 mRNA (rel. to wt control)
Ifit2 mRNA (fold induction)
Irf7 mRNA (rel. to wt control)
Irf7 mRNA (fold induction)
IFN-a [h]
IFN-α [h]
—
1
3
6
8


b protein
wt
SARM-/-
CCL5 protein [ng/ml]
IFN-a [U/ml]
—
200
1000


c
wt
SARM-/-
IFN-α [h]
-
0.25
0.5
1
3
6
p-STAT1
t-STAT1
β-actin
viperin

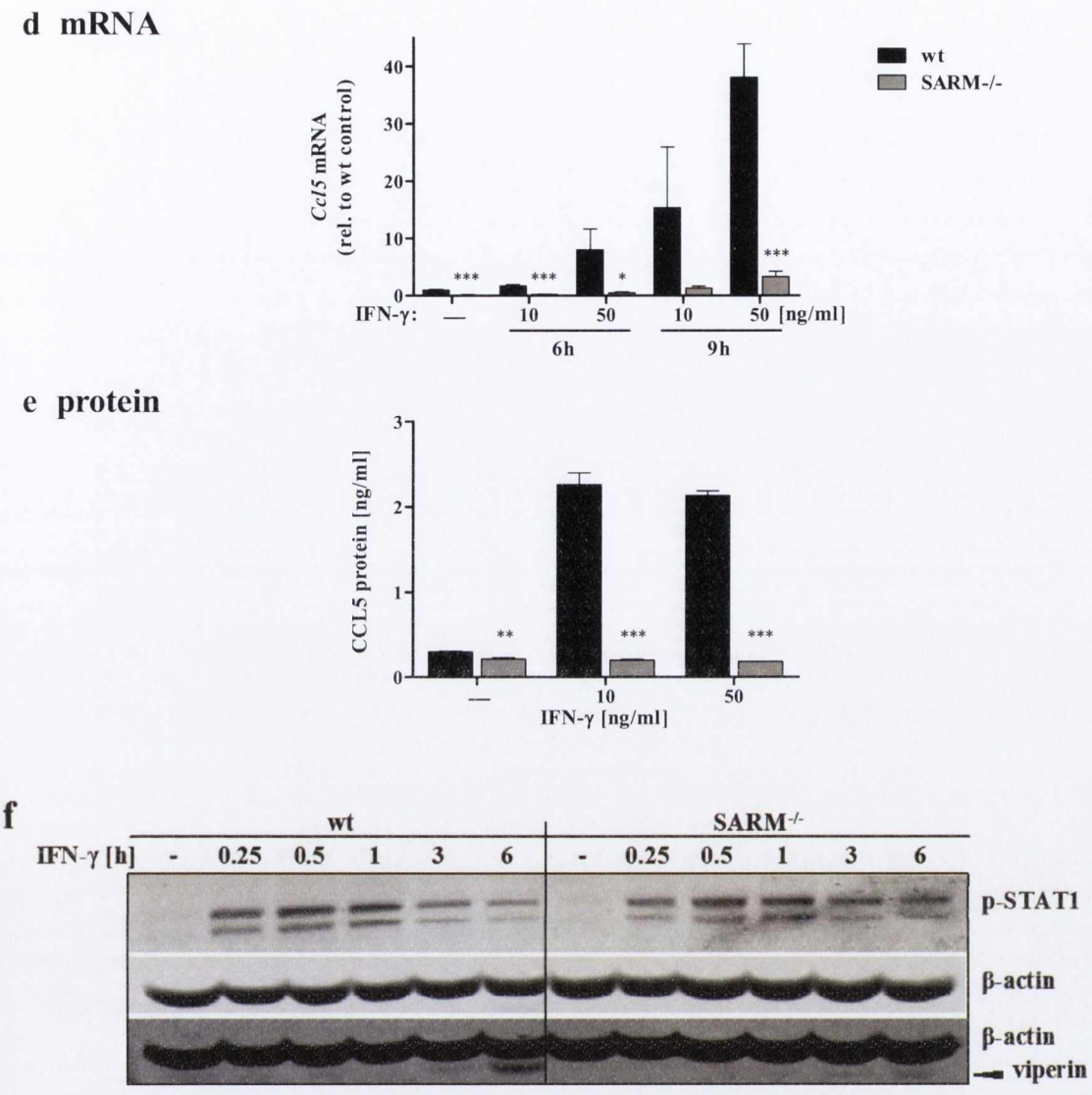


Figure 4.15: SARM is required for IFNAR- and IFNGR-induced CCL5 expression, but mostly dispensable for other IFN-mediated responses in immortalised BMDMs

(a) Quantitative real-time PCR analysis of *Ccl5*, *Ifit2* and *Irf7* mRNA expression in wt and *Sarm*$^{-/-}$ iBMDMs. Cells were seeded in 24 well plates and stimulated with IFN-α [1000U/ml] for the indicated time points or medium as control (—). mRNA level were normalised to the housekeeping gene *β-actin* and are presented relative to wt control (left) or as fold induction relative to each wt or *Sarm*$^{-/-}$ control (right). (b,e) Analysis of CCL5 protein expression in wt and *Sarm*$^{-/-}$ iBMDMs. Cells were seeded in 96 well plates and stimulated for 24h with the indicated concentrations of IFN-α (b) or IFN-γ (e). Medium-treated cells served as control (—). Supernatants were collected and assayed for CCL5 protein by ELISA. (c,f) Immunoblot analysis of p-STAT1 and viperin induction in wt and *Sarm*$^{-/-}$ iBMDMs. Cells were seeded in 6 well plates and stimulated with IFN-α [1000U/ml] (c) and IFN-γ [10ng/ml] (f) for the indicated time points or medium as control (—). Lysates were subjected to SDS-PAGE followed by Western Blotting using specific antibodies to detect tyrosine 701-phosphorylated STAT1 (p-STAT1), t-STAT1, viperin and β-actin as a loading control. (d) Quantitative real-time PCR analysis of wt and *Sarm*$^{-/-}$ iBMDMs treated with the indicated concentrations of IFN-γ for 6 and 9h or medium as control (—). *Ccl5* mRNA level were normalised to the housekeeping gene *β-actin* and are presented relative to wt control. Data are from one experiment representative of three (b, c, e), two (a) or one (d, f) (mean ± s.d.). * P<0.05, ** P<0.01, *** P<0.001, compared with wt (Student's *t*-test).

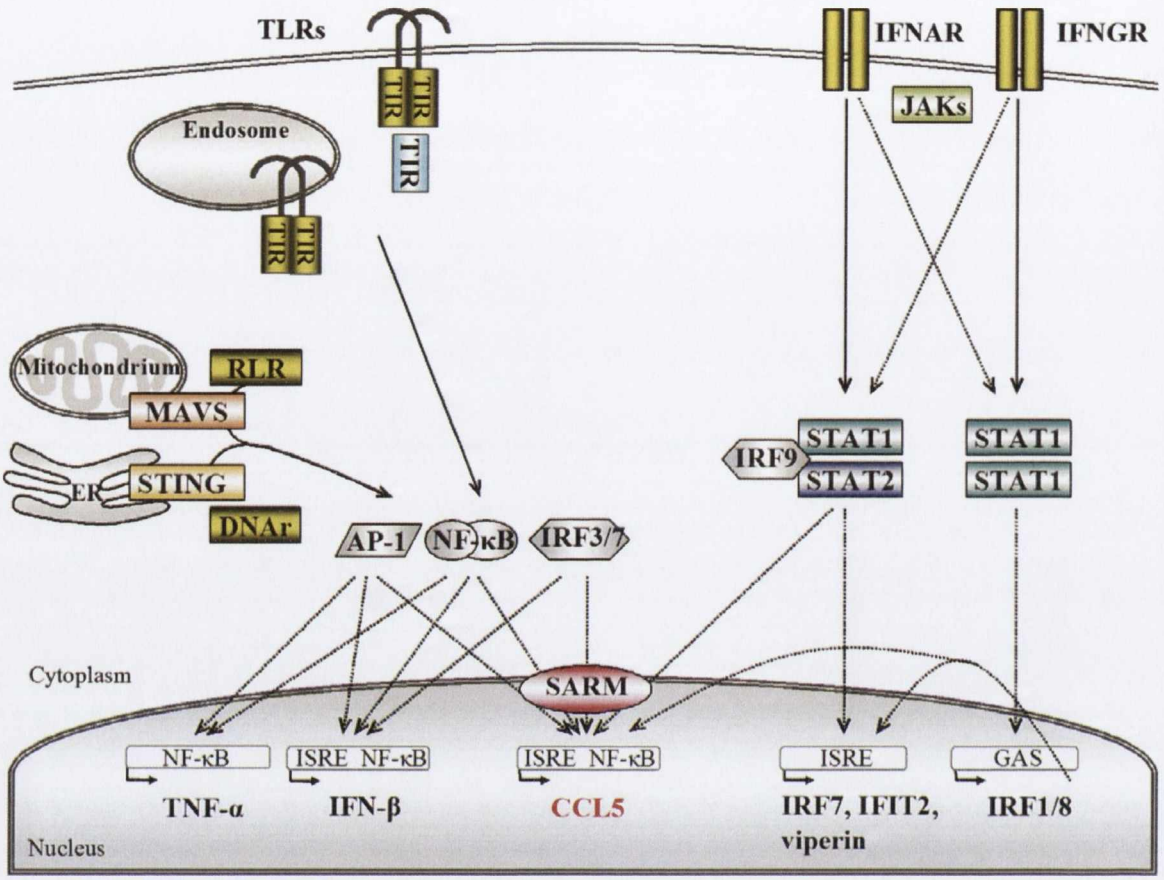


Figure 4.16: Signalling pathways showing SARM-dependent CCL5 expression in BMDMs

Schematic illustration of the various signalling pathways that showed a requirement for SARM for CCL5 expression in primary and immortalised BMDMs. After ligand binding, the various receptors engage with their specific adaptor proteins to initiate a signalling cascade that leads to transcription factor activation, nuclear translocation and selective gene induction. While the TLRs, RLRs and DNA receptors mainly activate the transcription factors AP-1, NF-κB and IRF3/7, the IFNAR and IFNGR induce the activation of STAT-containing transcriptional complexes. Thus, the different pathways upregulate CCL5 gene expression through different transcriptional activators, suggesting more a downstream regulatory role of SARM in CCL5 induction. Refer to text for a detailed description of the transcription factor complexes involved in induction of the various genes.

5 Investigating the CCL5-regulatory mechanism of SARM in murine BMDMs

5.1 Introduction

The analysis of the cytokine profile of murine wt and *Sarm*$^{-/-}$ BMDMs and BMDCs revealed a new function of SARM in positively regulating *Ccl5* gene expression in macrophages. In primary and immortalised BMDMs, SARM was consistently required for optimal CCL5 mRNA and protein expression following stimulation of TLR and non-TLR pathways, while it was dispensable for *Tnf-α* mRNA induction. Furthermore I obtained evidence that SARM might additionally promote IFN-β gene expression, however this observation was less consistent. In particular the immortalised BMDM cell line showed a strong dependency on SARM to express IFN-β, while the effects in primary cells were less significant. Due to this observation, experiments were performed to exclude an indirect, IFN-dependent modulation of CCL5 expression. This confirmed CCL5 as a primary response gene following TLR4 activation. Its expression was independent of a secondary produced factor and not modulated by IFN signalling or priming. Also the transcription factor IRF7 had no role in CCL5 expression. Thus SARM was regulating CCL5 directly in the primary transduction pathway. The main transcription factors activated by TLRs and the cytosolic PRRs are AP-1, NF-κB and IRF3/7; and CCL5 is known to be controlled synergistically by all of them, but with a particularly strong dependency on IRFs (259). The fact that SARM was dispensable for the mRNA induction of the NF-κB-regulated gene *Tnf-α* suggested that SARM might play a role in activating the IRF pathway. Further experiments determined that SARM was also selectively required for the IFNAR- and IFNGR-mediated upregulate of CCL5. Both pathways mainly initiate the formation of STAT1-containing transcriptional complexes, which differ significantly from the PRR-induced transcription factors. However STAT1 activation and the induction of other IFN-stimulated genes, such as *Irf7*, *Ifit2* and viperin, were not found to be dependent on SARM. Thus, the data suggested so far that SARM may control an alternative pathway with a particular strong role in CCL5 induction that is common to PRRs and IFN receptors. In this regard it was interesting to investigate the activation of the evolutionary conserved p38 MAPK, given that in *C. elegans* the homologue of mammalian SARM was shown to initiate this pathway to mediate immune responses. But SARM might also promote the

activation of IRF transcription factors, as they play a key role in PRR- and IFN receptor-induced CCL5 induction, although the type of IRF may vary between the pathways. PRR-induced CCL5 expression was shown to be mainly IRF3-dependent (259), while IRF1 and IRF8 were required for IFNGR-mediated CCL5 (250, 251). Furthermore, IRF9 is a component of the ISGF3 complex activated downstream of the IFNAR (191).

Thus, to elucidate the mechanism whereby SARM regulates CCL5 expression, I performed a detailed analysis of the activation of various transcription factors in wt and *Sarm*$^{-/-}$ BMDMs. Most of the studies were performed in primary and immortalised BMDMs, as this might also help to elucidate the cause of the different IFN-β profile between both cell types. The TLR4 pathway seemed appropriate to investigate the activation of MAPKs and the main transcription factors NF-κB and IRF3, as TLR4 was a potent inducer of all three pathways. Furthermore, TLR4 selectively activates those transcription factors via distinct TIR adaptors. The MyD88-dependent pathway mainly activates MAPKs and NF-κB, whereas the TRIF pathway is essential for IRF3 activation, and late-phase NF-κB and MAPKs (238, 272). Hence, TLR4-induced CCL5 and IFN-β are mainly controlled by the TRIF pathway, which was also interesting in light of the known SARM-TRIF interaction (44), even though the SARM-mediated CCL5 regulation was shown not to be restricted to TRIF. The other IRF family members, IRF1 and IRF8, are mainly controlled by their expression level, which is upregulated in response to type I and type II IFN receptor signalling (273). Whether SARM played a role in the expression of those transcription factors, which subsequently may participate in CCL5 induction, was also investigated in the following experiments.

5.2 Results

5.2.1 SARM is not required for the activation of MAPKs and the transcription factors NF-κB and IRF3

To investigate the mechanism by which SARM promoted CCL5 expression in BMDMs, I first examined if SARM-deficiency affected the activation of MAPKs and the transcription factors NF-κB and IRF3. All three pathways are important components of PRR-mediated gene induction, and were shown to cooperate for full CCL5 expression (259). Thus wt and *Sarm*$^{-/-}$ primary and immortalised BMDMs (p/iBMDMs) were stimulated for various times with LPS to trigger the TLR4 signalling cascade and subsequently the activation of MAPKs and transcription factors. Medium-treated cells served as negative control. The cell lysates were resolved on a 10% SDS-Polyacrylamide gel followed by Western Blotting using specific antibodies to detect the various signalling molecules and transcription factors. The activation of the three main MAPKs, p38, JNK1/2 and ERK1/2, were determined by detecting their phosphorylated form, while NF-κB activation was assessed indirectly by measuring the induced degradation of the NF-κB inhibitor IκB. At the same time, the blot was probed for the total protein levels of the MAPKs and the housekeeping gene β-actin as a loading control. In p/iBMDMs, I observed peak phosphorylation of all three MAPKs 15min after LPS stimulation, which decreased at 30min and returned to basal levels at 1h (Figure 5.1a, b). Also the degradation of IκB showed similar kinetics, with a complete abrogation of the protein observed 15min after LPS, which was restored to basal levels at 1h. I noted that pBMDMs had a slightly delayed IκB resynthesis compared to iBMDMs, whereby it took up to 3h to restore basal protein levels. However, I observed a similar degree of MAPKs and NF-κB activation in SARM-deficient p/iBMDMs in comparison with the corresponding wt. This excluded a role for SARM in TLR4 signalling pathways upstream of MAPKs and NF-κB activation. The normal activation of NF-κB was not surprising, as *Tnf-α* mRNA production was unaffected by SARM-deficiency. The fact that SARM was found to be specifically required for *Ccl5* and partially *Ifn-β* gene expression suggested a function in IRF3 activation. Several phosphorylation events have been described to be important for IRF3 activation, dimer formation, nuclear translocation and transcriptional activity (274). In particular Serine 396-phosphorylation of IRF3 was demonstrated to play a key role in the activation process (275), hence I decided to assess if SARM-deficiency would affect this phosphorylation

event. Wt and *Sarm*$^{-/-}$ p/iBMDMs were stimulated with LPS for various times and lysates were resolved on a SDS-Polyacrylamide gel. Immunoblot analysis was performed using specific antibodies to detect p396-IRF3 or total IRF3 protein and β-actin was used as a loading control. I noted that IRF3 was predominantly present as two forms, which was in agreement with published reports (276). The lower band most likely represented unphosphorylated IRF3 (form I), while the upper band was basally phosphorylated IRF3 (form II). In pBMDMs, both forms were equally detectable and it was the upper band that showed Ser 396-phosphorylation after LPS treatment (Figure 5.2a). In contrast, in iBMDMs the total IRF3 antibody detected mainly form I (Figure 5.2b). However, the phospho-specific antibody revealed both forms of IRF3 also in iBMDMs, with a more pronounced LPS-mediated Ser 396-phosphorylation of IRF3 form II. The IRF3 phosphorylation was mainly observed 1h after LPS stimulation, but could further accumulate at later times, as seen in some experiments of iBMDMs. However, SARM-deficiency did not cause alteration of TLR4-induced Ser 396-phosphorylation in p/iBMDMs. As a subsequent step in IRF3 activation, I assessed IRF3 dimer formation, which was additionally controlled by other phosphorylation events (277). Lysates of LPS-stimulated iBMDMs were resolved on a native gel, followed by immunoblotting against total IRF3 protein. But SARM was also not required for IRF3 dimerisation, indicated by the IRF3 dimer detected 1h after LPS in wt and SARM-deficient iBMDMs (Figure 5.2c). The blot was again probed for Ser 396-phosphorylated IRF3 and β-actin as a loading control.

Even though the initial activation of the transcription factors was found to be independent of SARM, it was still possible that SARM regulated another process required for full transcription factor activation. In particular IRF3 is known to be controlled by a multiplicity of activation events (274). As a subsequent step after successful activation, the transcription factor translocates from the cytosol to the nucleus to finally bind to specific DNA promoter elements and induce gene expression. Hence I decided to evaluate a requirement for SARM in the nuclear translocation of NF-κB and IRF3. Wt and *Sarm*$^{-/-}$ BMDMs were seeded on glass coverslips and treated with LPS and Sendai virus to trigger TLR4- and RIG-I-mediated transcription factor activation. Medium-treated cells served as control. Then the cells were fixed and intracellularly stained for the NF-κB subunit p65 and total IRF3 using specific antibodies followed by distinct fluorescent-labeled secondary antibodies. Nuclei were visualised using the DNA-intercalating dye DAPI. The confocal

microscopy analysis revealed a clear p65 and IRF3 nuclear translocation in pBMDMs treated with LPS and Sendai virus (Figure 5.3a, b). Following LPS stimulation, p65 translocated earlier and more pronounced than IRF3, but finally both transcription factors were detectable in the nucleus in almost every cell (Figure 5.3a). This was different to Sendai virus-activated cells, which showed the nuclear translocation, particularly of IRF3, only in a subset of cells, but then much stronger than the LPS-induced IRF3 translocation (Figure 5.3b). Overall, the stimulus-induced nuclear accumulation of p65 and IRF3 was comparable in wt and SARM-deficient pBMDMs. Consistently, SARM was also dispensable for the TLR4-induced translocation of both transcription factors in the immortalised cell line (Figure 5.3c). Of general note was that the *Sarm*$^{-/-}$ immortalised cells exhibited a different morphology compared to the corresponding wt iBMDMs. The cells were on average bigger and grew semi-adherent, while the wt cells were small and adherent. This can be seen to some extent in the confocal images, where less knockout cells adhered to the coverslip (Figure 5.3c). However, this phenotypical difference between wt and *Sarm*$^{-/-}$ iBMDMs was not observed in pBMDMs, and thus might not be related to SARM function. Together, the data demonstrated that SARM was neither required to activate the three main MAPKs, p38, JNK and ERK, nor did it control the activation and nuclear translocation of NF-κB and IRF3. This was surprising, as the divergent SARM-dependency on TNF-α versus CCL5 would have suggested a potential impairment of IRF3 activation; especially in iBMDMs, where SARM was absolutely required to upregulate both IRF3-dependent genes CCL5 and IFN-β. However during the immunoblot analysis of IRF3 I noted that SARM-deficient iBMDMs expressed lower level of total IRF3 protein than the corresponding wt, which will be addressed in the following experiments (see 5.2.2).

5.2.2 SARM has a role in enhancing basal IRF3 expression in immortalised BMDMs

From the previous study on IRF3 activation (see 5.2.1) it became evident that SARM might be required for IRF3 protein expression especially in iBMDMs, while this effect was less prominent in pBMDMs. As this could mechanistically explain, how SARM might regulate the IRF3-dependent genes *Ccl5* and *Ifn-β*, I decided to examine IRF3 expression and its regulation in these cells in more detail. First, I performed further immunoblot

analysis to directly compare IRF3 protein expression in primary and immortalised wt and SARM-deficient BMDMs, and also primary BMDCs. IRF3 protein was detected as described in 5.2.1 and β-actin was used as a loading control. Consistent with the previous observation (Figure 5.2b), the amount of IRF3 protein detected in *Sarm*$^{-/-}$ iBMDMs was only about half compared to the corresponding wt (Figure 5.4a, middle, arrows). In contrast in pBMDMs and pBMDCs, the lack of SARM did not affect IRF3 protein expression (Figure 5.4a, left, right). Consistent with the previous experiment, two main forms of IRF3 were detected, which most likely represented unphosphorylated (form I) and hyper-phosphorylated IRF3 (form II). While both forms were equally present in primary cells, iBMDMs mainly expressed form I, and the expression of this form was significantly elevated in iBMDMs compared to primary cells. As a side observation I noted that IRF3 protein levels were not found to be modulated by LPS stimulation within 1h or even up to 24h (Figure 5.4a, 5.2b). This was in agreement with the literature showing that IRF3 expression was constitutive and stimulus-independent (200). However, the different basal IRF3 expression between primary and immortalised BMDMs was surprising; hence I decided to assess IRF3 protein levels in other iBMDM cell lines. The immunoblot analysis revealed a similar enhanced basal IRF3 level in all other TIR adaptor knockout iBMDMs, *Trif*$^{-/-}$, *Tram*$^{-/-}$, *Myd88*$^{-/-}$ and *Mal*$^{-/-}$, with comparable amounts to wt iBMDMs (Figure 5.4b). Thus the elevated IRF3 expression was a general phenotype of iBMDMs and only suppressed in immortalised cells lacking SARM. To define at which step SARM was regulating IRF3 expression in iBMDMs, I next examined *Irf3* mRNA level in wt and *Sarm*$^{-/-}$ cells using quantitative real-time PCR. In correlation with the protein data I observed approximately 50% reduced basal *Irf3* mRNA in SARM-deficient iBMDMs compared to the corresponding wt, whereas the *Irf3* mRNA levels in pBMDMs were almost equal between both genotypes (Figure 5.4c, left graph). This demonstrated that SARM regulated IRF3 expression in iBMDMs at the mRNA level. Furthermore, the protein analysis revealed a divergence in the amount of basal IRF3 between primary and immortalised BMDMs. Therefore I performed a direct comparison of *Irf3* mRNA expression between both cell types. Interestingly, only the wt iBMDMs showed enhanced *Irf3* mRNA, while the level in SARM-deficient iBMDMs correlated with the level in primary cells (Figure 5.4c, right graph). Thus SARM might be required for the general upregulation of IRF3 in immortalised cells. Given that the *Sarm*$^{-/-}$ iBMDMs had a dramatic defect in IFN-β production, I wondered if constitutive IFNs were required to enhance basal IRF3

expression in this cell type. To evaluate the IFN-dependency of IRF3 expression, I first stimulated wt and *Sarm*$^{-/-}$ iBMDMs for various times with recombinant IFN-α and measured *Irf3* mRNA expression using quantitative real-time PCR. As a positive control I analysed *Irf7* mRNA, which is known to be highly dependent on type I IFNs (200). In line with previous experiments, I observed reduced basal *Irf3* mRNA levels in SARM-deficient iBMDMs, and also *Irf7* mRNA was dramatically impaired most likely due to the defective IFN priming in these cells (not visible in the graph since the unstimulated samples in both wt and *Sarm*$^{-/-}$ are set to 1). Hence, in order to assess the IFN-inducibility of *Irf3* and *Irf7*, disregarding the basal levels, I normalised each genotype to its individual control (set to 1) and presented the data as "fold induction" as opposed to the relative levels. In agreement with the literature (200), *Irf3* expression was not affected by IFN-α stimulation, while *Irf7* mRNA increased up to 12-fold 6h after IFN treatment (Figure 5.5a, b). The *Irf7* induction was similar in wt and SARM-deficient cells, confirming the previous observation that SARM was dispensable for the general upregulation of ISGs (see 4.2.6). To fully exclude that the defective IFN priming indirectly affected IRF3 expression in *Sarm*$^{-/-}$ iBMDMs, I assessed *Irf3* mRNA levels in wt iBMDMs treated overnight with an antibody specific to the IFNAR. This suppressed IFN priming effects usually mediated by basally produced and secreted IFNs (201). Cells without antibody treatment served as control. I observed that blocking the IFN response had no impact on basal *Irf3* mRNA expression, in contrast to *Irf7* mRNA, which was completely abrogated in the presence of the anti-IFNAR1 antibody (Figure 5.5c, d). This confirmed that *Irf3* mRNA was regulated independently of IFNs and gave evidence for a direct regulatory role of SARM in IRF3 expression. Apart from transcriptional regulation, it was possible that the enhanced *Irf3* mRNA was elicited by an increase in mRNA stability. To investigate if SARM controlled the stability of IRF3 mRNA, wt and *Sarm*$^{-/-}$ iBMDMs were treated for up to 3h with actinomycin D to block transcription. *Irf3* mRNA decay was monitored using quantitative real-time PCR. As a positive control for transcriptional inhibition, I additionally analysed the decay of the very unstable transcript *Tnf-α* (256). The mRNA levels were normalised to the housekeeping gene *β-actin* and presented as percent remaining compared to the untreated control. While *Tnf-α* mRNA decayed very rapidly with less than 10% remaining 1h after actinomycin D treatment, *Irf3* mRNA was found to be much more stable (Figure 5.6). No decrease in *Irf3* expression was observed 1h after actinomycin D treatment and even 3h later 60% of the transcript were still detectable. However, wt and SARM-deficient iBMDMs showed a

similar decay rate of *Irf3*, demonstrating that SARM was not required for *Irf3* mRNA stability. This suggested that SARM may directly enhance the transcription of IRF3. But as this function was restricted to iBMDMs and not apparent in primary cells, the exact mechanism was not further elucidated in this study.

5.2.3 SARM is dispensable for the induced upregulation of the transcription factors IRF1 and IRF8

Given that SARM was not found to regulate the activation of MAPKs and the classical transcription factors NF-κB and IRF3, I decided to investigate two other transcription factors, IRF1 and IRF8 that were implicated in mediating *Ccl5* gene expression in macrophages (250, 251). Both are upregulated by type I and type II IFNs and contribute to the induction of several genes in synergism with TLR-activated factors (273, 278). To assess if SARM played a role in IRF1 and IRF8 protein induction, I stimulated wt and *Sarm*$^{-/-}$ p/iBMDMs for various times with LPS, IFN-α and IFN-γ to activate TLR4, IFNAR and IFNGR signalling, respectively, and subsequently analysed the induction of the transcription factors via immunoblot. I observed a low basal expression of IRF8 in p/iBMDMs, which was enhanced only in IFN-γ-treated cells (Figure 5.7a, b). However, the upregulation observed 3 and 6h after IFN-γ stimulation was not affected by SARM-deficiency. IRF1 expression on the other hand was induced by all three stimuli, and an increase was detectable 1h after stimulation (Figure 5.7a, b). However IRF1 upregulation was also found to be independent of SARM, with a comparable level expressed in both genotypes. The LPS-mediated immediate-early upregulation of IRF1 was equal between wt and *Sarm*$^{-/-}$ cells, but showed a dependency for SARM in iBMDMs at the later times 3 and 6h (Figure 5.7b, top panel). However previous experiments have shown that IFN-β production was highly impaired in SARM-deficient iBMDMs (see 4.2.4), which suggests that the suppressed IRF1 expression at later times was most likely a secondary effect due to the lack of IFN-induced IRF1. According to this, the IRF1 expression observed at 1h was directly induced by the TLR4 pathway and independent of IFNs.

5.2.4 *Sarm*$^{-/-}$ mice harbour a polymorphism in the *Ccl5* gene promoter, which did not affect gene expression

The previous experiments have demonstrated that SARM did not regulate any of the main transcription factors described to be critical for CCL5 induction. Analysing the genomic localisation of the *Sarm* and *Ccl5* gene revealed that both genes were encoded on the same chromosome (Chr 11), with approximately 5 million base pair separation. To rule out that the targeted deletion of Exon 3-7 of the *Sarm* gene in *Sarm*$^{-/-}$ mice (220) accidentally disrupted the *Ccl5* gene, I decided to sequence part of the genomic *Ccl5* locus in BMDMs. Therefore I isolated genomic DNA of wt and *Sarm*$^{-/-}$ primary and immortalised BMDMs and PCR amplified a 927bp spanning DNA region around the transcriptional start site (designated +1) of the *Ccl5* gene (Figure 5.8a, b). This DNA fragment incorporated the 5'-proximal promoter with essential transcription factor binding sites, the first exon and part of intron 1. Sequencing of the PCR product was performed by Source BioScience with the same forward primer used to generate the DNA fragment. Alignments with the reference sequence (Ensembl release 68, July 2012: gene ID 20304) confirmed the expected DNA sequence in wt p/iBMDMs. However, the chromatogram of the *Sarm*$^{-/-}$ cells indicated a disruption of the sequencing at position -57 of the *Ccl5* gene promoter, which was not observed in the wt (Figure 5.8b, middle panel). A more detailed analysis revealed that this was caused by a heterozygous G-insertion in the knockout cell genome. Compared to the wt, the *Sarm*$^{-/-}$ sequence had at position -57 one G inserted on one allele and two G on the other allele, which resulted in a shift bringing both allele sequences out of alignment, while the sequence prior to the insertion was in alignment. I noted that the mutation was located at a 9G-mononucleotide repeat, and therefore at a region that is generally prone to mutations caused by DNA polymerase slippage during DNA replication. As the "slippage" can also happen as an error during PCR amplification (279), I repeated the sequence analysis several times and could confirm that the 10/11G repeat was only present in the *Sarm*$^{-/-}$ genome, while the wt consistently exhibited 9Gs at this position. The observation raised concerns about the role of SARM in CCL5 expression, as it was unclear if the 1-2bp insertion affected *Ccl5* promoter activity and hence caused the CCL5-defective phenotype artificially in the *Sarm*$^{-/-}$ BMDMs. In order to determine if the G-insertion was a mutation specific to the *Ccl5* promoter of *Sarm*$^{-/-}$ mice, I decided to sequence this DNA region in a range of other knockout iBMDMs from different sources. Unexpectedly, the analysis revealed the same 10/11G-repeat in two other TIR

adaptor knockout iBMDMs, *Trif*$^{-/-}$ and *Tram*$^{-/-}$, while the 9G-wt sequence was present in *Myd88*$^{-/-}$ and *Mal*$^{-/-}$ iBMDMs (Figure 5.8c). Also other knockout iBMDMs, including *Irak4*$^{-/-}$ and *caspase-1*$^{-/-}$, harboured 9Gs concordant with the reference sequence. Furthermore, the 9G-repeat was observed in genomic DNA isolated from mouse embryonic fibroblasts (MEFs) of an independently generated *Sarm*$^{-/-}$ mouse and the corresponding wt, kindly provided by Diamond et al. (221). Even though the 9G-repeat was most frequent, the analysis indicated that the 1-2bp G-insertion was most likely a polymorphism among different mouse substrains, as this sequence variation was present in *Sarm*-, *Trif*- and *Tram*-knockout iBMDMs and all knockout mice were bred on a C57BL/6 background. To assess if the observed mutation was already reported in substrains of C57BL/6 inbred mice, I consulted the sequencing resources of the Wellcome Trust Sanger Institute established in the course of the "Mouse Genomes Project" (www.sanger.ac.uk/resources/mouse/genomes/). Figure 5.9 shows the sequence alignment of the reverse complement DNA strand of C57BL/6 sequencing data from various sources, hence the Poly(G) region is represented by the C-repeat. The analysis revealed that the G-insertion at the Poly(G) region of the *Ccl5* promoter had not been documented so far, and therefore was not a known polymorphism amongst C57BL/6 substrains (Figure 5.9, right panel). Interestingly, I observed that a mouse strain, namely 129S1/SvlmJ, whose embryonic stem cells are frequently used to generate knockout mice, harboured the 1-2bp G-insertion (Figure 5.9, left panel). This strain was also initially used to generate the targeted disruption of the *Sarm* gene (220), which suggested that the observed sequence variation in *Sarm*-knockout BMDMs originated from residual genomic DNA of the 129S1/SvlmJ strain (further discussed in 5.3).

To directly assess if the 1-2bp G-insertion affected *Ccl5* promoter activity, I cloned the distinct 5'-proximal promoter sequences upstream of the firefly luciferase reporter gene in the promoterless pGL3 vector. As shown in Figure 5.10a, two different lengths of the *Ccl5* promoter were chosen according to the regulatory elements present. The longer pGL3 (-190/+57) construct contained all essential promoter elements, including the ISRE and NF-κB elements (251, 280), whereas the shorter pGL3 (-120/+53) construct was devoid of the potent ISRE element. Both fragments were PCR amplified from genomic DNA of wt and *Sarm*$^{-/-}$ pBMDMs, resulting in six different versions as they contained either 9, 10 or 11G repeats. The promoter fragments were subsequently inserted into the pGL3 reporter plasmid and sequenced to identify the individual G-repeat. A pGL3 vector containing the

constitutive SV40 promoter upstream of the luciferase gene served as positive control. As another control of the assay, I included the human *Ccl5* promoter reporter, which was successfully used in previous experiments by my colleagues (44). The functionalities of the various *Ccl5* promoter constructs were examined in human HEK293 and murine NIH3T3 cells. The cells were transiently transfected with the various firefly luciferase reporter constructs and cotransfected with a plasmid encoding renilla luciferase (pRL-TK) to normalise for transfection efficiency. The next day, cells were stimulated for 10h with LPS and Sendai virus to trigger transcription factor activation and induction of the *Ccl5* promoter. The reporter gene activity was subsequently measured in cell lysates. LPS stimulation of HEK293-TLR4 cells induced a potent activation of the long *Ccl5* promoter construct pGL3-190, which was not impaired by the 1-2bp G-insertion (Figure 5.10b). The activity of the shorter construct pGL3-120 was approximately 50% reduced compared to pGL3-190, indicating that the ISRE element was important for full *Ccl5* promoter activity. Nevertheless, also in the context of less regulatory elements in the promoter, the reporter gene activity was unaltered by the G-insertions. As the set of activated transcription factors varies slightly between different PRRs, I decided to additionally examine *Ccl5* promoter activity in response to a non-TLR, cytosolic receptor and used Sendai virus to trigger the RIG-I pathway. Sendai virus-stimulated HEK293 and NIH3T3 cells induced activity of the long pGL3-190 *Ccl5* promoter constructs, but were ineffective to activate the shorter pGL3-120 constructs (Figure 5.10c, d). This suggested that Sendai virus, in contrast to LPS, stimulated *Ccl5* promoter activity mainly via the ISRE element, which was in agreement with the literature (280). But also in the case of Sendai virus-mediated *Ccl5* promoter activity, the G-insertions did not influence the functionality of the promoter. This proved that the impaired CCL5 expression observed in SARM-deficient BMDMs was not caused artificially by the G-insertion and indicated a real SARM-mediated regulation of CCL5.

Interestingly, the 10/11G-repeat was also detected in *Trif*- and *Tram*-knockout iBMDMs, which allowed evaluation of the impact of the extra Gs on endogenous *Ccl5* promoter activity in comparison to the 9G-wt sequence. *Sarm*$^{-/-}$ cells, which also harboured the 10/11G polymorphism, were included in the analysis to assess specificity of the SARM-dependent CCL5 regulation. TRIF and TRAM are essential adaptor proteins in TLR4-mediated CCL5 induction (238). Thus to examine the functionality of the *Ccl5* promoter I used a TIR adaptor-independent stimulus to elicit CCL5 expression. IFN-α

seemed appropriate, as it triggered the IFNAR signalling cascade which differed significantly from PRRs, while LPS-induced CCL5 expression was additionally examined to control for the knockout phenotypes. As expected, TLR4-mediated CCL5 mRNA and protein expression was completely abrogated in iBMDMs lacking TRIF and TRAM (Figure 5.11b, d). And also the *Sarm*$^{-/-}$ iBMDMs showed dramatically impaired CCL5 expression in response to TLR4, which was consistent with previous observations (see 4.2.3). In contrast, the absence of those TIR adaptors did not affect the TLR4-mediated upregulation of *Tnf-α* mRNA, which is mainly regulated by the MyD88-dependent pathway, and thus confirmed the intact responsiveness of the cells (Figure 5.11a). The analysis of the IFN-α response revealed that *Trif*- and *Tram*-deficient iBMDMs were, like the wt, equally capable of upregulating CCL5, and that the defect in CCL5 expression was specific to cells lacking SARM (Figure 5.11c, e). Thus, I was able to demonstrate by two independent approaches that the polymorphism of the Poly(G)-region at position -57 of the *Ccl5* promoter did not affect gene induction.

5.2.5 Recruitment of RNA Polymerase II and transcription factors to the *Ccl5* promoter in the absence of SARM

As the previous studies did not reveal a transcription factor whose activity was regulated by SARM, I decided to investigate further downstream events, such as the binding of transcription factors to the *Ccl5* promoter and the subsequent recruitment of RNA Polymerase II (Pol II) (281). The Chromatin Immunoprecipitation (ChIP) assay allows studying the binding of specific proteins to a genomic DNA region of interest (282). First, cells were fixed with formaldehyde to form covalent cross-links between protein and DNA. Cell lysates were then sonicated to generate chromatin fragments of an average size of 200-1000bp. The sheared chromatin was applied to immunoprecipitation using a specific antibody to pull-down the protein-bound DNA fragment. The DNA was subsequently isolated from the complex and applied to PCR analysis to assay for the DNA region of interest. First, it was important to determine the sonication conditions that gave optimal DNA fragment size in BMDMs. To avoid excessive heating of the sample, the sonication process was performed in cycles, with each cycle consisting of 15 x 1sec pulses and a 45sec rest on ice using the Branson Sonifier 250. To evaluate fragment size, the DNA was resolved on a 1% agarose gel and visualised by ethidium bromide staining and

UV illumination. As depicted in Figure 5.12a, DNA fragment size decreased with the number of cycles and power 3 was found to be more efficient in shearing the chromatin than power 2. The best result was achieved after 10 cycles at power 3, generating 200-2000bp DNA fragments. This condition was used in the subsequent experiments. Before using the Pol II antibody in ChIP, I confirmed its specificity by immunoblot analysis on sheared chromatin lysates that were resolved on 8% SDS-Polyacrylamide gel. Two protein bands of expected molecular weight >200kDa were detected, which most likely corresponded to hypo- and hyperphosphorylated Pol II, as described in the literature (283). The last step of the ChIP analysis is to assay the immunoprecipitated DNA for the specific DNA region of interest using PCR. Thus I designed a pair of primers specific to the 5'-proximal *Ccl5* promoter, close to the transcription start site (designated +1), which is a region of transcription factor binding and assembly of the transcriptional machinery (Figure 5.12c). In addition I designed primers specific to the proximal *β-actin* promoter as control (region not shown). ChIP analysis was subsequently performed in wt and *Sarm*$^{-/-}$ iBMDMs treated for various times with LPS to stimulate transcription factor activation and binding to the endogenous *Ccl5* promoter. First, I determined the recruitment of Pol II, and as revealed by semi-quantitative PCR, LPS treatment triggered a significant increase of Pol II binding to the *Ccl5* promoter (Figure 5.13a). The Pol II recruitment was particularly prominent in the wt cells, while the SARM-deficient iBMDMs seemed to accumulate less of the protein. Many factors are involved in initiating Pol II recruitment, but given that IRF proteins play a crucial role in chromatin remodelling and CCL5 induction, I decided to specifically assay IRF3 and IRF1 binding to the *Ccl5* promoter (246, 250, 259). LPS induced the recruitment of both factors to the *Ccl5* promoter, albeit the detection was much weaker than for Pol II. However no significant differences were observed between wt and *Sarm*$^{-/-}$ cells. As the difference in Pol II detection could also result from variations in the chromatin "Input" sample of each reaction, I additionally measured the abundance of the *Ccl5* promoter in the Input DNA as a loading control. This did not reveal any major differences in DNA loading, but an exact quantification would be required to confirm this result using real-time PCR (described later). Furthermore, I confirmed the antibody-specific pull-down of the *Ccl5* DNA region using an isotype-control antibody (IgG). This revealed only a background detection of the *Ccl5* promoter and as expected did not lead to an LPS-mediated increase. As another negative control I assayed the immunoprecipitated DNA additionally for the *β-actin* promoter fragment (Figure 5.13b). The fact that the IRF3

and IRF1 antibody did not precipitate any *β-actin* DNA beyond the background level confirmed the specific reaction with the *Ccl5* promoter. Also in terms of the Pol II antibody I was able to verify its specific reaction, as Pol II was detected with high abundance at the *β-actin* promoter, independent of LPS stimulation, which was in agreement with the known constitutive transcription of housekeeping genes (264). Even though I obtained evidence for a role of SARM in mediating Pol II recruitment to the *Ccl5* promoter, the differences between wt and *Sarm*$^{-/-}$ BMDMs were quite subtle. Thus to perform more quantitative analysis, I next optimised the ChIP protocol for the detection using real-time PCR. After having resolved initial detection problems, I am now able to quantify the recruitment of a factor to the *Ccl5* promoter, as seen here for LPS-induced Pol II binding in wt iBMDMs (Figure 5.14). The recovered *Ccl5* promoter DNA fragments in the Pol II-immunoprecipitate were expressed as percentage relative to their abundance in the Input DNA sample, and thus normalised for sample variations. The successful establishment of the ChIP assay and the possibility of exact quantification will be useful for future studies in wt and SARM-deficient BMDMs to further elucidate the exact mechanism of SARM in regulating CCL5 expression.

5.3 Discussion

After having established that SARM was consistently required for full CCL5 expression in primary and immortalised BMDMs (p/iBMDMs), I wanted to gain further insights on the regulatory mechanism. The fact that SARM promoted CCL5 expression of TLR-dependent and -independent pathways, excluded that this function was mediated via its known interaction partner TRIF (44). Furthermore, the SARM-TRIF interaction in the human system resulted in inhibition of the TRIF pathway, whereas in murine BMDMs SARM was positively involved in selective gene induction. TLRs and the cytosolic RNA and DNA receptors use different adaptor proteins to initiate distinct signalling cascades, which converge further downstream to activate a similar set of transcription factors, including AP-1, NF-κB and IRFs, and induce gene expression. Given that PRR-induced CCL5 was induced in the primary response and independent of secreted type I IFNs, as defined in 4.2.5, SARM was likely to function more downstream in those receptor pathways, possibly at the level of transcription factor activation. The fact that SARM was dispensable for the NF-κB-dependent gene *Tnf-α*, but required for optimal CCL5 induction, suggested a potential regulatory role of SARM in the IRF pathway. Also the IRF3-dependent gene *Ifn-β* showed some dependency on SARM, which further supported this hypothesis. However, the effect on IFN-β was mainly restricted to iBMDMs and less significant in pBMDMs. Due to this discrepancy I performed the mechanistic studies in both cell types. Surprisingly, analysing the TLR4-mediated activation of MAPKs and the main transcription factors NF-κB and IRF3 in the absence of SARM did not reveal significant differences compared to the corresponding wt in p/iBMDMs. Also the nuclear translocations of the NF-κB-subunit p65 and IRF3 were normal in response to LPS and Sendai virus. The intact NF-κB activation was consistent with the unaffected *Tnf-α* mRNA induction observed in knockout BMDMs. However given the role of SARM in CCL5 and partially IFN-β expression, it was somewhat surprising that all key IRF3 activation events measured were intact in SARM-deficient p/iBMDMs, namely Ser 396-phosphorylation, IRF3 dimerisation and nuclear translocation. Interestingly, I noted in the immortalised cell line that the *Sarm*-knockout cells expressed about 50% less IRF3 mRNA and protein compared to the corresponding wt. Meanwhile the level in primary BMDMs was almost equal between both genotypes. Thus, it was likely that the diminished IRF3 expression in *Sarm*$^{-/-}$ iBMDMs caused the dramatic defect on the IRF3-dependent genes *Ccl5* and *Ifn-β*

in this cell type. Also it explained the discrepancy regarding IFN-β production of SARM-deficient primary and immortalised BMDMs. Strangely, a direct comparison of IRF3 mRNA and protein levels between both cell types revealed, that wt iBMDMs had in fact elevated IRF3 levels compared to primary cells. Furthermore the apparently reduced level in *Sarm*$^{-/-}$ iBMDMs was actually equal to the IRF3 expression in primary cells. Given that in primary BMDMs this amount of IRF3 was sufficient to upregulate normal levels of IFN-β, it was unlikely that the defective IFN-β production observed in *Sarm*$^{-/-}$ iBMDMs was solely caused by the IRF3 level; unless the sensitivity towards IRF3 had changed in immortalised compared to primary cells. Evidence for such a reprogramming in immortalised cells was the observation that all other TIR adaptor-knockout iBMDMs also showed the elevated basal IRF3 expression similar to wt iBMDMs. Only the SARM-deficient iBMDMs exhibited the lower IRF3 level, which indicated that SARM may play a role in upregulating basal IRF3 in immortalised cells, but not in primary BMDMs. The immortalised BMDM cell line was generated by infecting primary BMDMs with a recombinant J2 retrovirus carrying v-myc and v-raf/mil oncogenes (173, 228). It was surprising, that these "tumor-like" cells exhibited enhanced IRF3 levels, as IRF3 is generally considered as a tumor suppressor. Ectopic expression of IRF3 in normal and cancer cells inhibited cell proliferation, also in vivo, and the loss of IRF3 mediated oncogenic transformation in vitro (284-286). So far, the data on IRF3 in cancer are very limited, but a recent report described an aberrant expression of IRF3 in human lung cancer cells (287). Thus, in light of the observation in iBMDMs, I speculate that SARM may function as a tumor suppressor by increasing IRF3 expression in immortalised cells. Most interestingly, SARM was recently found to be associated with a good prognosis in patients with colon cancer (E. Ryan, personal communication). Also epigenetic changes of SARM are discussed as a biomarker for colorectal cancers (288). Therefore, it would be sensible to assess if the link between SARM and human cancers is a putative SARM-mediated regulation of IRF3 expression. If so, understanding the mechanism by which SARM enhances IRF3 level in cancer cells could become very relevant for cancer research and the development of novel therapies. As the *Sarm*$^{-/-}$ iBMDMs were devoid of any basal IFN-β production, I wanted to verify that the diminished IRF3 expression was not caused indirectly by the lack of IFN priming. But consistent with the literature (200), I observed that basal *Irf3* mRNA expression was independent of type I IFNs, as neither IFN-α treatment nor inhibition of IFNAR signalling affected *Irf3* expression in iBMDMs. This

confirmed that SARM was likely to regulate IRF3 expression directly. To gain insight into the mechanism, I tested if SARM mediated the enhanced *Irf3* mRNA level by increasing its stability. But *Irf3* mRNA stability was normal in the absence of SARM, which suggested a regulation at the transcriptional level. A recent report demonstrated that the constitutive expression of IRF3 is mediated by SP1 and SP3 transcription factors (289), while E2F1 negatively regulates its transcription (290, 291). Interestingly, the expression of those transcription factors is often enhanced in cancer cells and highly implicated in oncogenesis (195, 196). Also c-myc, the oncogene used for transforming the BMDMs, was shown to induce E2F1 accumulation (292). Thus, I propose that the elevated IRF3 level in iBMDMs may be a consequence of enhanced SP1 activity and SARM might positively regulate IRF3 expression either via SP1 or by inhibiting E2F1 function. A possible mechanism of E2F1 inhibition could be via the transcriptional corepressor KAP1, a negative regulator of E2F1 and also a potential binding partner of SARM, as recently revealed by mass spectrometry analysis in my laboratory ((293), M.Carty personal communication).

However, in primary BMDMs, IRF3 expression was not affected by SARM depletion and SARM more selectively regulated CCL5 induction, while IFN-β expression was mostly unaffected. But SARM was not found to regulate the main transcription factors required for PRR-induced CCL5 expression, such as NF-κB and IRF3. Also the MAPK cascades were found to be intact in the absence of SARM, which was surprising given that the SARM homologue TIR-1 functions upstream of the p38 MAPK in *C. elegans* (see 1.4, (212)). Thus, I explored alternative transcription factors implicated in CCL5 induction. In this regard it was interesting that SARM was also selectively required for optimal CCL5 expression in response to IFNAR and IFNGR stimulation, while SARM was dispensable for the expression of other IFN-stimulated genes (ISGs), such as *Irf7*, *Ifit2* and viperin (4.2.6). This indicated that also in the IFN pathway the formation of the main transcriptional complexes was independent of SARM, which was also demonstrated by the intact STAT1 activation in SARM-deficient BMDMs. Thus SARM may function in an alternative pathway activated by both PRR and IFN receptor stimulation. It emerged from several reports that IRF family members play a key role in CCL5 induction, thus IRF1 and IRF8 were two interesting candidates, as they were further upregulated by IFNs and shown to participate in CCL5 expression (250, 251). However the analysis in p/iBMDMs revealed that the IFNGR-mediated upregulation of both transcription factors, as well as the

induction of IRF1 following IFN-α and LPS stimulation were independent of SARM. Thus the data so far suggested a more downstream regulatory function of SARM after transcription factor activation and nuclear translocation, possibly at the *Ccl5* promoter level. During investigations of the *Ccl5* promoter I became aware that *Sarm* and *Ccl5* were encoded on the same chromosome (Chr 11). Although the genes were separated by over 5 million base pairs, I wanted to exclude that the genetic disruption of the *Sarm* gene had inadvertently affected regulatory elements of the *Ccl5* gene promoter in the *Sarm*-knockout mouse. The sequence analysis of a 5'-region of the *Ccl5* gene, which included the proximal promoter, the first exon and part of intron 1, revealed indeed a sequence variation in the genomic DNA of *Sarm*$^{-/-}$ BMDMs. While the wt completely matched the *Ccl5* reference sequence (Ensembl release 68, July 2012: gene ID 20304), the *Sarm*$^{-/-}$ DNA exhibited a heterozygous 1-2bp G-insertion at position -57 of the *Ccl5* promoter, and this was consistent in primary and immortalised BMDMs. The mutation was located at a mononucleotide Poly(G) region, which carried 9Gs in the wt and consequently 10/11Gs in the knockout. Interestingly, further analysis revealed that the 10/11G-sequence variation was also present in *Trif*- and *Tram*-knockout iBMDMs, although the wt sequence was most frequent among the tested knockout cell lines. This indicated that the 10/11G-repeat was most likely a polymorphism of the mouse strain, as all knockout mice were generated on a C57BL/6 background. However, the analysis of reported sequences from various sources of C57BL/6 mice on the Wellcome Trust Sanger Institute website established in the course of the "Mouse Genomes Project" (www.sanger.ac.uk/resources/mouse/genomes/) demonstrated that this 1-2bp G-insertion at position -57 of the *Ccl5* promoter had not been documented so far. The generation of a knockout mouse initially involves embryonic stem (ES) cells of a different mouse strain to establish the knockout genotype, which then get transferred into C57BL/6 blastocytes and after several rounds of systematic breeding leads to a knockout mouse on the C57BL/6 background. However, given that the *Ccl5* gene was in close proximity to the *Sarm* locus on chromosome 11, I wondered if some genomic DNA of the original strain was still present in the C57BL/6 knockout cells. As the ES cells used to generate the *Sarm*$^{-/-}$ mouse (220), and most likely other knockout mice, were derived from the 129/SvJ mouse strain, I additionally examined the sequencing data available for this strain on the Sanger Institute webpage. Most interestingly, this mouse strain exhibited a similar 1-2bp G-insertion at the Poly(G) region, as I had observed in the *Sarm*-knockout, and also *Trif*- and *Tram*-knockout genomic DNA. This suggested that the

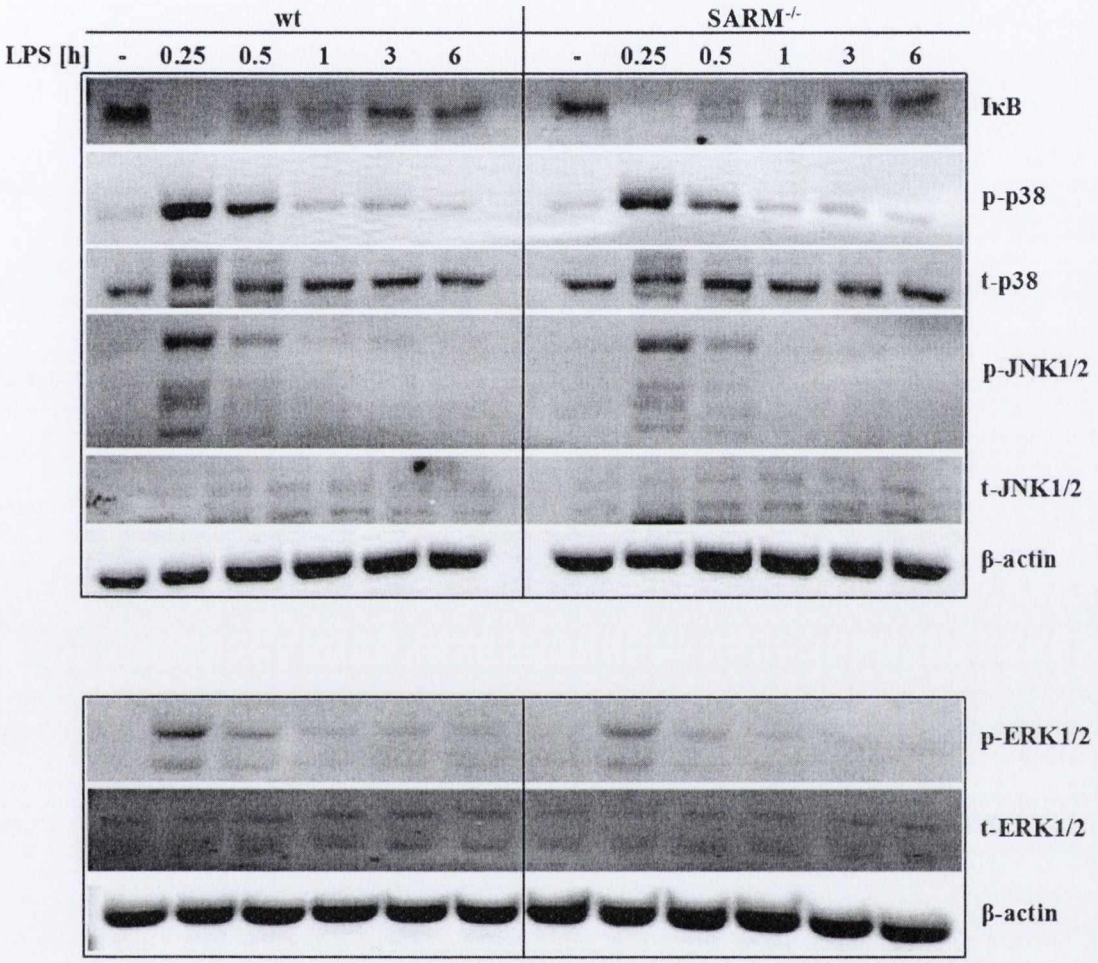
10/11G-repeat present in some knockout mice was most likely residual genomic DNA of the 129/SvJ ES cells.

Next, I evaluated if the 10/11G polymorphism had affected *Ccl5* promoter activity. I performed a bioinformatic analysis using MatInspector (Genomatix GmbH) to identify if the G-repeat was a potential transcription factor binding site (data not shown). The analysis revealed that the Poly(G) region was predisposed for binding of SP/KLF family members, which have a high affinity for specific GC-rich sequences (294). Particularly SP1 and KLF13 had been reported previously to regulate *Ccl5* expression in human NK cells and T lymphocytes, respectively (295, 296). Thus, there was a possibility that the 1-2bp G-insertion might have affected *Ccl5* promoter activity. I subsequently performed luciferase reporter gene assays using different constructs of the *Ccl5* promoter, containing 9, 10 or 11Gs at position -57 of the promoter. Two different length of the *Ccl5* promoter were investigated; a longer version that included the ISRE and NF-κB element and a shorter construct that was devoid of the potent ISRE element and that was more likely to reveal small differences in promoter activity caused by the G-insertion. Interestingly, the ligands LPS and Sendai virus varied in their potential to activate the different *Ccl5* promoter constructs, which illustrated the activation of a different set of transcription factors. Sendai virus, which signals via the cytosolic RIG-I receptor, required the ISRE element to induce promoter activity, while the TLR4 pathway could also induce the shorter, ISRE-deficient *Ccl5* promoter, albeit much weaker. Overall, the analysis clearly demonstrated that the G-sequence variation did not influence the functionality of the *Ccl5* promoter in response to both ligands. However, it is known that the endogenous *Ccl5* promoter is further controlled by chromatin remodelling events that can not be analysed via luciferase reporter gene assays (246). Also, the potential binding factors Sp1 and KLF13 were implicated in recruiting coactivators and chromatin remodelling proteins (297, 298). Thus as an independent approach to assess *Ccl5* promoter activity in the presence of the 10/11G-repeat, I used the *Trif*- and *Tram*-knockout iBMDMs, which similarly to SARM-deficient cells carried the polymorphism. Comparing the IFN-α-induced CCL5 expression of those cells with wt and *Sarm*$^{-/-}$ iBMDMs revealed that the polymorphism did not affect the functionality of the endogenous *Ccl5* promoter; and confirmed that SARM itself played a crucial role in CCL5 expression in BMDMs.

As the activation of the key transcription factors was found to be SARM-independent, I proposed that SARM may either regulate an alternative factor or mediate the assembly of

activator proteins at the promoter level. This was reasonable, as *Ccl5* is a tightly regulated gene, which initially requires the binding of various transcription factors to subsequently recruit coactivators and chromatin remodelling proteins, finally leading to formation of the transcriptional machinery (246, 259, 261). Accordingly, RNA Polymerase II (Pol II) is usually absent from the *Ccl5* promoter in the basal state, and its recruitment can be seen as a hallmark of prior transcription factor assembly and promoter activation. Thus I established a protocol for ChIP analysis and investigated the LPS-induced recruitment of Pol II to the *Ccl5* promoter, which was subsequently found to be impaired in SARM-deficient iBMDMs. This suggested that SARM might regulate one of the previous steps of protein assembly. It was reported that IRF transcription factors activated downstream of PRR and IFN receptor pathways play a key role in inducing chromatin remodelling by the SWI/SNF complex (246). Therefore, I next examined the binding of IRF3 and IRF1 molecules to the *Ccl5* promoter, but their recruitment was independent of SARM following LPS stimulation. However, to better quantify the accumulation of Pol II and other factors at the *Ccl5* promoter, I optimised a ChIP protocol for quantitative real-time PCR analysis to replace the semi-quantitative detection method. Using this protocol, future experiments in primary BMDMs will assess if SARM is consistently required for Pol II recruitment to the *Ccl5* promoter and will help to elucidate the exact mechanism of SARM in enhancing promoter activity.

a pBMDM


wt
SARM-/-
LPS [h] - 0.25 0.5 1 3 6
- 0.25 0.5 1 3 6
IκB
p-p38
t-p38
p-JNK1/2
t-JNK1/2
β-actin
p-ERK1/2
t-ERK1/2
β-actin

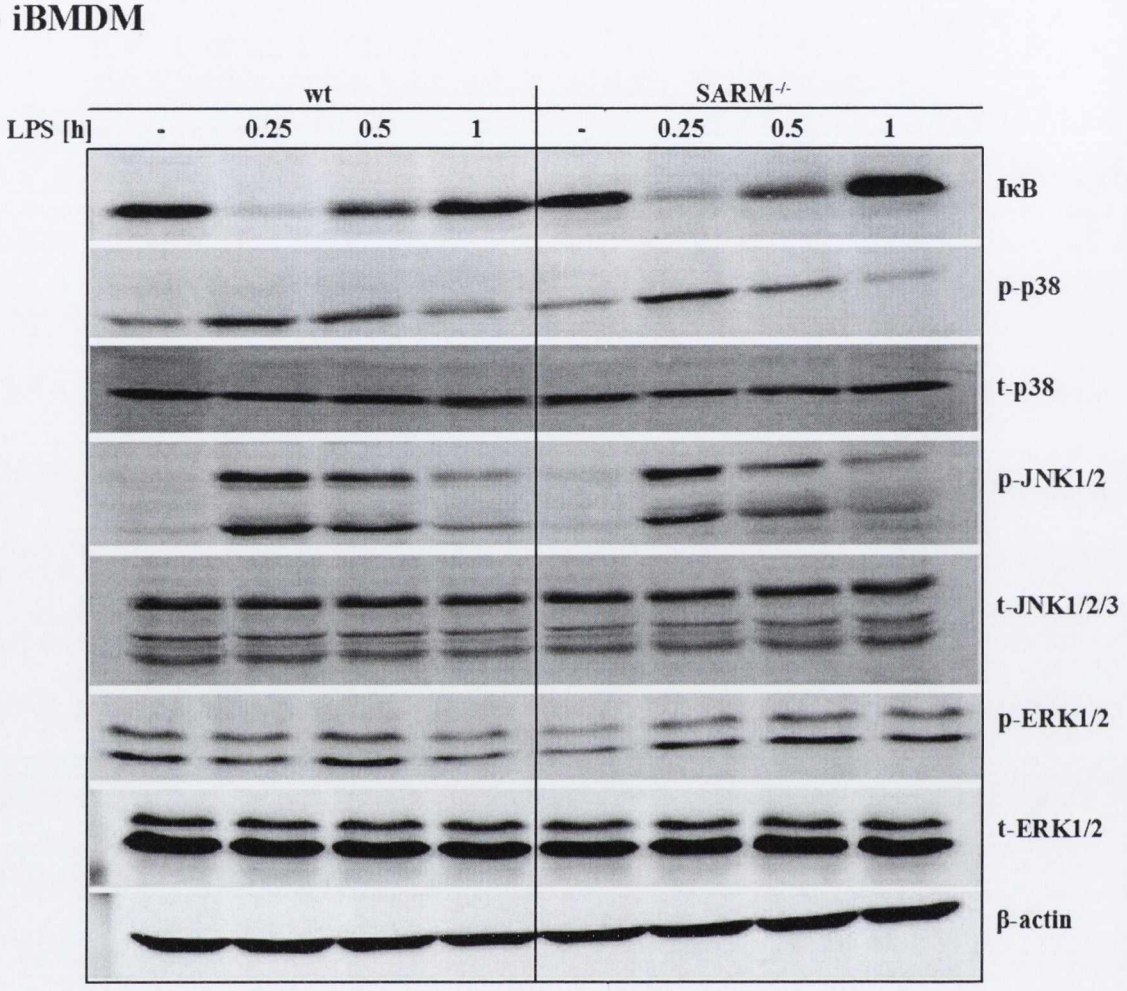


Figure 5.1: SARM is dispensable for TLR4-mediated activation of NF-κB and MAPKs in primary and immortalised BMDMs

Wt and *Sarm*$^{-/-}$ pBMDMs (a) and iBMDMs (b) were seeded in 6 well plates at $5x10^5$ cells/ml and stimulated for the indicated times with LPS [100ng/ml] or medium as control (—). Lysates were subjected to SDS-PAGE followed by Western blotting using specific antibodies to detect the degradation of the NF-κB inhibitor IκB or the phosphorylation of p38 (p-p38), JNK1/2 (p-JNK1/2) and ERK1/2 (p-ERK1/2). The detection of total protein, t-p38, t-JNK, t-ERK and β-actin served as loading control. Data are from one experiment representative of three.

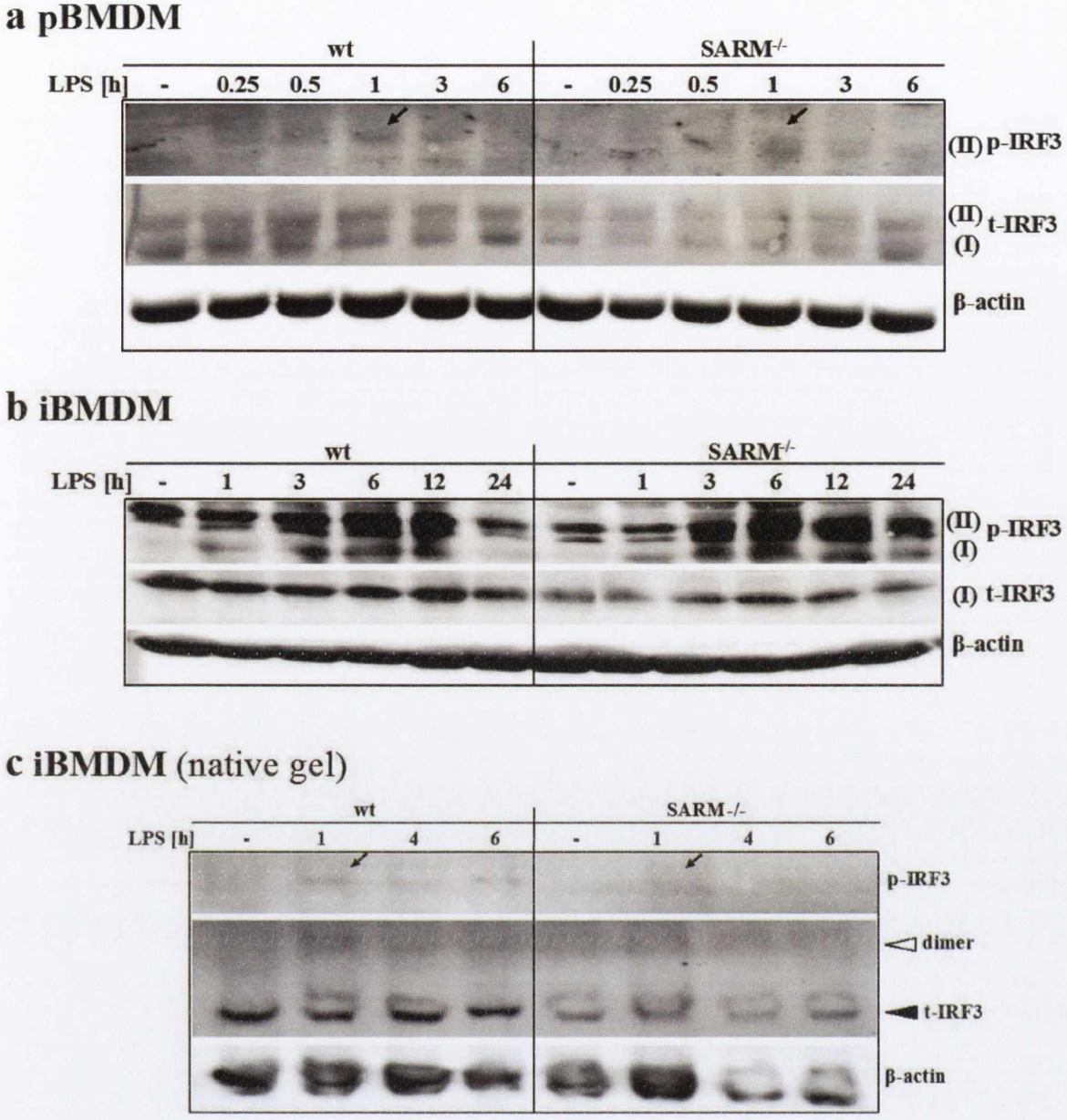
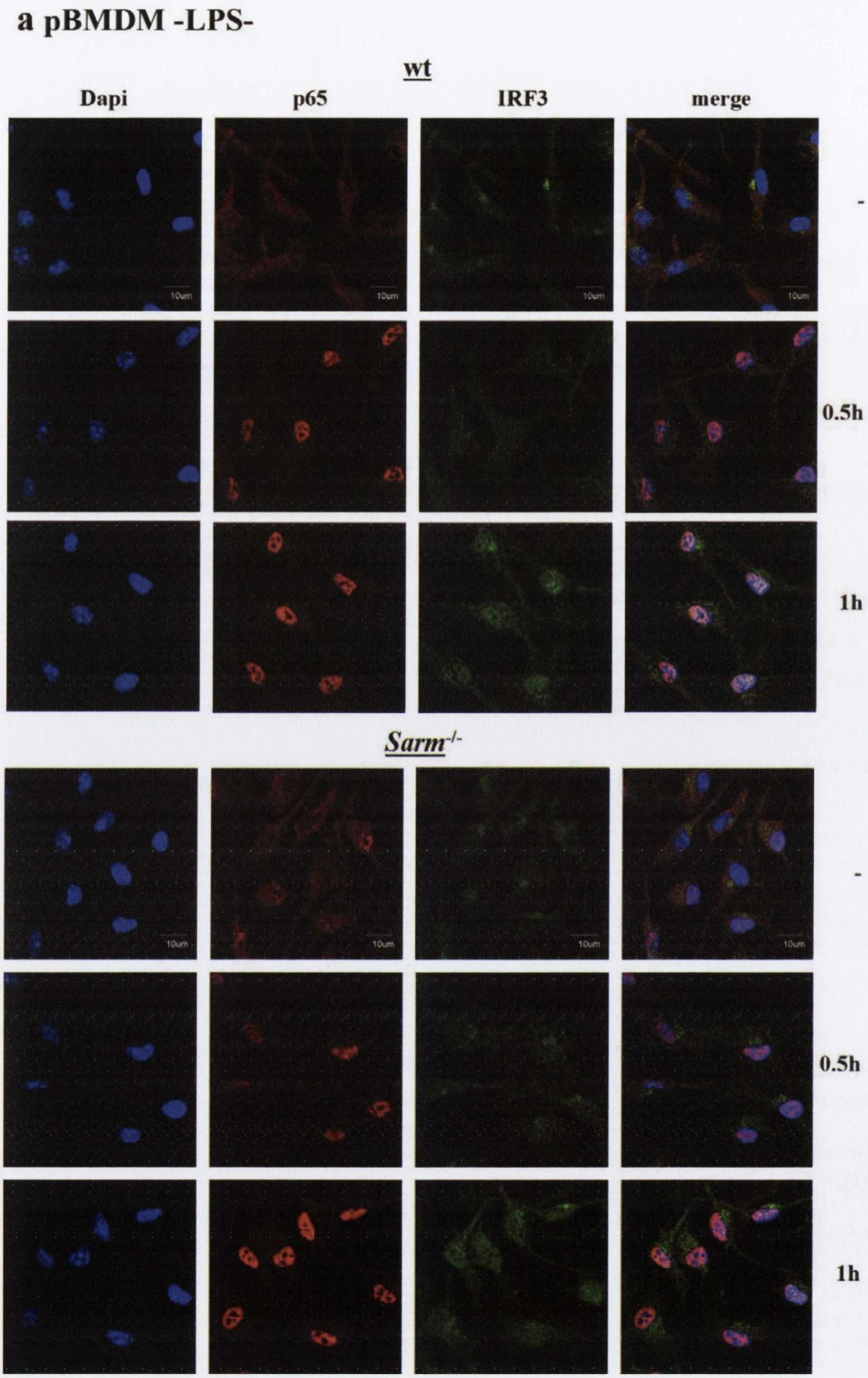
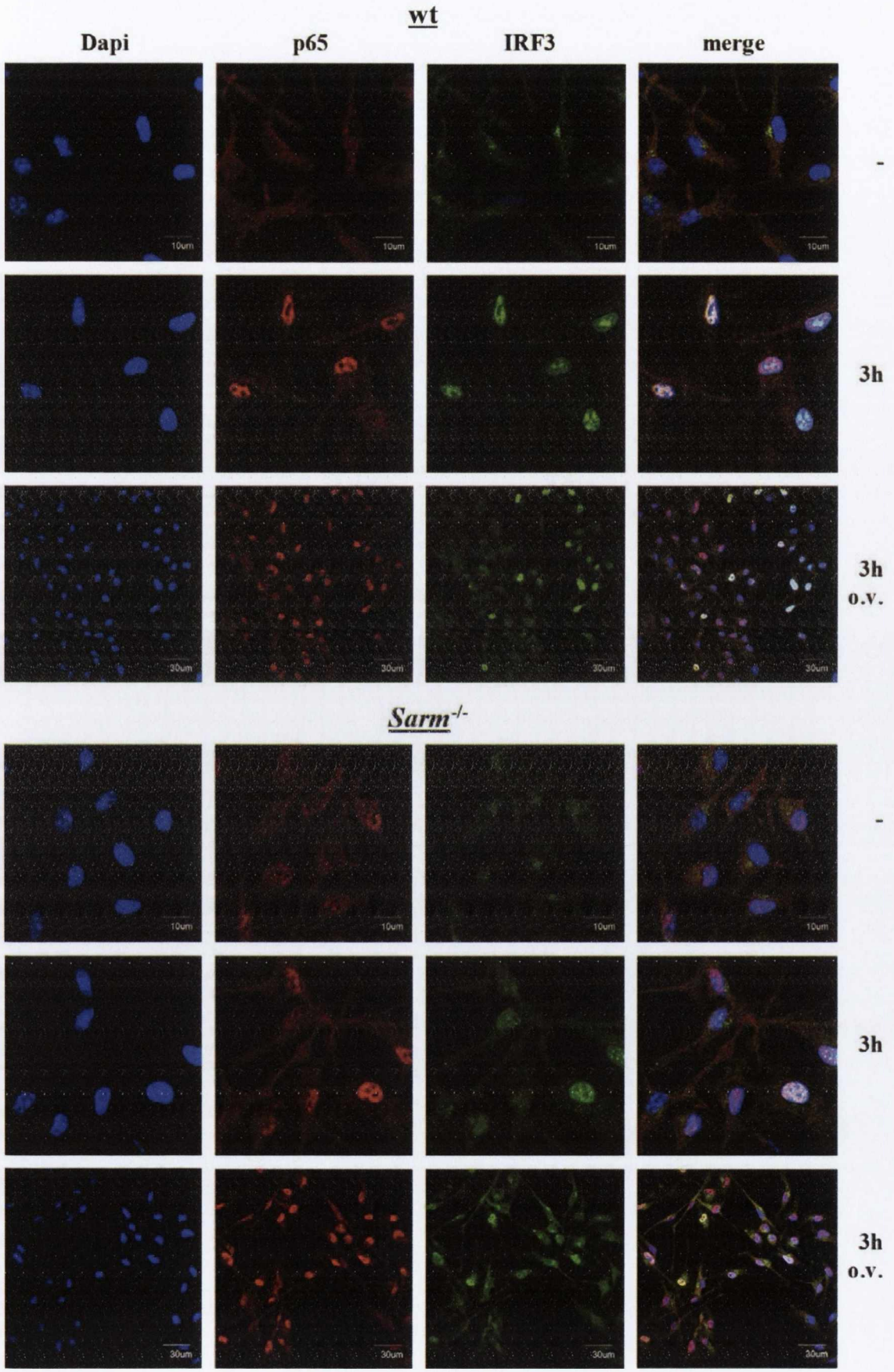


Figure 5.2: SARM is dispensable for TLR4-mediated IRF3 activation in primary and immortalised BMDMs

Immunoblot analysis of IRF3 activation in wt and *Sarm*$^{-/-}$ pBMDMs (a) and iBMDMs (b,c) following LPS stimulation. Cells were seeded in 6 well plates at 5x10^5 cells/ml and stimulated for the indicated times with LPS [100ng/ml] or medium as control (—). (a,b) Lysates were subjected to SDS-PAGE followed by Western blotting using specific antibodies to detect serine 396-phosphorylated IRF3 (p-IRF3), t-IRF3 and β-actin as a loading control. The Western Blot revealed two forms of IRF3, form (I) probably represented unphosphorylated IRF3, while form (II) was a higher phosphorylated IRF3. (c) Lysates were analysed by Native-PAGE to detect IRF3 dimer formation using the antibodies described above. The filled and open arrowheads indicate the IRF3 monomer and dimer, respectively. The black arrows in (a,c) highlight phosphorylated IRF3. Data are from one experiment representative of three.


a pBMDM -LPS-
wt
Dapi
p65
IRF3
merge
-
0.5h
1h
Sarm-/-
-
0.5h
1h
10um


b pBMDM -SeV-
wt
Dapi
p65
IRF3
merge
-
3h
3h
o.v.
Sarm-/-
-
3h
3h
o.v.
10um
30um

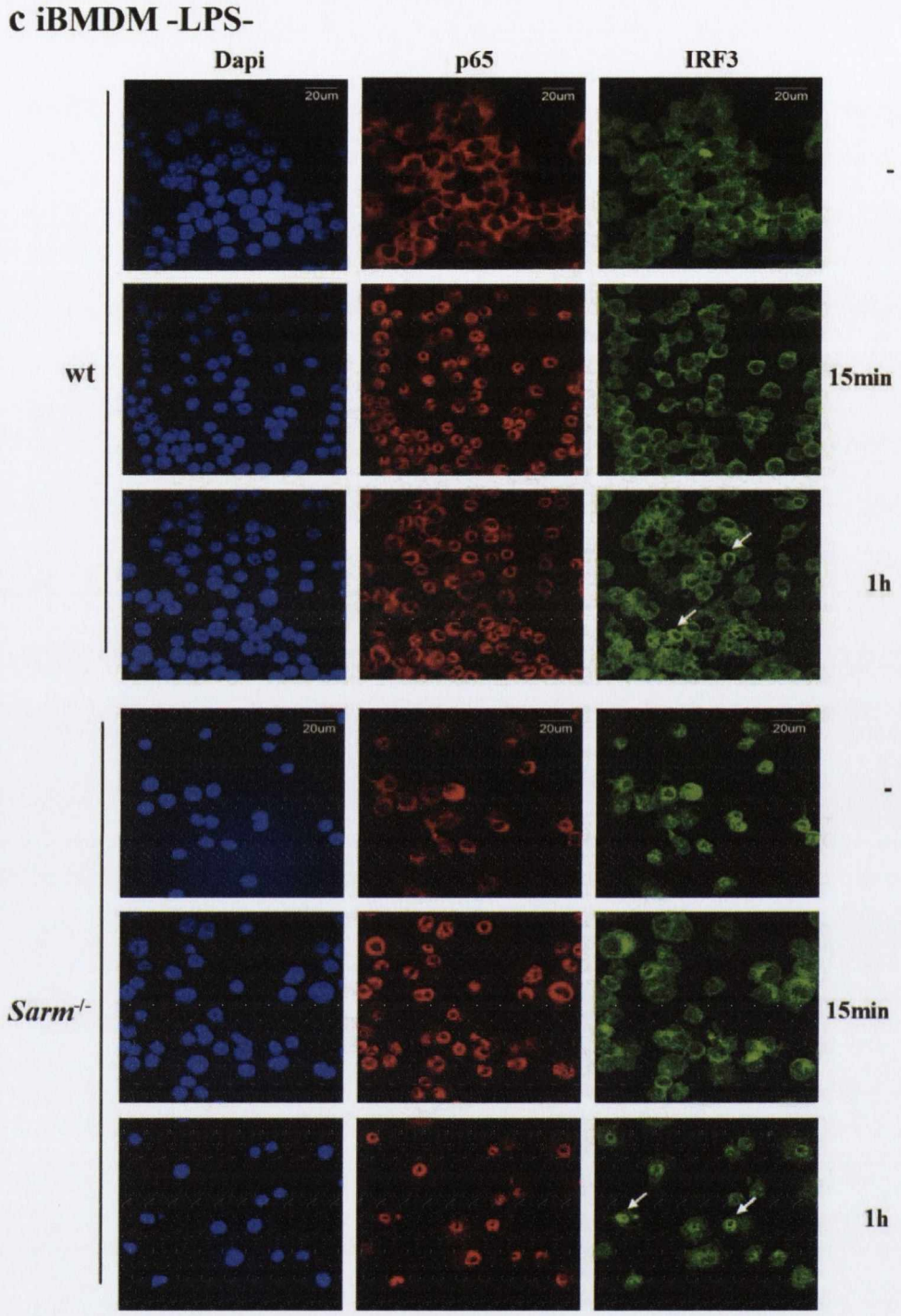


Figure 5.3: SARM is dispensable for TLR4- and non-TLR-mediated p65 and IRF3 nuclear translocation in primary and immortalised BMDMs

Confocal microscopy of wt and *Sarm*$^{-/-}$ pBMDMs (a,b) and iBMDMs (c). Cells were seeded on glass coverslips in 24 well plates at $3x10^5$ cells/ml and stimulated for the indicated times with LPS [100ng/ml] (a,c), Sendai virus (SeV) (b) or medium as control (—). Cells were fixed and stained for NF-κB p65 (red) and IRF3 (green) using specific antibodies followed by Alexa Fluor 647- and 488-conjugated secondary antibodies, respectively. Nuclei were visualised using the DNA-intercalating dye DAPI (blue). The scale bars are depicted in the control images and represent 10μm (a,b) or 20μm (c). An overview image (o.v.) is included in (b), with a scale bar indicating 30μm. The white arrows in (c) highlight the nuclear translocation of IRF3. Data are from one experiment representative of three.

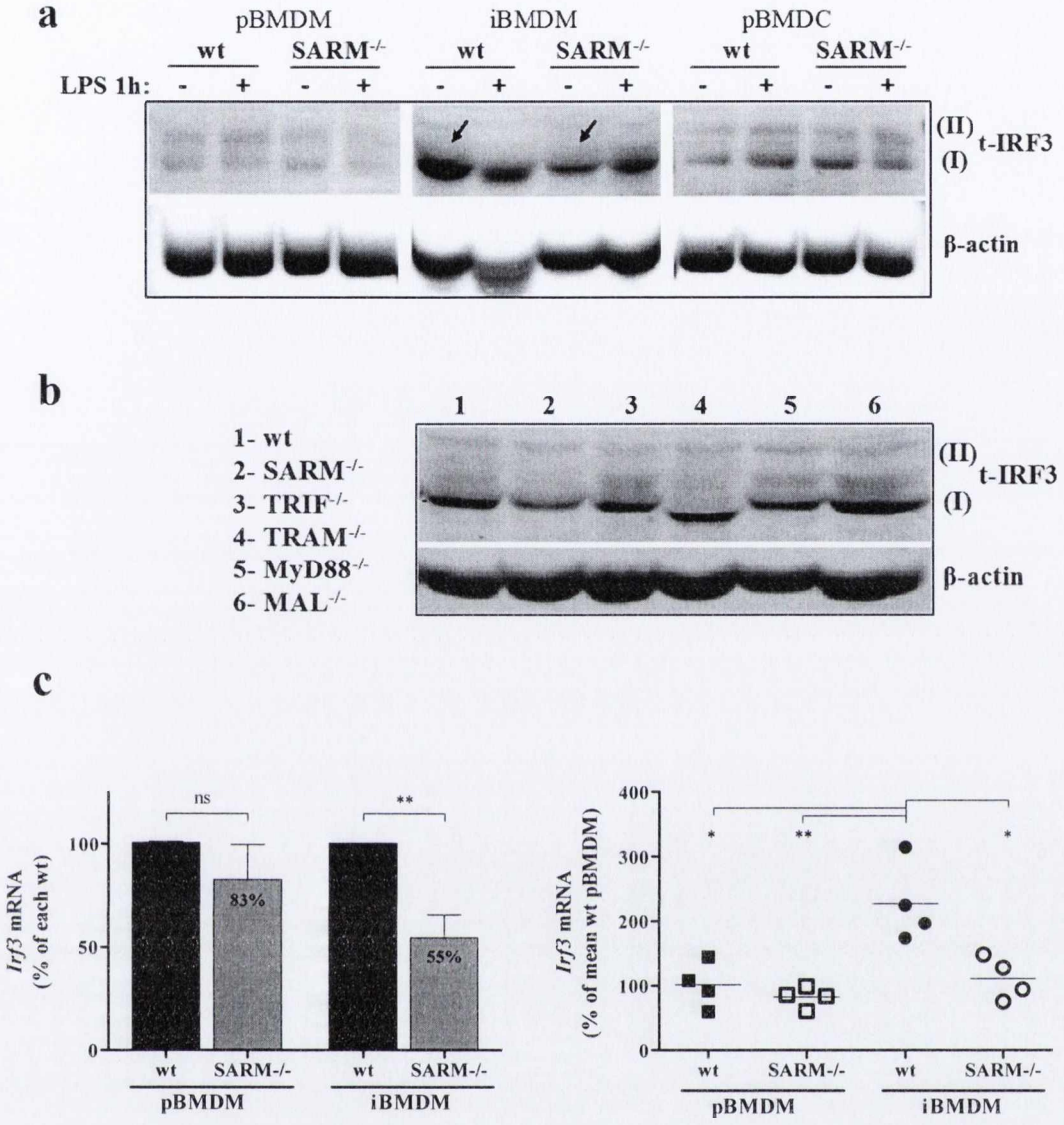


Figure 5.4: SARM is required for the elevated basal IRF3 expression in immortalised BMDMs, but dispensable for the IRF3 expression in primary BMDMs

Comparison of basal IRF3 mRNA and protein expression in wt and *Sarm*$^{-/-}$ pBMDMs and iBMDMs. (a) Immunoblot analysis of IRF3 protein expression in primary BMDMs and BMDCs compared with iBMDMs. Cells were seeded in 6 well plates at $5x10^5$ cells/ml and stimulated for 1h with LPS [100ng/ml] or medium as control (–). Lysates were subjected to SDS-PAGE followed by Western Blotting using specific antibodies to detect t-IRF3 and β-actin as a loading control. Two forms of IRF3 were detected with (I) probably representing an unphosphorylated form, while (II) might be a higher phosphorylated IRF3. The arrows indicate the difference in basal IRF3 protein expression in wt and *Sarm*$^{-/-}$ iBMDMs. The direct comparison was performed once. (b) Basal IRF3 protein expression of all TIR-adaptor knockout iBMDMs. Immunoblot analysis was performed as described in (a). Data are from one experiment representative of three. (c) Quantitative real-time PCR analysis of basal *Irf3* mRNA expression in pBMDMs and iBMDMs. Cells were seeded in 24 well plates at $5x10^5$ cells/ml and treated with medium only. *Irf3* mRNA was normalised to the housekeeping gene *β-actin* and is presented as percentage in *Sarm*$^{-/-}$ to each corresponding wt p/iBMDM (left panel) or as percentage of the mean level detected in wt pBMDMs (right panel). The left panel includes three (mean ± s.d.) and the right panel four independent experiments. * $P<0.05$, ** $P<0.01$, *** $P<0.001$ (Student's *t*-test).

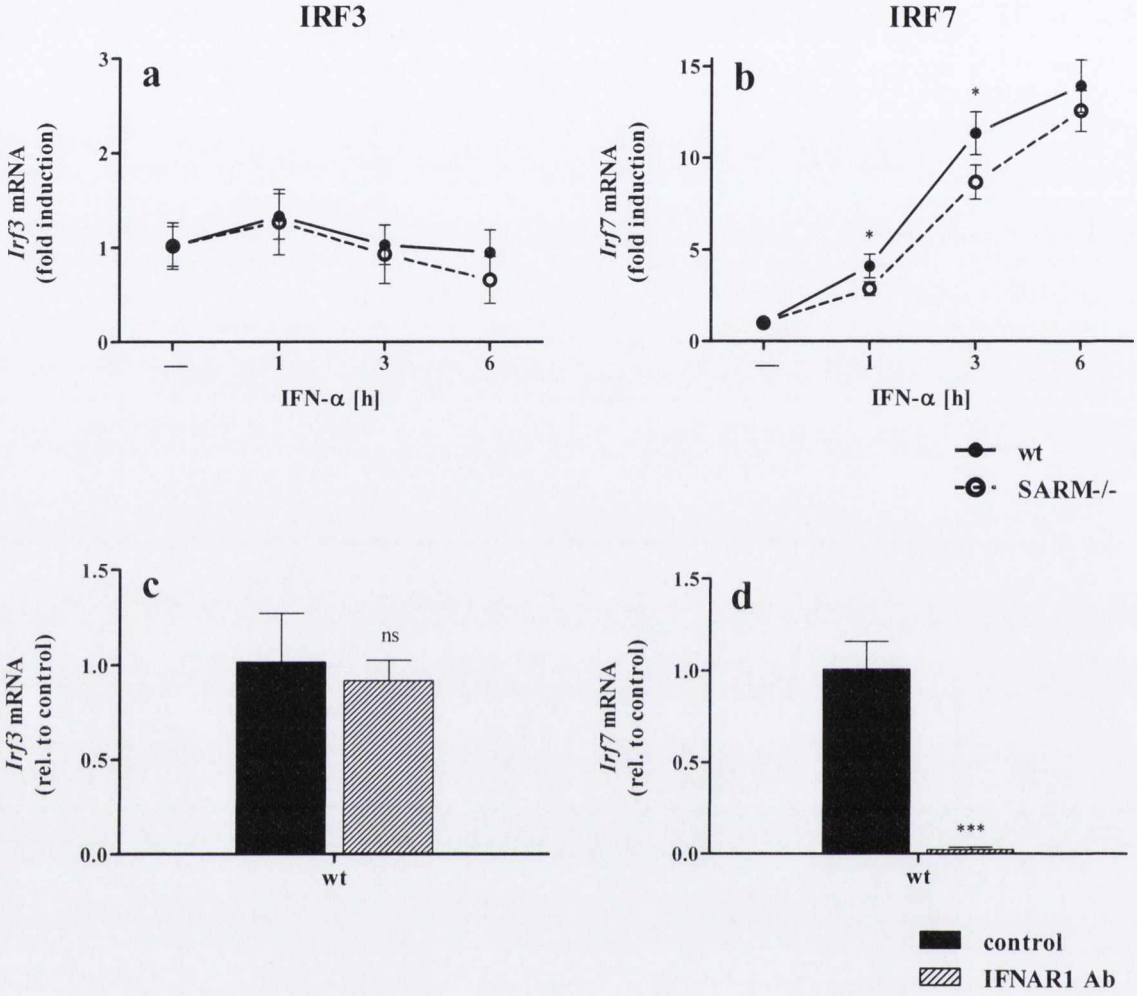


Figure 5.5: IRF3 expression is independent of type I IFNs in immortalised BMDMs

(a) Quantitative real-time PCR analysis of *Irf3* and *Irf7* mRNA expression in wt and *Sarm*$^{-/-}$ iBMDMs. Cells were seeded in 24 well plates and stimulated with IFN-α [1000U/ml] for the indicated times or medium as control (—). mRNA level were normalised to the housekeeping gene *β-actin* and are presented as fold induction relative to each wt or *Sarm*$^{-/-}$ control. (b) wt iBMDMs were seeded as in (a) and incubated overnight with anti-IFNAR1 antibody [5μg/ml] or medium as control. *Irf3* and *Irf7* mRNA expression were determined by quantitative real-time PCR as described above and are presented relative to control. Data are from one experiment representative of two (mean ± s.d.). * P<0.05, ** P<0.01, *** P<0.001, compared with wt (a) or control (b) (Student's *t*-test).

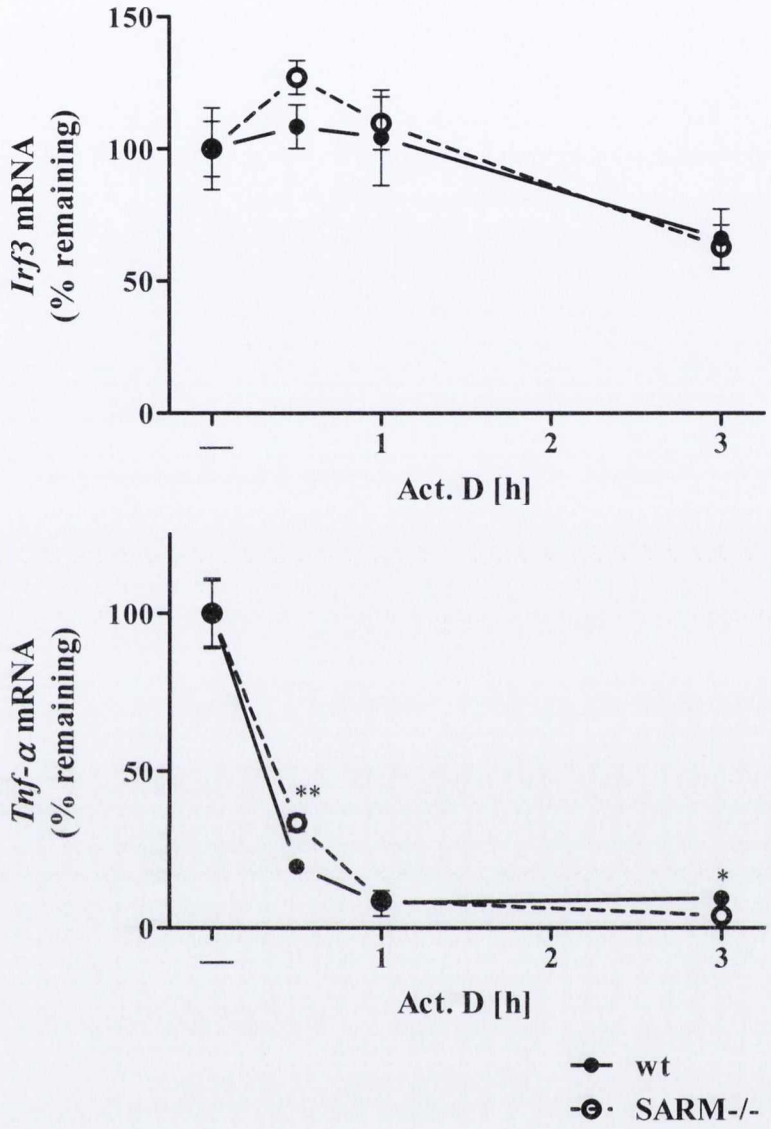
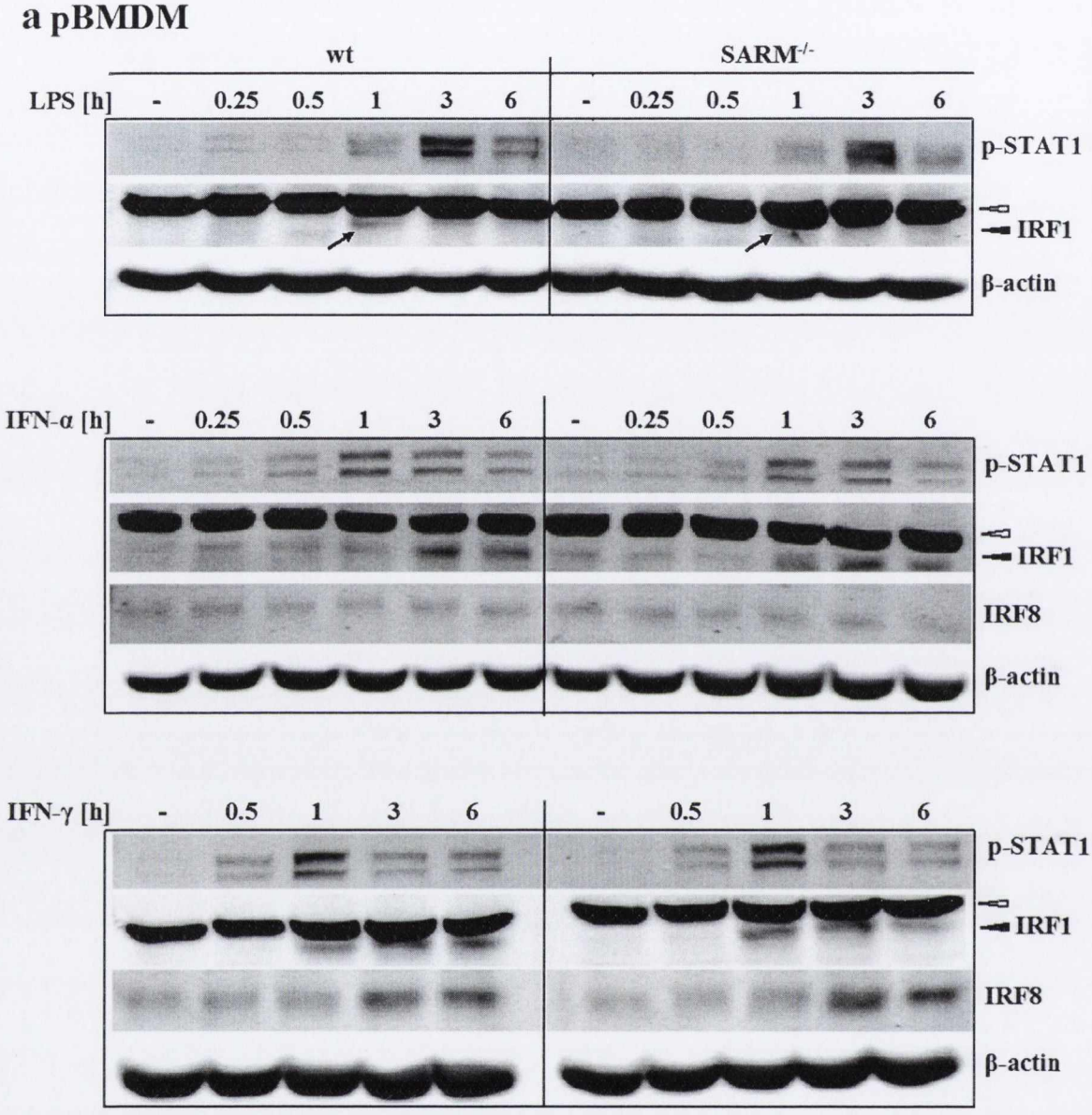


Figure 5.6: IRF3 mRNA stability is not regulated by SARM in immortalised BMDMs

To analyse *Irf3* mRNA stability, wt and *Sarm*$^{-/-}$ iBMDMs were seeded in 6 well plates at 5x10^5 cells/ml and treated for the indicated times with the transcriptional inhibitor actinomycin D [5µg/ml] or medium as control (—). *Irf3* and *Tnf-α* mRNA were determined by quantitative real-time PCR, normalised to the housekeeping gene *β-actin* and are presented as the percentage remaining compared with each wt or *Sarm*$^{-/-}$ control. The analysis of *Tnf-α* mRNA decay served as positive control for the actinomycin D treatment. Data are from one experiment representative of two (mean ± s.d.). * P<0.05, ** P<0.01, *** P<0.001, compared with wt (Student's *t*-test).


a pBMDM
wt
SARM-/-
LPS [h] - 0.25 0.5 1 3 6 - 0.25 0.5 1 3 6
p-STAT1
IRF1
β-actin
IFN-α [h] - 0.25 0.5 1 3 6 - 0.25 0.5 1 3 6
p-STAT1
IRF1
IRF8
β-actin
IFN-γ [h] - 0.5 1 3 6 - 0.5 1 3 6
p-STAT1
IRF1
IRF8
β-actin

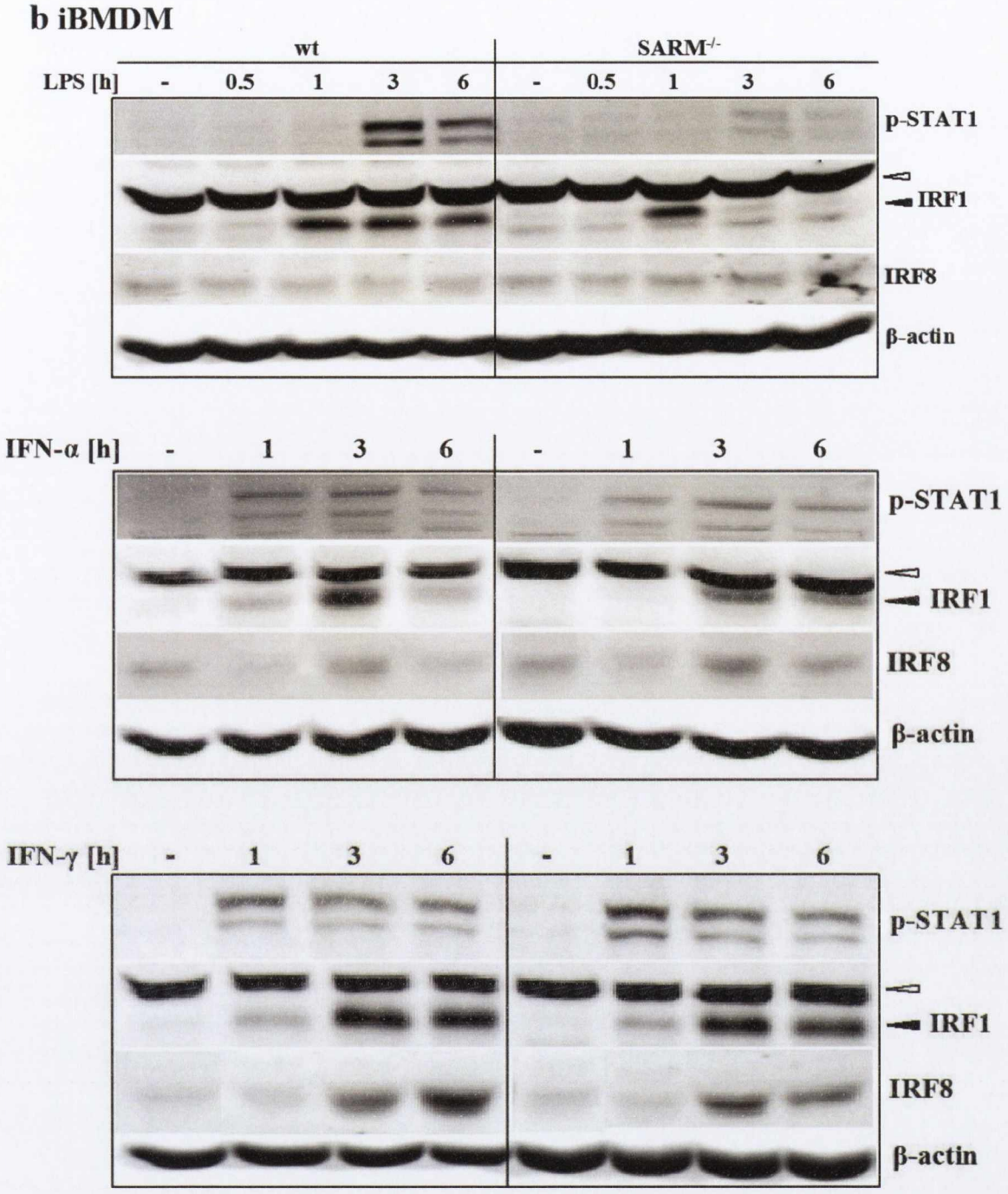


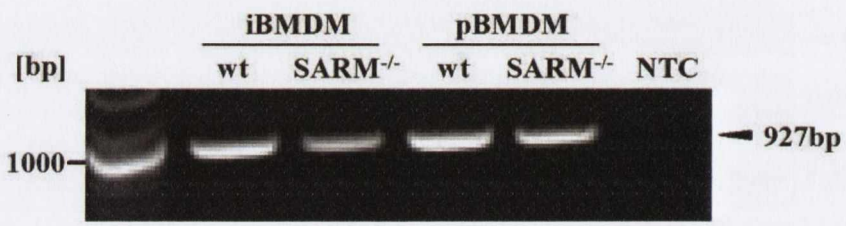
Figure 5.7: SARM is dispensable for TLR4- and IFNAR/IFNGR-mediated upregulation of IRF1 and IRF8 in primary and immortalised BMDMs

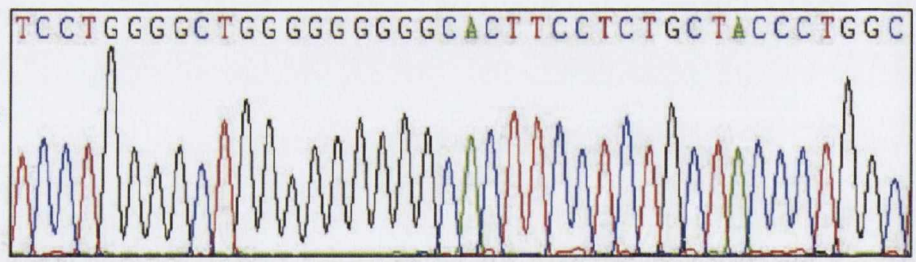
Immunoblot analysis of the induction of phosphorylated STAT1 and IRF1 and IRF8 in wt and *Sarm*$^{-/-}$ pBMDMs (a) and iBMDMs (b). Cells were seeded in 6 well plates at $5x10^5$ cells/ml and stimulated with LPS [100ng/ml], IFN-α [1000U/ml] and IFN-γ [10ng/ml] for the indicated times or medium as control (–). Lysates were subjected to SDS-PAGE followed by Western Blotting using specific antibodies to detect tyrosine 701-phosphorylated STAT1 (p-STAT1), IRF1, IRF8 and β-actin as a loading control. The filled arrowhead indicates the detection of IRF1 below a nonspecific band (open arrowhead). The black arrows in (a)-top panel indicate the upregulation of IRF1. Data are from one experiment representative of one (a) or two (b).

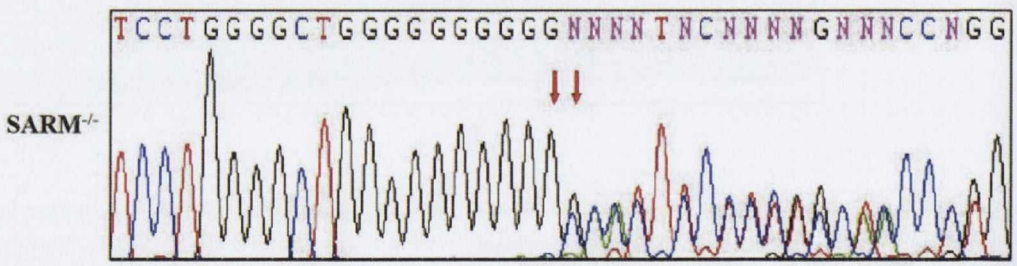
a

-600 CTCTCAGATCACATGTCACACACTAAGTGTAAGTATGCCTATATCTACCTAGTTATCTGG
GAATCAGGATTACCTGGCAAATTCCTTACAACAAATCTCCTATACCTTGTTAACTTATTG
TTATCAATGACACAAGTGTGGTCTGTTTCTGATATGGTATGCTCATGACAAATACTCTTC
CATGGAGAAAACAGAAAGACCAAAATCAAGTCTGGGCTACAACTTGGGAATTTGCCAAGT
GAAGACCAATGGCTTGACCTTAACTGACCCCTACTTGCCTTAAGACAACAGCTCCCTGCT
ACCTGGAGAGGCCCTGAGTGGGACGGCAGATCTGAGGGGGAGGGGGAGGGGGAGGAAGAA
ATTTTCCCCTACTGTATTTGGCCAGAGAGGGAGTCATCCTGGACTGGAGGGCAGTTAGAG
GCAGAGTCATACTTCCAAGGGTGATTTCAGTTTTCTTTTCCATTTTGTGTTTTCATTTTA
TGACAGCAACAAGTGTTTGGTGTCTTTTGTGGAAACTCCCCAAGTCCTGGGGCTGGGGGG
GGGCACTTCCTCTGCTACCCTGGCTCCCTATAAAAGGTCTGCCTGAGCTGCAGAGCACCC
+1 CTTGCAGAGGACTCTGAGACAGCACATGCATCTCCCACAGCCTCTGCCGCGGGTACC**ATG**
AAGATCTCTGCAGCTGCCCTCACCATCATCCTCACTGCAGCCGCCCTCTGCACCCCCGCA
CCTGCCTCACCATGTAAGTCGAGGGTTCTGACCATCACAGCCCCACTCTGCCTCGATGCC
AACCCATCTTGATACCCAGACCTCCCCTTCTTTCCAATCCTACTGTGTATGCTGCTGTAC
ATTCTTACGCATCCTTGACACGGCTACCCTGTCATCACTGTTAGATGTCTTGTATACTAA
TGGCAGGATCCTCTGAGGAACTTTTCTGTGTCTTCAAAGATGATATTATGAATTCTGCAG
GCACTCCTTATTGTGAACTGGTGCCGGGCTGACCTTTGAAAAATGACTTGCTCATATCTG
+420

b







wt	**(a1)**	-76	TCCTGGGGCTGGGGGGGGG--CACTTCCTCTGCTACCCTGGC
	(a2)	-76	TCCTGGGGCTGGGGGGGGG--CACTTCCTCTGCTACCCTGGC
SARM$^{-/-}$	**(a1)**	-76	TCCTGGGGCTGGGGGGGGG**G**-CACTTCCTCTGCTACCCTGGC
	(a2)	-76	TCCTGGGGCTGGGGGGGGG**GG**CACTTCCTCTGCTACCCTGGC

c

(I)

MyD88$^{-/-}$	-76 TCCTGGGGCTGGGGGGGGG -	-CACTTCCTCTGCTACCCTGGC
MAL$^{-/-}$	-76 TCCTGGGGCTGGGGGGGGG -	-CACTTCCTCTGCTACCCTGGC
TRIF$^{-/-}$	-76 TCCTGGGGCTGGGGGGGGG**G/GG**	CACTTCCTCTGCTACCCTGGC
TRAM$^{-/-}$	-76 TCCTGGGGCTGGGGGGGGG**G/GG**	CACTTCCTCTGCTACCCTGGC

(II)

IRAK4$^{-/-}$	-76 TCCTGGGGCTGGGGGGGGG -	-CACTTCCTCTGCTACCCTGGC
caspase-1$^{-/-}$	-76 TCCTGGGGCTGGGGGGGGG -	-CACTTCCTCTGCTACCCTGGC
gp91$^{phox-/-}$	-76 TCCTGGGGCTGGGGGGGGG -	-CACTTCCTCTGCTACCCTGGC
NLRP8$^{-/-}$	-76 TCCTGGGGCTGGGGGGGGG -	-CACTTCCTCTGCTACCCTGGC

(III)

wt	-76 TCCTGGGGCTGGGGGGGGG -	-CACTTCCTCTGCTACCCTGGC
SARM$^{-/-}$	-76 TCCTGGGGCTGGGGGGGGG -	-CACTTCCTCTGCTACCCTGGC

(another independently generated SARM$^{-/-}$ mouse)

Figure 5.8: *Sarm*$^{-/-}$ mice harbour a 1-2bp G-insertion in the proximal *Ccl5* gene promoter

(a) Nucleotide sequence of the murine *Ccl5* gene region (-600 to +420), including the proximal promoter (-600/-1), Exon 1 (+1/+133, highlighted in light grey) and part of Intron 1 (+134/+420) (ENSMUSG00000035042). The pair of PCR primers designed to amplify a 927bp fragment for sequencing is highlighted in dark grey. The putative ISRE element, NF-κB element and TATA box are indicated by the continuous, double and dotted line, respectively. Also shown are the transcriptional start site (arrow, designated +1) and the translational start site ATG (bold). The sequence depicted in (b,c) is highlighted in red. (b) A 927bp fragment of the 5'-region of the *Ccl5* gene was PCR amplified from genomic DNA of wt and *Sarm*$^{-/-}$ iBMDMs and pBMDMs. PCR products were visualised on a 1% agarose gel including a no template control (NTC) as negative control (top panel). DNA was purified from the PCR reactions and sent for sequence analysis using the forward primer. The chromatogram displays a region of the *Ccl5* promoter which shows a mutation in *Sarm*$^{-/-}$ pBMDMs and iBMDMs compared with the corresponding wt. At position -57 of the *Ccl5* gene, the *Sarm*$^{-/-}$ genomic DNA has a 1bp G-insertion on one allele (a1) and a 2-bp G-insertion on the other allele (a2) leading to a 10/11G-repeat compared with a 9G-sequence in wt (lower panel). The heterozygous insertion caused a shift in the sequence analysis of *Sarm*$^{-/-}$ cells, bringing the two allele sequences out of alignment after the insertion (indicated by the red arrows in the chromatogram). (c) Sequence analysis of the 5'-*Ccl5* gene locus in other knockout iBMDMs revealed the same mutation in the genomic DNA of *Trif*$^{-/-}$ and *Tram*$^{-/-}$ cells. Analysed was the 927bp DNA fragment of other TIR adaptor knockout iBMDMs (I), other knockout iBMDMs (II) and wt and *Sarm*$^{-/-}$ MEFs from an independent generated knockout mouse (a gift from MS. Diamond) (III). Data are representative of three (b, wt and *Sarm*$^{-/-}$ pBMDM), at least two (cI) or one (cII, III) independent analysis.

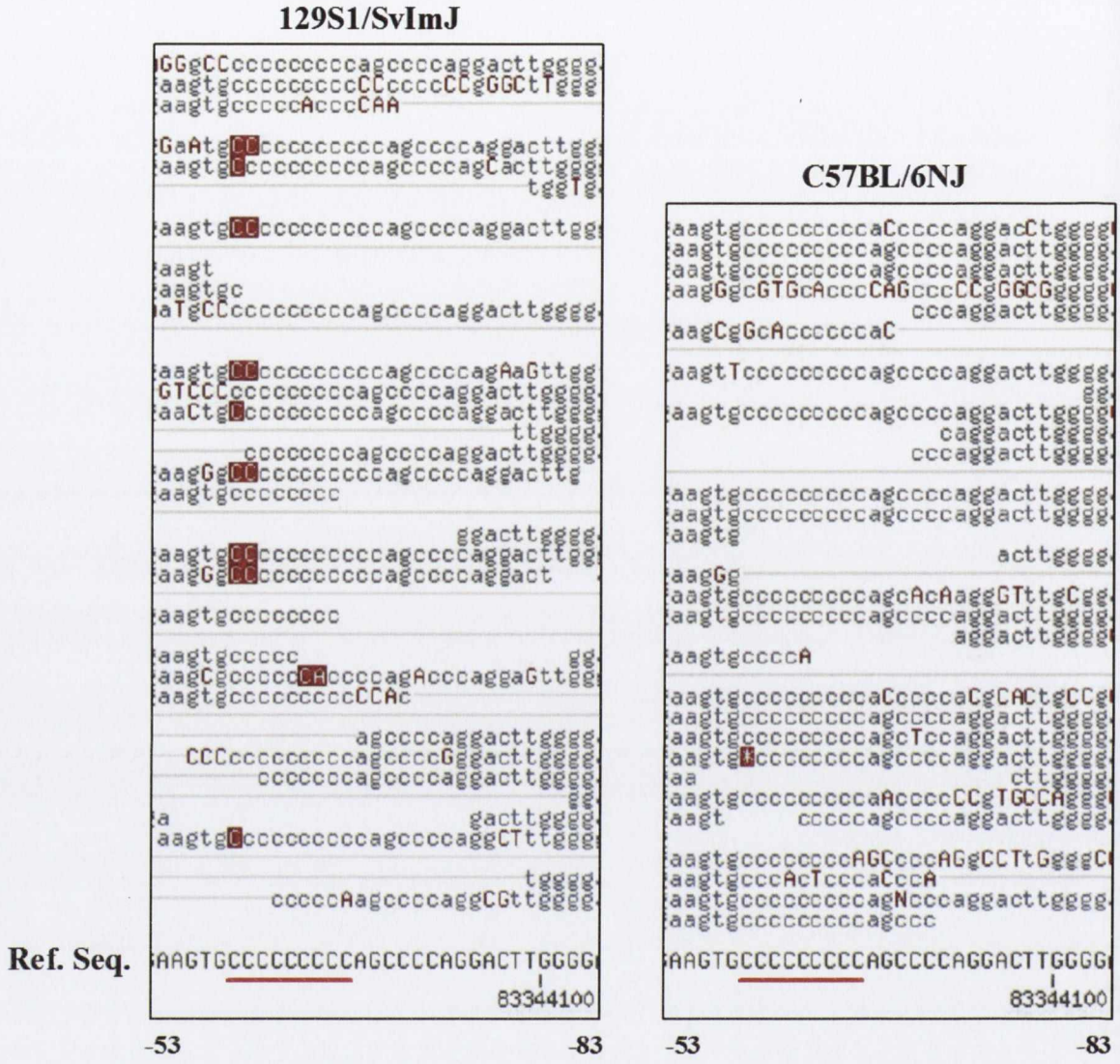


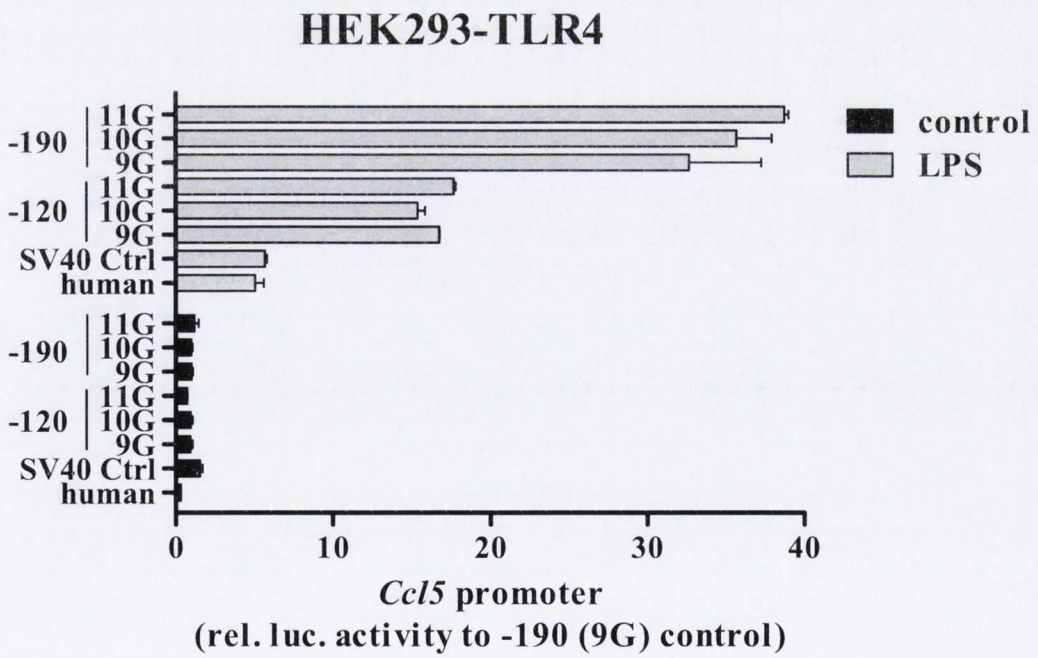
Figure 5.9: Sequence variations within the Poly(G:C) region of the *Ccl5* promoter in different mouse strains

Alignments of the 5'-proximal *Ccl5* promoter region (-53/-83) from different sequencing data of the 129S1/SvImJ and C57BL/6NJ mouse strains, as obtained from the Mouse Genomes Project of the Wellcome Trust Sanger Institute website (Sept.2012). Shown is the reverse complement strand of the previously described sequence (see Figure 5.8), consequently the 9G-repeat is represented by a 9C-sequence (underlined in red). The analysis displays the sequence variations within the respective mouse strain compaired to the reference sequence (Ref.Seq.), indicating mismatches (red characters), insertions (red boxes) and deletions (asterisk).

a


-190
-240 ATTTTCCCCTACTGTATTTGGCCAGAGAGGGAGTCATCCTGGACTGGAGGGCAGTTAGAG
GCAGAGTCATACTTCCAAGGGTGATTTCAGTTTTCTTTTCCATTTTGTGTTTTCATTTTA
-120
TGACAGCAACAAGTGTTTGGTGTCTTTTGTGGAAACTCCCCAAGTCCTGGGGCTGGGGGG
GGGCACTTCCTCTGCTACCCTGGCTCCCTATAAAAGGTCTGCCTGAGCTGCAGAGCACCC
+1
CTTGCAGAGGACTCTGAGACAGCACATGCATCTCCCACAGCCTCTGCCGCGGGTACCATG
+57
9G in wt
10/11G in SARM-/-
pGL3 (-190/+57)
ISRE
NF-κB
9/10/11 G
+57
luc
pGL3 (-120/+57)
NF-κB
9/10/11 G
+57
luc
pGL3-SV40 Ctrl
SV40
luc

b


HEK293-TLR4
-190
11G
10G
9G
-120
11G
10G
9G
SV40 Ctrl
human
-190
11G
10G
9G
-120
11G
10G
9G
SV40 Ctrl
human
control
LPS
0
10
20
30
40
Ccl5 promoter
(rel. luc. activity to -190 (9G) control)

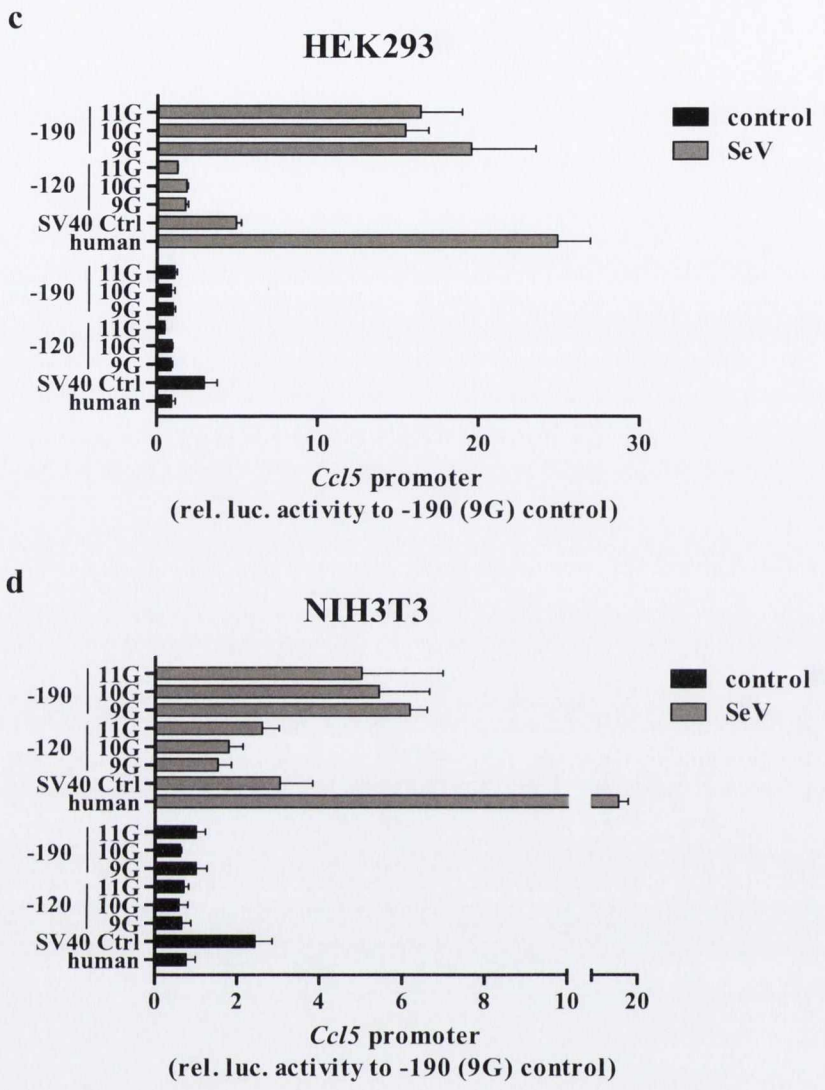


Figure 5.10: The 1-2bp G-insertion in the *Ccl5* promoter does not affect its activity

(a) Nucleotide sequence of the murine 5'-*Ccl5* gene region (-240 to +60), including the proximal promoter and the 5'-UTR (+1/+57, highlighted in light grey). The putative ISRE element, NF-κB element and TATA box are indicated by the continuous, double and dotted line, respectively. Also shown are the transcriptional start site (designated +1) and the translational start site ATG (bold). The sequence variation found in the G-repeat at position -57 as 9G in wt and 10/11G in *Sarm*$^{-/-}$ is highlighted in red. The two promoter regions cloned from wt and *Sarm*$^{-/-}$ genomic DNA into the pGL3-firefly luciferase reporter are indicated. The (-190/+57) construct includes the ISRE and NF-κB element, while the shorter (-120/+57) construct contains only the NF-κB element, as illustrated in the schematic. The cloning generated three versions of each construct with either 9 and 10 or 11Gs, corresponding to the wt and *Sarm*$^{-/-}$ genotype, respectively. pGL3-SV40 served as control vector with basal activity, containing the SV40 promoter upstream of the luciferase reporter gene. (b-d) Analysing the effect of the G-insertions on *Ccl5* promoter activity in human and murine cells. Human HEK293-TLR4, HEK293 and murine NIH3T3 cells were transiently transfected with the pGL3-firefly luciferase reporter constructs described in (a) and a human *Ccl5* promoter construct as positive control (human). Transfection efficiency was determined by cotransfection with a vector expressing renilla luciferase. 24h later, cells were stimulated for 10h with LPS [100ng/ml], Sendai virus (SeV) or medium as control. Firefly and renilla luciferase activity were determined in cell lysates. Firefly luciferase activity was normalised to renilla luciferase control and is presented relative to the untreated control of the -190 (9G) construct, which represents the longer wt *Ccl5* promoter region. Data are from one experiment representative of two (mean ± s.d.).

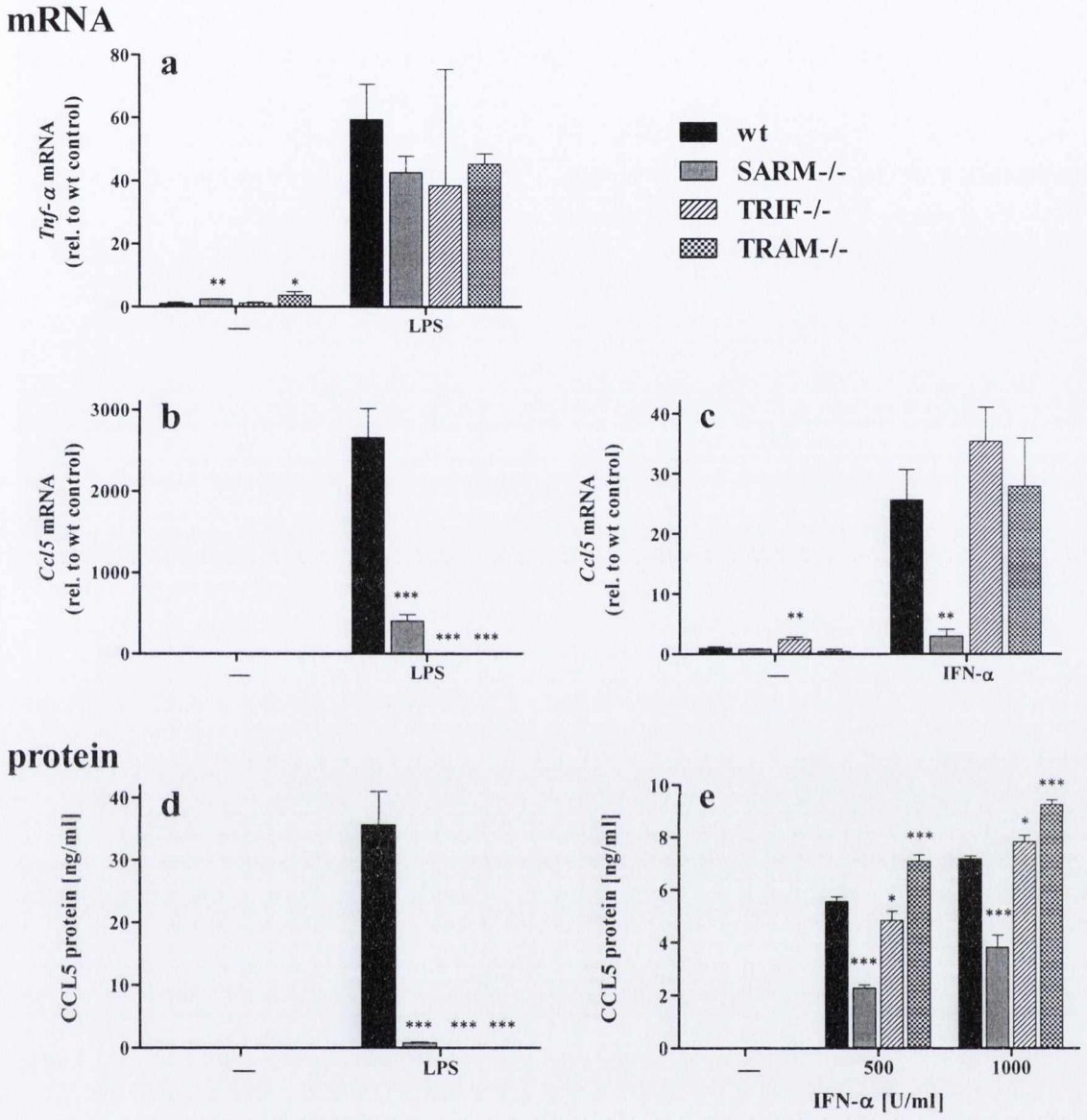


Figure 5.11: The Poly(G)-sequence variation does not affect endogenous CCL5 expression in *Trif*- and *Tram*-knockout immortalised BMDMs

(a-c) Quantitative real-time PCR analysis of *Tnf-α* and *Ccl5* mRNA expression in wt, *Sarm*$^{-/-}$, *Trif*$^{-/-}$ and *Tram*$^{-/-}$ iBMDMs. Cells were seeded in 24 well plates and stimulated with LPS [100ng/ml] and IFN-α [1000U/ml] for 3 and 6h, respectively, or medium as control (—). mRNA level were normalised to the housekeeping gene *β-actin* and are presented relative to wt control. (d,e) Analysis of CCL5 protein expression in the different iBMDMs described in (a). Cells were seeded in 96 well plates and stimulated for 24h with LPS [100ng/ml], IFN-α at the indicated concentrations or medium as control (—). Supernatants were collected and assayed for CCL5 protein by ELISA. LPS-treated cells served as control for the different knockout phenotypes. Data are from one experiment representative of two or three (mean ± s.d.). * $P<0.05$, ** $P<0.01$, *** $P<0.001$, compared with wt (Student's *t*-test).

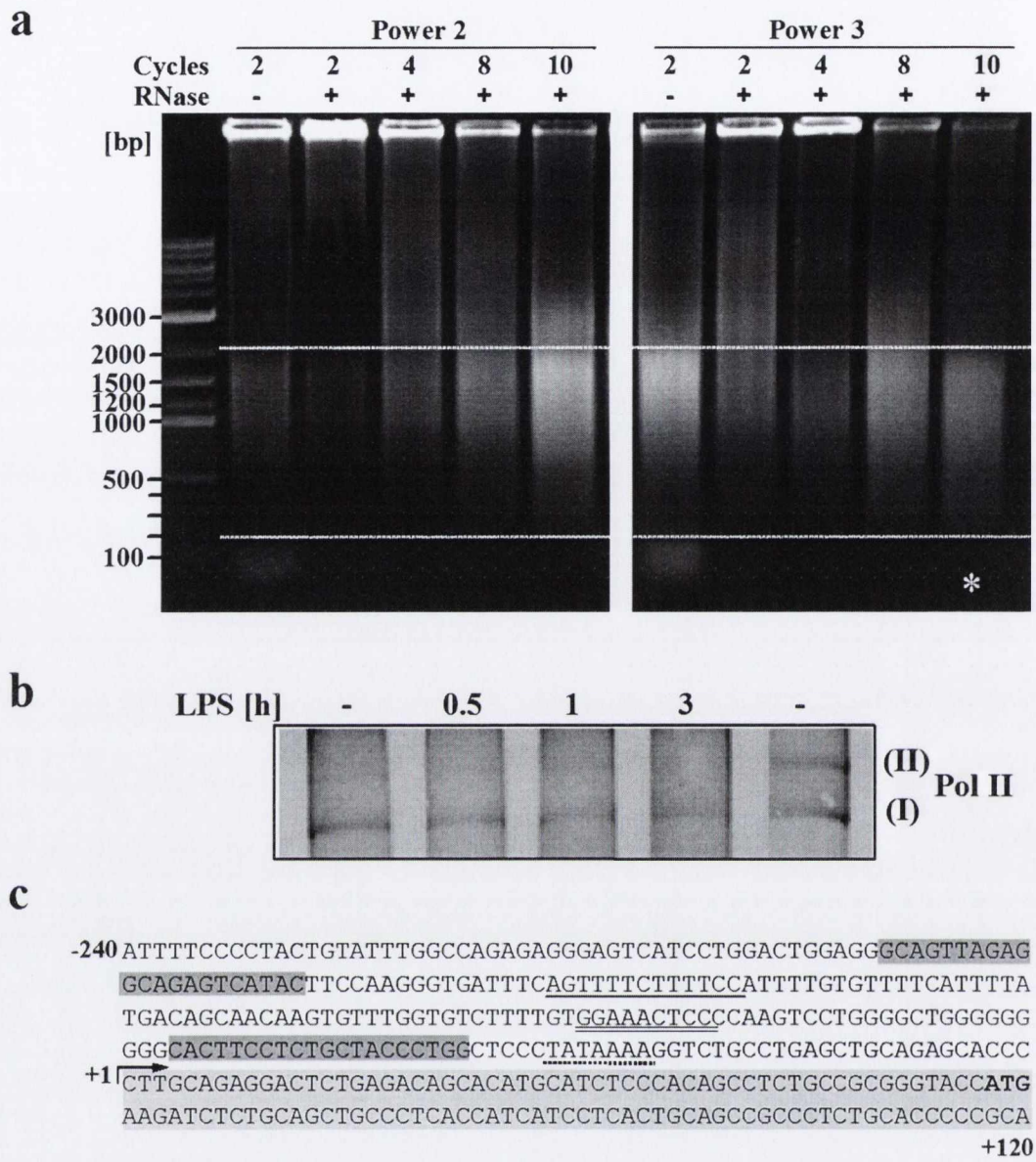
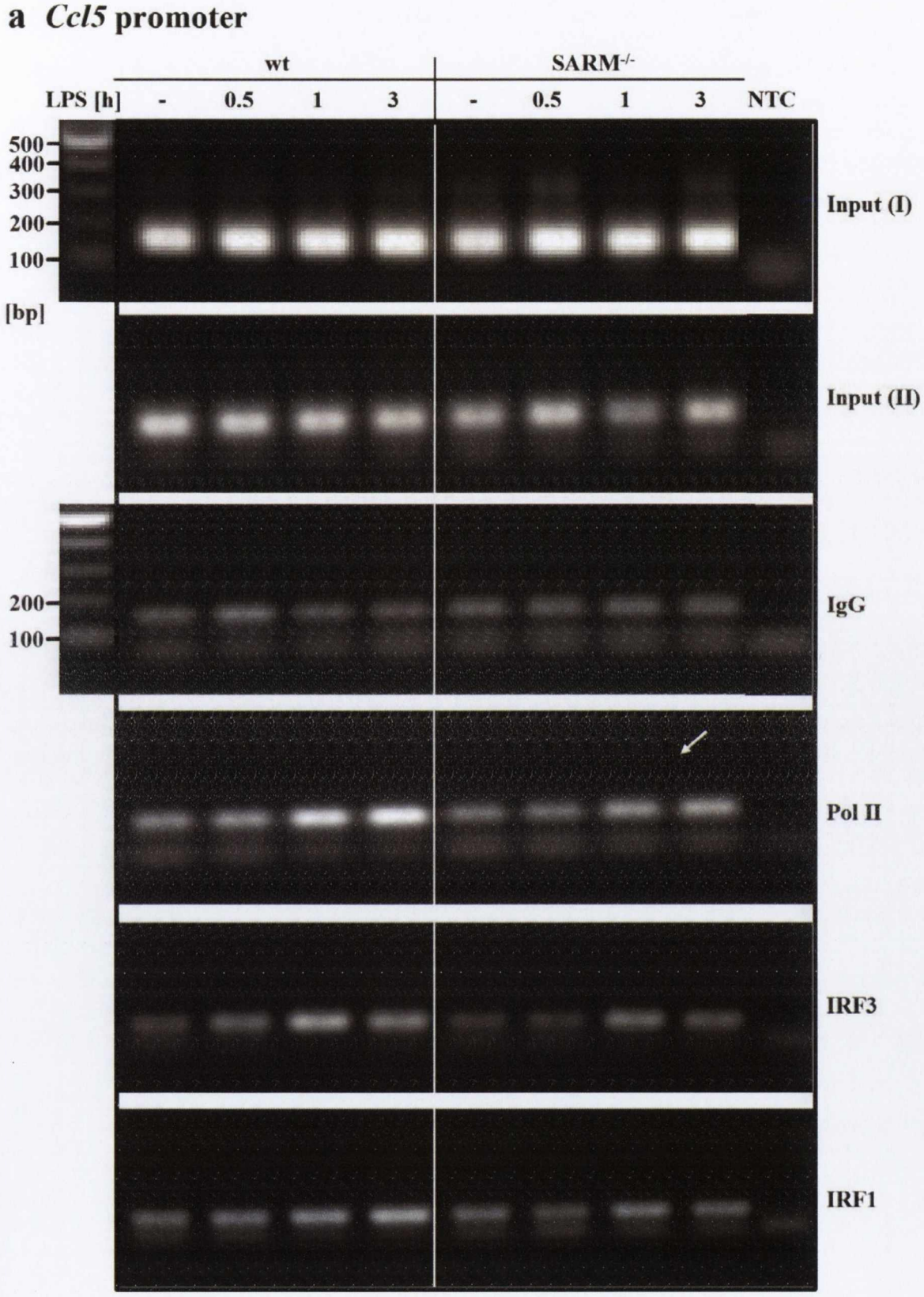


Figure 5.12: Optimisations for the Chromatin Immunoprecipitation (ChIP) assay

(a) Determining the optimal sonication conditions to achieve 200-1000bp sheared chromatin fragments required for the ChIP assay. Wt iBMDMs were seeded in 15cm dishes at $5x10^5$ cells/ml. The next day, cells were fixed and lysed at $1x10^7$ cells/ml. 2 to 10 cycles of 15x 1sec pulses, with 1min rest on ice between cycles, were applied to each 1ml lysate using a Branson Sonifier 250. The power output was 2 or 3 with 90% duty cycle. Shearing efficiency was examined on a 1% agarose gel after cross-linking was reversed, DNA isolated and treated with RNase. Optimal fragment sizes were obtained with 10 cycles at Power output 3, as indicated by the asterisk. (b) Immunoblot analysis confirmed the specific detection of RNA Polymerase II (Pol II) using the anti-Pol II antibody recommended for ChIP. Sheared chromatin lysates of wt iBMDMs stimulated for the indicated times with LPS [100ng/ml] or medium (—) and prepared as described in (a) were subjected to SDS-PAGE followed by Western Blotting using a specific Pol II antibody. Two forms of Pol II were detected, corresponding to hypo- (I) and hyper- (II) phosphoryled Pol II. Data are from one experiment representative of two. (c) Nucleotide sequence of the murine *Ccl5* promoter region (-240 to +120). Highlighted in dark grey is the pair of PCR primers designed to perform ChIP analysis. Light grey highlights part of Exon 1, with the arrow indicating the transcriptional start site (designated +1). The putative ISRE element, NF-κB element and the TATA box are indicated by the continuous, double and dotted line, respectively.


a Ccl5 promoter
wt
SARM-/-
LPS [h]
-
0.5
1
3
-
0.5
1
3
NTC
500
400
300
200
100
[bp]
Input (I)
Input (II)
200
100
IgG
Pol II
IRF3
IRF1

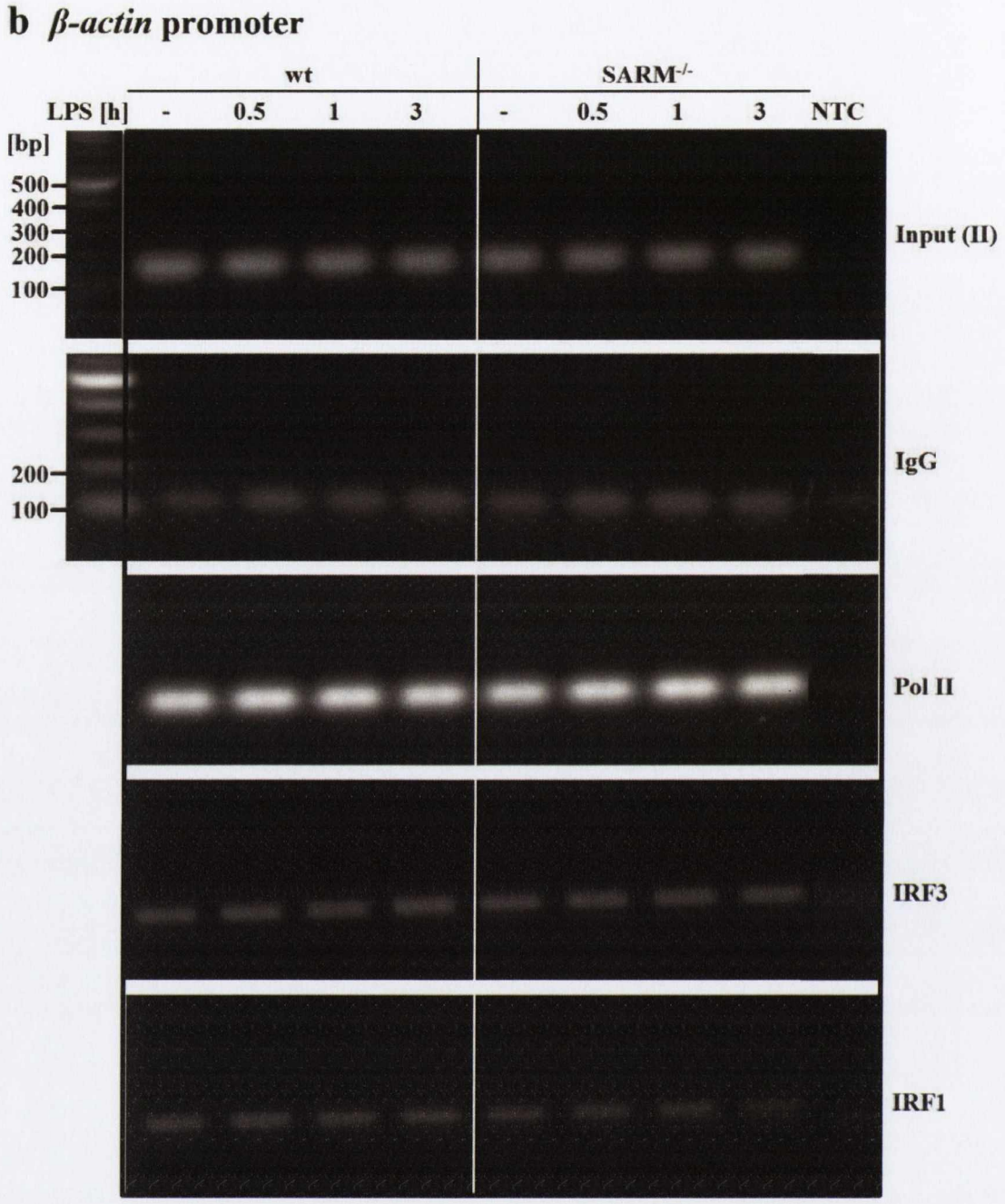


Figure 5.13: ChIP analysis of RNA Polymerase II and transcription factor binding to the *Ccl5* promoter in immortalised BMDMs in the presence and absence of SARM

Chromatin immunoprecipitation (ChIP) analysis of RNA Polymerase II (Pol II), IRF3 and IRF1 recruitment to the *Ccl5* promoter in wt and *Sarm*$^{-/-}$ iBMDMs. 2x10^{7} cells were seeded in 15cm dishes and stimulated with LPS [100ng/ml] for the indicated times or medium as control (—). Cells were fixed and the cross-linked, sheared chromatin was immunoprecipitated with specific antibodies to Pol II, IRF3 and IRF1 or an isotype-control antibody (IgG). Precipitated DNA was isolated and subjected to semi-quantitative PCR using primer pairs specific to the *Ccl5* promoter (a) or *β-actin* promoter as control (b), generating a 153bp or 112bp PCR product, respectively. Input DNA served as loading control for ChIP and was analysed in higher (I) and lower (II) concentration. The PCR analysis included a no template control (NTC) as negative control. Data are from one experiment representative of two.

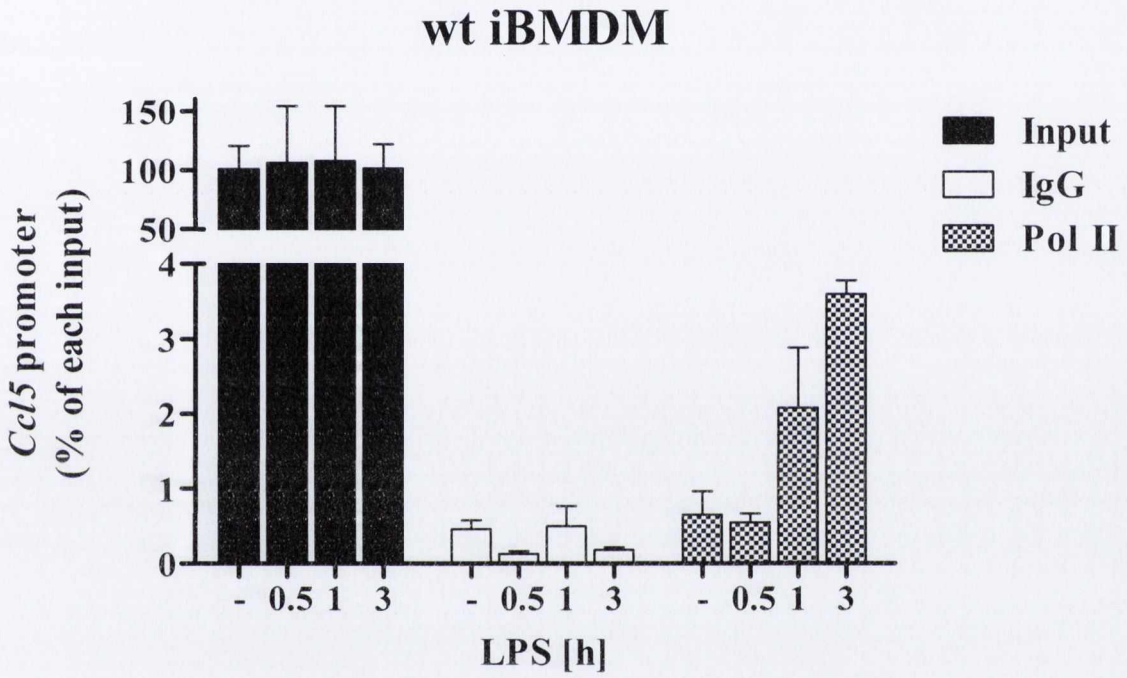


Figure 5.14: Optimisation of quantitative ChIP analysis in immortalised wt BMDMs

Quantitative ChIP analysis of RNA Polymerase II (Pol II) recruitment to the *Ccl5* promoter in wt iBMDMs using real-time PCR. $1.5x10^7$ cells were seeded in 15cm dishes and stimulated with LPS [100ng/ml] for the indicated times or medium as control (–). Cells were fixed and the cross-linked, sheared chromatin was immunoprecipitated with a specific Pol II antibody or an isotype-control antibody (IgG). Precipitated DNA was isolated and subjected to quantitative real-time PCR using primer pairs specific to the *Ccl5* promoter (indicated in Figure 5.12c). Input DNA served as loading control for ChIP. Data are presented as percentage of the level detected in each corresponding Input sample. Data are from one experiment representative of three.

6 Final discussion

Since the discovery of the TIR adaptor proteins, many of their functions in the TLR signalling pathway have been described (34). The four TIR adaptors MyD88, MAL, TRIF and TRAM are selectively involved in initiating downstream signalling from TLRs following their homotypic TIR-TIR interaction with the receptor complex. However the exact function of the fifth, most evolutionary conserved TIR adaptor SARM is still poorly understood and different roles have been assigned in the immune and nervous system; both in the lower organism *C. elegans* and in mammals (described in 1.4). Initially SARM was identified as a negative regulator of TRIF-dependent TLR pathways in human PBMCs and HEK293 cells via direct interaction with TRIF (44). However, studies on murine BMDMs from *Sarm*$^{-/-}$ mice could not confirm this TLR-regulatory role, as cells showed normal cytokine (TNF-α) and chemokine (MCP-1) expression after a range of TLR agonists (220). It was demonstrated that murine and human SARM is most abundantly expressed in the brain and only barely detectable in myeloid cells, including BMDMs. Since then several functions for SARM have been described in neurons in mediating cell death and neuronal morphology. Only one study in *Sarm*$^{-/-}$ mice addressed the immune role of SARM and revealed a requirement for SARM to restrict WNV pathogenesis (221). Here, SARM-deficiency was linked to reduced activation of CNS inflammatory cells, impaired TNF-α production and an increase in viral replication and neuronal death in the brainstem. These results were conflictive to the human data; hence the overall immune role of SARM was still enigmatic and required further investigations.

In the first part of my project, I performed expression analysis of SARM, which confirmed that SARM mRNA and protein were highly expressed in murine brain, compared to other tissues and BMDMs. Nevertheless, SARM was also detectable in human PBMCs and murine BMDMs and most interestingly, its mRNA expression was downregulated following TLR and IFN receptor stimulation. Unfortunately, I could not evaluate regulation of the protein level in more detail, as the available SARM antibodies, in particular in murine cells, nonspecifically detected another protein of the same molecular weight as SARM. Also efforts to generate our own SARM-specific antibody were not successful so far. However, in human PBMCs the SARM antibody was more reliable and studies by Carty et al. showed that PBMCs immediately increased SARM protein after TLR4 activation, which was most likely mediated by stabilisation of the

proteins N-terminus (44). This suggested that SARM protein might be regulated independently of the mRNA following immune stimulation. Overall the modulation of SARM expression was evidence for a role of SARM in immune responses in human PBMCs and murine BMDMs and indicated that its function might be controlled via its expression level.

However an immune function of SARM in murine BMDMs was questioned by Kim et al. (220). Thus I performed a detailed cytokine study in wt and *Sarm*$^{-/-}$ murine BMDMs and BMDCs, which unexpectedly revealed a crucial role of SARM in CCL5 mRNA and protein expression in macrophages. This was consistently observed in primary and immortalised BMDMs, and not as significant in BMDCs, which generally expressed much lower levels of the chemokine. Surprisingly, the regulatory function was not restricted to TRIF, the known interaction partner of SARM. In fact, all receptors tested required SARM for optimal CCL5 induction; namely the TLRs, the cytosolic RLRs and DNA sensors, as well as the PRR-independent IFNAR and IFNGR (Figure 6.1). These distinct pathways use completely unrelated adaptor proteins to mediate downstream signalling, like MyD88/TRIF, MAVS, STING and JAK-STAT molecules, respectively. Accordingly, it was unlikely that SARM mediated CCL5-regulation via the general TIR-TIR interaction mechanism. Strikingly, the expression of other genes was mostly unaffected by SARM-deficiency. Following activation of various PRRs, I observed normal mRNA induction of the NF-κB-dependent gene *Tnf-α*. Also IFN-β expression was mostly unaltered in primary *Sarm*$^{-/-}$ BMDMs, even though its transcriptional regulation was reported to be similar to CCL5, with important roles for NF-κB and IRF molecules (258, 259). Despite this similar transcription factor usage, it emerged that the regulatory mechanism between both genes differed slightly. CCL5 induction was found to be independent of IFNs and IRF7, while those in turn were required for optimal IFN-β expression. Also the kinetics of both cytokines differed, with an immediate and transient expression of IFN-β, but a delayed and consistent upregulation of CCL5. Regarding type I and type II IFN-mediated responses, SARM was dispensable for the upregulation of the ISGs IRF7, IFIT2 and viperin. Thus, the regulatory function of SARM in BMDMs was stimulus- and receptor-independent and most likely restricted to CCL5. To investigate if other genes are affected by SARM-deficiency, expression analysis on PRR-stimulated wt and SARM-deficient BMDMs are currently underway screening 100 genes simultaneously by using the NanoString Technology and the nCounter Analysis System. This will reveal if SARM selectively

regulates CCL5 or a specific set of genes with characteristic regulatory features or promoter organisation, hence specifying the subsequent mechanistic studies.

As PRR-induced type I IFNs subsequently signal via the IFNAR and upregulate ISGs in a secondary response, there was a possibility that SARM exclusively modulated the IFN-induced CCL5 expression. However I determined that PRR-induced CCL5 was directly upregulated in the primary pathway, independent of any secondary induced factors and also independent of IFN signalling and priming. Thus SARM regulated CCL5 in the context of constitutively expressed proteins. It is known that the signalling molecules, transcription factors and coactivators differ significantly between the PRR and IFN receptors. The various PRR pathways converge further downstream to activate a similar set of transcription factors, mainly AP-1, NF-κB and IRF3/7. On the contrary, gene expression of IFN receptors is mediated via STAT-containing transcriptional complexes, such as the ISGF3 complex composed of STAT1, STAT2 and IRF9 or other STAT homo- and heterodimers (Figure 6.1). Apart from CCL5, the expression of other genes analysed was unaffected, which indicated a downstream regulatory role of SARM, independent of the stimulus, the pathway and the distinct transcription factors, possibly acting at the *Ccl5* promoter level. However, as genes are selectively regulated by a specific combination of transcription factors, coactivators and chromatin modifications, there was still the possibility that SARM might act upstream and regulate the activation of a specific transcription factor or function in an alternative coactivator pathway, not required for the other genes (Figure 6.1, point 1). Subsequently, a detailed analysis revealed that SARM was dispensable for the activation of most transcription factors implicated in CCL5 induction. Those were NF-κB and IRF3 in response to TLR4, which showed normal activation and nuclear translocation in the absence of SARM. SARM-independent was also the tyrosine-phosphorylation of STAT1, which is essential for ISG expression, as well as the upregulation of IRF1 and IRF8, which were shown to play a role in IFN-γ-induced CCL5 expression. Of particular interest was the analysis of MAPK activation, as SARM functioned upstream of this evolutionary conserved cascade in *C. elegans*. Further intriguing, the MAPK pathway is stimulated by both, the PRR and IFN receptors, making it an attractive potential target of SARM for CCL5 regulation. However, SARM-deficient BMDMs showed normal activation of the three MAPKs, p38, JNK1/2 and ERK1/2. Given that none of the most relevant transcription factors for CCL5 expression were impaired in

their initial activation, it was likely that SARM controlled the proper assembly of those factors at the *Ccl5* promoter.

Ccl5 is a tightly regulated gene, and its promoter assembles into stable nucleosomes in the basal state preventing any transcriptional leakage (246). Thus the initiation of transcription requires several consecutive events, where transcription factor binding to the DNA leads to the recruitment of various proteins, initiating chromatin remodelling by the SWI/SNF complex and the formation of the transcriptional machinery, that includes RNA Polymerase II (Pol II). This complex regulation was also highlighted by the observed delay in TLR4-induced CCL5 expression in comparison to the immediate-early expression of genes, such as *Tnf-α* and *Ifn-β*. TNF-α belonged to a group of primary response genes (PRGs) that have Pol II preloaded at their promoter, but stalled by the negative elongation factor (NELF) complex (299). In contrast, Pol II and NELF are absent from the *Ccl5* promoter in resting cells, and LPS-dependent Pol II recruitment is regarded as the rate-limiting step in *Ccl5* transcription. Thus, as a hallmark of prior transcription factor binding, I assessed LPS-induced Pol II accumulation at the *Ccl5* promoter, which was slightly reduced in iBMDMs in the absence of SARM, suggesting a defect in one of the previous events required for Pol II recruitment. Referring to the literature, IRF molecules are key activators of CCL5 expression and IRF3 was demonstrated to play an essential role in chromatin remodelling at the *Ccl5* promoter (246). However, LPS-stimulated binding of IRF3 and IRF1 to the *Ccl5* promoter was mostly intact in SARM-deficient iBMDMs. Next, more quantitative experiments are required to exactly define the role of SARM in protein assembly at the *Ccl5* promoter (Figure 6.1, point 2), which will be addressed using the successfully established ChIP protocol for quantitative real-time PCR detection. At present, there is still a possibility that the slightly impaired Pol II recruitment in *Sarm*$^{-/-}$ cells was caused by an unequal loading of DNA Input in the ChIP assay, which was difficult to assess using the semi-quantitative read-out. Also ChIP and overexpressed Flag-tagged SARM will be used to directly assess the recruitment of SARM to the endogenous *Ccl5* promoter. In addition, SARM-mediated regulation of the *Ccl5* promoter will be investigated using the *Ccl5* luciferase reporter gene constructs established during the course of this study. These future experiments will distinguish, if SARM regulates a step prior to transcriptional initiation or if it controlled *Ccl5* mRNA expression at a later stage, such as transcriptional elongation, precursor (pre)-mRNA processing and maturation or mRNA stability (Figure 6.1, point 3 and 4), all processes are highly controlled by

multiprotein complexes. A role for SARM in *Ccl5* pre-mRNA processing can be evaluated by comparing the expression of precursor transcripts to mature, spliced mRNA using primer pairs specific to intron-exon or exon-exon sequences, respectively. According to the current model, transcriptional elongation and splicing are tightly coupled in both directions, meaning that the Pol II elongation complex recruits the splicing machinery, but also that pre-mRNAs are not synthesised unless the machinery for its processing is properly assembled (300). This may suggest that *Ccl5* precursor transcripts are difficult to detect. However, it was recently proposed by Baltimore et al. that late cytokine mRNA expression is controlled by a delay in splicing (301), thus *Ccl5* pre-mRNA might be induced and accumulate immediately after stimulation. If analysis will reveal SARM-independent Pol II recruitment, but a dependency for *Ccl5* pre-mRNA production, SARM might act at the level of transcriptional initiation to elongation. This could be examined by ChIP analysis measuring the presence of Serine 2-phosphorylated Pol II at the 3'end of the *Ccl5* gene, which is a hallmark of productive elongation.

In light of these potential functions of SARM in transcriptional regulation and RNA biogenesis it is interesting that SARM was recently found to interact with family members of the DExD/H-box RNA helicases, namely DDX3, DDX5, DDX17 and DHX9 (M. Carty personal communication). DEAD/DEAH-box proteins (DDX, DHX) are implicated in all aspects of RNA metabolism, from transcription to translation and mRNA decay (302). They mediate RNA unwinding via a helicase core with ATP- and RNA-binding sites, and additionally perform helicase-independent activities and modulate various RNA-protein interactions. It emerged more recently, that TIR proteins have the potential to interact with DExD/H-box proteins, besides their well known homotypic TIR-TIR interaction, whereby they perform functions also in TLR-independent pathways. This has been reported so far for a subset of DDXs implicated in cytosolic RNA and DNA sensing, like the TRIF interaction of the DDX1-DDX21-DHX36 complex or the MyD88-binding to DHX9/DHX36 ((132, 146), see 1.2.3, 1.2.4). The SARM interaction with DDX5 and DDX17 was particular intriguing as both proteins have been shown to function as transcriptional coactivators and were also part of the splicing machinery (303). Hence their adaptor functions were consistent with a model, where transcriptional initiation and splicing are closely coupled. DDX5/17 regulated the transcription factors ERα, p53, MyoD and Runx2, and they were also recruited to their target promoters. DDX5 also interacted with CBP, p300 and Pol II (304). Further, DDX5/17 and recently DHX9 were found in a

complex with Drosha regulating the processing of a selective set of microRNAs (miRNAs) (305, 306). miRNAs control gene expression by targeting specific mRNAs to mediate their degradation or translational repression. Interestingly, preliminary data by M. Carty from my laboratory indicated a potential SARM-Drosha interaction and also SARM-dependent expression of some miRNAs, which is currently further investigated. Thus, it is possible that SARM promoted *Ccl5* gene expression via modulation of distinct miRNAs. Besides miRNAs, the abundance of mRNAs is also regulated by mRNA stability, usually mediated via destabilising proteins that bind to AU-rich elements (ARE) in the 3'UTR of the mRNA. However, *Ccl5* mRNA was shown to be devoid of those elements, was very stable and accumulated even hours after stimulation (256). This was in agreement with my own preliminary data on *Ccl5* mRNA stability (data not shown) and suggested that *Ccl5* mRNA expression is mainly controlled by its initial transcriptional induction and sustained promoter activity. However, another study demonstrated that *Ccl5* mRNA was stabilised during replication-competent RSV infection by an unknown mechanism involving nucleotides 11-389 of the *Ccl5* gene (307). Thus, it is tempting to speculate that the generally observed stability of *Ccl5* mRNA might be mediated by a new, ARE-independent mechanism involving SARM. Given that *Ccl5* mRNA expression was affected, it is unlikely that SARM regulated the translational step of gene expression (Figure 6.1, point 5). However, it can not be excluded that SARM might additionally slightly enhance the translational machinery, as evident from data on TNF-α expression. Future analysis will exactly define if SARM positively regulated the transcriptional or posttranscriptional step of *Ccl5* gene expression and if DDXs were involved in the regulatory process.

At first, the discovered positive role of murine SARM in CCL5 expression was unexpected due to the previously described inhibitory functions of various SARM homologues in overexpression systems and siRNA-mediated knockdown studies. However, there is compelling evidence, also from an evolutionary perspective, that SARM was essential for optimal immune responses, which might highly depend on the specific cell type and environment. Accordingly, SARM was required for immune defence in *C. elegans* and WNV-infected mice in vivo (described in detail in 1.4). I propose that SARM function, either positive or negative, might be adjusted via its expression level, firstly because endogenous SARM levels were highly modulated following immune stimulation, and secondly because the inhibitory role was mainly observed, when SARM was

overexpressed. Also interesting was that the CCL5-regulatory role of SARM was not restricted to TLRs, similar to the positive, non-TLR immune function in *C. elegans*, and therefore might represent the evolutionary conserved immune function of SARM.

CCL5, a member of the C-C chemokine family, is an important mediator of inflammatory processes and implicated in many aspects of the innate and adaptive immune response, as its chemotactic activity leads to the recruitment of various immune cells, including monocytes, eosinophiles, basophiles, NK cells and T lymphocytes. Therefore, it is highly relevant to elucidate the exact mechanism of CCL5 regulation in macrophages, also in light of inflammatory diseases and cancer. CCL5 also plays a particular role during HIV-infection, as its receptor CCR5 serves as binding and entry site for macrophage-tropic HIV (R5 virus) (308, 309). CCL5 was first charcterised in T lymphocytes, where it is expressed 3-5 days after activation, hence it is also termed RANTES (regulated upon activation, normal T cell expressed and secreted). Responsible for the controlled late expression of CCL5 in T cells is the simultaneous translational induction of the transcriptional regulator Krüppel-like factor 13 (KLF13/RFLAT-1) (296, 310). KLF13 forms an enhanceosome with NF-κB and AP-1 at the *Ccl5* promoter and induces chromatin remodelling by recruiting various factors (311), but it is thought that the KLF13-dependent CCL5 regulation is restricted to T cells. Nevertheless it would be worth investigating if KLF13 plays a role in CCL5 induction in macrophages or vice versa if SARM is required for CCL5 expression in T cells, given that SARM is expressed in this cell type ((220) and data not shown). Interestingly, a microRNA that was found to be enhanced in *Sarm*$^{-/-}$ BMDMs, namely miR-125b (M. Carty, personal communication), was reported to potentially target KLF13 (312). And according to bioinformatic analysis by M. Carty miR-125b might also target SARM, which emphasises a putative function of both molecules in the same regulatory network.

In light of the abundant expression of SARM in the brain, I suspect that the SARM-mediated regulation of CCL5 is likely to be highly important for various immune responses of the central nervous system (CNS). It is well established that during infection with neurotropic viruses resident immune cells of the brain, such as microglia and astrocytes, secrete chemokines, including CCL5, to initiate leukocyte trafficking into the CNS (313). CCL5 and one of its receptors, CCR5, were shown to be particularly important for cell infiltration and subsequent control of WNV, which was also evident in patients with CCR5-deficiency and their increased risk of symptomatic WNV infection (314). In

this regard it is compelling that *Sarm*$^{-/-}$ mice also showed increased pathogenesis and enhanced mortality following infection with neurotropic WNV (221). It was stated that the phenotype was caused by decreased microglia activation, reduced TNF-α production and an increase in neuronal cell death. Although CCL5 was not analysed in this study, I speculate that a defect in CCL5 production in the absence of SARM might have contributed to the inability to control the infection. Furthermore, CCL5 has been implicated in pathogenesis of the autoimmune disease multiple sclerosis (MS), which is characterised by inflammatory lesions, demyelination and axonal loss in the CNS, mediated by recruited autoreactive T cells and innate immune cells (315, 316). CCL5 was also shown to participate in the pathophysiology of experimental autoimmune encephalomyelitis (EAE), which is the murine disease model for MS (317). It would be interesting to investigate the CCL5-regulatory role of SARM in various neuropathogenic disease models, such as EAE or pathogenic infection models, using SARM-deficient mice. The fact that CCL5 plays crucial roles in many physiological and pathological processes highlights the importance of elucidating the exact mechanism of CCL5 regulation. And if SARM selectively regulates its expression, SARM might become a potential target of new therapies.

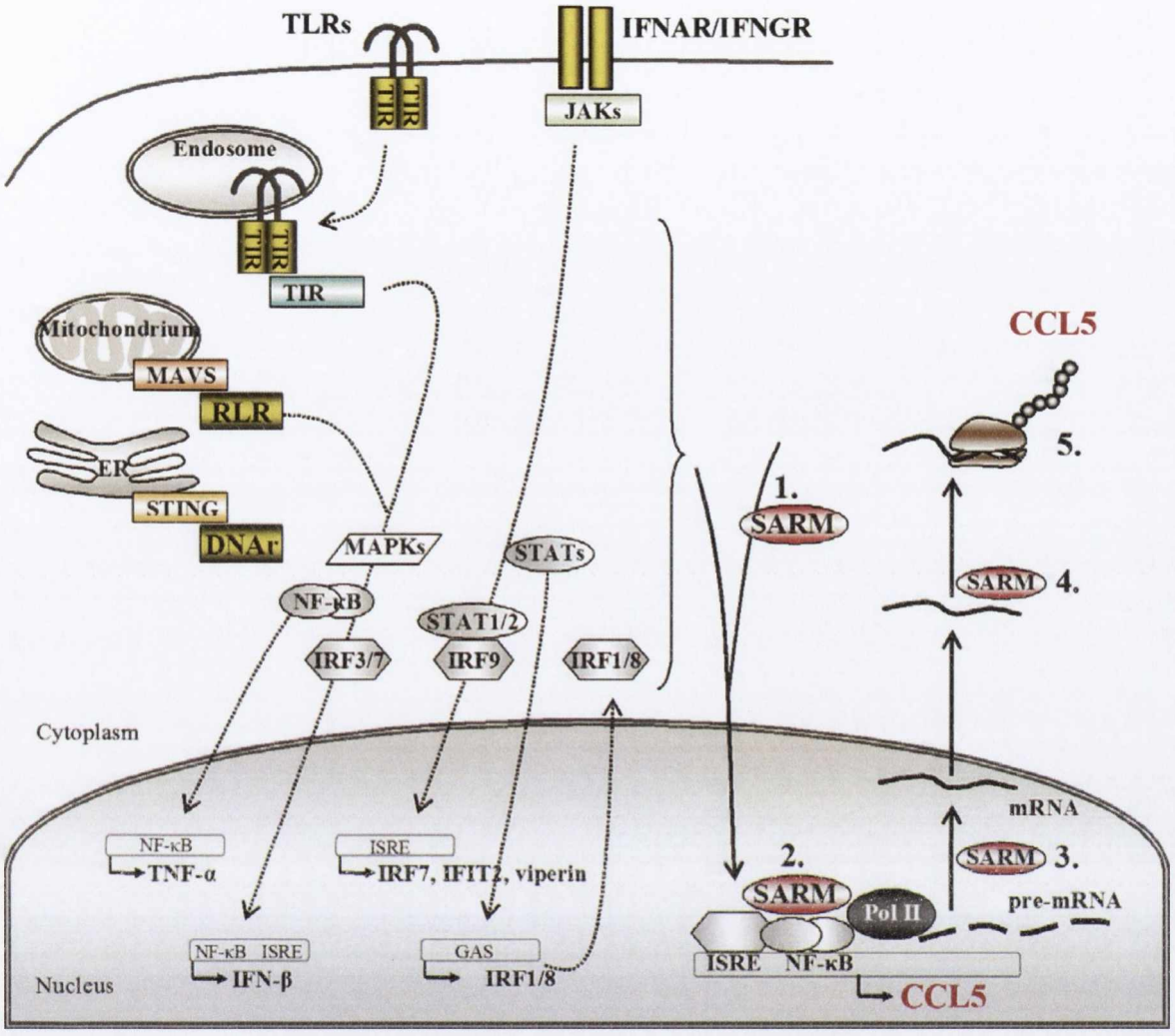


Figure 6.1: Potential mechanisms of SARM-mediated CCL5 regulation in BMDMs

Schematic of the CCL5-regulatory immune function of SARM in primary and immortalised BMDMs and illustration of the potential mechanism. SARM was required for CCL5 mRNA and protein expression downstream of TLRs and non-TLRs, including cytosolic RNA- and DNA sensors, as well as the type I and II IFN receptors. Following ligand binding, the various receptors engage with their specific adaptor proteins, namely TIR adaptors, MAVS, STING and JAKs, respectively, to initiate a signalling cascade leading to activation of distinct transcription factors and selective gene induction. SARM was found to be dispensable for the main activation events as follows: TLR4-induced activation of MAPKs and the transcription factors NF-κB and IRF3, IFNAR/IFNGR-mediated tyrosine 701-phosphorylation of STAT1 and the upregulation of the transcription factors IRF1 and IRF8. Accordingly the expression of most genes was unaffected by SARM-deficiency, such as PRR-induced TNF-α and IFN-β or the IFN-induced ISGs IRF7, IFIT2 and viperin. Thus SARM-mediated regulation was likely restricted to CCL5 with several possibilities of the mechanism: 1. SARM might function in a pathway common to both PRR and IFN receptors to activate a specific transcription factor or coactivator, 2. SARM might act at the *Ccl5* promoter to mediate transcriptional initiation via the assembly of activators, chromatin remodelling and Pol II recruitment, 3. SARM might be involved in the RNA maturation process, 4. SARM might stabilise *Ccl5* mRNA directly or by suppressing the production of specific miRNAs. However SARM is unlikely to function solely at the translational step (5.).

V. Acknowledgements

Firstly, I would like to thank my supervisor Prof. Andrew Bowie for offering this challenging project. I express my deep gratitude for your extensive support, encouragement and invaluable guidance during the planning and development of this work. Your enthusiasm was truly infectious and created a fantastic work environment. I couldn't have asked for any better.

I would also like to thank my cosupervisor Dr. Ed Lavelle and his group for the support during my rotation project in his lab, where I performed part of the dendritic cell and murine tissue studies. Also I am grateful for the fantastic collaboration with Prof. Aihao Ding (Weill Cornell Medical College, USA) and Dr. K. Fitzgerald (UMass, USA) for kindly providing the murine material for the studies in primary wild-type and SARM-deficient cells.

I am particularly thankful for the enormous help and advice given by Michael Carty. Your patience during my first year of the PhD is greatly appreciated and it was good to share the life of SARM with you in many discussions.
A huge thank you to all the past and current members of the Bowie lab for their constant help and support at all times, their brilliant suggestions during the lab meetings and for making the lab such an enjoyable place to work in -thanks Leonie, Julianne, Sinead K, Sinead F, Marcin, Alan, Tatyana, Orla, Geraldine & Laura.
Many thanks to all other friends of the department for being there for me and for the good times we had over the last four years.

I would also like to extend my thanks to Liam and Noel for their technical support, to Barry and Gavin at the FACS and confocal and to our secretaries Mary Pat and Miriam for keeping the school running.
Also I would like to thank Prof. Paul Moynagh, the director of the HRB PhD scholars programme in Immunology, for the possibility of participating in the very supportive PhD programme and I thank all HRB members for their valuable feedback during the research meetings.

Finally, I wish to thank my family and friends back home for their constant support: Mama und Papa, ich hoffe es ist euch bewusst, dass es euer Rückhalt ist, der mir die Kraft gibt meine Ziele zu erreichen. Ihr wart immer für mich da und habt meine Entscheidungen unterstützt, dafür bin ich euch endlos dankbar. Ich erinnere mich noch genau an den Moment, an dem ich euch aus Heidelberg anrief und euch von meinen Irlandplänen berichtete -und an die kurze Pause am Telefon. Mathias, ich bin ziemlich happy so einen Bruder wie dich zu haben und die Möglichkeit jederzeit bei euch aufschlagen zu können war super. Und natürlich möchte ich dir Amin dafür danken, dass du da bist und diese anstrengende Zeit der Entfernung mit mir durchgestanden hast. Du bist ein wichtiger Teil in meinem Leben geworden und ich freue mich so auf die kommende gemeinsame Zeit am gleichen Fleck!

Auch bin ich sehr froh solch guten Freunde zuhause zu haben. Dani, Mela & Lisa ich danke euch für eure Besuche und das wir uns nicht verloren haben während meiner Zeit in Dublin. Besonderer Dank geht an meine Schnecke Kiri, die es nun schon 28 Jahre mit mir aushält.

Ohne euch alle wäre dies nicht möglich gewesen, ihr seid die Besten!

This work was funded by the Health Research Board in Ireland under Grant No. PhD/ 20007/9.

VI. References

1. Janeway, C. A., Jr., and R. Medzhitov. 2002. Innate immune recognition. *Annu Rev Immunol* 20:197-216.
2. Moser, M., and O. Leo. 2010. Key concepts in immunology. *Vaccine* 28 Suppl 3:C2-13.
3. Janeway, C. A., Jr. 1989. Approaching the asymptote? Evolution and revolution in immunology. *Cold Spring Harb Symp Quant Biol* 54 Pt 1:1-13.
4. Iwasaki, A., and R. Medzhitov. 2010. Regulation of adaptive immunity by the innate immune system. *Science* 327:291-295.
5. Blander, J. M., and L. E. Sander. 2012. Beyond pattern recognition: five immune checkpoints for scaling the microbial threat. *Nat Rev Immunol* 12:215-225.
6. O'Leary, J. G., M. Goodarzi, D. L. Drayton, and U. H. von Andrian. 2006. T cell- and B cell-independent adaptive immunity mediated by natural killer cells. *Nat Immunol* 7:507-516.
7. Sun, J. C., J. N. Beilke, and L. L. Lanier. 2009. Adaptive immune features of natural killer cells. *Nature* 457:557-561.
8. Lemaitre, B., E. Nicolas, L. Michaut, J. M. Reichhart, and J. A. Hoffmann. 1996. The dorsoventral regulatory gene cassette spatzle/Toll/cactus controls the potent antifungal response in Drosophila adults. *Cell* 86:973-983.
9. Medzhitov, R., P. Preston-Hurlburt, and C. A. Janeway, Jr. 1997. A human homologue of the Drosophila Toll protein signals activation of adaptive immunity. *Nature* 388:394-397.
10. Hasan, U., C. Chaffois, C. Gaillard, V. Saulnier, E. Merck, S. Tancredi, C. Guiet, F. Briere, J. Vlach, S. Lebecque, G. Trinchieri, and E. E. Bates. 2005. Human TLR10 is a functional receptor, expressed by B cells and plasmacytoid dendritic cells, which activates gene transcription through MyD88. *J Immunol* 174:2942-2950.
11. Bell, J. K., G. E. Mullen, C. A. Leifer, A. Mazzoni, D. R. Davies, and D. M. Segal. 2003. Leucine-rich repeats and pathogen recognition in Toll-like receptors. *Trends Immunol* 24:528-533.
12. Botos, I., D. M. Segal, and D. R. Davies. 2011. The structural biology of Toll-like receptors. *Structure* 19:447-459.
13. Barbalat, R., S. E. Ewald, M. L. Mouchess, and G. M. Barton. 2011. Nucleic acid recognition by the innate immune system. *Annu Rev Immunol* 29:185-214.
14. Kim, Y. M., M. M. Brinkmann, M. E. Paquet, and H. L. Ploegh. 2008. UNC93B1 delivers nucleotide-sensing toll-like receptors to endolysosomes. *Nature* 452:234-238.
15. Shi, Z., Z. Cai, A. Sanchez, T. Zhang, S. Wen, J. Wang, J. Yang, S. Fu, and D. Zhang. 2011. A novel Toll-like receptor that recognizes vesicular stomatitis virus. *J Biol Chem* 286:4517-4524.
16. Pifer, R., A. Benson, C. R. Sturge, and F. Yarovinsky. 2010. UNC93B1 is essential for TLR11 activation and IL-12-dependent host resistance to Toxoplasma gondii. *J Biol Chem* 286:3307-3314.
17. Takahashi, K., T. Shibata, S. Akashi-Takamura, T. Kiyokawa, Y. Wakabayashi, N. Tanimura, T. Kobayashi, F. Matsumoto, R. Fukui, T. Kouro, Y. Nagai, K. Takatsu, S. Saitoh, and K. Miyake. 2007. A protein associated with Toll-like receptor (TLR) 4 (PRAT4A) is required for TLR-dependent immune responses. *J Exp Med* 204:2963-2976.

18. Yang, Y., B. Liu, J. Dai, P. K. Srivastava, D. J. Zammit, L. Lefrancois, and Z. Li. 2007. Heat shock protein gp96 is a master chaperone for toll-like receptors and is important in the innate function of macrophages. *Immunity* 26:215-226.
19. Park, B., M. M. Brinkmann, E. Spooner, C. C. Lee, Y. M. Kim, and H. L. Ploegh. 2008. Proteolytic cleavage in an endolysosomal compartment is required for activation of Toll-like receptor 9. *Nat Immunol* 9:1407-1414.
20. Beutler, B., and E. T. Rietschel. 2003. Innate immune sensing and its roots: the story of endotoxin. *Nat Rev Immunol* 3:169-176.
21. Akashi-Takamura, S., and K. Miyake. 2008. TLR accessory molecules. *Curr Opin Immunol* 20:420-425.
22. Hoebe, K., P. Georgel, S. Rutschmann, X. Du, S. Mudd, K. Crozat, S. Sovath, L. Shamel, T. Hartung, U. Zahringer, and B. Beutler. 2005. CD36 is a sensor of diacylglycerides. *Nature* 433:523-527.
23. Nilsen, N. J., S. Deininger, U. Nonstad, F. Skjeldal, H. Husebye, D. Rodionov, S. von Aulock, T. Hartung, E. Lien, O. Bakke, and T. Espevik. 2008. Cellular trafficking of lipoteichoic acid and Toll-like receptor 2 in relation to signaling: role of CD14 and CD36. *J Leukoc Biol* 84:280-291.
24. Uematsu, S., K. Fujimoto, M. H. Jang, B. G. Yang, Y. J. Jung, M. Nishiyama, S. Sato, T. Tsujimura, M. Yamamoto, Y. Yokota, H. Kiyono, M. Miyasaka, K. J. Ishii, and S. Akira. 2008. Regulation of humoral and cellular gut immunity by lamina propria dendritic cells expressing Toll-like receptor 5. *Nat Immunol* 9:769-776.
25. Botos, I., L. Liu, Y. Wang, D. M. Segal, and D. R. Davies. 2009. The toll-like receptor 3:dsRNA signaling complex. *Biochim Biophys Acta* 1789:667-674.
26. Heil, F., H. Hemmi, H. Hochrein, F. Ampenberger, C. Kirschning, S. Akira, G. Lipford, H. Wagner, and S. Bauer. 2004. Species-specific recognition of single-stranded RNA via toll-like receptor 7 and 8. *Science* 303:1526-1529.
27. Gorden, K. K., X. X. Qiu, C. C. Binsfeld, J. P. Vasilakos, and S. S. Alkan. 2006. Cutting edge: activation of murine TLR8 by a combination of imidazoquinoline immune response modifiers and polyT oligodeoxynucleotides. *J Immunol* 177:6584-6587.
28. Hemmi, H., O. Takeuchi, T. Kawai, T. Kaisho, S. Sato, H. Sanjo, M. Matsumoto, K. Hoshino, H. Wagner, K. Takeda, and S. Akira. 2000. A Toll-like receptor recognizes bacterial DNA. *Nature* 408:740-745.
29. Guan, Y., D. R. Ranoa, S. Jiang, S. K. Mutha, X. Li, J. Baudry, and R. I. Tapping. 2010. Human TLRs 10 and 1 share common mechanisms of innate immune sensing but not signaling. *J Immunol* 184:5094-5103.
30. Yarovinsky, F., D. Zhang, J. F. Andersen, G. L. Bannenberg, C. N. Serhan, M. S. Hayden, S. Hieny, F. S. Sutterwala, R. A. Flavell, S. Ghosh, and A. Sher. 2005. TLR11 activation of dendritic cells by a protozoan profilin-like protein. *Science* 308:1626-1629.
31. Hidmark, A., A. von Saint Paul, and A. H. Dalpke. 2012. Cutting Edge: TLR13 Is a Receptor for Bacterial RNA. *J Immunol* 189:2717-2721.
32. Oldenburg, M., A. Kruger, R. Ferstl, A. Kaufmann, G. Nees, A. Sigmund, B. Bathke, H. Lauterbach, M. Suter, S. Dreher, U. Koedel, S. Akira, T. Kawai, J. Buer, H. Wagner, S. Bauer, H. Hochrein, and C. J. Kirschning. 2012. TLR13 recognizes bacterial 23S rRNA devoid of erythromycin resistance-forming modification. *Science* 337:1111-1115.
33. Kumar, H., T. Kawai, and S. Akira. 2009. Toll-like receptors and innate immunity. *Biochem Biophys Res Commun* 388:621-625.

34. O'Neill, L. A., and A. G. Bowie. 2007. The family of five: TIR-domain-containing adaptors in Toll-like receptor signalling. *Nat Rev Immunol* 7:353-364.
35. Yamamoto, M., S. Sato, H. Hemmi, K. Hoshino, T. Kaisho, H. Sanjo, O. Takeuchi, M. Sugiyama, M. Okabe, K. Takeda, and S. Akira. 2003. Role of adaptor TRIF in the MyD88-independent toll-like receptor signaling pathway. *Science* 301:640-643.
36. Kagan, J. C., and R. Medzhitov. 2006. Phosphoinositide-mediated adaptor recruitment controls Toll-like receptor signaling. *Cell* 125:943-955.
37. Rowe, D. C., A. F. McGettrick, E. Latz, B. G. Monks, N. J. Gay, M. Yamamoto, S. Akira, L. A. O'Neill, K. A. Fitzgerald, and D. T. Golenbock. 2006. The myristoylation of TRIF-related adaptor molecule is essential for Toll-like receptor 4 signal transduction. *Proc Natl Acad Sci U S A* 103:6299-6304.
38. Kagan, J. C., T. Su, T. Horng, A. Chow, S. Akira, and R. Medzhitov. 2008. TRAM couples endocytosis of Toll-like receptor 4 to the induction of interferon-beta. *Nat Immunol* 9:361-368.
39. Gray, P., A. Dunne, C. Brikos, C. A. Jefferies, S. L. Doyle, and L. A. O'Neill. 2006. MyD88 adapter-like (Mal) is phosphorylated by Bruton's tyrosine kinase during TLR2 and TLR4 signal transduction. *J Biol Chem* 281:10489-10495.
40. Mansell, A., R. Smith, S. L. Doyle, P. Gray, J. E. Fenner, P. J. Crack, S. E. Nicholson, D. J. Hilton, L. A. O'Neill, and P. J. Hertzog. 2006. Suppressor of cytokine signaling 1 negatively regulates Toll-like receptor signaling by mediating Mal degradation. *Nat Immunol* 7:148-155.
41. Dunne, A., S. Carpenter, C. Brikos, P. Gray, A. Strelow, H. Wesche, N. Morrice, and L. A. O'Neill. 2010. IRAK1 and IRAK4 promote phosphorylation, ubiquitination, and degradation of MyD88 adaptor-like (Mal). *J Biol Chem* 285:18276-18282.
42. McGettrick, A. F., E. K. Brint, E. M. Palsson-McDermott, D. C. Rowe, D. T. Golenbock, N. J. Gay, K. A. Fitzgerald, and L. A. O'Neill. 2006. Trif-related adapter molecule is phosphorylated by PKC{epsilon} during Toll-like receptor 4 signaling. *Proc Natl Acad Sci U S A* 103:9196-9201.
43. Liberati, N. T., K. A. Fitzgerald, D. H. Kim, R. Feinbaum, D. T. Golenbock, and F. M. Ausubel. 2004. Requirement for a conserved Toll/interleukin-1 resistance domain protein in the Caenorhabditis elegans immune response. *Proc Natl Acad Sci U S A* 101:6593-6598.
44. Carty, M., R. Goodbody, M. Schroder, J. Stack, P. N. Moynagh, and A. G. Bowie. 2006. The human adaptor SARM negatively regulates adaptor protein TRIF-dependent Toll-like receptor signaling. *Nat Immunol* 7:1074-1081.
45. Martin, M. U., and H. Wesche. 2002. Summary and comparison of the signaling mechanisms of the Toll/interleukin-1 receptor family. *Biochim Biophys Acta* 1592:265-280.
46. Lin, S. C., Y. C. Lo, and H. Wu. 2010. Helical assembly in the MyD88-IRAK4-IRAK2 complex in TLR/IL-1R signalling. *Nature* 465:885-890.
47. George, J., P. G. Motshwene, H. Wang, A. V. Kubarenko, A. Rautanen, T. C. Mills, A. V. Hill, N. J. Gay, and A. N. Weber. 2011. Two human MYD88 variants, S34Y and R98C, interfere with MyD88-IRAK4-myddosome assembly. *J Biol Chem* 286:1341-1353.
48. Suzuki, N., S. Suzuki, G. S. Duncan, D. G. Millar, T. Wada, C. Mirtsos, H. Takada, A. Wakeham, A. Itie, S. Li, J. M. Penninger, H. Wesche, P. S. Ohashi, T. W. Mak, and W. C. Yeh. 2002. Severe impairment of interleukin-1 and Toll-like receptor signalling in mice lacking IRAK-4. *Nature* 416:750-756.
49. Flannery, S., and A. G. Bowie. 2010. The interleukin-1 receptor-associated kinases: critical regulators of innate immune signalling. *Biochem Pharmacol* 80:1981-1991.

50. Butler, M. P., J. A. Hanly, and P. N. Moynagh. 2007. Kinase-active interleukin-1 receptor-associated kinases promote polyubiquitination and degradation of the Pellino family: direct evidence for PELLINO proteins being ubiquitin-protein isopeptide ligases. *J Biol Chem* 282:29729-29737.
51. Keating, S. E., G. M. Maloney, E. M. Moran, and A. G. Bowie. 2007. IRAK-2 participates in multiple toll-like receptor signaling pathways to NFkappaB via activation of TRAF6 ubiquitination. *J Biol Chem* 282:33435-33443.
52. Maloney, G., M. Schroder, and A. G. Bowie. 2005. Vaccinia virus protein A52R activates p38 mitogen-activated protein kinase and potentiates lipopolysaccharide-induced interleukin-10. *J Biol Chem* 280:30838-30844.
53. Flannery, S. M., S. E. Keating, J. Szymak, and A. G. Bowie. 2011. Human Interleukin-1 Receptor-associated Kinase-2 Is Essential for Toll-like Receptor-mediated Transcriptional and Post-transcriptional Regulation of Tumor Necrosis Factor {alpha}. *J Biol Chem* 286:23688-23697.
54. Deng, L., C. Wang, E. Spencer, L. Yang, A. Braun, J. You, C. Slaughter, C. Pickart, and Z. J. Chen. 2000. Activation of the IkappaB kinase complex by TRAF6 requires a dimeric ubiquitin-conjugating enzyme complex and a unique polyubiquitin chain. *Cell* 103:351-361.
55. Kanayama, A., R. B. Seth, L. Sun, C. K. Ea, M. Hong, A. Shaito, Y. H. Chiu, L. Deng, and Z. J. Chen. 2004. TAB2 and TAB3 activate the NF-kappaB pathway through binding to polyubiquitin chains. *Mol Cell* 15:535-548.
56. Xia, Z. P., L. Sun, X. Chen, G. Pineda, X. Jiang, A. Adhikari, W. Zeng, and Z. J. Chen. 2009. Direct activation of protein kinases by unanchored polyubiquitin chains. *Nature* 461:114-119.
57. Wang, C., L. Deng, M. Hong, G. R. Akkaraju, J. Inoue, and Z. J. Chen. 2001. TAK1 is a ubiquitin-dependent kinase of MKK and IKK. *Nature* 412:346-351.
58. Yi, A. K., and A. M. Krieg. 1998. CpG DNA rescue from anti-IgM-induced WEHI-231 B lymphoma apoptosis via modulation of I kappa B alpha and I kappa B beta and sustained activation of nuclear factor-kappa B/c-Rel. *J Immunol* 160:1240-1245.
59. Beinke, S., M. J. Robinson, M. Hugunin, and S. C. Ley. 2004. Lipopolysaccharide activation of the TPL-2/MEK/extracellular signal-regulated kinase mitogen-activated protein kinase cascade is regulated by IkappaB kinase-induced proteolysis of NF-kappaB1 p105. *Mol Cell Biol* 24:9658-9667.
60. Dong, C., R. J. Davis, and R. A. Flavell. 2002. MAP kinases in the immune response. *Annu Rev Immunol* 20:55-72.
61. Hoshino, K., T. Sugiyama, M. Matsumoto, T. Tanaka, M. Saito, H. Hemmi, O. Ohara, S. Akira, and T. Kaisho. 2006. IkappaB kinase-alpha is critical for interferon-alpha production induced by Toll-like receptors 7 and 9. *Nature* 440:949-953.
62. Kawai, T., S. Sato, K. J. Ishii, C. Coban, H. Hemmi, M. Yamamoto, K. Terai, M. Matsuda, J. Inoue, S. Uematsu, O. Takeuchi, and S. Akira. 2004. Interferon-alpha induction through Toll-like receptors involves a direct interaction of IRF7 with MyD88 and TRAF6. *Nat Immunol* 5:1061-1068.
63. Uematsu, S., S. Sato, M. Yamamoto, T. Hirotani, H. Kato, F. Takeshita, M. Matsuda, C. Coban, K. J. Ishii, T. Kawai, O. Takeuchi, and S. Akira. 2005. Interleukin-1 receptor-associated kinase-1 plays an essential role for Toll-like receptor (TLR)7- and TLR9-mediated interferon-{alpha} induction. *J Exp Med* 201:915-923.
64. Takaoka, A., H. Yanai, S. Kondo, G. Duncan, H. Negishi, T. Mizutani, S. Kano, K. Honda, Y. Ohba, T. W. Mak, and T. Taniguchi. 2005. Integral role of IRF-5 in the gene induction programme activated by Toll-like receptors. *Nature* 434:243-249.

65. Meylan, E., K. Burns, K. Hofmann, V. Blancheteau, F. Martinon, M. Kelliher, and J. Tschopp. 2004. RIP1 is an essential mediator of Toll-like receptor 3-induced NF-kappa B activation. *Nat Immunol* 5:503-507.
66. Chang, M., W. Jin, and S. C. Sun. 2009. Peli1 facilitates TRIF-dependent Toll-like receptor signaling and proinflammatory cytokine production. *Nat Immunol* 10:1089-1095.
67. Pobezinskaya, Y. L., Y. S. Kim, S. Choksi, M. J. Morgan, T. Li, C. Liu, and Z. Liu. 2008. The function of TRADD in signaling through tumor necrosis factor receptor 1 and TRIF-dependent Toll-like receptors. *Nat Immunol* 9:1047-1054.
68. Ermolaeva, M. A., M. C. Michallet, N. Papadopoulou, O. Utermohlen, K. Kranidioti, G. Kollias, J. Tschopp, and M. Pasparakis. 2008. Function of TRADD in tumor necrosis factor receptor 1 signaling and in TRIF-dependent inflammatory responses. *Nat Immunol* 9:1037-1046.
69. Oganesyan, G., S. K. Saha, B. Guo, J. Q. He, A. Shahangian, B. Zarnegar, A. Perry, and G. Cheng. 2006. Critical role of TRAF3 in the Toll-like receptor-dependent and -independent antiviral response. *Nature* 439:208-211.
70. Kawai, T., and S. Akira. 2010. The role of pattern-recognition receptors in innate immunity: update on Toll-like receptors. *Nat Immunol* 11:373-384.
71. Barton, G. M., and J. C. Kagan. 2009. A cell biological view of Toll-like receptor function: regulation through compartmentalization. *Nat Rev Immunol* 9:535-542.
72. Dietrich, N., S. Lienenklaus, S. Weiss, and N. O. Gekara. 2010. Murine toll-like receptor 2 activation induces type I interferon responses from endolysosomal compartments. *PLoS One* 5:e10250.
73. Kadowaki, N., S. Ho, S. Antonenko, R. W. Malefyt, R. A. Kastelein, F. Bazan, and Y. J. Liu. 2001. Subsets of human dendritic cell precursors express different toll-like receptors and respond to different microbial antigens. *J Exp Med* 194:863-869.
74. Honda, K., Y. Ohba, H. Yanai, H. Negishi, T. Mizutani, A. Takaoka, C. Taya, and T. Taniguchi. 2005. Spatiotemporal regulation of MyD88-IRF-7 signalling for robust type-I interferon induction. *Nature* 434:1035-1040.
75. Zelensky, A. N., and J. E. Gready. 2005. The C-type lectin-like domain superfamily. *FEBS J* 272:6179-6217.
76. Geijtenbeek, T. B., and S. I. Gringhuis. 2009. Signalling through C-type lectin receptors: shaping immune responses. *Nat Rev Immunol* 9:465-479.
77. Kerrigan, A. M., and G. D. Brown. 2011. Syk-coupled C-type lectins in immunity. *Trends Immunol* 32:151-156.
78. Hughes, C. E., A. Y. Pollitt, J. Mori, J. A. Eble, M. G. Tomlinson, J. H. Hartwig, C. A. O'Callaghan, K. Futterer, and S. P. Watson. 2010. CLEC-2 activates Syk through dimerization. *Blood* 115:2947-2955.
79. Brown, G. D., and S. Gordon. 2001. Immune recognition. A new receptor for beta-glucans. *Nature* 413:36-37.
80. Rothfuchs, A. G., A. Bafica, C. G. Feng, J. G. Egen, D. L. Williams, G. D. Brown, and A. Sher. 2007. Dectin-1 interaction with Mycobacterium tuberculosis leads to enhanced IL-12p40 production by splenic dendritic cells. *J Immunol* 179:3463-3471.
81. Gross, O., A. Gewies, K. Finger, M. Schafer, T. Sparwasser, C. Peschel, I. Forster, and J. Ruland. 2006. Card9 controls a non-TLR signalling pathway for innate anti-fungal immunity. *Nature* 442:651-656.
82. Gringhuis, S. I., J. den Dunnen, M. Litjens, M. van der Vlist, B. Wevers, S. C. Bruijns, and T. B. Geijtenbeek. 2009. Dectin-1 directs T helper cell differentiation by

controlling noncanonical NF-kappaB activation through Raf-1 and Syk. *Nat Immunol* 10:203-213.

83. Slack, E. C., M. J. Robinson, P. Hernanz-Falcon, G. D. Brown, D. L. Williams, E. Schweighoffer, V. L. Tybulewicz, and C. Reis e Sousa. 2007. Syk-dependent ERK activation regulates IL-2 and IL-10 production by DC stimulated with zymosan. *Eur J Immunol* 37:1600-1612.
84. Shah, V. B., T. R. Ozment-Skelton, D. L. Williams, and L. Keshvara. 2009. Vav1 and PI3K are required for phagocytosis of beta-glucan and subsequent superoxide generation by microglia. *Mol Immunol* 46:1845-1853.
85. LeibundGut-Landmann, S., O. Gross, M. J. Robinson, F. Osorio, E. C. Slack, S. V. Tsoni, E. Schweighoffer, V. Tybulewicz, G. D. Brown, J. Ruland, and C. Reis e Sousa. 2007. Syk- and CARD9-dependent coupling of innate immunity to the induction of T helper cells that produce interleukin 17. *Nat Immunol* 8:630-638.
86. Gross, O., H. Poeck, M. Bscheider, C. Dostert, N. Hannesschlager, S. Endres, G. Hartmann, A. Tardivel, E. Schweighoffer, V. Tybulewicz, A. Mocsai, J. Tschopp, and J. Ruland. 2009. Syk kinase signalling couples to the Nlrp3 inflammasome for anti-fungal host defence. *Nature* 459:433-436.
87. Chen, L. F., S. A. Williams, Y. Mu, H. Nakano, J. M. Duerr, L. Buckbinder, and W. C. Greene. 2005. NF-kappaB RelA phosphorylation regulates RelA acetylation. *Mol Cell Biol* 25:7966-7975.
88. Osorio, F., and E. S. C. Reis. 2011. Myeloid C-type Lectin Receptors in Pathogen Recognition and Host Defense. *Immunity* 34:651-664.
89. Conti, H. R., and S. L. Gaffen. 2010. Host responses to Candida albicans: Th17 cells and mucosal candidiasis. *Microbes Infect* 12:518-527.
90. Cao, W., L. Zhang, D. B. Rosen, L. Bover, G. Watanabe, M. Bao, L. L. Lanier, and Y. J. Liu. 2007. BDCA2/Fc epsilon RI gamma complex signals through a novel BCR-like pathway in human plasmacytoid dendritic cells. *PLoS Biol* 5:e248.
91. Gringhuis, S. I., J. den Dunnen, M. Litjens, B. van Het Hof, Y. van Kooyk, and T. B. Geijtenbeek. 2007. C-type lectin DC-SIGN modulates Toll-like receptor signaling via Raf-1 kinase-dependent acetylation of transcription factor NF-kappaB. *Immunity* 26:605-616.
92. Marshall, A. S., J. A. Willment, H. H. Lin, D. L. Williams, S. Gordon, and G. D. Brown. 2004. Identification and characterization of a novel human myeloid inhibitory C-type lectin-like receptor (MICL) that is predominantly expressed on granulocytes and monocytes. *J Biol Chem* 279:14792-14802.
93. Meyer-Wentrup, F., A. Cambi, B. Joosten, M. W. Looman, I. J. de Vries, C. G. Figdor, and G. J. Adema. 2009. DCIR is endocytosed into human dendritic cells and inhibits TLR8-mediated cytokine production. *J Leukoc Biol* 85:518-525.
94. Steinman, R. M., and J. Banchereau. 2007. Taking dendritic cells into medicine. *Nature* 449:419-426.
95. Tacken, P. J., I. J. de Vries, R. Torensma, and C. G. Figdor. 2007. Dendritic-cell immunotherapy: from ex vivo loading to in vivo targeting. *Nat Rev Immunol* 7:790-802.
96. Yoneyama, M., M. Kikuchi, K. Matsumoto, T. Imaizumi, M. Miyagishi, K. Taira, E. Foy, Y. M. Loo, M. Gale, Jr., S. Akira, S. Yonehara, A. Kato, and T. Fujita. 2005. Shared and unique functions of the DExD/H-box helicases RIG-I, MDA5, and LGP2 in antiviral innate immunity. *J Immunol* 175:2851-2858.
97. Yoneyama, M., M. Kikuchi, T. Natsukawa, N. Shinobu, T. Imaizumi, M. Miyagishi, K. Taira, S. Akira, and T. Fujita. 2004. The RNA helicase RIG-I has an essential

function in double-stranded RNA-induced innate antiviral responses. *Nat Immunol* 5:730-737.

98. Kato, H., O. Takeuchi, S. Sato, M. Yoneyama, M. Yamamoto, K. Matsui, S. Uematsu, A. Jung, T. Kawai, K. J. Ishii, O. Yamaguchi, K. Otsu, T. Tsujimura, C. S. Koh, C. Reis e Sousa, Y. Matsuura, T. Fujita, and S. Akira. 2006. Differential roles of MDA5 and RIG-I helicases in the recognition of RNA viruses. *Nature* 441:101-105.
99. Kato, H., O. Takeuchi, E. Mikamo-Satoh, R. Hirai, T. Kawai, K. Matsushita, A. Hiiragi, T. S. Dermody, T. Fujita, and S. Akira. 2008. Length-dependent recognition of double-stranded ribonucleic acids by retinoic acid-inducible gene-I and melanoma differentiation-associated gene 5. *J Exp Med* 205:1601-1610.
100. Marques, J. T., T. Devosse, D. Wang, M. Zamanian-Daryoush, P. Serbinowski, R. Hartmann, T. Fujita, M. A. Behlke, and B. R. Williams. 2006. A structural basis for discriminating between self and nonself double-stranded RNAs in mammalian cells. *Nat Biotechnol* 24:559-565.
101. Pichlmair, A., O. Schulz, C. P. Tan, T. I. Naslund, P. Liljestrom, F. Weber, and C. Reis e Sousa. 2006. RIG-I-mediated antiviral responses to single-stranded RNA bearing 5'-phosphates. *Science* 314:997-1001.
102. Schlee, M., A. Roth, V. Hornung, C. A. Hagmann, V. Wimmenauer, W. Barchet, C. Coch, M. Janke, A. Mihailovic, G. Wardle, S. Juranek, H. Kato, T. Kawai, H. Poeck, K. A. Fitzgerald, O. Takeuchi, S. Akira, T. Tuschl, E. Latz, J. Ludwig, and G. Hartmann. 2009. Recognition of 5' triphosphate by RIG-I helicase requires short blunt double-stranded RNA as contained in panhandle of negative-strand virus. *Immunity* 31:25-34.
103. Hornung, V., J. Ellegast, S. Kim, K. Brzozka, A. Jung, H. Kato, H. Poeck, S. Akira, K. K. Conzelmann, M. Schlee, S. Endres, and G. Hartmann. 2006. 5'-Triphosphate RNA is the ligand for RIG-I. *Science* 314:994-997.
104. Saito, T., D. M. Owen, F. Jiang, J. Marcotrigiano, and M. Gale, Jr. 2008. Innate immunity induced by composition-dependent RIG-I recognition of hepatitis C virus RNA. *Nature* 454:523-527.
105. Ablasser, A., F. Bauernfeind, G. Hartmann, E. Latz, K. A. Fitzgerald, and V. Hornung. 2009. RIG-I-dependent sensing of poly(dA:dT) through the induction of an RNA polymerase III-transcribed RNA intermediate. *Nat Immunol* 10:1065-1072.
106. Chiu, Y. H., J. B. Macmillan, and Z. J. Chen. 2009. RNA polymerase III detects cytosolic DNA and induces type I interferons through the RIG-I pathway. *Cell* 138:576-591.
107. Malathi, K., B. Dong, M. Gale, Jr., and R. H. Silverman. 2007. Small self-RNA generated by RNase L amplifies antiviral innate immunity. *Nature* 448:816-819.
108. Rothenfusser, S., N. Goutagny, G. DiPerna, M. Gong, B. G. Monks, A. Schoenemeyer, M. Yamamoto, S. Akira, and K. A. Fitzgerald. 2005. The RNA helicase Lgp2 inhibits TLR-independent sensing of viral replication by retinoic acid-inducible gene-I. *J Immunol* 175:5260-5268.
109. Saito, T., R. Hirai, Y. M. Loo, D. Owen, C. L. Johnson, S. C. Sinha, S. Akira, T. Fujita, and M. Gale, Jr. 2007. Regulation of innate antiviral defenses through a shared repressor domain in RIG-I and LGP2. *Proc Natl Acad Sci U S A* 104:582-587.
110. Satoh, T., H. Kato, Y. Kumagai, M. Yoneyama, S. Sato, K. Matsushita, T. Tsujimura, T. Fujita, S. Akira, and O. Takeuchi. 2010. LGP2 is a positive regulator

of RIG-I- and MDA5-mediated antiviral responses. *Proc Natl Acad Sci U S A* 107:1512-1517.

111. Suthar, M. S., H. J. Ramos, M. M. Brassil, J. Netland, C. P. Chappell, G. Blahnik, A. McMillan, M. S. Diamond, E. A. Clark, M. J. Bevan, and M. Gale, Jr. 2012. The RIG-I-like Receptor LGP2 Controls CD8(+) T Cell Survival and Fitness. *Immunity* 37:235-248.
112. Takahasi, K., H. Kumeta, N. Tsuduki, R. Narita, T. Shigemoto, R. Hirai, M. Yoneyama, M. Horiuchi, K. Ogura, T. Fujita, and F. Inagaki. 2009. Solution structures of cytosolic RNA sensor MDA5 and LGP2 C-terminal domains: identification of the RNA recognition loop in RIG-I-like receptors. *J Biol Chem* 284:17465-17474.
113. Lu, C., H. Xu, C. T. Ranjith-Kumar, M. T. Brooks, T. Y. Hou, F. Hu, A. B. Herr, R. K. Strong, C. C. Kao, and P. Li. 2010. The structural basis of 5' triphosphate double-stranded RNA recognition by RIG-I C-terminal domain. *Structure* 18:1032-1043.
114. Kowalinski, E., T. Lunardi, A. A. McCarthy, J. Louber, J. Brunel, B. Grigorov, D. Gerlier, and S. Cusack. 2011. Structural basis for the activation of innate immune pattern-recognition receptor RIG-I by viral RNA. *Cell* 147:423-435.
115. Gee, P., P. K. Chua, J. Gevorkyan, K. Klumpp, I. Najera, D. C. Swinney, and J. Deval. 2008. Essential role of the N-terminal domain in the regulation of RIG-I ATPase activity. *J Biol Chem* 283:9488-9496.
116. Gack, M. U., Y. C. Shin, C. H. Joo, T. Urano, C. Liang, L. Sun, O. Takeuchi, S. Akira, Z. Chen, S. Inoue, and J. U. Jung. 2007. TRIM25 RING-finger E3 ubiquitin ligase is essential for RIG-I-mediated antiviral activity. *Nature* 446:916-920.
117. Zeng, W., L. Sun, X. Jiang, X. Chen, F. Hou, A. Adhikari, M. Xu, and Z. J. Chen. 2010. Reconstitution of the RIG-I pathway reveals a signaling role of unanchored polyubiquitin chains in innate immunity. *Cell* 141:315-330.
118. Liu, H. M., Y. M. Loo, S. M. Horner, G. A. Zornetzer, M. G. Katze, and M. Gale, Jr. 2012. The mitochondrial targeting chaperone 14-3-3epsilon regulates a RIG-I translocon that mediates membrane association and innate antiviral immunity. *Cell Host Microbe* 11:528-537.
119. Jiang, X., L. N. Kinch, C. A. Brautigam, X. Chen, F. Du, N. V. Grishin, and Z. J. Chen. 2012. Ubiquitin-induced oligomerization of the RNA sensors RIG-I and MDA5 activates antiviral innate immune response. *Immunity* 36:959-973.
120. Hou, F., L. Sun, H. Zheng, B. Skaug, Q. X. Jiang, and Z. J. Chen. 2011. MAVS forms functional prion-like aggregates to activate and propagate antiviral innate immune response. *Cell* 146:448-461.
121. Scott, I. 2010. The role of mitochondria in the mammalian antiviral defense system. *Mitochondrion* 10:316-320.
122. Dixit, E., S. Boulant, Y. Zhang, A. S. Lee, C. Odendall, B. Shum, N. Hacohen, Z. J. Chen, S. P. Whelan, M. Fransen, M. L. Nibert, G. Superti-Furga, and J. C. Kagan. 2010. Peroxisomes are signaling platforms for antiviral innate immunity. *Cell* 141:668-681.
123. Loo, Y. M., and M. Gale, Jr. 2011. Immune Signaling by RIG-I-like Receptors. *Immunity* 34:680-692.
124. Schroder, M., M. Baran, and A. G. Bowie. 2008. Viral targeting of DEAD box protein 3 reveals its role in TBK1/IKKepsilon-mediated IRF activation. *EMBO J* 27:2147-2157.

125. Wang, L., S. Li, and M. E. Dorf. 2012. NEMO Binds Ubiquitinated TANK-Binding Kinase 1 (TBK1) to Regulate Innate Immune Responses to RNA Viruses. *PLoS One* 7:e43756.
126. Takahashi, K., T. Kawai, H. Kumar, S. Sato, S. Yonehara, and S. Akira. 2006. Roles of caspase-8 and caspase-10 in innate immune responses to double-stranded RNA. *J Immunol* 176:4520-4524.
127. Poeck, H., M. Bscheider, O. Gross, K. Finger, S. Roth, M. Rebsamen, N. Hannesschlager, M. Schlee, S. Rothenfusser, W. Barchet, H. Kato, S. Akira, S. Inoue, S. Endres, C. Peschel, G. Hartmann, V. Hornung, and J. Ruland. 2010. Recognition of RNA virus by RIG-I results in activation of CARD9 and inflammasome signaling for interleukin 1 beta production. *Nat Immunol* 11:63-69.
128. Ishikawa, H., and G. N. Barber. 2008. STING is an endoplasmic reticulum adaptor that facilitates innate immune signalling. *Nature* 455:674-678.
129. Liu, X. Y., B. Wei, H. X. Shi, Y. F. Shan, and C. Wang. 2010. Tom70 mediates activation of interferon regulatory factor 3 on mitochondria. *Cell Res* 20:994-1011.
130. Pfaller, C. K., Z. Li, C. X. George, and C. E. Samuel. 2011. Protein kinase PKR and RNA adenosine deaminase ADAR1: new roles for old players as modulators of the interferon response. *Curr Opin Immunol* 23:573-582.
131. McAllister, C. S., N. Taghavi, and C. E. Samuel. 2012. Protein Kinase PKR Amplification of Interferon Beta Induction occurs through Initiation Factor eIF-2alpha-mediated Translational Control. *J Biol Chem.*
132. Zhang, Z., T. Kim, M. Bao, V. Facchinetti, S. Y. Jung, A. A. Ghaffari, J. Qin, G. Cheng, and Y. J. Liu. 2011. DDX1, DDX21, and DHX36 helicases form a complex with the adaptor molecule TRIF to sense dsRNA in dendritic cells. *Immunity* 34:866-878.
133. Park, J. H., S. H. Chang, M. C. Kim, S. H. Shin, H. J. Youn, J. K. Kim, Y. S. Jang, and C. W. Kim. 1998. Up-regulation of the expression of major histocompatibility complex class I antigens by plasmid DNA transfection in non-hematopoietic cells. *FEBS Lett* 436:55-60.
134. Ishii, K. J., C. Coban, H. Kato, K. Takahashi, Y. Torii, F. Takeshita, H. Ludwig, G. Sutter, K. Suzuki, H. Hemmi, S. Sato, M. Yamamoto, S. Uematsu, T. Kawai, O. Takeuchi, and S. Akira. 2006. A Toll-like receptor-independent antiviral response induced by double-stranded B-form DNA. *Nat Immunol* 7:40-48.
135. Keating, S. E., M. Baran, and A. G. Bowie. 2011. Cytosolic DNA sensors regulating type I interferon induction. *Trends Immunol* 32:574-581.
136. Rathinam, V. A., and K. A. Fitzgerald. 2011. Cytosolic surveillance and antiviral immunity. *Curr Opin Virol* 1:455-462.
137. Stetson, D. B., and R. Medzhitov. 2006. Recognition of cytosolic DNA activates an IRF3-dependent innate immune response. *Immunity* 24:93-103.
138. Burdette, D. L., K. M. Monroe, K. Sotelo-Troha, J. S. Iwig, B. Eckert, M. Hyodo, Y. Hayakawa, and R. E. Vance. 2011. STING is a direct innate immune sensor of cyclic di-GMP. *Nature* 478:515-518.
139. Takaoka, A., Z. Wang, M. K. Choi, H. Yanai, H. Negishi, T. Ban, Y. Lu, M. Miyagishi, T. Kodama, K. Honda, Y. Ohba, and T. Taniguchi. 2007. DAI (DLM-1/ZBP1) is a cytosolic DNA sensor and an activator of innate immune response. *Nature* 448:501-505.
140. Wang, Z., M. K. Choi, T. Ban, H. Yanai, H. Negishi, Y. Lu, T. Tamura, A. Takaoka, K. Nishikura, and T. Taniguchi. 2008. Regulation of innate immune responses by DAI (DLM-1/ZBP1) and other DNA-sensing molecules. *Proc Natl Acad Sci U S A* 105:5477-5482.

141. Rebsamen, M., L. X. Heinz, E. Meylan, M. C. Michallet, K. Schroder, K. Hofmann, J. Vazquez, C. A. Benedict, and J. Tschopp. 2009. DAI/ZBP1 recruits RIP1 and RIP3 through RIP homotypic interaction motifs to activate NF-kappaB. *EMBO Rep* 10:916-922.
142. Ishii, K. J., T. Kawagoe, S. Koyama, K. Matsui, H. Kumar, T. Kawai, S. Uematsu, O. Takeuchi, F. Takeshita, C. Coban, and S. Akira. 2008. TANK-binding kinase-1 delineates innate and adaptive immune responses to DNA vaccines. *Nature* 451:725-729.
143. Unterholzner, L., S. E. Keating, M. Baran, K. A. Horan, S. B. Jensen, S. Sharma, C. M. Sirois, T. Jin, E. Latz, T. S. Xiao, K. A. Fitzgerald, S. R. Paludan, and A. G. Bowie. 2010. IFI16 is an innate immune sensor for intracellular DNA. *Nat Immunol* 11:997-1004.
144. Jin, T., A. Perry, J. Jiang, P. Smith, J. A. Curry, L. Unterholzner, Z. Jiang, G. Horvath, V. A. Rathinam, R. W. Johnstone, V. Hornung, E. Latz, A. G. Bowie, K. A. Fitzgerald, and T. S. Xiao. 2012. Structures of the HIN domain:DNA complexes reveal ligand binding and activation mechanisms of the AIM2 inflammasome and IFI16 receptor. *Immunity* 36:561-571.
145. Li, T., B. A. Diner, J. Chen, and I. M. Cristea. 2012. Acetylation modulates cellular distribution and DNA sensing ability of interferon-inducible protein IFI16. *Proc Natl Acad Sci U S A* 109:10558-10563.
146. Kim, T., S. Pazhoor, M. Bao, Z. Zhang, S. Hanabuchi, V. Facchinetti, L. Bover, J. Plumas, L. Chaperot, J. Qin, and Y. J. Liu. 2010. Aspartate-glutamate-alanine-histidine box motif (DEAH)/RNA helicase A helicases sense microbial DNA in human plasmacytoid dendritic cells. *Proc Natl Acad Sci U S A* 107:15181-15186.
147. Zhang, Z., B. Yuan, M. Bao, N. Lu, T. Kim, and Y. J. Liu. 2011. The helicase DDX41 senses intracellular DNA mediated by the adaptor STING in dendritic cells. *Nat Immunol* 12:959-965.
148. Zhang, X., T. W. Brann, M. Zhou, J. Yang, R. M. Oguariri, K. B. Lidie, H. Imamichi, D. W. Huang, R. A. Lempicki, M. W. Baseler, T. D. Veenstra, H. A. Young, H. C. Lane, and T. Imamichi. 2011. Cutting edge: Ku70 is a novel cytosolic DNA sensor that induces type III rather than type I IFN. *J Immunol* 186:4541-4545.
149. Yang, P., H. An, X. Liu, M. Wen, Y. Zheng, Y. Rui, and X. Cao. 2010. The cytosolic nucleic acid sensor LRRFIP1 mediates the production of type I interferon via a beta-catenin-dependent pathway. *Nat Immunol* 11:487-494.
150. Martinon, F., K. Burns, and J. Tschopp. 2002. The inflammasome: a molecular platform triggering activation of inflammatory caspases and processing of proIL-beta. *Mol Cell* 10:417-426.
151. Hornung, V., A. Ablasser, M. Charrel-Dennis, F. Bauernfeind, G. Horvath, D. R. Caffrey, E. Latz, and K. A. Fitzgerald. 2009. AIM2 recognizes cytosolic dsDNA and forms a caspase-1-activating inflammasome with ASC. *Nature* 458:514-518.
152. Fernandes-Alnemri, T., J. W. Yu, P. Datta, J. Wu, and E. S. Alnemri. 2009. AIM2 activates the inflammasome and cell death in response to cytoplasmic DNA. *Nature* 458:509-513.
153. Burckstummer, T., C. Baumann, S. Bluml, E. Dixit, G. Durnberger, H. Jahn, M. Planyavsky, M. Bilban, J. Colinge, K. L. Bennett, and G. Superti-Furga. 2009. An orthogonal proteomic-genomic screen identifies AIM2 as a cytoplasmic DNA sensor for the inflammasome. *Nat Immunol* 10:266-272.
154. Roberts, T. L., A. Idris, J. A. Dunn, G. M. Kelly, C. M. Burnton, S. Hodgson, L. L. Hardy, V. Garceau, M. J. Sweet, I. L. Ross, D. A. Hume, and K. J. Stacey. 2009.

HIN-200 proteins regulate caspase activation in response to foreign cytoplasmic DNA. *Science* 323:1057-1060.

155. Kerur, N., M. V. Veettil, N. Sharma-Walia, V. Bottero, S. Sadagopan, P. Otageri, and B. Chandran. 2011. IFI16 Acts as a Nuclear Pathogen Sensor to Induce the Inflammasome in Response to Kaposi Sarcoma-Associated Herpesvirus Infection. *Cell Host Microbe* 9:363-375.
156. Stetson, D. B., J. S. Ko, T. Heidmann, and R. Medzhitov. 2008. Trex1 prevents cell-intrinsic initiation of autoimmunity. *Cell* 134:587-598.
157. Yasutomo, K., T. Horiuchi, S. Kagami, H. Tsukamoto, C. Hashimura, M. Urushihara, and Y. Kuroda. 2001. Mutation of DNASE1 in people with systemic lupus erythematosus. *Nat Genet* 28:313-314.
158. Yoshida, H., Y. Okabe, K. Kawane, H. Fukuyama, and S. Nagata. 2005. Lethal anemia caused by interferon-beta produced in mouse embryos carrying undigested DNA. *Nat Immunol* 6:49-56.
159. Crow, Y. J., B. E. Hayward, R. Parmar, P. Robins, A. Leitch, M. Ali, D. N. Black, H. van Bokhoven, H. G. Brunner, B. C. Hamel, P. C. Corry, F. M. Cowan, S. G. Frints, J. Klepper, J. H. Livingston, S. A. Lynch, R. F. Massey, J. F. Meritet, J. L. Michaud, G. Ponsot, T. Voit, P. Lebon, D. T. Bonthron, A. P. Jackson, D. E. Barnes, and T. Lindahl. 2006. Mutations in the gene encoding the 3'-5' DNA exonuclease TREX1 cause Aicardi-Goutieres syndrome at the AGS1 locus. *Nat Genet* 38:917-920.
160. Kanneganti, T. D. 2010. Central roles of NLRs and inflammasomes in viral infection. *Nat Rev Immunol* 10:688-698.
161. Bauernfeind, F., A. Ablasser, E. Bartok, S. Kim, J. Schmid-Burgk, T. Cavlar, and V. Hornung. 2011. Inflammasomes: current understanding and open questions. *Cell Mol Life Sci* 68:765-783.
162. Duncan, J. A., D. T. Bergstralh, Y. Wang, S. B. Willingham, Z. Ye, A. G. Zimmermann, and J. P. Ting. 2007. Cryopyrin/NALP3 binds ATP/dATP, is an ATPase, and requires ATP binding to mediate inflammatory signaling. *Proc Natl Acad Sci U S A* 104:8041-8046.
163. Franchi, L., R. Munoz-Planillo, and G. Nunez. 2012. Sensing and reacting to microbes through the inflammasomes. *Nat Immunol* 13:325-332.
164. Puren, A. J., G. Fantuzzi, and C. A. Dinarello. 1999. Gene expression, synthesis, and secretion of interleukin 18 and interleukin 1beta are differentially regulated in human blood mononuclear cells and mouse spleen cells. *Proc Natl Acad Sci U S A* 96:2256-2261.
165. Hsu, L. C., S. R. Ali, S. McGillivray, P. H. Tseng, S. Mariathasan, E. W. Humke, L. Eckmann, J. J. Powell, V. Nizet, V. M. Dixit, and M. Karin. 2008. A NOD2-NALP1 complex mediates caspase-1-dependent IL-1beta secretion in response to Bacillus anthracis infection and muramyl dipeptide. *Proc Natl Acad Sci U S A* 105:7803-7808.
166. Gong, Y. N., and F. Shao. 2012. Sensing bacterial infections by NAIP receptors in NLRC4 inflammasome activation. *Protein Cell* 3:98-105.
167. Lightfield, K. L., J. Persson, S. W. Brubaker, C. E. Witte, J. von Moltke, E. A. Dunipace, T. Henry, Y. H. Sun, D. Cado, W. F. Dietrich, D. M. Monack, R. M. Tsolis, and R. E. Vance. 2008. Critical function for Naip5 in inflammasome activation by a conserved carboxy-terminal domain of flagellin. *Nat Immunol* 9:1171-1178.

168. Petrilli, V., S. Papin, C. Dostert, A. Mayor, F. Martinon, and J. Tschopp. 2007. Activation of the NALP3 inflammasome is triggered by low intracellular potassium concentration. *Cell Death Differ* 14:1583-1589.
169. Ichinohe, T., I. K. Pang, and A. Iwasaki. 2010. Influenza virus activates inflammasomes via its intracellular M2 ion channel. *Nat Immunol* 11:404-410.
170. Martinon, F., V. Petrilli, A. Mayor, A. Tardivel, and J. Tschopp. 2006. Gout-associated uric acid crystals activate the NALP3 inflammasome. *Nature* 440:237-241.
171. Dostert, C., V. Petrilli, R. Van Bruggen, C. Steele, B. T. Mossman, and J. Tschopp. 2008. Innate immune activation through Nalp3 inflammasome sensing of asbestos and silica. *Science* 320:674-677.
172. Halle, A., V. Hornung, G. C. Petzold, C. R. Stewart, B. G. Monks, T. Reinheckel, K. A. Fitzgerald, E. Latz, K. J. Moore, and D. T. Golenbock. 2008. The NALP3 inflammasome is involved in the innate immune response to amyloid-beta. *Nat Immunol* 9:857-865.
173. Hornung, V., F. Bauernfeind, A. Halle, E. O. Samstad, H. Kono, K. L. Rock, K. A. Fitzgerald, and E. Latz. 2008. Silica crystals and aluminum salts activate the NALP3 inflammasome through phagosomal destabilization. *Nat Immunol* 9:847-856.
174. Eisenbarth, S. C., O. R. Colegio, W. O'Connor, F. S. Sutterwala, and R. A. Flavell. 2008. Crucial role for the Nalp3 inflammasome in the immunostimulatory properties of aluminium adjuvants. *Nature* 453:1122-1126.
175. Zhou, R., A. Tardivel, B. Thorens, I. Choi, and J. Tschopp. 2010. Thioredoxin-interacting protein links oxidative stress to inflammasome activation. *Nat Immunol* 11:136-140.
176. Bauernfeind, F. G., G. Horvath, A. Stutz, E. S. Alnemri, K. MacDonald, D. Speert, T. Fernandes-Alnemri, J. Wu, B. G. Monks, K. A. Fitzgerald, V. Hornung, and E. Latz. 2009. Cutting edge: NF-kappaB activating pattern recognition and cytokine receptors license NLRP3 inflammasome activation by regulating NLRP3 expression. *J Immunol* 183:787-791.
177. Magalhaes, J. G., M. T. Sorbara, S. E. Girardin, and D. J. Philpott. 2011. What is new with Nods? *Curr Opin Immunol* 23:29-34.
178. Kanneganti, T. D., M. Lamkanfi, and G. Nunez. 2007. Intracellular NOD-like receptors in host defense and disease. *Immunity* 27:549-559.
179. Ting, J. P., J. A. Duncan, and Y. Lei. 2010. How the noninflammasome NLRs function in the innate immune system. *Science* 327:286-290.
180. Kersse, K., M. J. Bertrand, M. Lamkanfi, and P. Vandenabeele. 2011. NOD-like receptors and the innate immune system: coping with danger, damage and death. *Cytokine Growth Factor Rev* 22:257-276.
181. Bertrand, M. J., K. Doiron, K. Labbe, R. G. Korneluk, P. A. Barker, and M. Saleh. 2009. Cellular inhibitors of apoptosis cIAP1 and cIAP2 are required for innate immunity signaling by the pattern recognition receptors NOD1 and NOD2. *Immunity* 30:789-801.
182. Hsu, Y. M., Y. Zhang, Y. You, D. Wang, H. Li, O. Duramad, X. F. Qin, C. Dong, and X. Lin. 2007. The adaptor protein CARD9 is required for innate immune responses to intracellular pathogens. *Nat Immunol* 8:198-205.
183. Sabbah, A., T. H. Chang, R. Harnack, V. Frohlich, K. Tominaga, P. H. Dube, Y. Xiang, and S. Bose. 2009. Activation of innate immune antiviral responses by Nod2. *Nat Immunol* 10:1073-1080.

184. Dugan, J. W., A. Albor, L. David, J. Fowlkes, M. T. Blackledge, T. M. Martin, S. R. Planck, H. L. Rosenzweig, J. T. Rosenbaum, and M. P. Davey. 2009. Nucleotide oligomerization domain-2 interacts with 2'-5'-oligoadenylate synthetase type 2 and enhances RNase-L function in THP-1 cells. *Mol Immunol* 47:560-566.
185. Watanabe, T., N. Asano, S. Fichtner-Feigl, P. L. Gorelick, Y. Tsuji, Y. Matsumoto, T. Chiba, I. J. Fuss, A. Kitani, and W. Strober. 2010. NOD1 contributes to mouse host defense against Helicobacter pylori via induction of type I IFN and activation of the ISGF3 signaling pathway. *J Clin Invest* 120:1645-1662.
186. Moore, C. B., D. T. Bergstralh, J. A. Duncan, Y. Lei, T. E. Morrison, A. G. Zimmermann, M. A. Accavitti-Loper, V. J. Madden, L. Sun, Z. Ye, J. D. Lich, M. T. Heise, Z. Chen, and J. P. Ting. 2008. NLRX1 is a regulator of mitochondrial antiviral immunity. *Nature* 451:573-577.
187. Tattoli, I., L. A. Carneiro, M. Jehanno, J. G. Magalhaes, Y. Shu, D. J. Philpott, D. Arnoult, and S. E. Girardin. 2008. NLRX1 is a mitochondrial NOD-like receptor that amplifies NF-kappaB and JNK pathways by inducing reactive oxygen species production. *EMBO Rep* 9:293-300.
188. Isaacs, A., and J. Lindenmann. 1957. Virus interference. I. The interferon. *Proc R Soc Lond B Biol Sci* 147:258-267.
189. Gonzalez-Navajas, J. M., J. Lee, M. David, and E. Raz. 2012. Immunomodulatory functions of type I interferons. *Nat Rev Immunol* 12:125-135.
190. Li, M., X. Liu, Y. Zhou, and S. B. Su. 2009. Interferon-lambdas: the modulators of antivirus, antitumor, and immune responses. *J Leukoc Biol* 86:23-32.
191. Platanias, L. C. 2005. Mechanisms of type-I- and type-II-interferon-mediated signalling. *Nat Rev Immunol* 5:375-386.
192. Li, Y., A. Sassano, B. Majchrzak, D. K. Deb, D. E. Levy, M. Gaestel, A. R. Nebreda, E. N. Fish, and L. C. Platanias. 2004. Role of p38alpha Map kinase in Type I interferon signaling. *J Biol Chem* 279:970-979.
193. Sun, D., and A. Ding. 2006. MyD88-mediated stabilization of interferon-gamma-induced cytokine and chemokine mRNA. *Nat Immunol* 7:375-381.
194. Gough, D. J., D. E. Levy, R. W. Johnstone, and C. J. Clarke. 2008. IFNgamma signaling-does it mean JAK-STAT? *Cytokine Growth Factor Rev* 19:383-394.
195. Joshi, S., S. Kaur, B. Kroczynska, and L. C. Platanias. 2010. Mechanisms of mRNA translation of interferon stimulated genes. *Cytokine* 52:123-127.
196. Du, Z., L. Wei, A. Murti, S. R. Pfeffer, M. Fan, C. H. Yang, and L. M. Pfeffer. 2007. Non-conventional signal transduction by type 1 interferons: the NF-kappaB pathway. *J Cell Biochem* 102:1087-1094.
197. Wei, L., M. R. Sandbulte, P. G. Thomas, R. J. Webby, R. Homayouni, and L. M. Pfeffer. 2006. NFkappaB negatively regulates interferon-induced gene expression and anti-influenza activity. *J Biol Chem* 281:11678-11684.
198. Gough, D. J., N. L. Messina, C. J. Clarke, R. W. Johnstone, and D. E. Levy. 2012. Constitutive type I interferon modulates homeostatic balance through tonic signaling. *Immunity* 36:166-174.
199. Hata, N., M. Sato, A. Takaoka, M. Asagiri, N. Tanaka, and T. Taniguchi. 2001. Constitutive IFN-alpha/beta signal for efficient IFN-alpha/beta gene induction by virus. *Biochem Biophys Res Commun* 285:518-525.
200. Sato, M., N. Hata, M. Asagiri, T. Nakaya, T. Taniguchi, and N. Tanaka. 1998. Positive feedback regulation of type I IFN genes by the IFN-inducible transcription factor IRF-7. *FEBS Lett* 441:106-110.

201. Thomas, K. E., C. L. Galligan, R. D. Newman, E. N. Fish, and S. N. Vogel. 2006. Contribution of interferon-beta to the murine macrophage response to the toll-like receptor 4 agonist, lipopolysaccharide. *J Biol Chem* 281:31119-31130.
202. Mink, M., B. Fogelgren, K. Olszewski, P. Maroy, and K. Csiszar. 2001. A novel human gene (SARM) at chromosome 17q11 encodes a protein with a SAM motif and structural similarity to Armadillo/beta-catenin that is conserved in mouse, Drosophila, and Caenorhabditis elegans. *Genomics* 74:234-244.
203. Jault, C., L. Pichon, and J. Chluba. 2004. Toll-like receptor gene family and TIR-domain adapters in Danio rerio. *Mol Immunol* 40:759-771.
204. Meijer, A. H., S. F. Gabby Krens, I. A. Medina Rodriguez, S. He, W. Bitter, B. Ewa Snaar-Jagalska, and H. P. Spaink. 2004. Expression analysis of the Toll-like receptor and TIR domain adaptor families of zebrafish. *Mol Immunol* 40:773-783.
205. Tewari, R., E. Bailes, K. A. Bunting, and J. C. Coates. 2010. Armadillo-repeat protein functions: questions for little creatures. *Trends Cell Biol* 20:470-481.
206. Kim, C. A., and J. U. Bowie. 2003. SAM domains: uniform structure, diversity of function. *Trends Biochem Sci* 28:625-628.
207. Panneerselvam, P., L. P. Singh, B. Ho, J. Chen, and J. L. Ding. 2012. Targeting of pro-apoptotic TLR adaptor SARM to mitochondria: definition of the critical region and residues in the signal sequence. *Biochem J* 442:263-271.
208. Couillault, C., N. Pujol, J. Reboul, L. Sabatier, J. F. Guichou, Y. Kohara, and J. J. Ewbank. 2004. TLR-independent control of innate immunity in Caenorhabditis elegans by the TIR domain adaptor protein TIR-1, an ortholog of human SARM. *Nat Immunol* 5:488-494.
209. Kim, D. H., R. Feinbaum, G. Alloing, F. E. Emerson, D. A. Garsin, H. Inoue, M. Tanaka-Hino, N. Hisamoto, K. Matsumoto, M. W. Tan, and F. M. Ausubel. 2002. A conserved p38 MAP kinase pathway in Caenorhabditis elegans innate immunity. *Science* 297:623-626.
210. Troemel, E. R., S. W. Chu, V. Reinke, S. S. Lee, F. M. Ausubel, and D. H. Kim. 2006. p38 MAPK regulates expression of immune response genes and contributes to longevity in C. elegans. *PLoS Genet* 2:e183.
211. Shivers, R. P., D. J. Pagano, T. Kooistra, C. E. Richardson, K. C. Reddy, J. K. Whitney, O. Kamanzi, K. Matsumoto, N. Hisamoto, and D. H. Kim. 2010. Phosphorylation of the conserved transcription factor ATF-7 by PMK-1 p38 MAPK regulates innate immunity in Caenorhabditis elegans. *PLoS Genet* 6:e1000892.
212. Irazoqui, J. E., J. M. Urbach, and F. M. Ausubel. 2010. Evolution of host innate defence: insights from Caenorhabditis elegans and primitive invertebrates. *Nat Rev Immunol* 10:47-58.
213. Shivers, R. P., T. Kooistra, S. W. Chu, D. J. Pagano, and D. H. Kim. 2009. Tissue-specific activities of an immune signaling module regulate physiological responses to pathogenic and nutritional bacteria in C. elegans. *Cell Host Microbe* 6:321-330.
214. Chuang, C. F., and C. I. Bargmann. 2005. A Toll-interleukin 1 repeat protein at the synapse specifies asymmetric odorant receptor expression via ASK1 MAPKKK signaling. *Genes Dev* 19:270-281.
215. Peng, J., Q. Yuan, B. Lin, P. Panneerselvam, X. Wang, X. L. Luan, S. K. Lim, B. P. Leung, B. Ho, and J. L. Ding. 2010. SARM inhibits both TRIF- and MyD88-mediated AP-1 activation. *Eur J Immunol* 40:1738-1747.
216. Belinda, L. W., W. X. Wei, B. T. Hanh, L. X. Lei, H. Bow, and D. J. Ling. 2008. SARM: a novel Toll-like receptor adaptor, is functionally conserved from arthropod to human. *Mol Immunol* 45:1732-1742.

217. Yuan, S., K. Wu, M. Yang, L. Xu, L. Huang, H. Liu, X. Tao, S. Huang, and A. Xu. 2010. Amphioxus SARM involved in neural development may function as a suppressor of TLR signaling. *J Immunol* 184:6874-6881.
218. Zhou, X., T. Jiang, X. Du, P. Zhou, Z. Jiang, J. J. Michal, and B. Liu. 2012. Molecular characterization of porcine SARM1 and its role in regulating TLRs signaling during highly pathogenic porcine reproductive and respiratory syndrome virus infection in vivo. *Dev Comp Immunol.*
219. Pudla, M., K. Limposuwan, and P. Utaisincharoen. 2011. Burkholderia pseudomallei-Induced Expression of a Negative Regulator, Sterile-{alpha} and Armadillo Motif-Containing Protein, in Mouse Macrophages: a Possible Mechanism for Suppression of the MyD88-Independent Pathway. *Infect Immun* 79:2921-2927.
220. Kim, Y., P. Zhou, L. Qian, J. Z. Chuang, J. Lee, C. Li, C. Iadecola, C. Nathan, and A. Ding. 2007. MyD88-5 links mitochondria, microtubules, and JNK3 in neurons and regulates neuronal survival. *J Exp Med* 204:2063-2074.
221. Szretter, K. J., M. A. Samuel, S. Gilfillan, A. Fuchs, M. Colonna, and M. S. Diamond. 2009. The immune adaptor molecule SARM modulates tumor necrosis factor alpha production and microglia activation in the brainstem and restricts West Nile Virus pathogenesis. *J Virol* 83:9329-9338.
222. Chen, C. Y., C. W. Lin, C. Y. Chang, S. T. Jiang, and Y. P. Hsueh. 2011. Sarm1, a negative regulator of innate immunity, interacts with syndecan-2 and regulates neuronal morphology. *J Cell Biol* 193:769-784.
223. Osterloh, J. M., J. Yang, T. M. Rooney, A. N. Fox, R. Adalbert, E. H. Powell, A. E. Sheehan, M. A. Avery, R. Hackett, M. A. Logan, J. M. MacDonald, J. S. Ziegenfuss, S. Milde, Y. J. Hou, C. Nathan, A. Ding, R. H. Brown, Jr., L. Conforti, M. Coleman, M. Tessier-Lavigne, S. Zuchner, and M. R. Freeman. 2012. dSarm/Sarm1 is required for activation of an injury-induced axon death pathway. *Science* 337:481-484.
224. Blum, E. S., M. C. Abraham, S. Yoshimura, Y. Lu, and S. Shaham. 2012. Control of nonapoptotic developmental cell death in Caenorhabditis elegans by a polyglutamine-repeat protein. *Science* 335:970-973.
225. Molday, L. L., W. W. Wu, and R. S. Molday. 2007. Retinoschisin (RS1), the protein encoded by the X-linked retinoschisis gene, is anchored to the surface of retinal photoreceptor and bipolar cells through its interactions with a Na/K ATPase-SARM1 complex. *J Biol Chem* 282:32792-32801.
226. Piao, W., C. Song, H. Chen, M. A. Diaz, L. M. Wahl, K. A. Fitzgerald, L. Li, and A. E. Medvedev. 2009. Endotoxin tolerance dysregulates MyD88- and Toll/IL-1R domain-containing adapter inducing IFN-beta-dependent pathways and increases expression of negative regulators of TLR signaling. *J Leukoc Biol* 86:863-875.
227. de Vos, A. F., J. M. Pater, P. S. van den Pangaart, M. D. de Kruif, C. van 't Veer, and T. van der Poll. 2009. In vivo lipopolysaccharide exposure of human blood leukocytes induces cross-tolerance to multiple TLR ligands. *J Immunol* 183:533-542.
228. Roberson, S. M., and W. S. Walker. 1988. Immortalization of cloned mouse splenic macrophages with a retrovirus containing the v-raf/mil and v-myc oncogenes. *Cell Immunol* 116:341-351.
229. Genin, P., M. Algarte, P. Roof, R. Lin, and J. Hiscott. 2000. Regulation of RANTES chemokine gene expression requires cooperativity between NF-kappa B and IFN-regulatory factor transcription factors. *J Immunol* 164:5352-5361.

230. Anderson, P. 2010. Post-transcriptional regulons coordinate the initiation and resolution of inflammation. *Nat Rev Immunol* 10:24-35.
231. Hochstrasser, M. 1996. Ubiquitin-dependent protein degradation. *Annu Rev Genet* 30:405-439.
232. O'Neill, L. A., F. J. Sheedy, and C. E. McCoy. 2011. MicroRNAs: the fine-tuners of Toll-like receptor signalling. *Nat Rev Immunol* 11:163-175.
233. Pedersen, I. M., G. Cheng, S. Wieland, S. Volinia, C. M. Croce, F. V. Chisari, and M. David. 2007. Interferon modulation of cellular microRNAs as an antiviral mechanism. *Nature* 449:919-922.
234. Liew, F. Y., D. Xu, E. K. Brint, and L. A. O'Neill. 2005. Negative regulation of toll-like receptor-mediated immune responses. *Nat Rev Immunol* 5:446-458.
235. West, A. P., G. S. Shadel, and S. Ghosh. 2011. Mitochondria in innate immune responses. *Nat Rev Immunol* 11:389-402.
236. Robbins, M., A. Judge, and I. MacLachlan. 2009. siRNA and innate immunity. *Oligonucleotides* 19:89-102.
237. Sakaguchi, S., H. Negishi, M. Asagiri, C. Nakajima, T. Mizutani, A. Takaoka, K. Honda, and T. Taniguchi. 2003. Essential role of IRF-3 in lipopolysaccharide-induced interferon-beta gene expression and endotoxin shock. *Biochem Biophys Res Commun* 306:860-866.
238. Fitzgerald, K. A., D. C. Rowe, B. J. Barnes, D. R. Caffrey, A. Visintin, E. Latz, B. Monks, P. M. Pitha, and D. T. Golenbock. 2003. LPS-TLR4 signaling to IRF-3/7 and NF-kappaB involves the toll adapters TRAM and TRIF. *J Exp Med* 198:1043-1055.
239. Banchereau, J., and R. M. Steinman. 1998. Dendritic cells and the control of immunity. *Nature* 392:245-252.
240. Hoebe, K., E. M. Janssen, S. O. Kim, L. Alexopoulou, R. A. Flavell, J. Han, and B. Beutler. 2003. Upregulation of costimulatory molecules induced by lipopolysaccharide and double-stranded RNA occurs by Trif-dependent and Trif-independent pathways. *Nat Immunol* 4:1223-1229.
241. Shen, H., B. M. Tesar, W. E. Walker, and D. R. Goldstein. 2008. Dual signaling of MyD88 and TRIF is critical for maximal TLR4-induced dendritic cell maturation. *J Immunol* 181:1849-1858.
242. Kamon, H., T. Kawabe, H. Kitamura, J. Lee, D. Kamimura, T. Kaisho, S. Akira, A. Iwamatsu, H. Koga, M. Murakami, and T. Hirano. 2006. TRIF-GEFH1-RhoB pathway is involved in MHCII expression on dendritic cells that is critical for CD4 T-cell activation. *EMBO J* 25:4108-4119.
243. Mengozzi, M., and P. Ghezzi. 1993. Cytokine down-regulation in endotoxin tolerance. *Eur Cytokine Netw* 4:89-98.
244. Biswas, S. K., P. Bist, M. K. Dhillon, T. Kajiji, C. Del Fresno, M. Yamamoto, E. Lopez-Collazo, S. Akira, and V. Tergaonkar. 2007. Role for MyD88-independent, TRIF pathway in lipid A/TLR4-induced endotoxin tolerance. *J Immunol* 179:4083-4092.
245. Freudenberg, M. A., and C. Galanos. 1988. Induction of tolerance to lipopolysaccharide (LPS)-D-galactosamine lethality by pretreatment with LPS is mediated by macrophages. *Infect Immun* 56:1352-1357.
246. Ramirez-Carrozzi, V. R., D. Braas, D. M. Bhatt, C. S. Cheng, C. Hong, K. R. Doty, J. C. Black, A. Hoffmann, M. Carey, and S. T. Smale. 2009. A unifying model for the selective regulation of inducible transcription by CpG islands and nucleosome remodeling. *Cell* 138:114-128.

247. Fleetwood, A. J., H. Dinh, A. D. Cook, P. J. Hertzog, and J. A. Hamilton. 2009. GM-CSF- and M-CSF-dependent macrophage phenotypes display differential dependence on type I interferon signaling. *J Leukoc Biol* 86:411-421.
248. Nakaya, T., M. Sato, N. Hata, M. Asagiri, H. Suemori, S. Noguchi, N. Tanaka, and T. Taniguchi. 2001. Gene induction pathways mediated by distinct IRFs during viral infection. *Biochem Biophys Res Commun* 283:1150-1156.
249. Menachery, V. D., and D. A. Leib. 2009. Control of herpes simplex virus replication is mediated through an interferon regulatory factor 3-dependent pathway. *J Virol* 83:12399-12406.
250. Liu, J., X. Guan, and X. Ma. 2005. Interferon regulatory factor 1 is an essential and direct transcriptional activator for interferon {gamma}-induced RANTES/CCl5 expression in macrophages. *J Biol Chem* 280:24347-24355.
251. Liu, J., and X. Ma. 2006. Interferon regulatory factor 8 regulates RANTES gene transcription in cooperation with interferon regulatory factor-1, NF-kappaB, and PU.1. *J Biol Chem* 281:19188-19195.
252. Cremer, I., J. Ghysdael, and V. Vieillard. 2002. A non-classical ISRE/ISGF3 pathway mediates induction of RANTES gene transcription by type I IFNs. *FEBS Lett* 511:41-45.
253. Noppert, S. J., K. A. Fitzgerald, and P. J. Hertzog. 2007. The role of type I interferons in TLR responses. *Immunol Cell Biol* 85:446-457.
254. Shaw, G., and R. Kamen. 1986. A conserved AU sequence from the 3' untranslated region of GM-CSF mRNA mediates selective mRNA degradation. *Cell* 46:659-667.
255. Carballo, E., W. S. Lai, and P. J. Blackshear. 1998. Feedback inhibition of macrophage tumor necrosis factor-alpha production by tristetraprolin. *Science* 281:1001-1005.
256. Hao, S., and D. Baltimore. 2009. The stability of mRNA influences the temporal order of the induction of genes encoding inflammatory molecules. *Nat Immunol* 10:281-288.
257. Shakhov, A. N., M. A. Collart, P. Vassalli, S. A. Nedospasov, and C. V. Jongeneel. 1990. Kappa B-type enhancers are involved in lipopolysaccharide-mediated transcriptional activation of the tumor necrosis factor alpha gene in primary macrophages. *J Exp Med* 171:35-47.
258. Ford, E., and D. Thanos. 2010. The transcriptional code of human IFN-beta gene expression. *Biochim Biophys Acta* 1799:328-336.
259. Casola, A., R. P. Garofalo, H. Haeberle, T. F. Elliott, R. Lin, M. Jamaluddin, and A. R. Brasier. 2001. Multiple cis regulatory elements control RANTES promoter activity in alveolar epithelial cells infected with respiratory syncytial virus. *J Virol* 75:6428-6439.
260. Sato, M., H. Suemori, N. Hata, M. Asagiri, K. Ogasawara, K. Nakao, T. Nakaya, M. Katsuki, S. Noguchi, N. Tanaka, and T. Taniguchi. 2000. Distinct and essential roles of transcription factors IRF-3 and IRF-7 in response to viruses for IFN-alpha/beta gene induction. *Immunity* 13:539-548.
261. Medzhitov, R., and T. Horng. 2009. Transcriptional control of the inflammatory response. *Nat Rev Immunol* 9:692-703.
262. Saccani, S., S. Pantano, and G. Natoli. 2001. Two waves of nuclear factor kappaB recruitment to target promoters. *J Exp Med* 193:1351-1359.
263. Zhou, W., P. Zhu, J. Wang, G. Pascual, K. A. Ohgi, J. Lozach, C. K. Glass, and M. G. Rosenfeld. 2008. Histone H2A monoubiquitination represses transcription by inhibiting RNA polymerase II transcriptional elongation. *Mol Cell* 29:69-80.

264. Hargreaves, D. C., T. Horng, and R. Medzhitov. 2009. Control of inducible gene expression by signal-dependent transcriptional elongation. *Cell* 138:129-145.
265. Krausgruber, T., K. Blazek, T. Smallie, S. Alzabin, H. Lockstone, N. Sahgal, T. Hussell, M. Feldmann, and I. A. Udalova. 2011. IRF5 promotes inflammatory macrophage polarization and TH1-TH17 responses. *Nat Immunol* 12:231-238.
266. Lacey, D. C., A. Achuthan, A. J. Fleetwood, H. Dinh, J. Roiniotis, G. M. Scholz, M. W. Chang, S. K. Beckman, A. D. Cook, and J. A. Hamilton. 2012. Defining GM-CSF- and macrophage-CSF-dependent macrophage responses by in vitro models. *J Immunol* 188:5752-5765.
267. Beutler, B., N. Krochin, I. W. Milsark, C. Luedke, and A. Cerami. 1986. Control of cachectin (tumor necrosis factor) synthesis: mechanisms of endotoxin resistance. *Science* 232:977-980.
268. Gais, P., C. Tiedje, F. Altmayr, M. Gaestel, H. Weighardt, and B. Holzmann. 2010. TRIF signaling stimulates translation of TNF-alpha mRNA via prolonged activation of MK2. *J Immunol* 184:5842-5848.
269. Buxade, M., J. L. Parra, S. Rousseau, N. Shpiro, R. Marquez, N. Morrice, J. Bain, E. Espel, and C. G. Proud. 2005. The Mnks are novel components in the control of TNF alpha biosynthesis and phosphorylate and regulate hnRNP A1. *Immunity* 23:177-189.
270. Li, S., L. Wang, M. Berman, Y. Y. Kong, and M. E. Dorf. 2011. Mapping a dynamic innate immunity protein interaction network regulating type I interferon production. *Immunity* 35:426-440.
271. Wan, Y., H. Xiao, J. Affolter, T. W. Kim, K. Bulek, S. Chaudhuri, D. Carlson, T. Hamilton, B. Mazumder, G. R. Stark, J. Thomas, and X. Li. 2009. Interleukin-1 receptor-associated kinase 2 is critical for lipopolysaccharide-mediated post-transcriptional control. *J Biol Chem* 284:10367-10375.
272. Lu, Y. C., W. C. Yeh, and P. S. Ohashi. 2008. LPS/TLR4 signal transduction pathway. *Cytokine* 42:145-151.
273. Takaoka, A., T. Tamura, and T. Taniguchi. 2008. Interferon regulatory factor family of transcription factors and regulation of oncogenesis. *Cancer Sci* 99:467-478.
274. Chen, W., and W. E. Royer, Jr. 2010. Structural insights into interferon regulatory factor activation. *Cell Signal* 22:883-887.
275. Chen, W., H. Srinath, S. S. Lam, C. A. Schiffer, W. E. Royer, Jr., and K. Lin. 2008. Contribution of Ser386 and Ser396 to activation of interferon regulatory factor 3. *J Mol Biol* 379:251-260.
276. Servant, M. J., B. ten Oever, C. LePage, L. Conti, S. Gessani, I. Julkunen, R. Lin, and J. Hiscott. 2001. Identification of distinct signaling pathways leading to the phosphorylation of interferon regulatory factor 3. *J Biol Chem* 276:355-363.
277. Clement, J. F., A. Bibeau-Poirier, S. P. Gravel, N. Grandvaux, E. Bonneil, P. Thibault, S. Meloche, and M. J. Servant. 2008. Phosphorylation of IRF-3 on Ser 339 generates a hyperactive form of IRF-3 through regulation of dimerization and CBP association. *J Virol* 82:3984-3996.
278. Negishi, H., Y. Fujita, H. Yanai, S. Sakaguchi, X. Ouyang, M. Shinohara, H. Takayanagi, Y. Ohba, T. Taniguchi, and K. Honda. 2006. Evidence for licensing of IFN-gamma-induced IFN regulatory factor 1 transcription factor by MyD88 in Toll-like receptor-dependent gene induction program. *Proc Natl Acad Sci U S A* 103:15136-15141.

279. Clarke, L. A., C. S. Rebelo, J. Goncalves, M. G. Boavida, and P. Jordan. 2001. PCR amplification introduces errors into mononucleotide and dinucleotide repeat sequences. *Mol Pathol* 54:351-353.
280. Lokuta, M. A., J. Maher, K. H. Noe, P. M. Pitha, M. L. Shin, and H. S. Shin. 1996. Mechanisms of murine RANTES chemokine gene induction by Newcastle disease virus. *J Biol Chem* 271:13731-13738.
281. Kadonaga, J. T. 2004. Regulation of RNA polymerase II transcription by sequence-specific DNA binding factors. *Cell* 116:247-257.
282. Nelson, J. D., O. Denisenko, and K. Bomsztyk. 2006. Protocol for the fast chromatin immunoprecipitation (ChIP) method. *Nat Protoc* 1:179-185.
283. Dubois, M. F., V. T. Nguyen, S. Bellier, and O. Bensaude. 1994. Inhibitors of transcription such as 5,6-dichloro-1-beta-D-ribofuranosylbenzimidazole and isoquinoline sulfonamide derivatives (H-8 and H-7) promote dephosphorylation of the carboxyl-terminal domain of RNA polymerase II largest subunit. *J Biol Chem* 269:13331-13336.
284. Kim, T. K., J. S. Lee, S. Y. Oh, X. Jin, Y. J. Choi, T. H. Lee, E. Lee, Y. K. Choi, S. You, Y. G. Chung, J. B. Lee, R. A. DePinho, L. Chin, and H. Kim. 2007. Direct transcriptional activation of promyelocytic leukemia protein by IFN regulatory factor 3 induces the p53-dependent growth inhibition of cancer cells. *Cancer Res* 67:11133-11140.
285. Duguay, D., F. Mercier, J. Stagg, D. Martineau, J. Bramson, M. Servant, R. Lin, J. Galipeau, and J. Hiscott. 2002. In vivo interferon regulatory factor 3 tumor suppressor activity in B16 melanoma tumors. *Cancer Res* 62:5148-5152.
286. Kim, T. Y., K. H. Lee, S. Chang, C. Chung, H. W. Lee, J. Yim, and T. K. Kim. 2003. Oncogenic potential of a dominant negative mutant of interferon regulatory factor 3. *J Biol Chem* 278:15272-15278.
287. Tokunaga, T., Y. Naruke, S. Shigematsu, T. Kohno, K. Yasui, Y. Ma, K. J. Chua, I. Katayama, T. Nakamura, Y. Hishikawa, T. Koji, Y. Yatabe, T. Nagayasu, T. Fujita, T. Matsuyama, and H. Hayashi. 2010. Aberrant expression of interferon regulatory factor 3 in human lung cancer. *Biochem Biophys Res Commun* 397:202-207.
288. Quyun, C., Z. Ye, S. C. Lin, and B. Lin. 2010. Recent patents and advances in genomic biomarker discovery for colorectal cancers. *Recent Pat DNA Gene Seq* 4:86-93.
289. Xu, H. G., R. Jin, W. Ren, L. Zou, Y. Wang, and G. P. Zhou. 2012. Transcription factors Sp1 and Sp3 regulate basal transcription of the human IRF-3 gene. *Biochimie* 94:1390-1397.
290. Xu, H. G., W. Ren, L. Zou, Y. Wang, R. Jin, and G. P. Zhou. 2011. Direct repression of the human IRF-3 promoter by E2F1. *Immunogenetics* 63:189-196.
291. Xu, H. G., W. Ren, C. Lu, and G. P. Zhou. 2010. Characterization of the human IRF-3 promoter and its regulation by the transcription factor E2F1. *Mol Biol Rep* 37:3073-3080.
292. Leone, G., J. DeGregori, R. Sears, L. Jakoi, and J. R. Nevins. 1997. Myc and Ras collaborate in inducing accumulation of active cyclin E/Cdk2 and E2F. *Nature* 387:422-426.
293. Wang, C., F. J. Rauscher, 3rd, W. D. Cress, and J. Chen. 2007. Regulation of E2F1 function by the nuclear corepressor KAP1. *J Biol Chem* 282:29902-29909.
294. Black, A. R., J. D. Black, and J. Azizkhan-Clifford. 2001. Sp1 and kruppel-like factor family of transcription factors in cell growth regulation and cancer. *J Cell Physiol* 188:143-160.

295. Kumar, D., J. Hosse, C. von Toerne, E. Noessner, and P. J. Nelson. 2009. JNK MAPK pathway regulates constitutive transcription of CCL5 by human NK cells through SP1. *J Immunol* 182:1011-1020.
296. Song, A., Y. F. Chen, K. Thamatrakoln, T. A. Storm, and A. M. Krensky. 1999. RFLAT-1: a new zinc finger transcription factor that activates RANTES gene expression in T lymphocytes. *Immunity* 10:93-103.
297. Li, L., and J. R. Davie. 2010. The role of Sp1 and Sp3 in normal and cancer cell biology. *Ann Anat* 192:275-283.
298. Ahn, Y. T., B. Huang, L. McPherson, C. Clayberger, and A. M. Krensky. 2007. Dynamic interplay of transcriptional machinery and chromatin regulates "late" expression of the chemokine RANTES in T lymphocytes. *Mol Cell Biol* 27:253-266.
299. Adelman, K., M. A. Kennedy, S. Nechaev, D. A. Gilchrist, G. W. Muse, Y. Chinenov, and I. Rogatsky. 2009. Immediate mediators of the inflammatory response are poised for gene activation through RNA polymerase II stalling. *Proc Natl Acad Sci U S A* 106:18207-18212.
300. Zhou, Q., T. Li, and D. H. Price. 2012. RNA polymerase II elongation control. *Annu Rev Biochem* 81:119-143.
301. Shengli Hao, a. D. B. 2012. RNA splicing regulates the temporal order of TNF-induced gene expression. *J Immunol, Meeting Abstract* 188, 167.5.
302. Linder, P., and E. Jankowsky. 2011. From unwinding to clamping - the DEAD box RNA helicase family. *Nat Rev Mol Cell Biol* 12:505-516.
303. Fuller-Pace, F. V., and S. Ali. 2008. The DEAD box RNA helicases p68 (Ddx5) and p72 (Ddx17): novel transcriptional co-regulators. *Biochem Soc Trans* 36:609-612.
304. Rossow, K. L., and R. Janknecht. 2003. Synergism between p68 RNA helicase and the transcriptional coactivators CBP and p300. *Oncogene* 22:151-156.
305. Fukuda, T., K. Yamagata, S. Fujiyama, T. Matsumoto, I. Koshida, K. Yoshimura, M. Mihara, M. Naitou, H. Endoh, T. Nakamura, C. Akimoto, Y. Yamamoto, T. Katagiri, C. Foulds, S. Takezawa, H. Kitagawa, K. Takeyama, B. W. O'Malley, and S. Kato. 2007. DEAD-box RNA helicase subunits of the Drosha complex are required for processing of rRNA and a subset of microRNAs. *Nat Cell Biol* 9:604-611.
306. Kawai, S., and A. Amano. 2012. BRCA1 regulates microRNA biogenesis via the DROSHA microprocessor complex. *J Cell Biol* 197:201-208.
307. Koga, T., E. Sardina, R. M. Tidwell, M. Pelletier, D. C. Look, and M. J. Holtzman. 1999. Virus-inducible expression of a host chemokine gene relies on replication-linked mRNA stabilization. *Proc Natl Acad Sci U S A* 96:5680-5685.
308. Berger, E. A., P. M. Murphy, and J. M. Farber. 1999. Chemokine receptors as HIV-1 coreceptors: roles in viral entry, tropism, and disease. *Annu Rev Immunol* 17:657-700.
309. Levy, J. A. 2009. The unexpected pleiotropic activities of RANTES. *J Immunol* 182:3945-3946.
310. Nikolcheva, T., S. Pyronnet, S. Y. Chou, N. Sonenberg, A. Song, C. Clayberger, and A. M. Krensky. 2002. A translational rheostat for RFLAT-1 regulates RANTES expression in T lymphocytes. *J Clin Invest* 110:119-126.
311. Krensky, A. M., and Y. T. Ahn. 2007. Mechanisms of disease: regulation of RANTES (CCL5) in renal disease. *Nat Clin Pract Nephrol* 3:164-170.
312. Ooi, A. G., D. Sahoo, M. Adorno, Y. Wang, I. L. Weissman, and C. Y. Park. 2010. MicroRNA-125b expands hematopoietic stem cells and enriches for the lymphoid-

balanced and lymphoid-biased subsets. *Proc Natl Acad Sci U S A* 107:21505-21510.

313. Hosking, M. P., and T. E. Lane. 2010. The role of chemokines during viral infection of the CNS. *PLoS Pathog* 6:e1000937.
314. Lim, J. K., C. Y. Louie, C. Glaser, C. Jean, B. Johnson, H. Johnson, D. H. McDermott, and P. M. Murphy. 2008. Genetic deficiency of chemokine receptor CCR5 is a strong risk factor for symptomatic West Nile virus infection: a meta-analysis of 4 cohorts in the US epidemic. *J Infect Dis* 197:262-265.
315. Goverman, J. 2009. Autoimmune T cell responses in the central nervous system. *Nat Rev Immunol* 9:393-407.
316. Gade-Andavolu, R., D. E. Comings, J. MacMurray, R. K. Vuthoori, W. W. Tourtellotte, R. M. Nagra, and L. A. Cone. 2004. RANTES: a genetic risk marker for multiple sclerosis. *Mult Scler* 10:536-539.
317. dos Santos, A. C., M. M. Barsante, R. M. Arantes, C. C. Bernard, M. M. Teixeira, and J. Carvalho-Tavares. 2005. CCL2 and CCL5 mediate leukocyte adhesion in experimental autoimmune encephalomyelitis--an intravital microscopy study. *J Neuroimmunol* 162:122-129.